

Hans-Klaus Roth, Klaus Heinemann, Gerhard Gobsch

4th International Symposium
Technologies for Polymer Electronics - TPE 10 -

Special thanks of the editors go to Mrs. BIANCA KÄMMER.

She helped us again most conscientiously to cope with the wealth of abstracts and showed also remarkable patience in preparing this proceedings of TPE 10.

Volume 1

Proceedings

**4th International Symposium Technologies
for Polymer Electronics
- TPE 10 -**

Thuringian Institute of Textile and
Plastics Research, Rudolstadt
and
Ilmenau University of Technology

18. - 20. May 2010, Rudolstadt/Germany

ed. by
Hans-Klaus Roth, Klaus Heinemann
and Gerhard Gobsch



Universitätsverlag Ilmenau
2010

Impressum

Bibliografische Information der Deutschen Nationalbibliothek

Die Deutsche Nationalbibliothek verzeichnet diese Publikation in der Deutschen Nationalbibliografie; detaillierte bibliografische Angaben sind im Internet über <http://dnb.d-nb.de> abrufbar.

Technische Universität Ilmenau/Universitätsbibliothek

Universitätsverlag Ilmenau

Postfach 10 05 65

98684 Ilmenau

www.tu-ilmenau.de/universitaetsverlag

Herstellung und Auslieferung

Thüringisches Institut für Textil- und Kunststoff-Forschung e.V.

Breitscheidstr. 97

07407 Rudolstadt

www.titk.de

ISBN 978-3-939473-66-4 (Druckausgabe)

urn:nbn:de:gbv:ilm1-2010100013

Symposium Board

International Advisory Committee

Prof. Dr. R. Baumann (TU Chemnitz, D)
Prof. Dr. M. Berggren (Uni Linköping, S)
Dr. Ch. Brabec (Uni Erlangen, Erlangen D)
Prof. Dr. K.-H. Bock (TU Berlin, D)
Prof. Dr. G. Gobsch (TU Ilmenau, D)
Prof. Dr. D. Fichou (CEA Saclay, F)
Prof. Dr. G. Gobsch (TU Ilmenau, D)
Prof. Dr. G. Horowitz (Uni Paris, F)
Prof. Dr. O. Inganäs (Uni Linköping, S)
Prof. Dr. G. E. Jabbour (Adv. PV. C., Uni Arizona, USA)
Prof. Dr. R. Janssen (TU Eindhoven, NL)
Dr. S. Kirchmeyer (H. C. Starck Clevios, Leverkusen, D)
Dr. F. Krebs (RISO National Laboratory, DK)
Dr. J. Kroon (ECN, Petten, NL)
Dr. Th. Kugler (CDT, Cambridge, UK)
Prof. Dr. N. Martin (Uni Madrid, E)
Dr. A. Lux (Novaled AG, Dresden, D)
Dr. K. Schmidt (PolyIC, Fürth, D)
Dr. D. Müller (Merck Adv. Tech., Darmstadt, D)
Prof. Dr. J.-M. Nunzi (Uni Limoges, Limoges, F)
Prof. Dr. G. Paasch (IFW, Dresden, D)
Prof. Dr. H.-K. Roth (TITK, Rudolstadt, D)
Prof. Dr. V. F. Razumov (ICP Chernogolovka, RUS)
Prof. Dr. N. S. Sariciftci (Uni Linz, A)
Prof. Dr. U. S. Schubert (Uni Jena, D)
Dr. M. Shkunov (Uni Surrey, UK)
Prof. Dr. H. Sirringhaus (Plastic Logic, Cambridge, UK)
Prof. Dr. G. A. Sotzing (Uni Connecticut, USA)
Dr. B. Stadlober (Joanneum Research, Weiz, A)
Prof. Dr. L. Torsi (Uni Bari, I)
Prof. Dr. D. Vanderzande (Uni Hasselt, B)

Local Conference Committee

Dr. R.-U. Bauer (TITK, Rudolstadt)
Prof. Dr. G. Gobsch (TU Ilmenau)
Prof. Dr. K. Heinemann (TITK, Rudolstadt)
Dr. H. Hoppe (TU Ilmenau)
Mrs. B. Kämmer (TITK, Rudolstadt)
Prof. Dr. H.-K. Roth (TITK, Rudolstadt)
Prof. Dr. P. Scharff (TU Ilmenau)
Dr. S. Scheinert (TU Ilmenau)
Dr. M. Schrödner (TITK, Rudolstadt)
Dr. S. Sensfuss (TITK, Rudolstadt)

CONTENTS Vol. 1

Introductions

- Fichou, D.;** GIF-SUR-YVETTE (F) 1
Supramolecular self-assembly on surfaces: a bottom-up strategy towards novel 2D multicomponent networks
- Schubert, U.;** Jena (D) 6
Synthesis, characterization and inkjet printing of functional materials
- Berggren, M.;** Tybrandt, K.; Larsson, K.; Bolin, M.; Persson, K.; Svennersten, K.; Simon, D.; Jager, E.; Richter-Dahlfors, A.; Norrköping (S) 13
Organic Bioelectronics

OLEDs and related 1

- Neher, D.;** Barge, S.; Potsdam (D) 16
Polymer-based white-emitting OLED's: Function and Perspectives
- Da Como, E.;** Hallermann, M.; Feldmann, J.; München (D) 20
Suppression of Exciton-Charge Quenching and Electrode Photon Losses in Organic Light-Emitting Devices
- Hasselgruber, M.;** Todt, U.; Finger, F.; May, C.; Baumann, R.; Dresden (D) 22
Low cost fabrication of OLED-substrates for Large-Area Lighting: The application of printing technologies for OLED-substrate structuring
- Malliaras, G. ;** Gardanne (F) 27
Organic electronics at the interface with biology

OFET's and devices 1

- Horowitz, G.;** Battaglini, N.; Braga, D.; Kergoat, L.; Kim, H; Paris (F) 29
New architectures for the organic transistors
- Melzer, C.;** von Seggern, H.; Schidleja, M.; Feldmeier, E.; Darmstadt (D) 32
Ambipolar charge transport and light emission in organic field-effect transistors
- Nakayama, K.;** Yonezawa (J) 37
Development of vertical-type metal-base organic transistors
- Turner, M.;** Madec, M.B.; Morrison, J.J.; Yeates, S.G.; Wedge, D.C.; Kell, D.B.; Kettle, J.; Song, A.; Das, A.; Grell, M.; Richardson, T.H.; Manchester (UK) 42
Low cost sensing arrays using organic semiconductors

Materials & Methods 1

Sariciftci, S.; Linz (A) 46
New materials for organic and bio-organic optoelectronic devices

Kirchmeyer, S.; Leverkusen (D) 48
Material challenges for printed electronics

Müller, D.; Backlund, T.; Brookes, P.; Canisius, J.; Lloyd, G.; Miskiewicz, P.;
Carrasco-Orozco, M.; Tierney, S.; Darmstadt (D) 51
Development of Stable, High-Performing Organic Semiconductors and TFTs

Solar cells / OPV 1

Jabbour, G.; Arizona (USA) 54
Interfacial effects in photovoltaics and progress in printed Quantum Dot LEDs

Brabec, Ch.; Erlangen (D) 55
Reliability and failure mechanisms of organic solar cells

van Assche, G.; Zhao, J.; Demir, F.; Van den Brande, N.; Bertho, S.; Vanderzande, D.;
Van Mele, B.; Brüssel (B) 56
On the relation between thermal transformations and morphological stability of polymer:
fullerene solar cells

Berny, S.; Torteck, L.; Véber, M.; Fichou, D.; Gif-sur Yvette (F) 62
Improved hole collection in organic solar cells using dithiapyrranylidene ultra-thin films
as anodic interlayers

Presselt, M.; Herrmann, F.; Seeland, M.; Bärenklau, M.; Engmann, S.; Roesch, R.;
Shokhovets, S.; Hoppe, H.; Gobsch, G.; Ilmenau (D) 65
Observation of charge-transfer complex absorption and emission in polymer solar cells

OFET and devices

Wagner, V.; Gburek, B.; Balster, T.; Bremen (D) 68
From ultra-thin model systems to flexible thin film transistors

Paasch, G.; Scheinert, S.; Dresden (D) 71
The influence of gaussian disorder on the performance of organic devices

Caironi, M.; Gili, E.; Sirringhaus, H.; Cambridge (UK) 77
Printed CMOS-like inverters for fast-switching organic logic circuits

Meyer-Friedrichsen, T.; Ponomarenko, S.A.; Borshchev, O.V.; Leverkusen (D) 81
Design of organic semiconductors for self assembled monolayer field effect transistors
(SAM-FETs)

Halik, M. ; Erlangen (D) Approaches in flexible thin film electronics	86
Irimia-Vladu, M. ; Bauer, S.; Sariciftci, N.S.; Linz (A) New strategies and materials for organic field effect transistors	89
Kugler, T. ; Othman, K.; Newsome, C.; Wilson, R.; Burroughes, J.; Godmanchester (UK) Interface engineering for optimising solution-processed high-mobility OTFTs	95
Shkunov, M. ; Opoku, C.; Guildford (UK) Solution processable nanomaterial field-effect transistors	97
von Hauff, E. ; Fuchs, K.; Parisi, J.; Oldenburg (D) Molecularly imprinted polymer layers for the regulation of L-Glutamate	101
 OLEDs and related 2	
Leo, K. ; Dresden (D) Highly efficient organic devices	104
Fernández-Lázaro, F. ; Rodriguez-Redondo, J.L.; Céspedes-Guirao, F.J.; Costa, R.D.; Gierschner, J.; Ortí, E.; Bolink, H.J.; Sastre-Santos, A.; Elche (E) Red-Light-Emitting electrochemical cells based on Iridium(III) complexes	105
Padilla, J. ; Invernale, M.; Ding, Y.; Mamangun, D.; Sotzing, G.A.; Cartagena (E) Optimizing contrast in dual electrochromic devices with optically transparent ion-storage layers	107
 Materials & Methods 2	
Roth, H.-K. ; Konkin, A.; Krinichnyi, V.I.; Schroedner, M.; Rudolstadt (D) Photoinduced electron transfer and transient states in organic composites studied by ESR	112
Urbina, A. ; Garcia-Sakai, V.; Tyagi, M.; Espinosa, N.; Diaz-Paniagua, C.; F.; Garcia Valverde, R.; Padilla, J.; Abad, J.; Batallán and F.; Murcia (E) Molecular dynamics of poly-alkyl-thiophenes: experimental study by neutron scattering, rheology and calorimetry	123
Schmidt, W. ; Osnabrück (D) Paper based substrates for polymer electronics	129
Voit, W. ; Reinhold, I.; Zapka, W.; Gaiser, D.; Järfälla (S) Deposition of PEDOT: PSS dispersions with industrial inkjet printheads	131

Paraschuk, D.Yu.; Gromchenko, A.A.; Zapunidi, S.A.; Bruevich, V.V.; Khlopin, N.A.; Dyakov, V.A.; Gvozdokova, I.A.; Tsikalova, M.V.; Novikov, Yu.N.; Moskau (RUS) 138
Metallocomplexes of fullerenes for polymer solar cells with enhanced photovoltage

Solar cells / OPV 2

Nunzi, J.-M.; Derbal, H.; Bergeret, C.; Cousseau, J.; Limoges (F) 143
Functionalized single wall carbon nanotubes significantly improve the performances of polymer solar cells

Sensfuss, S.; Blankenburg, L.; Schache, H.; Shokhovets, S.; Gobsch, G.; Konkin, A.; Sell, S.; Klemm, E.; Dellith, A.; Andrae, G.; Rudolstadt (D) 150
Improvements of thienopyrazine-PPV based polymer solar cells by thiol additives

Vanderzande, D.; Oosterbaan, W.D.; Vrindts, V.; Bertho, S.; Bolsée, J.C.; Gadisa, A.; Vandewal, K.; Manca, J.; Lutsen, L.; Cleij, T.J.; Haen, J.D.; Zhao, J.; Van Assche, G.; Van Mele, B.; Diepembeek (B) 158
Use of Nanofibers in bulk heterojunction solar cells: The effect of order and morphology on the performance of P3HT: PCBM blends

Veenstra, S.; Verhees, W.J.H.; Slooff, L.H.; Kroon, J.M.; Galagan, Y.; Grossiord, N.; Andriessen, R.A.; Petten (NL) 166
Exploring device concepts for efficient, stable and cost effective printed polymer PV

Troshin, P.A.; Susarova, D.K.; Khalina, E.A.; Goryachev, A.E.; Egbe, D.; Ponomarevko, S.A.; Sariciftci, N.S.; Razumov, V.F.; Chernogolovka, (RUS) 168
Solubility and molecular structure effects of donor and acceptor materials in bulk heterojunction organic solar cells

Stadler, P.; Track, A.M.; Ullah, M.; Sitter, H.; Matt, G.J.; Neugebauer, H.; Singh, T.B.; Sariciftci, N.S.; Koller, G.; Ramsey, M.; Linz (A) 169
Correlation between the energy level alignment and device performance in organic field effect transistors

Hoppe, H.; Bärenklau, M.; Schoonderbeek, A.; Roesch, R.; Muhsin, B.; Stute, U.; Teckhaus, D.; Gobsch, G.; Ilmenau (D) 175
Towards roll-to-roll processing of flexible polymer solar modules

CONTENTS Vol. 2

Posters

- Abad, J.;** Espinosa, N.; Urbina, A.; Colchero, J.; Murcia (E) 176
Nanoscale ultraviolet and ozone degradation of P3OT thin films studied by scanning probe microscopy and related techniques
- Auner, C.;** Stadlober, B.; Gold, H.; Haase, A.; Palfinger, U.; Haber, T.; Sezen, M.; Grogger, W.; Jakopic, G.; Weiz (A) 181
Residue-free NIL structuring techniques for submicron OTFT's
- Blankenburg, L.;** Schultheis, K.; Sensfuß, S.; Schrödner, M.; Schache, H.; Rudolstadt (D) 186
Reel-to-reel wet coating for the formation of thin functional layers in bulk-heterojunction polymer solar cells
- Berny, S.;** Torteck, L.; Fichou, D.; Gif-sur-Yvette (F) 187
Recombination-limited photocurrent in dithiapyranylidene/PCBM bulk heterojunctions
- Bober, P.;** Trchová, M.; Stejskal, J.; Prag (CZ) 188
Polyaniline – silver composites
- Borchert, H.;** Zutz, F.; Heinemann, M.D.; Witt, F.; Kruszynska, M.; Radychev, N.; Lokteva, I.; von Hauff, E.; von Maydell, K.; Kolny-Olesia, J.; Riedel, I.; Parisi J.; Oldenburg (D) 191
Organic-based solar cells with CdSe nanoparticles as electron acceptor materials
- Carbonera, C.;** Bernardi, A.; Allegramente G.; Pellegrino, A.; Po, R.; Giannotta, G.; Savoini, A.; Novara (I) 199
P3HT-Peryeryleneimide solar cells: performances of bulk heterojunctions vs. bilayer architectures
- Do, T. H.;** Vogeler, H.; Bott, A.; Pütz, A.; Colsmann, A.; Lemmer, U.; Karlsruhe (D) 206
Low voltage solution processed organic light emitting p-i-n diodes
- Espinosa, N.;** Garcia-Valverde, R.; Garcia-Cascales, M.S.; Urbina, A.; Cartagena (E) 209
Multi-criteria decision method applied to film forming techniques in polymer solar cells
- Georgakopoulos, S.;** Sparrowe, D.; Shkunov, M.; Guildford (UK) 221
Stability in bottom-and top-gate organic field-effect transistors
- Da Como, E.;** Hallermann, M.; Feldmann, J.; München (D) 225
Recombination via charge transfer excitons in polymer/fullerene blends: the role of Morphology and molecular conformation

Dittrich, C.; Kolbusch, T.; Dormagen (D)	226
Production technologies for large area flexible electronics and OPV	
Konyushenko, E.N.; Trchová, M.; Stejskal, J.; Prag (CZ)	228
Polyaniline, MWCNTs/PANI composites-their properties and possible application	
Kostyanovskiy, V. A.; Troshin, P.A.; Susarova, D.K.; Khalina, E.A.; Getachew, A.;	234
Peregudov, A.S.; Razumov, V.F.; Chernogolovka (RUS)	
Novel low band gap electron donor materials for organic solar cells	
Nazmutdinova, G.; Schrödner, M.; Schache, H.; Raabe, D.; Rudolstadt (D)	235
Electrochemical studies on new electrochromic polymer	
Reinhold, I.; Stürmer, M.; Steinhäuser, F.; Madjarov, A.; Sutter, T.;	239
Voit, W.; Zapka, W.; Järfälla (S)	
Grayscale inkjet printing of phase change materials with increased reliability	
Reuter, K.; Deshmukh, K.D.; Kempa, H.; Katz, H.E.; Hübler, A.C.; Chemnitz (D)	243
Printed full-swing inverters using charged dielectrics	
Scheipl, G.; Stadlober, B.; Zirkl, M.; Kraker, E.; Kuna, L.; Magnien, J.; Jakopic, G.;	246
Krenn, J.R.; Sawatdee, A.; Bodö, P.; Weiz (A)	
Fully printed PVDF based pyroelectrical Sensors	
Sinwel, D.; Egginger, M.; Sariciftci, N.S.; Linz (A)	252
Electrical characterization of organic vertical transistors	
Susarova, D.K.; Troshin, P.A.; Babenko, S.D.; Moskvina, Yu.L.; Razumov, V.F.;	253
Chernogolovka (RUS)	
Effect of various chemical additives on the active layer morphology and photovoltaic performance of the fullerene/polymer bulk heterojunction solar cells	
Berny, S.; Tortech, L.; Matzen, S.; Moussy, J.-B.; Fichou, D.; Gif-sur-Yvette (F)	254
Growth of ultra-thin organic films for magnetic decoupling in hybrid organic inorganic heterostructures	
Tunc, A.V.; Hauff, v. E.; Parisi, J.; Oldenburg (D)	255
Investigations of the dependence of the saturation behaviour and charge carrier mobility on the film thickness and channel length in MDMO-PPV organic field effect measurements	
Valozhyn, A.; Solntsev, A.; Zhdanok, S.; Kwiatkowska, M.; Roslaniec, Z.;	257
Petukhou, Yu.; Uglov, V.; Zenker, M.; Subocz, J.; Minsk (BY)	
Dielectric properties of PET films modified by functional carbon nanomaterials	

Berson, S.; Guillerez, S.; Mourao, J.; Barret, M.; Pierron, P.; Dieudonné, M.; Sonntag, P.; Grenoble (F) Development of an inkjet printing process for the production of OPV modules : the solarjet project	262
Ghani, F.; Kristen, J.; Riegler, H.; Potsdam (D) Nanoaggregates of phthalocyanine for organic photovoltaic applications	263
Pradana, A.; Threm, D.; Rädler, M.; Gerken, M.; Kiel (D) Integration of two different spin-coated optoelectronic devices on a single substrate	264
Riedel, B.; Hauss, J.; Kaiser, I.; Guetlein, J.; Geyer, U.; Huska, K.; Lemmer, U.; Gerken, M.; Karlsruhe (D) Methods to enhance the efficiency of organic light emitting devices	267
Sapurina, I.; Trchova, M.; Stejskal, J.; St. Petersburg (RUS) Nafion membrane modification for application in fuel cells	272
Stejskal, J.; Sapurina, I.; Trchova, M.; Prague (CZ) Polyaniline: the presence and the future	275

Part I:

Introductions

SUPRAMOLECULAR SELF-ASSEMBLY ON SURFACES: A BOTTOM-UP STRATEGY TOWARD NOVEL 2D MULTICOMPONENT NETWORKS

Denis Fichou^{1,2}

¹ CEA-Saclay, Groupe Nanostructures & Semi-Conducteurs Organiques, IRAMIS/SPCSI, 91191 Gif-sur-Yvette, France

² Institut Parisien de Chimie Moléculaire, UMR CNRS 7201, Université Paris VI, France

denis.fichou@cea.fr

Supramolecular networks are attracting considerable interest as highly ordered functional materials for applications in nanotechnology and organic electronic devices. The challenge consists in directing the ordering of predesigned molecular species into periodic architectures over extended length scales with atomic precision. The self-assembly of functionalized organic molecules on surfaces is governed by an intricate balance of adsorbate-substrate and adsorbate-adsorbate interactions. The ability to disentangle these competing interactions would enable to design target 2D patterns having the desired structure and properties (optical, magnetic, etc). Highly-organized supramolecular 2D arrays can be obtained by self-assembly of molecules which interlock via either chemical (H-bonds) or physical (shape recognition) interactions. An alternative approach aimed at tailoring multicomponent networks consists in trapping guest molecules into a host open network to form guest-host architectures. We report here on various recent 2D self-organized systems that we generated at the liquid/solid interface and investigated by scanning tunnelling microscopy.¹⁻⁷

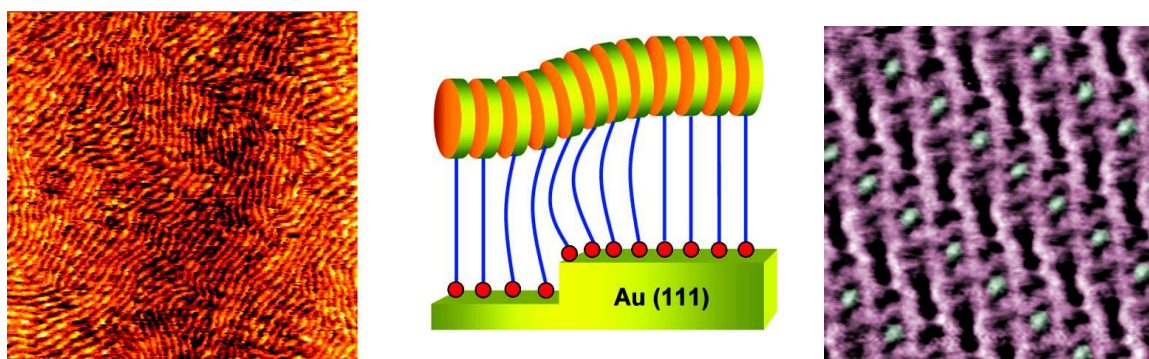


Figure 1 STM image ($115 \times 115 \text{ nm}^2$) and schematic structure of HBC nanocolumns chemisorbed on Au(111) showing the “soft” step crossing of HBC molecules when they bear a long and flexible grafting chain. *From Ref.5*

Figure 2 STM image of a self-organized supramolecular guest-host 2D network on graphite ($21 \times 21 \text{ nm}^2$). Vertical cavities (dark contrast) remain empty while horizontal cavities are filled with a C_{60} molecule (in green). *From Ref.1*

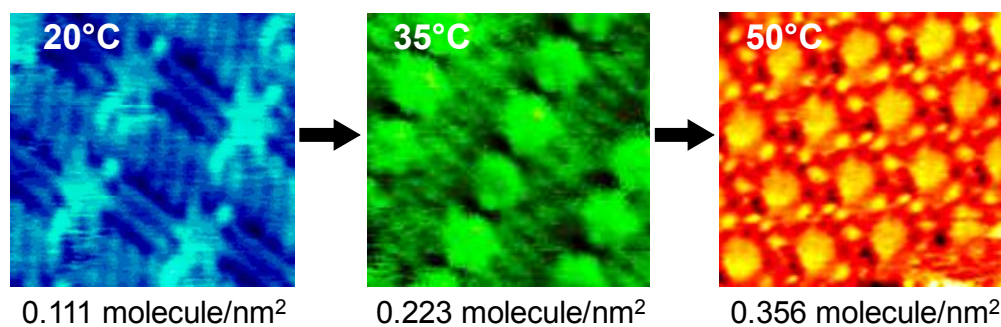
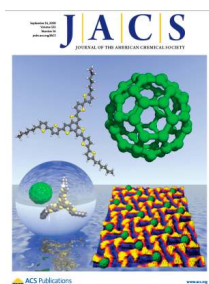


Figure 3 Tuning the packing density of 2D supramolecular self-assemblies at the solid-liquid interface using variable temperature. *From Ref.3*



1. L. Piot, F. Silly, L. Torteck, Y. Nicolas, P. Blanchard, J. Roncali, D. Fichou *J. Am. Chem. Soc.* **2009**, *131*, 12864.
2. M. Zhao, K. Deng, P. Jiang, X. Peng, S. Xie, D. Fichou, and C. Jiang, *J. Phys. Chem. C* **2010**, *114*, 1646.
3. C. Marie, F. Silly, L. Torteck, K. Müllen, D. Fichou, *ACS Nano* **2010**, *4*, 1288.
4. A. Popoff and D. Fichou, *J. Mol. Struct.* **2009**, *936*, 156.
5. L. Piot, C. Marie, X. Dou, X. Feng, K. Müllen, D. Fichou, *J. Am. Chem. Soc.* **2009**, *131*, 1378.
6. A. Popoff and D. Fichou, *Col. Surf. B: Biointerfaces* **2008**, *63*, 153.
7. L. Piot, C. Marie, X. Feng, K. Müllen, and D. Fichou, *Adv. Mater.* **2008**, *20*, 3854.

Curriculum vitae

Professor Dr. Denis Fichou
CEA Saclay
SPSCI/IRAMIS
91191 Gif-sur-Yvette Cédex
France
Tel: +33-1 69 08 43 74
Fax: +33-1 69 08 84 46



Prof. Dr. Denis Fichou is a 1st class Research Director at CNRS in France. He is the current Head of the *Laboratory of Organic Nanostructures and Semiconductors* that he founded in CEA-Saclay, close to Paris, in 2001. His lab is a joint unit between CNRS, CEA-Saclay and Pierre et Marie Curie University.

From 1987, D. Fichou has pioneered organic transistors and their applications in “plastic electronics”. Since then, he has been developing organic semiconductors and devices and has published more than 150 articles in international journals such as *Advanced Materials*, *J. Am. Chem. Soc.*, *Nature*, etc.

Since 2001, his research is oriented towards nanosciences and nanotechnologies of organic semiconductors and devices. A major topic is to tailor supramolecular self-assemblies on atomically flat surfaces and implement them as the active materials in field-effect transistors and photovoltaic solar cells. Another research axis is the study of single crystalline organic semiconductors at the micro and nanoscale. Scanning tunneling microscopy (STM) and spectroscopy (STS) are the main techniques used in these programs. Therefore, the lab is equipped with various facilities for near-field microscopies (STM at the liquid-solid interface, UHV/STM, light-assisted STM, etc), device characterizations (microprobe station, lasers, etc)

Besides, D. Fichou has been appointed as Professor of Organic Chemistry in France (1981), Morocco (1982), Japan (1986 and 1992) and is currently a Visiting Professor at the Nanyang Technological University (NTU) of Singapore since 2005. Finally, he has been acting as the coordinator or partner of several research programs in France, Europe, Japan, Singapore, etc, and is a member of various scientific committees. He is also the organizer of several international conferences worldwide such as APS, SPIE, ECME, etc.

Selected recent publications

- 1 Immobilization of paracetamol and benzocaine pro-drug derivatives as long-range self-organized monolayers on graphite.
A. Popoff, D. Fichou, *Colloids and Surfaces B: Biointerfaces*, **2008**, *63*, 153-158.
- 2 Investigation on the nature of the chemical link between acetylenic organosilane self-assembled monolayers and Au(111) by means of synchrotron radiation photoelectron spectroscopy and scanning tunneling microscopy.
N. Katsonis, A. Marchenko, D. Fichou, and N. Barrett, *Surface Science*, **2008**, *602*, 9-16.
- 3 9,10-ter-anthrylene-ethynylene: a new molecular architecture for solution processed anthracene-based thin film transistors.
Dell'Aquila, F. Marinelli, J. Tey, P. Keg, Y-M. Lam, O. Kapitanchuk, P. Mastrorilli, C. F. Nobile, P. Cosma, A. Marchenko, D. Fichou, S. G. Mhaisalkar, G-P. Suranna, and L. Torsi, *J. Mater. Chem.*, **2008**, *18*, 786-791.
- 4 Two-dimensional self-assembly and complementary base-pairing between amphiphathic nucleotides on graphite.
I. Bestel, N. Campins, A. Marchenko, D. Fichou, M. W. Grinstaff, and P. Barthélémy, *Journal of Colloid and Interface Science*, **2008**, (doi:10.1016/j.jcis.2008.04.042)
- 5 Direct Observation of Alkyl Chain Interdigitation in Conjugated Polyquarterthiophene Self-Organized on Graphite.
P. Keg, A. Lohani, D. Fichou, Y.M. Lam, Y. Wu, B.S. Ong, S.G. Mhaisalkar, *Macromol. Rapid Commun.* **2008**, *29*, (doi: 10.1002/marc.200800012).
- 6 A self-rechargeable and flexible polymer solar battery.
S. Bereznev, P. Birke, G. Dennler, D. Fichou, M. Krebs, A. Labouret, C. Lungenschmied, A. Marchenko, D. Meissner, E. Melikov, J. Méot, A. Meyer, T. Meyer, H. Neugebauer, N. S., Sariciftci, S. Taillemite, T. Wöhrle, *Solar Energy* **2007**, *81*, 947.
- 7 Solution processed n-type organic field-effect transistors with high on/off current ratios based on fullerene derivatives.
S. P. Tiwari, E. B. Namdas, V. Ramgopal Rao, D. Fichou and S. G. Mhaisalkar, *IEEE Letters* **2007**, *28*, 880.
- 8 Steady-state and transient photocurrents in rubrene single crystal free-space dielectric Transistors.
N. Mathews, D. Fichou, E. Menard, V. Podzorov, and S. G. Mhaisalkar, *Appl. Phys. Lett.* **2007**, *91*, 212108.
- 9 Rectangular nanostructuring of Au(111) surfaces by self-assembly of size-selected thiocrown ether macrocycles.
A. Nion, P. Jiang, A. Popoff and D. Fichou, *J. Am. Chem. Soc.* **2007**, *129*, 2450.
- 10 Hole-vibronic coupling in oligothiophenes: impact of backbone torsional flexibility on relaxation energies.
D. A. da Silva Filho, V. Coropceanu, D. Fichou, N.E. Gruhn, T. G. Bill, J. Gierschner, J. Cornil and J-L. Brédas, *Phil. Trans. R. Soc. A* **2007**, *365*, 1435.
- 11 Nanoscale surface morphology and rectifying behaviour of a bulk single crystal organic semiconductor.
E. Menard, A. Marchenko, V. Podzorov, M. E. Gershenson, D. Fichou, J. A. Rogers, *Advanced Materials* **2006**, *18*, 1552.

- 12** Time-resolved observation of fracture events in mica single crystals using scanning tunneling microscopy.
A. Marchenko, D. Fichou, D. Bonamy, and E. Bouchaud, *Appl. Phys. Lett.* **2006**, *89*, 093124.
- 13** Rotational polymorphism in 2-naphthalenethiol self-assembled monolayers.
P. Jiang, A. Nion, A. Marchenko, L. Piot, D. Fichou, *J. Am. Chem. Soc.* **2006**, *128*, 12390.
- 14** Structural evolution of hexa-peri-hexabenzocoronene adlayers on *n*-pentacontane template monolayers.
L. Piot, J. Wu, A. Marchenko, K. Müllen, D. Fichou, *J. Am. Chem. Soc.* **2005**, *127*, 16245.
- 15** Synthesis and self-assembling properties of triazatrinaphthylene, a new star-shaped prochiral derivative with C₃ symmetry.
N. Saettel, N. Katsonis, A. Marchenko, M-P. Teulade-Fichou, D. Fichou, *J. Mater. Chem.* **2005**, *15*, 3175.
- 16** Adsorption and self-assembly of C₇₀ molecules at the Au(111)/*n*-tetradecane interface studied by scanning tunneling microscopy.
N. Katsonis, A. Marchenko and D. Fichou, *Adv. Mater.* **2004**, *16*, 309.
- 17** Substrate-induced pairing in 2,3,6,7,10,11-hexakis-undecalkoxy-triphenylene self-assembled monolayers on Au(111).
N. Katsonis, A. Marchenko and D. Fichou, *J. Am. Chem. Soc.* **2003**, *125*, 13682.
- 18** Long-range self-assembly of a polyunsaturated linear organosilane at the *n*-tetradecane/Au(111) interface studied by STM.
A. Marchenko, N. Katsonis, D. Fichou, C. Aubert, and M. Malacria, *J. Am. Chem. Soc.* **2002**, *124*, 9998.
- 19** Nanoscale STM detection of photocurrents in organic semiconductors.
D. Fichou, F. Charra, and A. Gusev, *Adv. Mater.* **2001**, *13*, 555.
- 20** Coulomb blockade transport in single crystal organic thin film transistors.
W.A. Schoonveld, J. Wildeman, D. Fichou, P.A. Bobbert, B.J. van Wees, T.M. Klapwijk, *Nature* **2000**, 977.

SYNTHESIS, CHARACTERIZATION AND INKJET PRINTING OF FUNCTIONAL MATERIALS

Ulrich S. Schubert

Laboratory of Organic and Macromolecular Chemistry,
Friedrich-Schiller-University Jena,
Humboldtstr. 10, 07743 Jena, Germany.
ulrich.schubert@uni-jena.de; www.schubert-group.de

Abstract

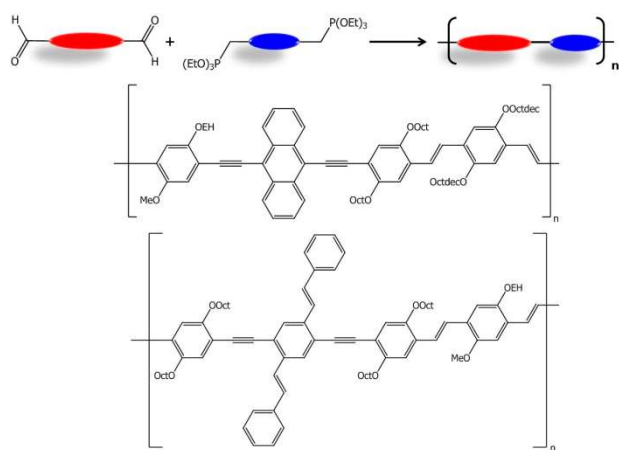
Inkjet printing is an interesting tool for scientific research that enables on demand deposition of functional materials. It can be used for the rapid and easy film preparation in a combinatorial approach. Upon variation of the ink composition or the printing parameters, a fast characterization of the film properties, including optical and topography, can be performed. In this way, structure-property relationships between ink composition, printing parameters and film qualities can be identified. In combination with the synthesis of various promising conjugated polymer materials, the loop from materials research to functional device properties can be closed.

1. Introduction

Printing techniques, such as inkjet printing, are interesting alternatives to conventional photolithography for the production of electronics.^[1] The advantage of printing lies in the ease of mass production, low cost and flexibility. Compared to other printing techniques (*e.g.* screen printing), inkjet printing lacks production speed. However, the flexibility of inkjet printing makes it very well suited for rapid prototyping applications. In addition, it allows the use of inviscid fluids, like dilute polymer solutions or suspensions without binder added. Inkjet printing has been used to transfer digital documents into high-resolution copies on paper, but today it is also used as an advanced dispensing technique for scientific research,^[2] for example organic photovoltaics,^[3] flexible batteries,^[4] field effect transistors (FET) and thin film transistors (TFT),^[5,6] sensor arrays^[7] and radio frequency identification (RFID) tags.^[8] Amongst the current challenges in the inkjet technology one particular example is the continuous drive to improve its resolution: scientists are manipulating droplets in order to make them smaller in order to produce features with a finer resolution.^[9,10]

2. Synthesis of conduction polymers

Conjugated polymers are widely used in organic electronics (e.g., solar cells or OLEDs). Their structures can be manipulated chemically and by this manner also their material properties can be changed. Therefore, a wide range of optoelectronic properties could be achieved with functional conjugated polymers, using e.g. the prominent examples polythiophene, polyphenylenevinylenes (PPVs), and poly-phenylene-ethynyls (PPEs). Poly(*p*-phenylene-ethynylene)-*alt*-poly(phenylenevinylene)s (PPE-PPVs) combines the properties of the well-known PPVs and PPEs. The introduction of the rigid acetylene units into the PPV backbone lead to polymers with outstanding optoelectronic properties.^[11] The PPE-PPVs are synthesized *via* the Horner-Wadsworth-Emmons (HWE) olefination reaction from the corresponding luminophoric dialdehydes and bisphosphonate esters (Scheme 1). Only short reaction times are required to obtain polymers with high molar masses. The synthetic approach is modular, therefore different building blocks can be combined in order to achieve polymers with tailor-made properties. The systematic variation of the different monomers, for example introduction of anthracene^[12] or styryl sidegroups^[13], and of their position in the polymer chain was applied to adjust the optical properties of these polymers. Already small changes in the structure can lead to rather large differences of the optoelectronic properties, which result in different efficiencies in solar cells.^[14]



Scheme 1. Schematic presentation of the modular synthesis of PPE-PPVs (top); schematic representation of two exemplary polymer structures (bottom).

Inkjet printing of thin film libraries allows a combinatorial workflow from thin film preparation to structure-property relation investigations.^[15] With this approach, the

influence of ink composition, substrate properties, and different printing parameters to the film properties can be studied in a fast and reproducible way. Hereto we have inkjet printed libraries of various PPE-PPV copolymers and investigated their optical properties as a function of film thickness.^[16,17] By investigation of the film formation and the optical properties, these materials can be used for optoelectronic devices.

3. LED's and organic solar cells

The impact of a droplet has a significant influence on the final printed feature, but also of great concern is a frequently observed in-homogeneous drying effect of liquid droplets on a non-absorbing substrate, the so-called “coffee drop” effect.^[18,19] The solute that is present in the solution deposits near the boundary of inkjet printed droplets – this behavior is similar comparing to drops of coffee that are spilt on the table. When using the technique of inkjet printing, for example for the application of organic light emitting diodes (OLED), this effect should be minimized for correct device functionality.^[20] Therefore, much research has been conducted to prevent the coffee ring effect, for example by applying an increased substrate temperature, in order to stimulate solvent evaporation, which subsequently minimizes line or film bleeding,^[21] and by combining a high and low boiling solvent, which reduces the high evaporation rate at a liquid feature's edge (see Figure 1).^[22]

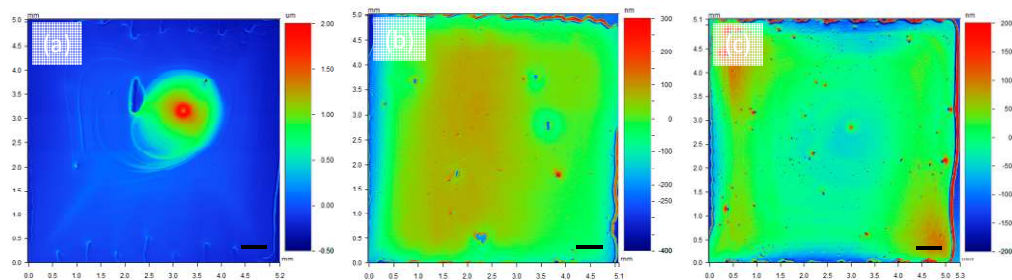


Figure 1. Improvement of film formation of inkjet printed films: (a) printed from a single solvent, (b) printed from a solvent mixture and (c) same as (b) but with additional plasma treatment of the glass substrate prior printing. The scale bar represents 500 μm.

For photovoltaic applications we prepared homogeneous films by inkjet printing of polymer:fullerene blends.^[23] Therefore, two polymers and two fullerene derivatives were studied in various blend ratios in a combinatorial screening. Inkjet printing was used as a precise and fast dispensing technique for the preparation of thin film libraries. Morphological and optical properties of the inkjet printed films were investigated and compared to other deposition techniques, like spin-coating. It was found that inkjet printing

allowed a combinatorial workflow from film preparation to property investigations. A selection of the inkjet printed polymer:fullerene samples are currently being tested for their performance in organic solar cells.

4. Inkjet printing of functional materials

In order to achieve the multi-micron feature resolution typically associated with rapid prototyping techniques, inkjet printing was considered as a synthesis tool. This new technique is also called reactive inkjet printing, and is a precise method for building up small structures using certain reactive materials.^[24] Towards this aim, the synthesis of polyurethane-based materials was seen as a particularly illustrative example. The chemistry of this involves the preparation of two separate inks, one containing a diol, and the second containing a diisocyanate. In our experiments we have used hydroxyl-terminated telechelic poly(propylene glycol) (PPG) as diol and isophorone diisocyanate (IPDI) as diisocyanate. The reactive components were inkjet printed from separate nozzles. The droplets merge on the substrate and polymerize in-situ to form a solid polyurethane (PU) structure within three minutes. The addition of a fluorescent dye allowed for the investigation of the system with confocal laser scanning fluorescence microscopy, and showed the homogeneous mixing of both solutions on the substrate. This fast, in-situ polymerization reaction that forms solid PU at the surface opens a new route for rapid-prototyping and multi-micron-PU structures on surfaces. The resulting structures were measured using optical profilometry, as shown in Figure 2.

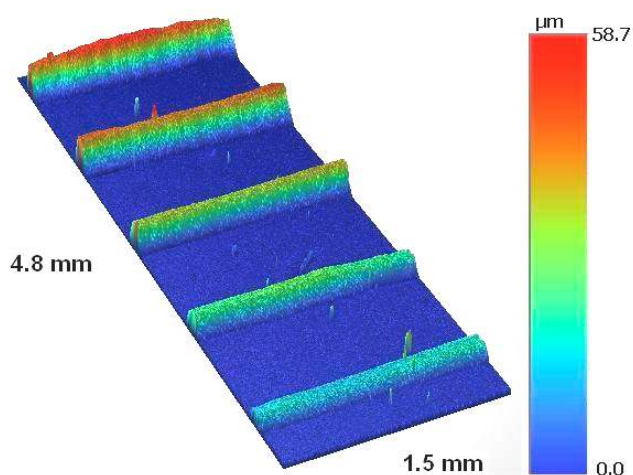


Figure 2. Five inkjet printed lines of in-situ formed polyurethane. From top to bottom, the parallel lines consist of an increased number of layers, where each layer consists of two print runs from both reactants. From top to bottom the number of layer decreases from 5 to 1, respectively. Reprinted from Ref. [24].

Furthermore, inkjet printers have been used in several studies in order to produce a series of equal-sized droplets, which allowed the reduction of errors in the measurements and significantly increased the experimental reproducibility.^[25] For example, the deposition behavior of uniformly sized silica particles in drying aqueous droplets has been investigated to gain an improved understanding of the coffee drop effect.^[19] When aqueous droplets consisting of monomodal silica microspheres were inkjet printed, the 'coffee ring' effect was observed. However, the exact location of the microspheres strongly depends on their size: large particles sediment further away from the contact line than small particles, hence the 'coffee rings' from large particles were smaller than those from small particles. When the contact angle is increased to 90° or higher, the discrimination of particle size vanishes and all particle sizes show a similar dried droplet diameter on a substrate with a low surface energy (Figure 3). This observation of a self-organization is very important for the fabrication of photonic crystals. These materials show interesting properties for manipulation of light due to their photonic bandgaps.^[26]

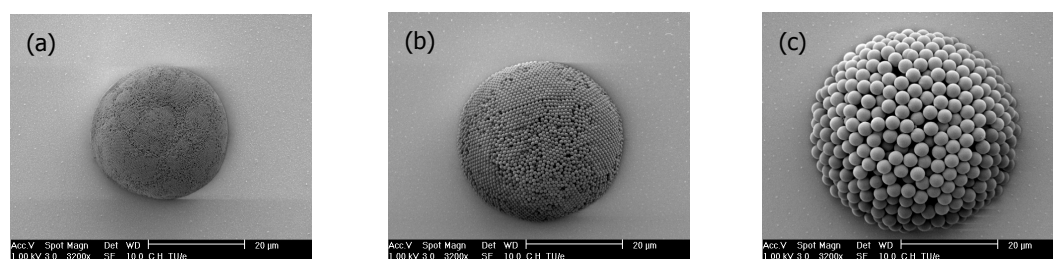


Figure 3. Scanning Electron Microscopy (SEM) images of silica particles with a particle diameter of 0.33 μm (a), 1 μm (b), and 3 μm (c) on OTS coated glass slides. Reprinted from Ref. [19].

5. Summary

The main advantage of printing lies in its flexibility, low cost, ease of processing and its potential for mass production. Therefore, inkjet printing is an attractive tool for combinatorial screening of functional materials for printed electronic applications. Inkjet printers can be used for the preparation of well-defined thin-film libraries that allow a fast and efficient characterization of their optical and morphological properties. Upon variation of the ink composition or the printing parameters, the structure-property relationship between ink and processing can be identified, which is important for functional device preparation in plastic electronic applications. In combination with the in-house synthesis of various promising conjugated polymers, we can close the loop from materials research to functional device properties.

6. Acknowledgements

The Dutch Polymer Institute and the EU is greatly acknowledged for the financial support.

7. References

- [1] B.-J. de Gans, P. C. Duineveld, U. S. Schubert, *Adv. Mater.* 2004, 16, 203.
- [2] E. Tekin, P. J. Smith, U. S. Schubert, *Soft Matter* 2008, 4, 703.
- [3] Special issue on “Solar Cells”, *J. Mater. Chem.* 2009, 19, 5261 (eds. R. A. J. Jansen, M. Grätzel).
- [4] C. C. Ho, K. Murata, D. A. Steingart, J. W. Evans, P. K. Wright, *J. Micromech. Microeng.* 2009, 19, 094013.
- [5] S. Gamerith, A. Klug, H. Schreiber, U. Scherf, E. Moderegger, E. J. W. List, *Adv. Funct. Mater.* 2007, 17, 3111.
- [6] D. Kim, S. Jeong, S. Lee, B. Kyun Park, J. Moon, *Thin Solid Films* 2007, 515, 7692.
- [7] V. R. Marinov, Y. A. Atanasov, A. Khan, D. Vaselaar, A. Halvorsen, D. L. Schulz, D. B. Chrisey, *IEEE Sens. J.* 2007, 7, 937.
- [8] V. Subramanian, J. M. J. Fréchet, P. C. Chang, D. Huang, J. B. Lee, S. E. Molesa, A. R. Murphy, D. R. Redinger, S. K. Volkman, *Proc. IEEE* 2005, 93, 1330.
- [9] T. H. J. van Osch, J. Perelaer, A. W. M. de Laat, U. S. Schubert, *Adv. Mater.* 2008, 20, 343.
- [10] H. Meier, U. Löffelmann, D. Mager, P. J. Smith and J. G. Korvink, *Phys. Status Solidi A*, 2009, 206, 1626.
- [11] E. Tekin, H. Wiljaars, E. Holder, D. A. M. Egbe, U. S. Schubert, *J. Mater. Chem.* 2006, 16, 4294.
- [12] A. Wild, D. A. M. Egbe, E. Birckner, V. Cimrová, R. Baumann, U.-W. Grummt, U. S. Schubert, *Polym. Sci. A: Polym. Chem.* 2009, 47, 2243.
- [13] D. A. M. Egbe, E. Tekin, E. Birckner, A. Pivrikas, N. S. Sariciftci, U. S. Schubert, *Macromolecules* 2007, 40, 7786.
- [14] S. Günes, A. Wild, E. Cevik, A. Pivrikas, D. A. M. Egbe, U. S. Schubert, *Sol. Energy Mater. Sol. Cells* 2010, in press.
- [15] B.-J. de Gans, E. Kazancioglu, W. Meyer, U. S. Schubert, *Macromol. Rapid Commun.* 2004, 25, 292.
- [16] E. Tekin, H. Wijlaars, E. Holder, D. A. M. Egbe, U. S. Schubert, *J. Mater. Chem.* 2006, 16, 4294.
- [17] A. Teichler, R. Eckardt, C. Friebe, J. Perelaer, U. S. Schubert, submitted.
- [18] R. D. Deegan, O. Bakajin, T. F. Dupont, G. Huber, S. R. Nagel, T. A. Witten, *Phys. Rev. E* 2000, 62, 756.
- [19] J. Perelaer, P. J. Smith, C. E. Hendriks, A. M. J. van den Berg, U. S. Schubert, *Soft Matter* 2008, 4, 1072.
- [20] D. B. van Dam, J. G. M. Kuerten, *Langmuir* 2008, 24, 582.
- [21] J. Perelaer, B.-J. de Gans, U. S. Schubert, *Adv. Mater.* 2006, 18, 2101.
- [22] E. Tekin, B.-J. de Gans, U. S. Schubert, *J. Mater. Chem.* 2004, 14, 2627.
- [23] A. Teichler, R. Eckardt, C. Friebe, J. Perelaer, M. Morana, C. J. Brabec, U. S. Schubert, manuscript in preparation.
- [24] P. Kroeber, J. T. Delaney, J. Perelaer, U. S. Schubert, *J. Mater. Chem.* 2009, 19, 5234.
- [25] J. Perelaer, P. J. Smith, E. van den Bosch, S. S. C. van Grootel, P. H. J. M. Ketelaars, U. S. Schubert, *Macromol. Chem. Phys.* 2009, 210, 495.
- [26] S. H. Kim, H. S. Park, J. H. Choi, J. W. Shim, S. M. Yang, *Adv. Mater.* 2010, 22, 946.

Prof. Dr. Ulrich S. Schubert

Laboratory of Organic and Macromolecular Chemistry
Friedrich-Schiller-Universität Jena & Dutch Polymer Institute
Humboldtstr. 10, D-07743 Jena, Germany
Tel.: +49 (0)3641 9482-00, Fax: +49 (0)3641 9482-02
E-Mail: ulrich.schubert@uni-jena.de,
<http://www.iomc.uni-jena.de>; <http://www.researcherid.com/rid/B-5777-2009>
Laboratory of Macromolecular Chemistry and Nanoscience
Eindhoven University of Technology & Dutch Polymer Institute
P.O. Box 513, NL-5600 MB Eindhoven, The Netherlands



8. Short curriculum vitae

Ulrich S. Schubert was born in Tübingen/Germany in 1969. He studied chemistry and Biochemistry at the Universities of Frankfurt, Bayreuth (both Germany) and Richmond (USA). His Ph.D. work was performed under the supervision of Professor Eisenbach (Bayreuth, Germany) and Professor Newkome (Florida, USA). In 1995, he obtained his doctorate with Prof. Eisenbach. After a postdoctoral training with Professor Lehn (Nobel laureate 1987) at the Université Strasbourg (France), he moved to the Technische Universität München (Germany) to obtain his habilitation in 1999 (with Professor Nuyken). From 1999 to spring 2000, he held a temporary position as a professor at the Center for Nano-Science (CeNS) at the Ludwig-Maximilians-Universität München (Germany). From June 2000 to March 2007, he was Full Professor at the Eindhoven University of Technology (Chair for Macromolecular Chemistry and Nanoscience), combined with several scientific and management functions at the Dutch Polymer Institute (2003-2005: program manager of the cluster "High-throughput experimentation" and member of the management team DPI; 2005-2010: scientific chairman of the cluster HTE/CMR and member of the board of the DPI cooperate research). Since April 2007, he is Full Professor for Organic and Macromolecular Chemistry (Chair) at the Friedrich-Schiller-Universität Jena (Germany; since October 2007 also director of the Institute for Organic and Macromolecular Chemistry as well as since February 2008 scientific director ("Sprecher") of the "Forschungsschwerpunkt Innovative Materialien und Technologien" of the Friedrich-Schiller-Universität Jena). In addition, he is Part-time Professor at the Eindhoven University of Technology (up to 6/2010) as well as scientific chairman of the DPI cluster HTE.

His awards include the Bayerischer Habilitations-Förderpreis, the Habilitandenpreis of the GDCh (Fachgruppe Makromolekulare Chemie), the Heisenberg-Stipendium of the DFG and the Dozenten-Stipendium of the Fonds der Chemischen Industrie. In January 2004, he was awarded with the VICI award by NWO (1.25 M€ price) and with the Jan Pieter Lemstra Innovation award of the Dutch Polymer Institute in 2009. In 2010, he will receive the International Biannual Belgian Polymer Group Award. He is currently member of the Board of the Center for NanoMaterials (cNM) Eindhoven, member of the Editorial Advisory Board of *Soft Matter*, *Macromol. Rapid Commun.*, *J. Comb. Chem.*, *Macromol. Chem. Phys.*, *Polymer Chem.*, *e-Polymers*, *QRAR & Comb. Chem.*, *Design. Monomers Polym.* and *J. Polym. Sci.: Part A: Polym. Chem.*, member of the CeNS in München as well as member of the Kuratorium of ENAS/Fraunhofer Chemnitz and DKI/Darmstadt. He acted as Guest Editor for five special issues in *Macromol. Rapid Commun.* and *J. Comb. Chem.*, edited two books and wrote one textbook on "Modern terpyridine chemistry".

The major focus of his research interest relates to tailor-made functional macromolecules, supramolecular materials, metal-containing polymers, organic heterocyclic chemistry, combinatorial material research, inkjet printing, bio-based/bio-inspired materials, bioactive surfaces and nanoscience.

Total number of referred publications: >370, h-index: 49, total numbers of citations: >8500. Web-of-Science ranking in Chemistry: #301, in Materials: #710. External funding 2000-2009: >15 M€.

Additional activities/interests

Concerts as clarinet player in chamber music ensembles and orchestra (e.g. Alte Oper Frankfurt, Markgräfliches Opernhaus Bayreuth, Prinzregenten-Theater München, Gasteig München, Philharmonie Bratislava, Tampa Bay Performing Art Center Florida): chamber music courses with Prof. Alfons Kontarsky, Hagen-String-Quartett, Abegg-Trio, Jan Doormann (Soloclarinet Staatskapelle Weimar), Prof. Francois Benda (Musikhochschule Basel) and others.

Funder and artistic director of the concert series "Forum Junger Musiker" and the "INTERNATIONALE JUNGE ORCHESTERAKADEMIE", artistic director ("Intendant") of the Bayreuther Osterfestival (www.osterfestival.de)

Organization of over 320 benefit concerts for children with cancer in Germany, the Netherlands, Austria and the Slovak Republic (raising > 800000 € for dedicated projects), production of 16 benefit CD's.

Establishment of a foundation (Kultur- und Sozialstiftung), "Vorstandsvorsitzender" (chairman of the board).

ORGANIC BIOELECTRONICS

- to regulate biology, in vitro and in vivo

Magnus Berggren*, Klas Tybrandt*, Karin Larsson**, Maria Bolin*, Kristin Persson*, Karl Svennersten**, Daniel Simon*, Edwin Jager*, Agneta Richter-Dahlfors**

*Organic Electronics, ITN-Campus Norrköping, Linköping University, Sweden

**Swedish Medical Nanoscience Center, Karolinska Institutet, Solna, Sweden

Signal translation across the biology-technology interface has been a long-standing challenge all since the early experiments of Luigi Galvani in the late 18th century. Charge polarisation at metal-biology interfaces has widely been used to sense or induce signalling in systems of various eukaryotic species. In organic electronic materials the signal carrier can include ions, electrons, peptides etc, which makes them promising to transduce bio-identical signals into electronic ones, and vice versa.

We report and review progresses achieved during the last years in our group regarding using organic electronics to regulate physiology and growth, of epithelial and neurons, and as a prosthesis technology to regulate sensory functions of mammals.

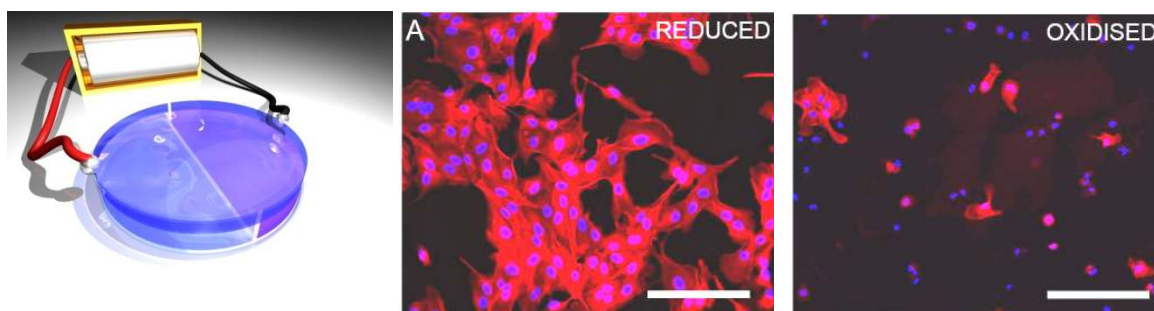


Figure 1. Left, an illustration of ESS manufactured along the floor of a Petri dish. Right, Fluorescence microscopy images of MDCK cells grown along the PEDOT:Tosylate ESS pads, switched to the reduced and oxidised state, respectively. Cells adhere in much greater density and forms tissues only along the reduced electrode [1]

In one technology, electronic surface switches (ESS) have been explored as a dynamic cell hosting surface, enabling regulation of the seeding, spreading, proliferation and also the release of cells and tissues. The ESS devices are composed of electrode pads based on PEDOT:Tosylate or similar materials. As the electrochemical state of these electrodes is changed, the binding characteristics for matrix proteins are controlled. This dictates the conformation of the matrix proteins, which further regulates the binding and spreading of cells along the surface [1]. Those pads can also be incorporated within the channel of electrochemical transistors, thus enabling gate- and drain-addressed control of the adhesion

and growth of cells. Along this transistor channel, electrochemical gradients are formed as the gate and drain contacts are electrically biased. As cells are seeded along these channels they mimic the gradients along the channel and forms stratified structures on one side which gradually converts into tight junction tissues at the other side [2]. We have also explored using ESS devices to achieve electronics control of the release of grown tissues.

In a second technology, we utilise the combined ionic and electronic transport properties of PEDOT:PSS to electronically control the release of neurotransmitters and cations to regulate physiology, *in vitro*, and sensory function, *in vivo*. A source reservoir, containing the biomolecule to be delivered, is connected via a PEDOT:PSS channel with a receiving target reservoir, which contains the cells to be stimulated and also associated growth media. This organic electronic ion pump (OEIP) includes two or more addressing electrodes to enable electrophoretic pumping of ions from the source to the target reservoir [3]. The PEDOT:PSS channel, connecting the two reservoirs, has been electrochemically over-oxidised, which renders the PSS phase ionically conducting but PEDOT electronically insulating.

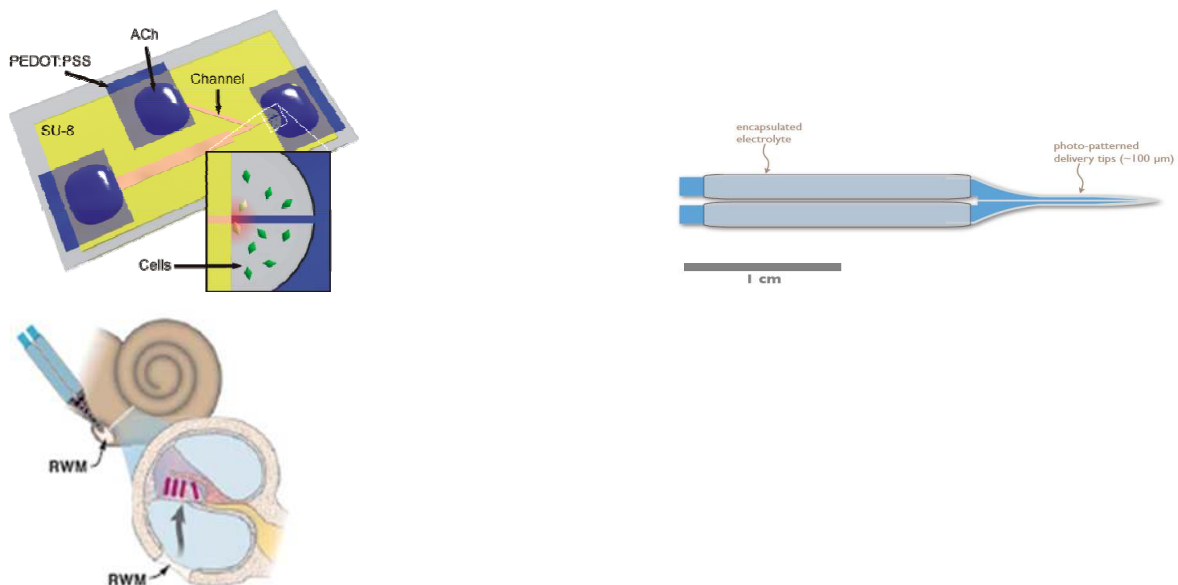


Figure 2. Left: the miniaturised OEIP device [4]. Middle: the pen-shaped OEIP for *in vivo* applications, such as pumping to pump Glutamate in order to regulate the hair cells inside the cochlear (right) [5].

This device can be miniaturised to enable regulation of intracellular signalling at very high spatiotemporal resolution. Further, the device can also be shaped into a pen-like device for *in vivo* applications. In this configuration the device has been applied to the round window

membrane at the cochlear. By electronically pumping Glutamate the sensitivity of the hair cells are regulated, thus enabling electronic control of the sound sensory function.

References

- [1] K. Svennersten, M. H. Bolin, E. W. H. Jager, M. Berggren, A. Richter-Dahlfors, *Biomaterials* **2009**, *30*, 6257.
- [2] M. H. Bolin, K. Svennersten, D. Nilsson, A. Sawatdee, E. W. H. Jager, A. Richter-Dahlfors, M. Berggren, *Advanced Materials* **2009**, *21*, 4379.
- [3] J. Isaksson, P. Kjäll, D. Nilsson, N. Robinson, M. Berggren, A. Richter-Dahlfors, *Nature Materials* **2007**, doi:10.1038/nmat1963.
- [4] K. Tybrandt, K. C. Larsson, S. Kurup, D. T. Simon, P. Kjall, J. Isaksson, M. Sandberg, E. W. H. Jager, A. Richter-Dahlfors, M. Berggren, *Advanced Materials* **2009**, *21*, 4442.
- [5] D. T. Simon, S. Kurup, K. C. Larsson, R. Hori, K. Tybrandt, M. Goiny, E. H. Jager, M. Berggren, B. Canlon, A. Richter-Dahlfors, *Nature Materials* **2009**, *8*, 742.

Part II:

OLEDs and related 1

POLYMER-BASED WHITE-EMITTING OLEDs: FUNCTION AND PERSPECTIVES

D. Neher* and S. Bange⁺

*University of Potsdam, Institute for Physics and Astronomy, Karl-Liebknecht-Str. 24-25, 14476 Potsdam-Golm, Germany

⁺ present address: Department of Physics and Astronomy, University of Utah, 115 South 1400 East # 201, Salt Lake City, UT 84112-0830, USA

The growing demand for efficient lighting has triggered intense research on solid state white light sources. One attractive approach is the realisation of large area devices with white-emitting polymers. Recently, various strategies to attain white emission from single polymers have been developed. For the commercialisation of such devices, several problems regarding the efficiency and the colour stability have to be solved.

We investigated the role of charge density, notably hole density, in determining the emission spectrum and performance of white-emitting polymer diodes fabricated from the conjugated copolymer shown below. The treatment involved a rate equation approach for the effective emission zone assuming that trapping of electrons on the deep trap formed by red chromophores can be treated in terms of first-order trapping rates despite the energetic disorder present in these amorphous polymers. The polymers investigated here are especially suited to test the predictions made by the proposed model, the dominant hole currents allowing for a significant simplification of the equations involved. The model's predictions concerning the temperature dependence of the emission spectrum are consistent with experimental results over the whole range of operating voltages. Electrical conditioning effects of the optical device behaviour were observed and could be consistently explained using the proposed model by relating the conditioning to an enhancement of the hole injection barrier at the anode/polymer interface during operation. Most notably, these effects are quantitatively explained by the model without involving free parameters. Being based on a faithful decomposition of the emission spectrum into the contributions of each chromophore, the model additionally allowed for a quantitative analysis of the electron trapping process. In variance with a previous analysis, trapping by diffusive electron motion was found to be insignificant for electric fields larger than 10^6 V/m. Based on an effective lattice hopping formalism, we calculated that in an applied electric field, electrons move between conjugated segments that on average comprise four

monomer units. The low contribution of diffusion-driven electron trapping is found to be accordance with the notion of diffusion in quasi one-dimensional percolation pathways.

In addition, detailed information was obtained on the efficiency of charge injection into the active layer. Though the energy scheme shown in Figure 3 suggest that an Ohmic contact forms between the polymer and PEDOT:PSS, a significant barrier for hole injection was revealed. Also, the detailed study of the electron transport properties and the current in electron-only devices showed that the electron current is injection limited. Without doubt, the development of novel strategies to reduce these injection barriers will further booster the efficiency of such white-emitting polymer OLEDs.

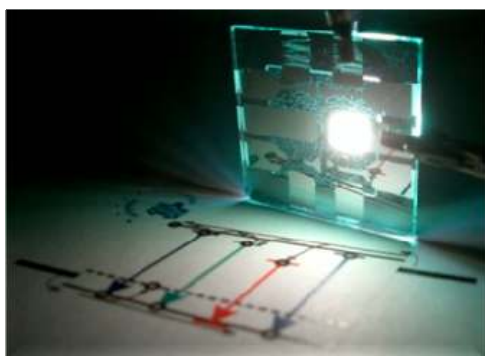
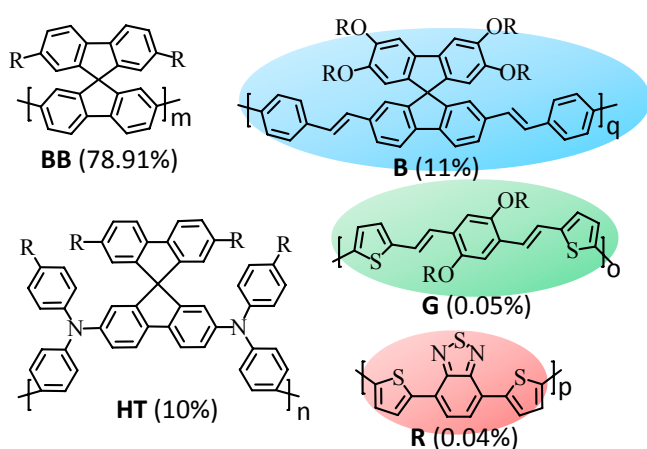


Figure 1: Chemical structure of the white-emitting polymer studied here and a polymer white-emitting OLED driven at high brightness.

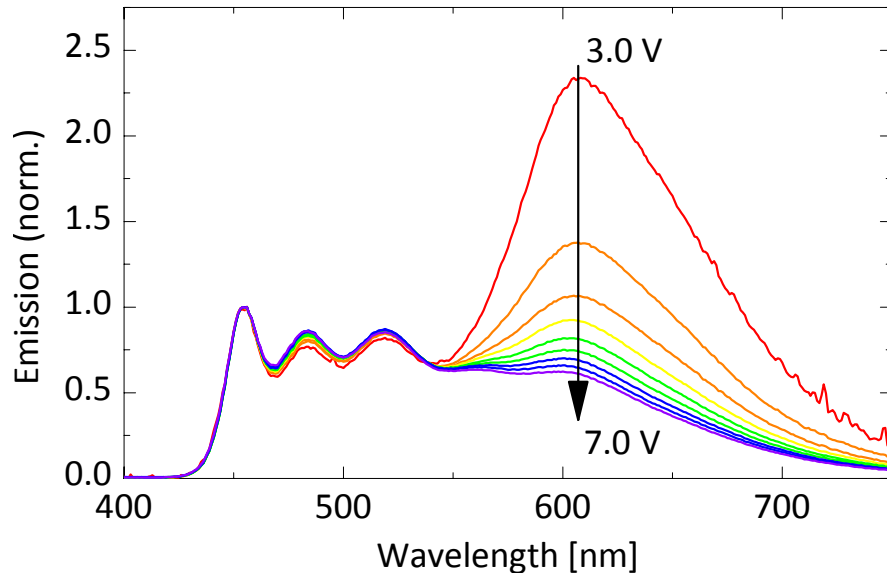


Figure 2: EL spectrum of a white-emitting polymer OLED measured at different bias.

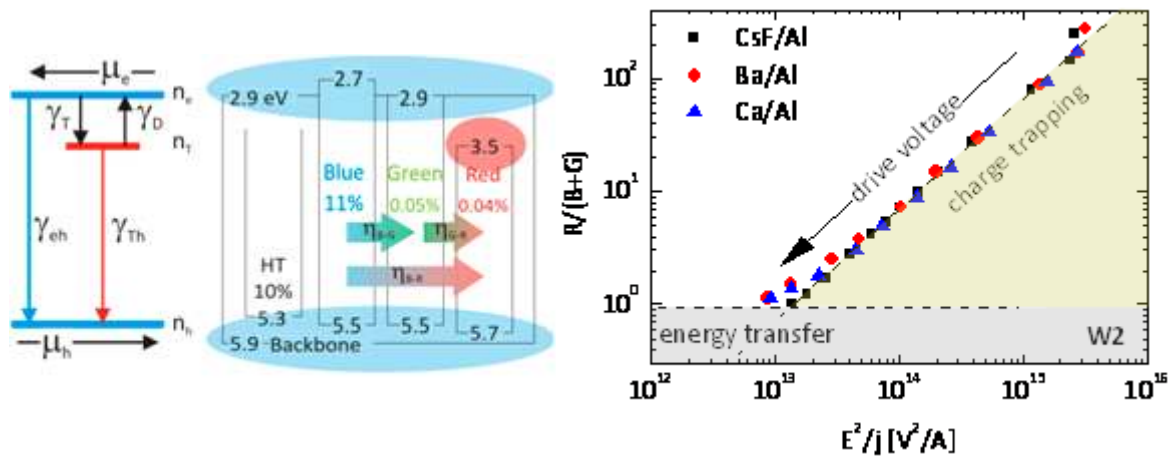


Figure 3: Scheme of the rate model to describe the pronounced color shift in the studied WOLED and red/blue emission ratio parametric in the electric field E and current density j .

BIOGRAPHIC DATA OF PROFESSOR DIETER NEHER

Dieter Neher studied physics at the Johannes-Gutenberg-University in Mainz, Germany. He gained his PhD with Prof. Dr. Wegner at the MPI for Polymer Research in Mainz. From 1990-1992 he was postdoc with Prof. G. Stegeman at the Optical Sciences Centre in Tuscon and at the Centre for Research in Electrooptics and Lasers



in Orlando. He joined again the group of Prof. G. Wegner as a group leader, with focus on electrooptical phenomena in polymers. He entered his current position as Professor of Soft Matter Physics at the Institute for Physics at the University of Potsdam in November 1998. Current research interests are the optical, electrical and optoelectronic properties of polymers, with special focus on multicomponent systems with well-controlled structural characteristics.

RECOMBINATION VIA CHARGE TRANSFER EXCITONS IN POLYMER/FULLERENE BLENDS: THE ROLE OF MORPHOLOGY AND MOLECULAR CONFORMATION

M. HALLERMANN; E. DA COMO*; J. FELDMANN

Photonics and Optoelectronics Group, Department of Physics and CeNS, Ludwig-Maximilians-University, Amalienstraße 54; 80799 Munich; Germany

Blends between conjugated polymers and fullerene derivatives constitute a promising material combination for organic photovoltaics with current efficiencies of up to 6.77%. To make this technology competitive, a thorough understanding of loss mechanisms in carrier photogeneration is mandatory. Recombination appears to be a major limit, although a clear picture on the electronic states and molecular parameters controlling this process is still lacking.

In this communication, we unravel the origin of charge transfer excitons (CTE) [1] forming in such blends and we discuss their importance for recombination processes after the initial photoinduced charge transfer. We show that CTE photoluminescence can be observed in several material combinations. For example, in conjugated polymers such as poly(3-hexylthiophene) and poly(phenylenevinylene) when blended with the fullerene acceptor PCBM. By combining transmission electron microscopy and photoluminescence spectroscopy, we show that CTE recombination is only slightly influenced by the mesoscopic morphology. Surprisingly, large differences in CTE recombination have origin in the polymer chain conformation. [2] We discuss new insights on limiting recombination via CTE in polymer/fullerene solar cells.

[1] M. Hallermann, S. Haneder, and E. Da Como, *Applied Physics Letters* 93, 053307 (2008).

[2] M. Hallermann, I. Kriegel, E. Da Como, J. M. Berger, E. von Hauff, J. Feldmann, *Advanced Functional Materials*, 19, 3662 (2009).

CURRICULUM VITAE ET STUDIORUM OF ENRICO DA COMO

Personal information

Place of birth: Modena (Italy), May 16th 1978.
Address: Volkartstraße 18, 80634, Munich (Germany)
E-Mail: Enrico.dacomo@physik.uni-muenchen.de
Website: http://www.phog.physik.uni-muenchen.de/people/da_como_enrico/index.html



Present position

Assistant at the Photonics and Optoelectronics group, Department of Physics, Ludwig-Maximilians-University Munich, Germany. www.phog.physik.uni-muenchen.de

Education and scientific appointments

- September 1997 to October 2002: **Laurea in Chemical Physics (equivalent to 5 years Master)**, 110/110 *cum laude*. Department of Chemistry, University of Modena (Italy). (Advisor Prof. F. Momicchioli)
- January 2003 to March 2006: **Ph.D. degree in Chemical Physics** at the Istituto per lo Studio dei Materiali Nanostrutturati, National Research Council, Bologna (Italy) (Advisors Dr. M. Muccini/Prof. A Brillante)
- April 2006 to December 2007: **Postdoc** at the Photonics and Optoelectronics group, Department of Physics, Ludwig-Maximilians-University Munich (Germany).
- Since January 2008: **Assistant in experimental physics** at the Photonics and Optoelectronics group, Department of Physics, Ludwig-Maximilians-University Munich (Germany) and extraordinary member of CeNS.
- August 2008 and August 2009: **visiting scientist** at the Department of Physics, University of Utah, UT (USA).

LOW-COST FABRICATION OF OLED-SUBSTRATES FOR LARGE-AREA LIGHTING: THE APPLICATION OF PRINTING TECHNOLOGIES FOR OLED-SUBSTRATE STRUCTURING

M. HASSELGRUBER¹; U. TODT¹; F. FINGER¹; C. MAY¹; R. BAUMANN²

¹Fraunhofer Institute for Photonic Microsystems (IPMS); Center for Organic Materials and Electronic Devices Dresden (COMEDD); Maria-Reiche-Straße 2; 01109 Dresden; Germany

²PmTUC Chemnitz, Reichenhainer Str. 70, 09126 Chemnitz, Germany

Beside conventional inorganic LEDs, OLEDs are considered as the solid-state-lighting technology for new flat, large-area, and efficient lighting solutions. However, in order to achieve a large market penetration in a segment like lighting, the cost issue of the complete fabrication chain is the major key for commercialisation.

Currently the standard manufacturing process for OLED-Substrates is photolithography, as this is the mayor structuring technology for MEMS, LCD or OLED-Display application. In the field of OLED signage and lighting alternative structuring technologies have the potential for considerable cost saving compared to standard photolithography. This is realized with much less requirements for the structuring resolution of the OLED-substrate layers. A first cost price reduction can be already reached when high resolving LCD lithography equipment would be replaced by less accurate printed-circuit-board lithography equipment. Printing technologies like screen printing or ink-jet are even more cost-effective and capable of providing the structuring of all layers needed for OLED substrates.

The Fraunhofer IPMS has developed a printing process with respect to the requirements of large area OLED substrates. This substrate fabrication process is fully based on the thick film technology screen printing. IPMS has established a screen-printing line for the fabrication of OLED-substrates on Gen.2 glass (470x370mm²). These substrates are used for pilot production of OLED panel for signage and lighting within the Center for Organic Materials and Electronics Devices in Dresden (“COMEDD”, cp. /1/).

The process flow can be seen in the fig. 1. It offers inexpensive and straight forward structuring of the transparent anode (Indium Tin Oxid, ITO), the metal shunt lines (metallization) and the passivation layer. The structuring facilities are installed in a clean room class 10 at the IPMS and include the following setup:

- A handling system, supporting batches of 20 substrates with a substrate size of 370x470mm²
- An automatic screen printer providing a tact time below 1min

- A clean room oven for annealing
- Divers cleaning facilities with mega sonic, ultra sonic and different tenside bathes

Polymer pastes are used as materials for screen print. Contrary to widely used pastes based on glass particles, polymer pastes require lower firing temperatures of $<200^{\circ}\text{C}$, which is essential for sustaining the quality of the ITO-coated glass substrates [2].

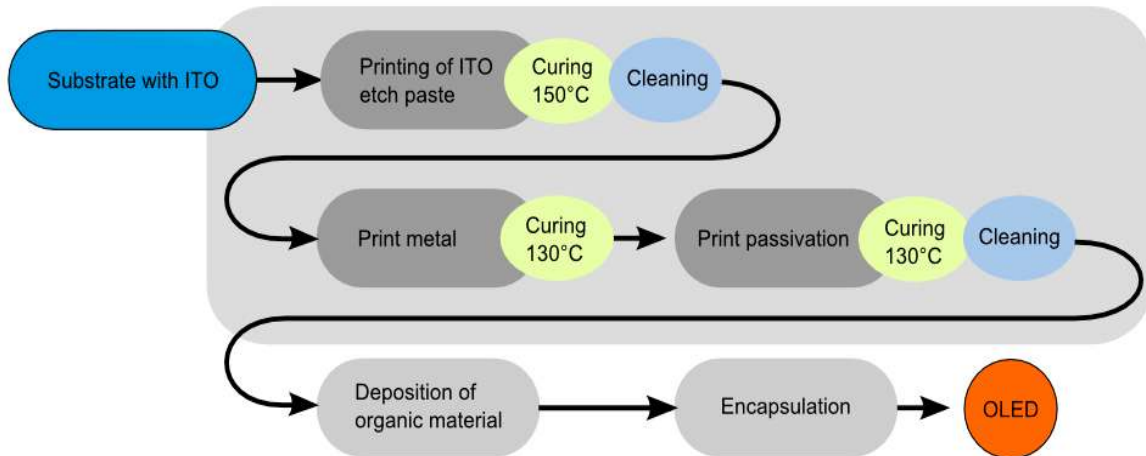


Figure 1: Production flow for the alternative structuring of OLED-substrates via screen printing

The ITO layer on the glass substrate is structured using an ITO-etch paste. The screen-printed etch-paste is activated under nitrogen atmosphere at 150°C . After cleaning of the etch paste, only the structured ITO-layer remains on the glass. The main challenge here concerns the cleanliness of the process: all residues of the paste have to be removed without damaging the ITO-surface. Advantages are the abdication of wet etching processes, low facility costs and high tact time. With the setup of paste and printer a resolution of $100\mu\text{m}$ for line and space is feasible. No change of the ITO itself concerning surface roughness or electrical parameters due to the structuring process has been observed.

In a second step, contact lines and a metal grid are printed upon the anode to adjust the insufficient sheet resistance of the ITO-layer. The silver filled polymer paste is about $10\text{-}20\mu\text{m}$ thick, which is much higher then common conductive thin films, but required for an adequate sheet resistance of the metallisation. The development of this process step also focused on the contact resistivity to the underlying ITO. This should be as good or better than $30\text{m}\Omega/\text{mm}^2$ which is state-of-the-art for lithographic structured metallisation. With the

current setup, a contact resistivity of $26\text{m}\Omega/\text{mm}^2$ has been reached. The sheet resistance is about $22\text{m}\Omega/\square$ (@ $8\mu\text{m}$ mean thickness). Lines and spaces of about $150\mu\text{m}$ can be printed.

In the last step a passivation layer is added that softens the edges of the metallization and prevents shortcuts to the cathode or organic thin film layers. The screen printed passivation has a shape angle of $<10^\circ$ which enables the thin organic layers to be deposited without ripping. The thickness of the passivation is about $20\mu\text{m}$. Both the metallization and the passivation have to be heated at 130°C for about 1h to expel the solvents.

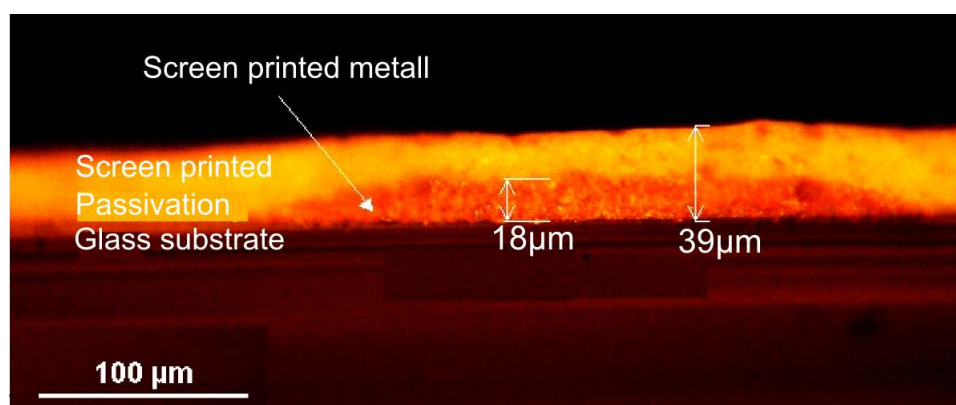


Figure 2: lateral picture of the screen printed layers of an OLED substrate

With the current setup, the manufactured OLEDs on screen printed substrates reach performance parameters comparable to substrates structured by lithography as can be seen in the table below. Especially driving voltage and luminous efficacy (indicator for appropriate anode and metallisation parameters) as well as the reverse current density (an indicator for the quality of the passivation) are as good as on state-of-the-art OLED substrates.

Driving voltage [V] @ 1000 cd/m²			
Substrate type	Min	Typ	Max
Lithografic	2,55	2,62	2,68
Screen printed	2,39	2,60	2,74

Revers current [mA/cm²] @ -5V			
	Min	Typ	Max
Lithografic	0,0003	0,12	0,87
Screen printed	0,04	0,24	0,88

Tab. 1: Driving voltage and reverse current for an orange PIN-OLED on lithografic and screen printed substrates

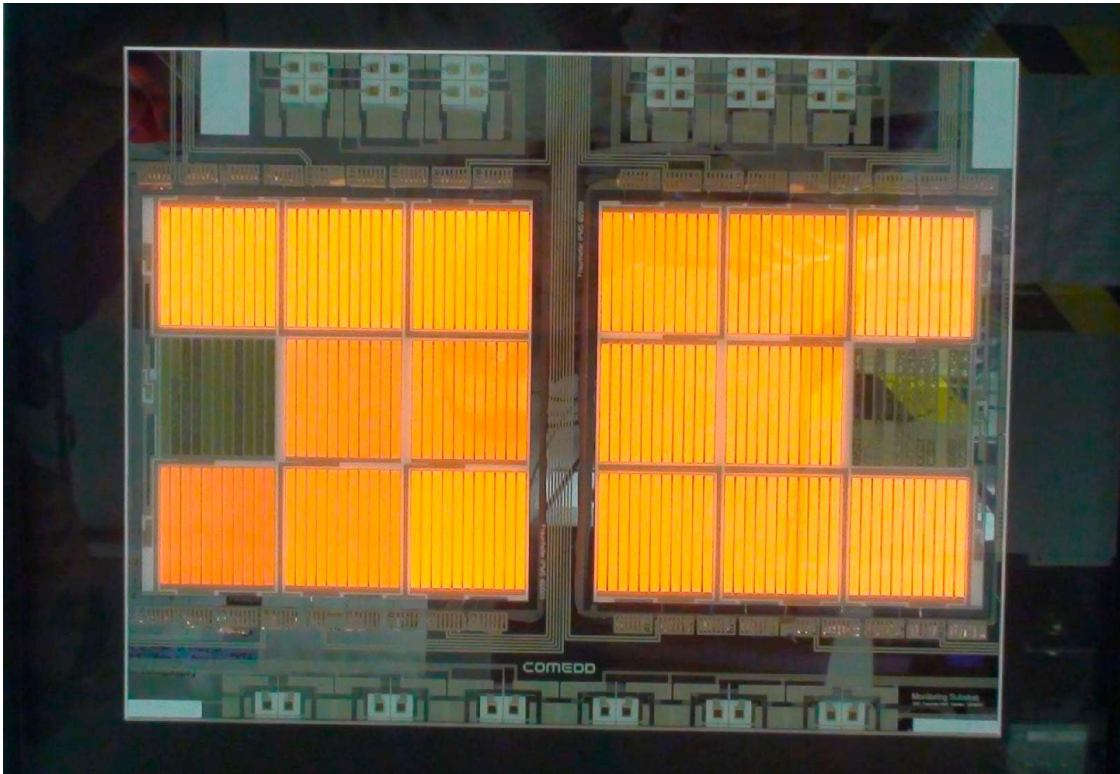


Figure 3: OLED on screen-printed substrate of GEN.2 size

Acknowledgements

This work has been funded by SMWK Saxony ministry within the framework for technology promotion by means of the European Fund for Regional Development (EFRE).

References

- [1] U. Todt, et al, "OLED for Large Area Lighting as well as for optoelectronic Microsystems: Center for Organic Materials and Electronic Devices Dresden – COMEDD (TPE08), 20-22 May 2008, TITK Rudolstadt
- [2] Balasundaraprabhua, M: "Effect of heat treatment on ITO film properties and ITOp-Si interface". In: Materials Chemistry and Physics 114 (2009.), S. 425-429

BIOGRAPHIC DATA OF MORITZ HASSELGRUBER

Dipl. Ing. Moritz Hasselgruber was born in Göttingen, Germany, in 1981. During his studies at the Technische Universität Dresden he specialised in micro mechanics and optical micro systems, especially organic light emitting diodes (OLEDs). From 2008 till 2009 he worked in the department of clean room robotic systems at Wikodema, Dresden, developing systems for automated wafer handling. He wrote his diploma thesis about alternative structuring



technologies for organic LED and organic photovoltaic applications and received his diploma in mechatronics from the University of Technology, Dresden, in 2009.

He went on dealing with organic light emitting diodes at the Fraunhofer IPMS, department of organic materials and systems (OMS) where he started his PhD work to investigate the possibilities of alternative structuring processes for large OLED and OPV substrates. He is responsible for the development of the thickfilm structuring at the COMEDD line at IPMS.

ORGANIC ELECTRONICS AT THE INTERFACE WITH BIOLOGY

George G. Malliaras

Department of Bioelectronics, Centre Microélectronique de Provence,
Ecole Nationale Supérieure des Mines de Saint Etienne,
880, route de Mimet, 13541 Gardanne, France
malliaras@emse.fr

Organic electronics seems to be ideally suited for the interface with biology. The “soft” nature of organic materials offers better mechanical compatibility with tissue than traditional electronic materials, while their natural compatibility with mechanically flexible substrates suits the non-planar form factors often required for bioelectronic implants. More importantly, their ability to conduct ions in addition to electrons and holes opens up a new communication channel with biology. I will review recent progress in the field and subsequently focus on two emerging areas: (a) The development of biosensors using conducting polymer transistors, and in particular their integration with microfluidics to create multi-analyte sensors, and, (b) the development of active substrates for cell growth, in which a potential applied on a conducting polymer substrate controls cell density and morphology.

BIOGRAPHIC DATA OF PROFESSOR GEORGE MALLIARAS

Professor **George Malliaras** is the Head of the Department of Bioelectronics (BEL) at the Centre Microélectronique de Provence of the Ecole Nationale Supérieure des Mines de Saint Etienne. He received a BS in Physics from the Aristotle University (Greece) in 1991, and a PhD in Mathematics and Physical Sciences, *cum laude*, from the University of Groningen (the Netherlands) in 1995. After a two year postdoc at the IBM Almaden Research Center (California), he joined the faculty in the Department of Materials Science and Engineering at Cornell University (New York). From 2006 to 2009 he served as the *Lester B. Knight* Director of the Cornell NanoScale Science & Technology Facility. He joined the Centre Microélectronique de Provence in the Fall of 2009. His research on organic electronics and bioelectronics has been recognized with awards from the New York Academy of Sciences, the US National Science Foundation, and DuPont. He is a co-author of 150+ publications in peer-reviewed journals that have received over 4,000 citations. He serves as the chairman of the Editorial Board of the *Journal of Materials Chemistry*.



Part III:

OFETs and devices 1

NEW ARCHITECTURES FOR THE ORGANIC TRANSISTOR

G. HOROWITZ*; N. BATTAGLINI; D. BRAGA; L. KERGOAT; H. KIM

ITODYS, Université Paris Diderot, 75205 Paris cedex 13, France

The interest in organic transistors is growing worldwide as new applications are emerging. Among the most appealing advantages of these devices are the possibility of using low-cost, large throughput fabrication methods based on printing techniques, and the feasibility of the device on flexible substrates. Moreover, the performance of organic transistors has substantially increased during the last years to reach a level at which its utilization in less demanding applications, such as radio-frequency identification (RFID) tags or active matrices for liquid-crystal (LCD), or even organic light-emitting diode (OLED) displays, can be envisioned. Up to now, the large majority of organic transistors were built according to the insulated-gate field-effect geometry, in which the gate electrode is isolated from the organic semiconductor active film by an insulating dielectric layer. However, a major drawback of this architecture is an operating voltage of a few tens of volts, which considerably restrains its development in practical applications. For this reason, considerable work has been devoted to the development of ultra-thin dielectric films, for instance with the help of self-assembled monolayers, where the thickness of the insulator is reduced to a single molecular layer.

In the present communication, we present two alternative architectures that have been investigated in our group. The first one is characterized by the absence of any gate dielectric. Instead, the gate is made a non-injecting electrode, a structure that more or less mimics the metal-semiconductor field-effect (MESFET) architecture. Like in its inorganic counter-part, the organic metal-semiconductor (MS) transistor is a normally on device; that is, the maximum current occurs when no voltage is applied to the gate. However, we show that, unlike the MESFET, the organic MS structure does not operate through the modulation of a space charge layer width. This statement primarily rests on a careful analysis of the operating mode of the organic metal-semiconductor diode, in which the current is controlled by the injection at both electrodes. First results on a numerical simulation of the organic MESFET will be presented. We will show that the shape of the current-voltage curves is mainly controlled by the density of free charges and the heights of the injection barrier at both the source and the gate electrodes.

In the second structure, the gate dielectric is replaced by a simple droplet of pure water in which the gate electrode is dipped. The main advantages of the structure reside in the simplicity of its realization and the fact that the device operates at very low voltages (less than 1V). Typical transfer characteristics are shown in Figure 1. The curves were obtained with a rubrene single crystal, and two different gate electrodes, gold and tungsten. A noticeable feature in these curves is the fact that the threshold voltage is significantly dependent on the nature of the gate electrode. This is due to the limited operating voltage range, which lies within the variation of the work function of the gate electrode. The operating mode and other limitations of this structure will be discussed.

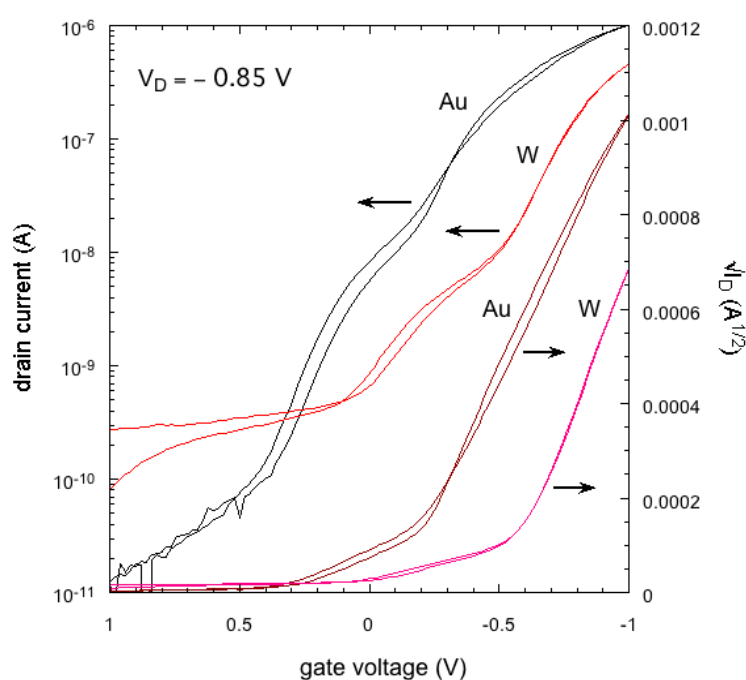


Figure 1. Transfer characteristics of a water-gated rubrene single crystal organic transistor, under semi-log (left scale) and square-root (right scale) plots, with two different gate electrodes (Au and W). The curves were recorded under a drain bias of 0.85 V.

BIOGRAPHIC DATA OF PROFESSOR GILLES HOROWITZ

Gilles Horowitz received a MS degree in solid state physics at the University Paris 7 in 1973. He was hired as Senior Scientist (“Chargé de Recherche”) by the “Centre National de la Recherche Scientifique” (CNRS) in 1976. He defended his PhD thesis in solid state physics at the University Paris 7 in 1981. In 1982, he moved to the “Laboratoire des Matériaux Moléculaires” in Thiais, near Paris, and in 1989 he started a research program in organic electronics that led the same year



to the realization of the first organic transistor made of a conjugated oligomer. He joined the University Paris Diderot in 2000 and was appointed professor in 2005. He currently leads a research group of four permanent personnel and five PhD students and two post-docs. His current research themes include the modification of organic electronic device interfaces with self-assembled monolayers and the modeling of organic thin-film transistors. He has recently launched a program on organic-based biosensors. He is the author or coauthor of nearly 150 publications and communications in international journals and conference proceedings.

AMBIPOLAR CHARGE TRANSPORT AND LIGHT EMISSION IN ORGANIC FIELD-EFFECT TRANSISTORS

C. Melzer, M. Schidleja, E. Feldmeier, H. von Seggern

Institute of Materials Science, Technische Universität Darmstadt,
Petersenstrasse 23, 64287 Darmstadt, Germany
Corresponding author email: melzer@e-mat.tu-darmstadt.de

Since the discovery of light emission from organic field-effect transistors (OFETs) in 2003 by Hepp et al.¹, OFETs have become an interesting device for the investigation of ambipolar charge transport and might even serve in the near future in highly integrated optoelectronic systems.

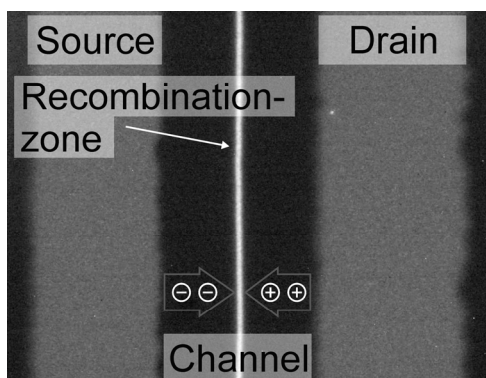


Fig 1: Optical micrograph of a light-emitting field-effect transistor. The device consists of: a PMMA gate dielectric, F8BT and Au source / drain terminals. The optical micrograph was taken at gate and drain voltages of 55 V und 100 V, respectively. The recombination zone appears as a narrow luminescent line in the middle of the transistor channel.

In this contribution, recent progress on organic light-emitting field-effect transistors will be reported. First, the importance of the gate insulator and the charge-carrier injection properties at the source and drain contacts on the OFET performance will be reviewed^{2, 3}. It will be demonstrated how ambipolar transport can be initiated and suppressed by the choice of an appropriate dielectric or contact metal allowing for a spatially controllable recombination zone or not⁴. Second, the performance of ambipolar light-emitting field-effect transistors will be discussed (Fig. 1). Using luminescent organic materials the position of the recombination zone is

monitored by optical microscopy and in combination with the emitted light intensity and current-voltage characteristics a comprehensive set of experimental data is available to characterize the OFET. Using this complementary experimental data the impact of the contact formation between semiconductor and source and drain electrodes in bottom-gate, top-contact transistors on the luminescence-voltage characteristic is unveiled^{5, 6}. It will be shown that for good contacts, the luminescent region moves from one of the employed electrodes across the organic semiconductor thin-film to the channel which is finally traversed. This property is ultimately used for the realization of a light-emitting field-effect transistor changing its emission colour by adjusting the applied bias⁷.

In order to realize ambipolar light-emitting field-effect transistors balanced charge carrier transport properties are of inherent importance. In this context, it can be demonstrated on basis of a selection of polymeric insulators that the polarity of organic thin film transistors is not only sensitive to the transport properties of the semiconductor but rather on the dielectric employed². Using an insulator allowing for ambipolar charge-carrier transport it is then only a matter of the appropriate metallization of the source and drain contacts to define whether the transistor acts unipolar n-type, unipolar p-type or even ambipolar³. Again ambipolarity requires balanced charge carrier injection properties meaning that comparable injection rates for electrons and holes should prevail.

Balanced charge carrier injection properties at the source and the drain contacts can be realized by using the same metal for electron and hole injection with a Fermi level centring

the bandgap of the used semiconductor. A prominent example is the poly(9,9-di-n-octyl-fluorene-alt-benzothiadiazole) (F8BT) based light-emitting thin film transistor with a poly(methylmethacrylate) (PMMA) gate insulator and gold source and drain contacts⁸. A transistor comprising such identical source and drain contacts is strongly impeded by the prevailing large injection barriers and hence, the description of the current voltage behaviour requires an extension of the existing analytical ambipolar OFET model⁹ towards a barrier limited charge carrier injection rate into the transistor channel⁶. The simulated electrical characteristics including such a barrier reproduce well the experimental observations. With respect to the luminescence properties, the transistor essentially emits in the ambipolar regime. Approaching the unipolar transistor regime the emission region moves towards one metal contact and finally the channel depletes from one of the charge carrier species and light-emission stops.

The transistor characteristic changes once the injection barriers are reduced by choosing low and high work function metals for electron and hole injection, respectively, while still maintaining the balance in injection barriers^{3, 5}. Once good contacts are achieved for electron and hole injection the light emission of the transistor retains even in the unipolar regimes. Since the current is smallest in the ambipolar regime and increases strongly once the transistor is driven towards the unipolar regimes, the emission intensity can be strongly increased even though the luminescence efficiency is reduced due to the emerging proximity of the emission zone and the contact metal.

The discrepancy in the emission characteristic of the different transistor types can be understood on basis of the contact formation between semiconductor and metal. Contacting a metal and an organic semiconductor with different work functions carriers will diffuse from the metal into the semiconductor establishing space-charge regions in both materials¹⁰. The self induced electric field of the carriers prevents a deep penetration of the carriers in the semiconductor and the metal and thus a charge carrier reservoir establishes in the organic semiconductor in the vicinity of the metal contact. Whether this reservoir remains even under an external bias naturally depends on the injection rate across the metal/semiconductor interface refilling the reservoir and thus on the charge carrier injection barrier.

For low barriers, the reservoir can be hardly depleted and the contact does not limit the current. Now, driving an organic transistor in the ambipolar regime the established reservoirs supply sufficient electrons and holes to the channel where they recombine. However, once the transistor enters the unipolar regime only one reservoir feeds the transistor channel, the carrier traverse the channel and are ejected into the reservoir of the complementary carrier species established at the counter electrode. The device emits light even in the unipolar regime.

The depicted mechanism can be used to design an organic light-emitting field-effect transistor

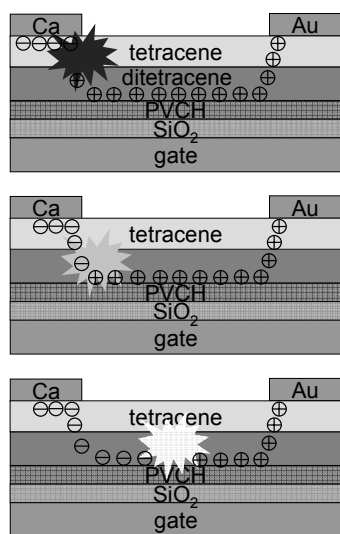


Fig 2: Possible positions of the recombination zone in a light emitting OFET with a double layered transport stack. Dependent of the applied biases the emission zone moves from on luminescent material to the other thus changing the emission colour of the light-emitting field-effect transistor.

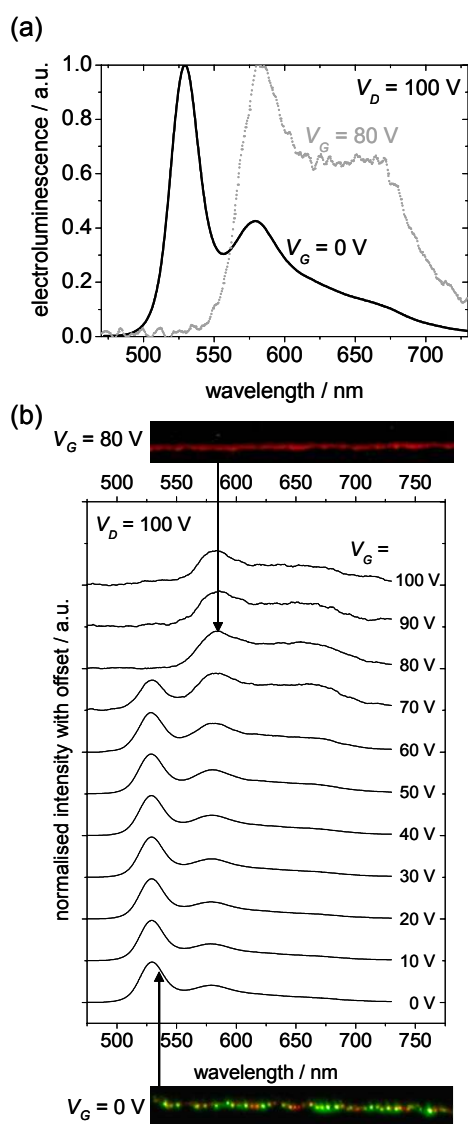


Fig 3: Transistor with a ditetracene¹/tetracene stack as semiconductor and calcium/gold contacts (a) electroluminescence spectra at $V_G = 0$ V and 80 V (b) electroluminescence spectra at different V_G and $V_D = 100$ V

contacts. On the other hand, the realization of the voltage controlled colour change in one light emitting pixel envisions a broad applicability of light-emitting organic field-effect transistor in the future.

The authors thank the German Research Foundation for financial support through projects SE941/13-3 and Graduiertenkolleg 1037 (TICMO). Prof. Dr. M. Rehn and his coworkers of the Ernst-Berl-Institut for Technical and Macromolecular Chemistry at the Technische Universität Darmstadt are acknowledged for providing the employed ditetracene. The material ditetracene is protected by the patent WO/2007/000268. The patent is a property of the Dritte Patentportfolio Beteiligungsgesellschaft mbH & Co. KG.

whose emission colour can be controlled by the applied bias⁷. The realized bottom-gate, top-contact transistor consists of a double-layer structure of two different acenes, namely tetracene and ditetracene¹, which possess different bandgaps and thus emission colours. The light-emitting OFETs include balanced low-barrier contacts for electron and hole injection made out of Ca and Au, respectively. As gate insulator a SiO₂/polyvinylcyclohexane (PVCH) double layer is used. To change the emission colour we use the property that the emission zone in such a light-emitting OFET can be moved from the established reservoir of one contact through the double layer stack towards the channel and further to the counter electrode by simply changing the applied biases. As a consequence, the emission zone will move from one organic layer to the other thus changing the colour of the emitted light. This is seen in Fig. 2. In Fig. 3 the emission spectra for a series of gate biases V_G at a given drain bias V_D of 100 V clearly demonstrate the change in emission colour. In CIE coordinates, a shift from (0.42, 0.57) to (0.59, 0.41) can be achieved by changing V_G from 0 V to 80 V. On the one hand, the colour change supports the above depicted scenario of the movement of the recombination zone in ambipolar light-emitting field-effect transistors with ohmic con-

¹ The material ditetracene is protected by the patent WO/2007/000268.

The patent is a property of the Dritte Patentportfolio Beteiligungsgesellschaft mbH & Co. KG.

Literature

- [1] Hepp, A., Heil, H., Weise, W., Ahles, M., Schmechel, R. and von Seggern, H., "Light-emitting field-effect transistor based on a tetracene thin film", *Phys. Rev. Lett.*, 91(15), 157406 (2003).
- [2] Benson, N., Melzer, C., Schmechel, R. and von Seggern, H., "Electronic states at the dielectric/semiconductor interface in organic field effect transistors", *Phys. Stat. Solidi A*, 205(3), 475-487 (2008).
- [3] Melzer, C., Schidleja, M. and von Seggern, H., "Organic field-effect transistors: from unipolar to ambipolar to light emission", *Proc. of the SPIE*, 74515,741516 (2009).
- [4] Schidleja, M., Melzer, C. and von Seggern, H., "Electroluminescence from a pentacene based ambipolar organic field-effect transistor", *Appl. Phys. Lett.*, 94(12), 123307 (2009).
- [5] Schidleja, M., Melzer, C., Roth, M., Schwalm, T., Gawrisch, C., Rehahn, M. and von Seggern, H., "The impact of contact formation on the light emission from ambipolar transistors", *Appl. Phys. Lett.*, 95(11), 113303 (2009).
- [6] Schidleja, M., Melzer, C. and von Seggern, H., "Investigation of charge carrier injection in ambipolar organic light-emitting field-effect transistors", *Adv. Mater.*, 21,1172-1176 (2009).
- [7] Feldmeier, E. J., Schidleja, M., Melzer, C. and von Seggern, H., "A colour tuneable light-emitting transistor", *Adv. Mater.*, accepted for publication,(2009).
- [8] Zaumseil, J., Friend, R. H. and Sirringhaus, H., "Spatial control of the recombination zone in an ambipolar light-emitting organic transistors", *Nature Materials*, 5(1), 69-74 (2006).
- [9] Schmechel, R., Ahles, M. and von Seggern, H., "A pentacene ambipolar transistor: Experiment and theory", *J. Appl. Phys.*, 98(8), 084511 (2005).
- [10] Neumann, F., Genenko, Y. A., Melzer, C., Yampolskii, S. V. and von Seggern, H., "Self-consistent analytical solution of a problem of charge-carrier injection at a conductor/insulator interface", *Phys. Rev. B*, 75,205322 (2007).

BIOGRAPHIC DATA OF DR. CHRISTIAN MELZER

Date of birth: 12.05.1970



Scientific career

- 1991-1999 Studies of physics at the TH Karlsruhe (Germany) and the CNRS Strasbourg (France), Diploma Thesis „Photorefractive Polymers“ (Prof. Dr. R. Levy, Prof. Dr. H. Kalt)
- 1999-2004 Graduation at the Rijksuniversiteit Groningen, Material Science Centre (The Netherlands), Ph.D. thesis „Organic Semiconductors and Optoelectronic Elements“ (Prof. Dr. G. Hadziioannou)
- 2003 PostDoc at the Rijksuniversiteit Groningen, Material Science Centre (The Netherlands), Group “Physics of organic semiconductors” (Prof. Dr. P.W.M. Blom)
- since 2005 Scientific staff at the Institute of Materials Science, Department Electronic Materials (Prof. Dr. H. von Seggern), TU Darmstadt (Germany)

DEVELOPMENT OF VERTICAL-TYPE METAL-BASE ORGANIC TRANSISTORS

K. NAKAYAMA¹

¹Department of Organic Device Engineering; Graduate School of Science and Engineering; Yamagata University; 4-3-16 Jonan; Yonezawa; Yamagata 992-8510; Japan

The vertical-type organic transistor is a promising device structure that can make the channel length much shorter, leading to low voltage and high current operation. So far several vertical-type devices have been proposed, polymer grid triodes [1], organic static induction transistors [2], organic/inorganic hybrid transistors [3], and unique architecture vertical transistors [4]. However, these devices often require complicated fabrication process and suffer from poor reproducibility. Recently, we have reported a high performance vertical transistor having a simple layered structure composed of organic/metal/organic layers [5,6]. This device was named a metal-base organic transistor (MBOT), because the inserted middle electrode behaves like a base layer in the bipolar transistors.

Figure 1 shows the device structure and measurement system. The device was fabricated by vacuum deposition. The first organic layer (collector layer) of perylenetetracarboxylic derivatives (Me-PTC) was deposited on an ITO glass substrate of a collector electrode. The base electrode of aluminum was deposited with a thickness of 20 nm. Here, the device was subjected to heat treatment in air to reduce off current [7]. The second organic layer (emitter layer) of C₆₀ and the emitter electrode of Ag were deposited.

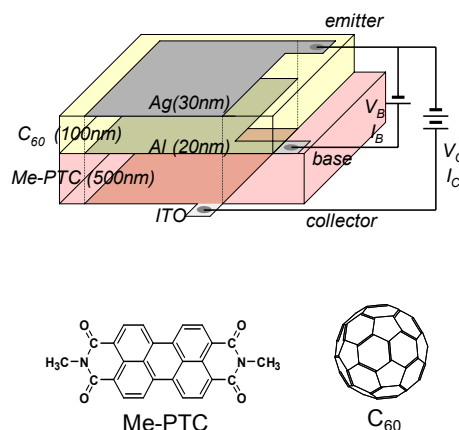


Figure 1 The device structure of the metal-base organic transistors and the chemical structure of used materials.

The current modulation was measured in the glove box using emitter common circuit (Figure 1) with two sets of source measure unit. The output collector current (I_C) was measured for sweeping input base voltage (V_B) under constant collector voltage (V_C).

Figure 2 shows the typical current modulation characteristics ($I_C - V_C$ curves at various V_B) for the MBOT. The output current was markedly increased by base voltage application with 5 orders of magnitude. It should be noted that very large output current density exceeding 100 mA/cm^2 was obtained with low operation voltage of $V_C = 5\text{V}$ and $V_B = 2\text{V}$.

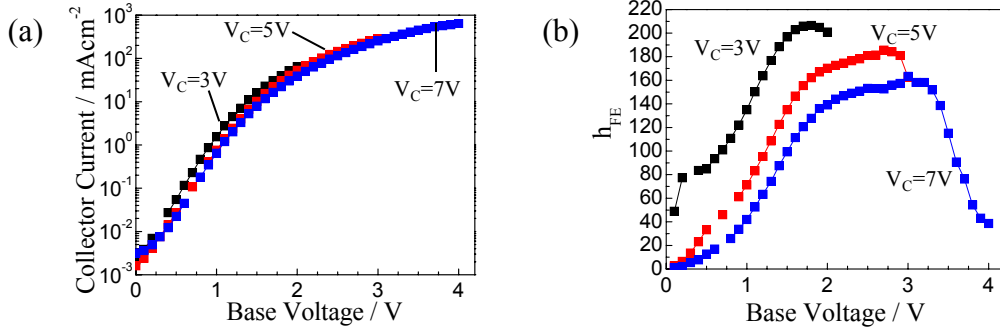


Figure 2 Typical modulation characteristics of the MBOT, (a) output current modulation characteristics (I_C - V_B curves), (b) current amplification factor (h_{FE}).

The current flow in the MBOT device is shown in Figure 3. In this case, the input base current (I_B) remains small value in spite of V_B application; therefore, input base current (I_B) can be amplified to large output current (I_C). This behaviour can be quantified by current amplification factor (h_{FE}), that is defined as the ratio of the change in I_C to I_B for V_B application. Typical value of h_{FE} in MBOTs is several hundreds.

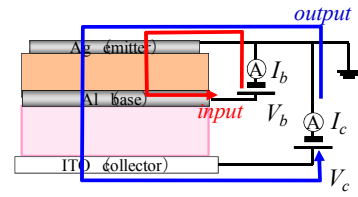


Figure 3 The input and output current flow in the MBOT device.

The operation mechanism of the MBOTs can be explained by the energy diagram as shown in Figure 4. In the off state ($V_C > 0$, $V_B = 0$), output current is small because the electron injection from the base electrode is blocked by heat treatment [7]. In the on state ($V_C > 0$, $V_B > 0$), electrons injected from the emitter electrode can pass through the base electrode with high probability. As a result, almost all electrons can reach the collector electrode leading to large output current (I_C). Small part of electrons falls into the base electrode leading to input current (I_B). This is why large current amplification can be achieved in this system.

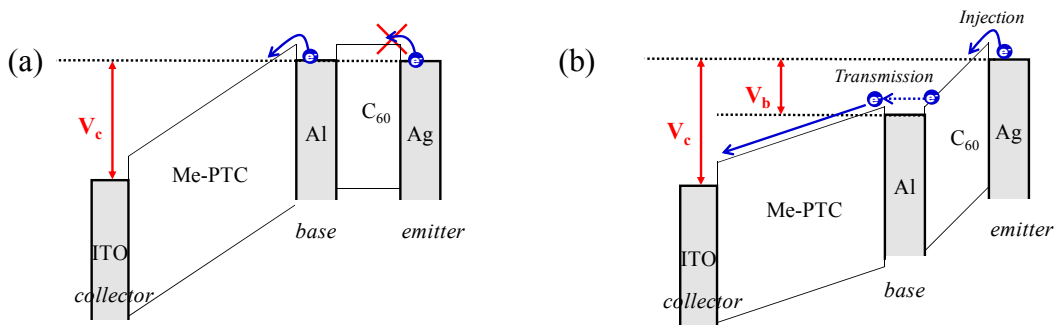


Figure 4 The energy diagram of MBOT, (a) in the off state ($V_C > 0$, $V_B = 0$), and (b) in the on state ($V_C > 0$, $V_B > 0$).

The transmission mechanism has not been clarified in detail. Unfortunately, there are few kinds of materials showing amplification in the MBOT. In our knowledge, this combination of Me-PTC as a collector layer and C₆₀ as an emitter layer brings about the best performance. One of important parameters is the LUMO level of the used semiconductor material. Figure 5 shows the energy levels of these materials and electrodes. We can say that enough deep LUMO levels are necessary for smooth transport of electrons from the emitter to collector leading to current amplification.

The MBOTs are generally fabricated on the ITO glass substrate. Therefore, it can be easily fabricated on an ITO plastic substrate. Figure 6 is a picture of the MBOT device fabricated on a polyethylene naphthalate (PEN) substrate. The device showed almost same performance with that on the ITO glass substrate.

In conclusion, the metal-base organic transistor has novel and promising device structure that can be fabricated simply and achieve low voltage and high current operation. In addition, its unique function of current amplification would be more suitable for analog amplifier and wireless communication rather than organic field-effect transistors.

REFERENCES

- [1] Y. Yang and A. J. Heeger, *Nature* **372**, 344 (1994).
- [2] K. Kudo, D. X. Wang, M. Iizuka, S. Kuniyoshi, and K. Tanaka, *Thin Solid Films* **331**, 51 (1998).
- [3] M. S. Meruvia, I. A. Hümmelgen, M. L. Sartorelli, A. A. Pasa, W. Schwarzacher, *Appl. Phys. Lett.* **84**, 3978 (2004).
- [4] L. P. Ma and Y. Yang, *Appl. Phys. Lett.* **85**, 5084 (2004).
- [5] S. Fujimoto, K. Nakayama, M. Yokoyama, *Appl. Phys. Lett.* **87**, 133503 (2005).
- [6] K. Nakayama, S. Fujimoto, M. Yokoyama, *Appl. Phys. Lett.* **88**, 153512 (2006).
- [7] K. Nakayama, S. Fujimoto, M. Yokoyama, *Org. Electron.* **10**, 543 (2009).

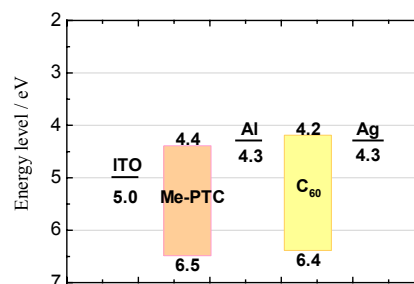


Figure 5 Energy levels of organic semiconductors and electrodes used in the MBOT.

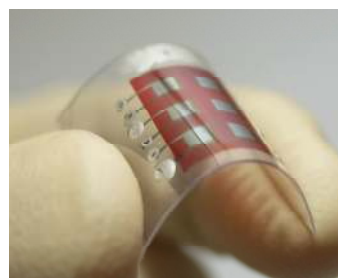


Figure 6 The MBOT device fabricate on a flexible ITO substrate.

CURRICULUM VITAE OF KEN-ICHI NAKAYAMA (PH. D)



Personal Information

Affiliation:

Department of Organic Device Engineering,
Graduate School of Science and Engineering,
Yamagata University, Japan

Work Address: 4-3-16, Jonan, Yonezawa, Yamagata 992-8510, Japan

Nationality: Japan

Email: nakayama@yz.yamagata-u.ac.jp

Phone/FAX: +81-238-26-3713

Educations and Working Experiences

- 2006.8 – Associate Professor, Department of Organic Device Engineering, Graduate School of Science and Engineering, Yamagata University, Japan.
- 2006.10 – 2010.3 Research Associate of Japan Science and Technology Agency.
- 2000.4 – 2006.7 Assistant Professor, Graduate School of Engineering, Osaka University, Japan.
- 1996.4 – 2000.3 Ph. D. (Applied Chemistry), Department of Material and Life Science, Graduate School of Engineering, Osaka University, Japan.
- 1994.4 – 1996.3 M.S. (Applied Chemistry), Department of Material and Life Science, Graduate School of Engineering, Osaka University, Japan.
- 1991.4. – 1994.3 B.S. (Applied Chemistry), Department of Applied Chemistry, Faculty of Engineering, Osaka University, Japan.

Research

- 2000 – Vertical-type organic transistors (Metal-Base Organic Transistor).
- 2000 – Organic field-effect transistors (n-type OFET materials and hetero-layered OFET).
- 2001 – 2006 Application of carbon nanotubes for wet-processed field-effect transistor.
- 1998 – 2006 Structural and electronic properties at organic/metal interface and its relationship with photoelectric properties of organic electronic devices.
- 1994 – 2004 Organic Photosensor (Photocurrent multiplication phenomena) and related organic materials.

Awards

1. Konica Minolta Imaging Science Foundation Award (2007).
2. Prize for Encouragement in Molecular and Bio Electronics Branch in the Japan Society of Applied Physics (2007).
3. Paper Award in the Japanese Liquid Crystal Society (2008).
4. Paper Award in the Japan Imaging Society (2009).

Selected Papers

1. M. Hiramoto, K. Nakayama, T. Katsume, and M. Yokoyama, "Field-activated structural traps at organic pigment/metal interfaces causing photocurrent multiplication phenomena", *Appl. Phys. Lett.* **73**, 2627-2629 (1998).
2. K. Nakayama, M. Hiramoto, and M. Yokoyama, "Direct tracing of the photocurrent multiplication process in an organic pigment film", *J. Appl. Phys.* **84**, 6154-6156 (1998).
3. K. Nakayama, M. Hiramoto, and M. Yokoyama, "Photocurrent multiplication at organic/metal interface and surface morphology of organic films", *J. Appl. Phys.* **87**, 3365-3369 (2000).
4. K. Nakayama, M. Hiramoto, and M. Yokoyama, "A high-speed photocurrent multiplication device based on an organic double-layered structure", *Appl. Phys. Lett.* **76**, 1194-1196 (2000).
5. K. Nakayama, Y. Niguma, Y. Matsui, and M. Yokoyama, "Electronic interactions in codeposited films of naphthalene tetracarboxylic derivatives and metals", *J. Appl. Phys.* **94**, 3216-3221 (2003).
6. S. Fujimoto, K. Nakayama, and M. Yokoyama, "Fabrication of a vertical-type organic transistor with a planar metal base", *Appl. Phys. Lett.* **87**, 133503 (2005).
7. H. Tachikawa, H. Kawabata, R. Miyamoto, K. Nakayama, and M. Yokoyama, "Experimental and theoretical studies on the organic anorganic hybrid compound: Aluminum-NTCDA co-deposited film", *J. Phys. Chem. B* **109**, 3139-3145 (2005).
8. K. Nakayama, S. Fujimoto, and M. Yokoyama, "High-current and low-voltage operation of metal-base organic transistors with LiF/Al emitter", *Appl. Phys. Lett.* **88**, 153512 (2006).
9. Y. Shimizu, K. Oikawa, K. I. Nakayama, and D. Guillon, "Mesophase semiconductors in field effect transistors", *J. Mater. Chem.*, **17**, 4223-4229 (2007).
10. K. Nakayama, S. Fujimoto, and M. Yokoyama, "Improvement in the on/off ratio of a vertical-type metal-base organic transistor by heat treatment in air", *Org. Electron.*, **10**, 543-546 (2009).
11. K. Nakayama, M. Ishikawa, and M. Yokoyama, "Improvement in Mobility and stability of n-type organic field-effect transistors with a hole transporting interfacial layer", *Appl. Phys. Express*, **2**, 021501-1-3 (2009).

LOW COST SENSING ARRAYS USING ORGANIC SEMICONDUCTORS

M.-B. MADEC,^a J.J. MORRISON,^a M. L. TURNER,^{*,a} S.G. YEATES,^a D.C. WEDGE,^b D. B. KELL,^b J. KETTLE,^c A. SONG,^c A. DAS,^d M. GRELL,^d T.H. RICHARDSON^d

^a *Organic Materials Innovation Centre, School of Chemistry, Oxford Road, University of Manchester, Manchester, M13 9PL, UK;*

^b *Manchester Interdisciplinary Biocentre, 131 Princess Street, Manchester M1 7DN, UK;*

^c *School of Electrical and Electronic Engineering, University of Manchester, Manchester, M13 9PL, UK;*

^d *Department of Physics and Astronomy, University of Sheffield, Hicks Building, Hounsfield Road, Sheffield, S3 7RH, UK.*

Organic semiconductors have been utilised in many applications, e.g. OLEDs, OFETs, OPV, RFID tags [1,2]. One application of organic semiconductors that is currently emerging is their use in sensor systems. The versatility of organic chemistry allows the attachment of specific recognition sites, the most celebrated example being the work of Swager and others on the optical sensing of explosives such as TNT, with a functionalised poly(*p*-phenylene ethynylene) [3]. A more generic, electronically read, organic semiconductor-based sensor concept is the ‘chemiresistor’, where the electrical resistance of a material is monitored during analyte exposure [4]. Recently, sensors based on organic field effect transistors (OFETs) have received increasing interest [5,6]. The OFET’s source–drain current, I_{SD} , in the ‘on’ state is orders-of-magnitude larger than in the ‘off’ state with no gate voltage applied and most OFET-based sensor research has used the OFET as an ‘amplified’ chemiresistor [7–9]. In principle, however, OFET sensors allow a more sophisticated mode of operation, where the transistor undergoes a full characterization rather than simple monitoring of I_{SD} . The most common ‘full characterisation’ of an OFET comprises the recording of a saturated transfer characteristic, that is I_{SD} vs. V_G , with source–drain voltage (V_{SD}) kept larger or equal to V_G . A saturated transfer characteristic allows separate extraction of carrier mobility, μ , threshold V_T , and off-current, or on/off ratio. The full characterization gives a ‘multiparameter’ data set that gives a more selective odour response. Torsi et al. [10] have reported extensively on OFET sensors under multiparameter characterisation, showing enhanced selectivity thanks to the simultaneous extraction of several parameters.

Saturated transfer characteristics are typically recorded with expensive semiconductor parameter analysers, which are slow, immobile due to their weight and dependent on mains electricity. For a truly portable, low cost, multiparameter sensor system, we require a low-cost, battery powered unit that returns multiparameter data in real time.

In this presentation the selective detection of airborne analytes in real time using arrays of organic field-effect transistors (OFETs) based on libraries of polytriarylaminines is demonstrated. [11] The fabrication of OFETs with low voltage operation is discussed and the rapid characterisation of the performance of these devices using the “Gain” method presented (see **Figure 1**).[12] The use of multiple parameters – on resistance, off current threshold voltage and mobility – collected from multiple transistors coated with amorphous semiconducting polymers gives dramatic improvements in the specificity and speed of sensing of arrays of OFETs.[13]

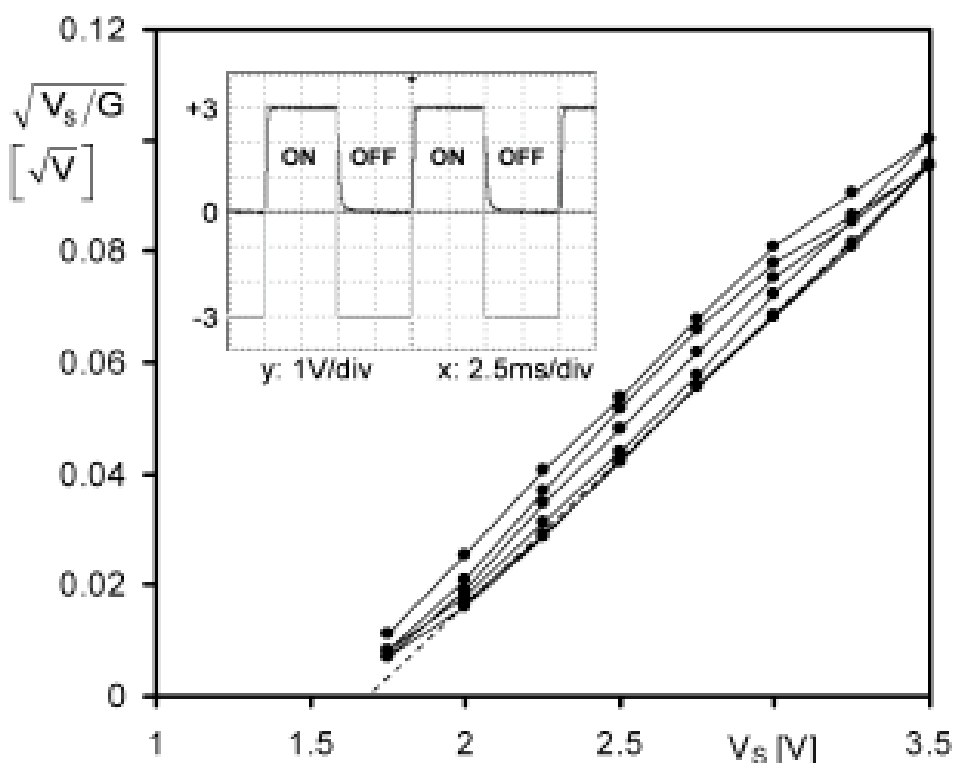


Figure 1: Characterisation of a PTAA OFET using the “Gain“ method in less than 1s.

Computer-controlled data collection allows the identification of analytes in real-time, with a time-lag between exposure and detection of the order of a few seconds. The incorporation of genetic programming into the analysis of the collected data is demonstrated to be an effective method for the identification of patterns in the multiparametric data obtained.[14]

References

- [1] H. Sirringhaus, Device physics of solution-processed organic field-effect transistors, *Adv. Mater.* 17 (2005) 2411.
- [2] A. Dodabalapur, Organic and polymer transistors for electronics, *Mater. Today*, 9 (2006) 24.
- [3] J.-S. Yang, T.M. Swager, Porous shape persistent fluorescent polymer films: an approach to TNT sensory materials, *J. Am. Chem. Soc.* 120 (1998) 5321.
- [4] H. Bai, G. Shi, Gas sensors based on conducting polymers, *Sensors* 7 (2007) 267.
- [5] L. Torsi, G.M. Farinola, F. Marinelli, M.C. Tanese, O.H. Omar, L. Valli, F. Babudri, F. Palmisano, P.G. Zambonin, F. Naso, A sensitivity-enhanced field-effect chiral sensor, *Nat. Mater.* 7 (2008) 412.
- [6] L. Torsi, M.C. Tanese, N. Cioffi, M.C. Gallazzi, L. Sabbatini, P.G. Zambonin, Alkoxy-substituted polyterthiophene thin-film-transistors as alcohol sensors, *Sens. Actuators B* 98 (2004) 204.
- [7] F. Liao, C. Chen, V. Subramanian, Organic TFTs as gas sensors for electronic nose applications, *Sens. Actuators B* 107 (2005) 849.
- [8] L. Wang, D. Fine, A. Dodabalapur, Nanoscale chemical sensor based on organic thin film transistors, *Appl. Phys. Lett.* 85 (2004) 6386.
- [9] L. Torsi, M.C. Tanese, N. Cioffi, M.C. Gallazzi, L. Sabbatini, P.G. Zambonin, G. Raos, S.V. Meille, M.M. Giangregorio, Side-chain role in chemically sensing conducting polymer field-effect transistors, *J. Phys. Chem. B* 107 (2003) 7589.
- [10] L. Torsi, A. Dodabalapur, L. Sabbatini, P.G. Zambonin, Multi-parameter gas sensors based on organic thin-film-transistors, *Sens. Actuators B* 67 (2000) 312.
- [11] I.-W. Shen, M.C. McCairn, J.J. Morrison, M.L. Turner, Synthesis of polytriarylamines via microwave-assisted palladium, *Macromol. Rapid Commun.* 28 (2007) 449.
- [12] R. Dost, A. Das, M. Grell, A novel characterization scheme for organic field-effect transistors, *J. Phys. D: Appl. Phys.* 40 (2007) 3563.
- [13] A. Das, R. Dost, T.H. Richardson, M. Grell, J.J. Morrison, M.L. Turner, A nitrogen dioxide sensor based on an organic transistor, *Adv. Mater.* 19 (2007) 4018.
- [14] D. C. Wedge, A. Das, R. Dost, J. Kettle, M.-B. Madec, J.J. Morrison, M. Grell, D. B. Kell, T. H. Richardson, S.G. Yeates and M. L. Turner, *Sens. Actuators B*, 143 (2009) 365.

BIOGRAPHIC DATA OF PROFESSOR M.L. TURNER

School of Chemistry, University of Manchester, Manchester, M13 9PL, UK



Biography

Mike Turner is Professor of Materials Chemistry (www.omec.org.uk/MLTurner/) and Director of the Organic Materials Innovation Centre (www.omic.org.uk) within the School of Chemistry. He obtained his first degree and a PhD from the University of Bristol, working with Professor Selby Knox on the synthesis of new organometallic complexes, before moving to the United States to work with Professor Harry Allcock investigating new routes to polyphosphazenes. He returned to the UK to work at the University of Sheffield with Professor Peter Maitlis on the mechanism of the Fischer-Tropsch reaction and was awarded a Royal Society University Research Fellowship in 1993 to investigate the synthesis of novel polymers. He joined the staff of the Department of Chemistry, University of Sheffield as a Reader in 2000 and in April 2004 moved to the University of Manchester to a Chair in Materials Chemistry and to be Director of OMIC. Professor Turner is coordinator of the Organic Materials for Electronics Consortium (www.omec.org.uk) and was Senior Editor for Reactive and Functional Polymers 2002-8. He is principal investigator for the Knowledge Centre for Materials Chemistry (www.materialschemistry.org) at the University of Manchester. The KCMC is a virtual centre of expertise providing multi-disciplinary research and innovative knowledge transfer based on world class capabilities in applied materials chemistry.

Research Interests

My principal research interests concern the synthesis of novel conjugated molecules, particularly conjugated liquid crystals and conjugated polymers, and in using these novel molecules in organics electronic and electrooptical devices such as organic transistors, organic light emitting diodes, sensors and solar cells. This research is carried out as part of the Organic Materials for Electronics Consortium (www.omec.org.uk) of the EPSRC, an interdisciplinary consortium that consists of research groups from the School of Chemistry, University of Manchester, the Department of Physics and Astronomy and the Department of Chemistry at the University of Sheffield and the Department of Physics and Astronomy at Imperial College. Other areas of interest include sol-gel chemistry, polymer synthesis, auxetic materials and device fabrication at the nanoscale.

Selected publications

- Das A, Dost R, Richardson TH, Grell M, Wedge DC, Kell DB, Morrison JJ, Turner ML. Low cost, portable, fast multiparameter data acquisition system for organic transistor odour sensors. *Sens. Actuators, B*. 2009; B137: 586-591.
- Spring AM, Yu C, Horie M, Turner ML. MEH-PPV by microwave assisted ring-opening metathesis polymerisation. *Chem. Commun. (Cambridge, U. K.)*. 2009; 2676-2678.
- Horie M, Luo Y, Morrison JJ, Majewski LA, Song A, Saunders BR, Turner ML. Triarylamine polymers by microwave-assisted polycondensation for use in organic field-effect transistors. *J. Mater. Chem.* 2008; 18: 5230-5236.
- Maunoury M, Howse JR, Turner ML. Melt-processing of conjugated liquid crystals: a simple route to fabricate OFETs. *Adv. Mater. (Weinheim, Ger.)*. 2007; 19: 805-809.
- Yu C, Turner M. Soluble poly(p-phenylenevinylene)s through ring-opening metathesis polymerization. *Angew. Chem., Int. Ed.* 2006; 45: 7797-7800.
- Coppo P, Turner ML. Cyclopentadithiophene based electroactive materials. *J. Mater. Chem.* 2005; 15: 1123-1133.

The abstract of the lecture Professor Sariciftci
entitled
“New materials for organic and bio-organic
optoelectronic devices”
was not available to the editorial deadline.

BIOGRAPHIC DATA OF PROFESSOR NIYAZI SERDAR SARICIFTCI

Prof. Sariciftci is ordinarius (chair) professor for physical chemistry and the founding director of the Linzer Institute for Organic Solarcells (LIOS) at the Johannes Kepler University of Linz/Austria.

He studied at the University of Vienna (Austria) and graduated as PhD in physics in 1989. After two years postdoctoral study at the University of Stuttgart (Germany) he joined the Institute for Polymers and Organic Solids at



the University of California, USA, by Prof. Alan J. HEEGER, Nobel laureate 2000 for Chemistry. His major contributions are in the fields of photoinduced optical, magnetic resonance and transport phenomena in semiconducting and metallic polymers. He is the inventor of conjugated polymer and fullerene based solar cells. Prof. Sariciftci published over 400 publications, 6 books with over 17000 citations and h-factor of 57. He educated several academic and industrial scientists. He also initiated seven spin off companies for organic optoelectronics. He is recipient of several prizes among them the National Science Prize of Turkey 2006 and the Austria 2008 Prize for Scientific Research. He is a Fellow of SPIE, Fellow of the Royal Society of Chemistry (FRSC) and member of several societies such as American Chemical Society, Materials Research Society, SPIE, Austrian Chemical Society and Austrian Physical Society.

Part IV:

Materials & Methods 1

MATERIAL CHALLENGES FOR PRINTED ELECTRONICS

S. Kirchmeyer*, H.C. Starck Clevis GmbH, Chempark Leverkusen, Building B 202,
51368 Leverkusen, Germany

Printed electronics is believed to open a field of low-cost electronics with new fields of applications. Printing semiconductors, conductors and dielectrics will be a critical task to fulfill cost targets. We will discuss challenges facing this technology which result from the properties of materials during processing and during operation of the devices.

Integrated electronic circuits are constructed from a manifold of active electronic components like diodes, transistors and passive components like e.g. resistors. The vision of printed electronics includes the mass-printing of interacting circuits, photovoltaic cells and displays at low costs. Therefore the availability of low-cost printing processes with high accuracy will be critical for this vision to become true.

Besides sophisticated electronic structures like transistors also energy sources will be needed. Organic solar cells and printable batteries might be options, RFID-tags may operate using the energy absorbed from an electrical field. But even silicon based chips have not been able to integrate another important passive component into the chip: capacitors. Capacitors are needed for the signal processing devices and to ensure a stable energy supply during operation. Limited attempts have been made to produce capacitors by printing techniques. Capacitors with high capacity i.e. high surfaces will be difficult to manufacture by printing organic materials.

Single components that form the integrated chip will be made by combining three basic materials being conductors, semiconductors and dielectrics. The development of materials is still ongoing, the main challenges being charge carrier mobility and lifetime for semiconductors and conductivity and transparency for conductors. Polymeric conductors have become mature technical materials available in technical quantities. Polymeric and organic semiconductors have experienced a rapid development within the last 10 years. Dielectric polymers and inorganic printable conductors, semiconductors and dielectrics complement the portfolio of materials for printed electronic devices. Polymeric dielectrics are already available but so far compared to inorganic dielectrics exhibit only limited dielectric constants.

All materials employed will need to match the intended production processes. Regarding suitable production processes the discussion is still ongoing. In the meantime it has become clear that the production of complex electronic devices will need a combination of several deposition techniques each selected by the intended electronic structure. A challenge will be to meet the cost target in case of complex combinations of deposition techniques.

Homogeneous, highly smooth layers will be required as transparent electrodes which may be achieved either by coating or printing as well. Coating is a suitable technique for highly smooth layers, but will have the disadvantage that in most cases some structures will be necessary, e.g. OLED's will require non coated areas near the edge needed for sealing. Silk screen, ink jet and gravure printing have been proven to be suitable for large area homogeneous printing, but the challenge will be to meet the desired smoothness in the sub nanometer level.

Metal electrodes for source, drain and gate in OFETs are most commonly deposited by photolithographic etching or by evaporating metals through a shadow mask to achieve small patterns with dimensions in the order of microns. Polymers like PEDOT:PSS for gate-electrodes were deposited by screen printing technique.¹ The resolution of the pattern is limited to approximate 100 μm defined by the coarseness of the screen. Recently the resolution of screen prints has rapidly progressed and a resolution of 20 μm might be achievable.

For ink jet printing a concept has been proposed that allows the deposition of PEDOT:PSS electrodes with a channel resolution of $L = 5 \mu\text{m}$ using the segregation of surfactants.²

An approach to reach high resolution electrodes was realized for PEDOT:PSS by self-alignment employing ink-jet deposition on structures made by contact printing of a self-assembled monolayer (SAM), which turns the surface hydrophobic at those parts where PEDOT:PSS-wetting should be inhibited³. However these processes will still face challenges during scaling into the technical scale and adoption for high printing speed.

Vertical interconnects (vias) will be essential to connect lines and have been accomplished by creating contact holes with standard photolithography subsequently filled by PEDOT:PSS.⁴ For real production processes it will be necessary that the vias are solely produced by printing.

For the material manufacturers it has become clear that all materials will have to be adopted to the intended deposition techniques and the desired function. For example, the

formulation of the conductor PEDOT:PSS will be not only quite different for ink jet and silk screen printing but also for homogeneous layer and fine line printing.

Another challenge will be the design of material interfaces. The interface of PEDOT and semiconductors in OLEDs have been extensively studied since degradation of the interface have been made responsible for their limited life times. Similar issues can also be expected for the interfaces between semiconductors and conductors in organic transistors, OPV and organic sensors. This problem may be expected to become even more severe if organic and inorganic materials are combined in devices.

-
- ¹⁾ E. Becker, R. Parashkov, G. Ginev, D. Schneider, S. Hartmann, F. Brunetti, T. Dobbertin, D. Metzdorf, T. Riedl, H.-H. Johannes and W. Kowalsky. 2003. All-organic thin-film transistors patterned by means of selective electropolymerization. *Appl Phys Lett* 83(19):4044-4046
 - ²⁾ H. Sirringhaus, T. Kawase, R. H. Friend, T. Shimoda, M. Inbasekaran, W. Wu and W. P. Woo. 2000. High-Resolution Inkjet Printing of All-Transistor Circuits. *Science* 290:2123-2126
 - ³⁾ S. P. Li, C. J. Newsome, T. Kugler, M. Ishida and S. Inoue. 2007. Polymer thin film transistors with self-aligned gates fabricated using ink-jet printing. *Appl Phys Lett* 90:172103/1-172103/3
 - ⁴⁾ F. J. Touwslager, N. P. Willard and D. M de Leeuw. 2002. I-Line lithography of poly(ethylenedioxythiophene) electrodes and application in all-polymer integrated circuits. *Appl Phys Lett* 81:4556-4558

Development of Stable, High-Performing Organic Semiconductors and TFTs

T. Backlund, P. Brookes, J. Canisius, G. Lloyd, P. Miskiewicz,
D. Mueller*, M. Carrasco-Orozco, S. Tierney,

Merck, Advanced Technologies – Chilworth, Merck Chemicals Ltd., University Parkway,
Southampton, SO16 7QD, United Kingdom

* Merck, Advanced Technologies – Innovation Management, Merck KGaA, Frankfurterstr. 250,
64293 Darmstadt, Germany

The Abstract of this lecture is not available!

The Abstract of this lecture is not available!

BIOGRAPHIC DATA OF DR. DAVID MUELLER

David Mueller has worked in the field of organic electronics for over 12 years. He received his diploma and PhD from the University of Munich, specializing in physical organic chemistry and organic light emitting diodes. After postdoctoral research at the University of Cologne, he joined the organic electronics team at Avecia, Manchester in 2004 and more recently, Merck, following the acquisition of the Avecia group in March 2005. At Merck's Technical Centre in Chilworth,



Southampton, he was leading a group responsible for the development, formulation and integration of active and passive materials in organic electronic devices, thereby mainly focusing on organic transistors. In mid of 2009 he returned to Germany to join the Merck head quarter in Darmstadt. He is currently responsible for the Merck activities and investments in the German cluster of excellence "Forum organic Electronics" in Heidelberg.

Part V:

Solar cells / OPV 1

The abstract of the lecture Professor Jabbour
entitled
“Interfacial effects in photovoltaics and progress in
printed Quantum Dot LEDs”
was not available to the editorial deadline.

The abstract of the lecture Professor Brabec
entitled

“Reliability and failure mechanisms of
organic solar cells”

was not available to the editorial deadline.

ON THE RELATION BETWEEN THERMAL TRANSFORMATIONS AND MORPHOLOGICAL STABILITY OF POLYMER:FULLERENE SOLAR CELLS

G. VAN ASSCHE¹; J. ZHAO¹; F. DEMIR¹; N. VAN DEN BRANDE¹; S. BERTHO²;
D. VANDERZANDE²; B. VAN MELE¹

¹Vrije Universiteit Brussel; Research unit Physical chemistry and Polymer Science; Pleinlaan 2; 1050 Brussels; Belgium

²Institute for Materials Research; Hasselt University; Wetenschapspark 1; 3590 Diepenbeek; Belgium

High-performance polymer solar cells based on regioregular poly(3-hexyl thiophene) (P3HT, donor) and [6,6]-phenyl C₆₁-butyric acid methyl ester (PCBM, acceptor) represent the current state-of-the-art in organic photovoltaics.^{1,2} Reaching the highest efficiencies for these devices requires an optimum bulk heterojunction morphology, consisting of a co-continuous network with a maximum interface area and a mean domain size of 5-10 nm.³⁻⁶ Such a morphology can be approached by post-production thermal annealing processes, during which reorganization, aggregation, and further crystallization within the initially amorphous or nanocrystalline deposited films result in the formation of “larger” well-organized domains.⁷⁻¹³ In general, the initial morphology of the deposited blend films is the result of a kinetically frozen phase separation or crystallization. Consequently, both thermodynamic and kinetic parameters are responsible for the morphology obtained.^{6,14,15} In this contribution, we will present a comprehensive study of the phase behaviour of P3HT/PCBM blends over the whole composition range and compare it to the phase behaviour obtained for other conjugated polymers. These phase diagrams are of key importance to gain a fundamental understanding and control of morphology development in said blends of donor-acceptor materials.^{16,17} Moreover, it should be emphasized that the phase diagram is essential in the understanding of the long-term stability of the blended film morphology and consequently of the photovoltaic performance of the corresponding solar cells.¹⁸ It has in fact been demonstrated that long-term operation of various types of polymer/PCBM solar cells (including P3HT/PCBM) at elevated temperatures results in a significant change of the film morphology and a remarkable decrease of the photovoltaic performance.¹⁹

In this paper, the use of advanced thermal analysis techniques to obtain the phase diagram for polymer/PCBM blends will be discussed. The use of conventional and modulated temperature differential scanning calorimetry (DSC and MTDSC, respectively), as well as fast-scanning differential scanning calorimetry (RHC) to obtain the transition temperatures and kinetics will be discussed.

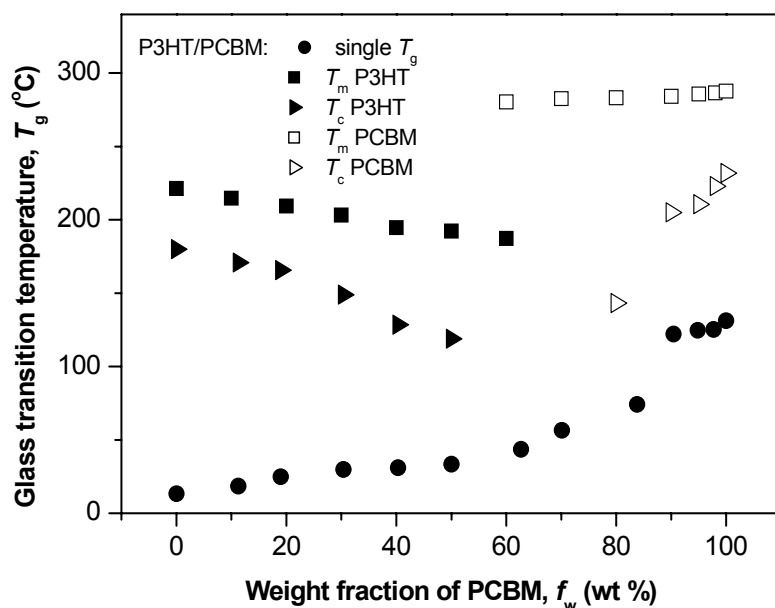


Figure 1. Phase diagram of P3HT:PCBM blends displaying the melting T_m , crystallization T_c , and glass transition T_g temperatures.

The knowledge about the phase diagram of these blends has important implications on the operating window for the thermal annealing and on the expected long-term thermal stability of the morphology in solar cell applications.

The isothermal annealing of P3HT:PCBM blends was studied from 60°C to 160°C using RHC. As the heat flow during annealing is too small to be measured accurately, the subsequent melting of the annealed sample was studied (Figure 2). In many cases, crystallization during heating is observed prior to melting.

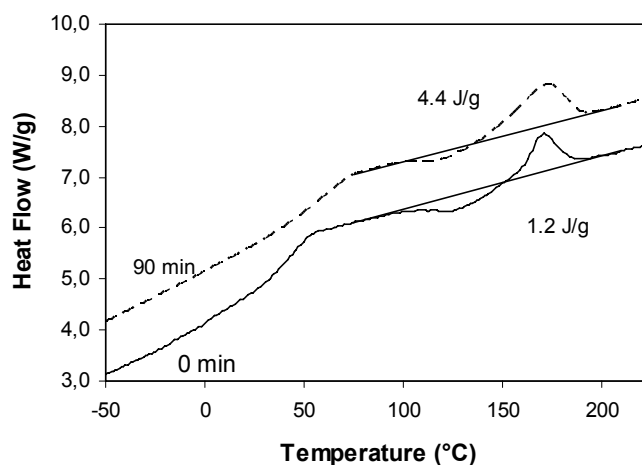


Figure 2. Heating at 250 K/min of a quenched P3HT:PCBM 50:50 blend after isothermal annealing at 60°C, showing the glass transition, cold crystallization, and melting.

Plotting the melting enthalpy as a function of the annealing time, accounting for crystallization during heating, results in sigmoidal curves (Figure 3). These curves were fitted using the Avrami equation,²⁰ to obtain the time constant for crystallization. The reciprocal of the Avrami time constant is a measure for the crystallization rate.

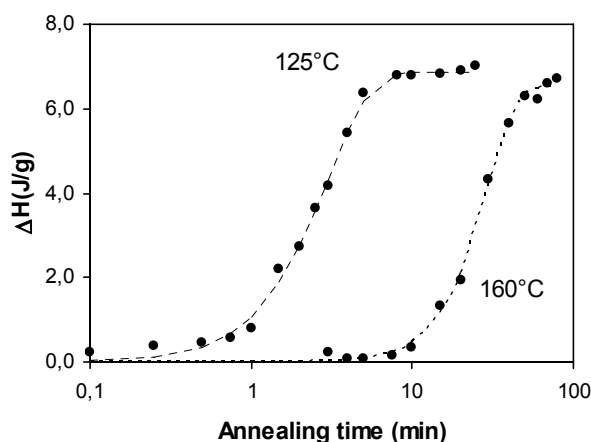


Figure 3. Melting enthalpy as a function of annealing time for a P3HT:PCBM 50:50 blend for annealing at 125°C and 160°C. Dashed lines are fits of the Avrami model for crystallization.

Plotting the reciprocal of the time constant versus the annealing temperature results in a bimodal plot, as has been observed previously for homopolymers.²¹ The crystallization rate rapidly decreases as the annealing temperature approaches the melting temperature or the glass transition temperature the 50:50 P3HT:PCBM blend, as usually observed in homopolymers. Nevertheless, the results indicate that at 60°C, about 25°C above the glass transition temperature, the crystallization is nearing completion within about 60 minutes.

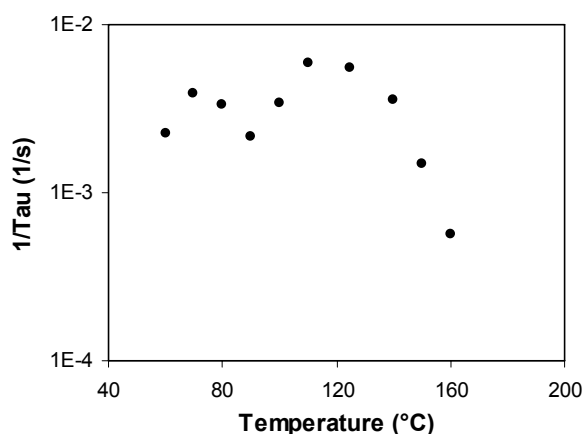


Figure 4. Plots of the crystallization rate $1/\tau$ for a P3HT:PCBM 50:50 blend as determined by fitting the Avrami model for crystallization.

At 110°C, it takes less than two minutes for the melting enthalpy to reach half of the final value, and less than eight minutes to reach 95% of the final value. Microscopy studies of the morphological development on solar cells have shown that at 110°C PCBM needles are formed and continuously grow over hours, gradually decreasing the efficiency.¹⁹ During this continued morphological development is a gradual growing of larger, more stable crystals, at the expense of smaller, less stable ones. The further increase in melting enthalpy involved in this perfecting process is too small to be measured using the presented calorimetric method. However, for an optimal efficiency, reaching a sufficiently high crystallinity is needed, as it improves the charge mobility, but growing larger needles is not expected to be beneficial.

Using the calorimetric approach presented, the initial crystallization involved in the annealing process can be followed quantitatively in a straightforward manner. The results indicate that the crystallization is advancing in a sigmoidal fashion versus annealing time and that its rate is going through a maximum as a function of the annealing temperature. They also strengthen the understanding of the stability of polymer solar cells.

- (1) Li, G.; Shrotriya, V.; Huang, J.; Yao, Y.; Moriarty, T.; Emery, K.; Yang, Y. *Nat. Mater.* 2005, 4, 864-868.
- (2) Ma, W.; Yang, C.; Gong, X.; Lee, K.; Heeger, A. J. *Adv. Funct. Mater.* 2005, 15, 1617-1622.
- (3) Halls, J. J. M.; Walsh, C. A.; Greenham, N. C.; Marseglia, E. A.; Friend, R. H.; Moratti, S. C.; Holmes, A. B. *Nature* 1995, 376, 498-500.
- (4) Yu, G.; Gao, J.; Hummelen, J. C.; Wudl, F.; Heeger, A. J. *Science* 1995, 270, 1789-1791.
- (5) Yu, G.; Heeger, A. J. *J. Appl. Phys.* 1995, 78, 4510-4515.
- (6) Thompson, B. C.; Frechet, J. M. J. *Angew. Chem. Int. Ed.* 2008, 47, 58-77.
- (7) Riedel, I.; Parisi, J.; Dyakonov, V.; Lutsen, L.; Vanderzande, D.; Hummelen, J. C. *Adv. Funct. Mater.* 2004, 14, 38-44.
- (8) Yang, X.; Loos, J.; Veenstra, S. C.; Verhees, W. J. H.; Wienk, M. M.; Kroon, J. M.; Michels, M. A. J.; Janssen, R. A. J. *Nano Lett.* 2005, 5, 579-583.
- (9) Mihailetschi, V. D.; Koster, L. J. A.; Blom, P. W. M.; Melzer, C.; de Boer, B.; van Duren, J. K. J.; Janssen, R. A. J. *Adv. Funct. Mater.* 2005, 15, 795-801.
- (10) Riedel, I.; von Hauff, E.; Parisi, J.; Martin, N.; Giacalone, F.; Dyakonov, V. *Adv. Funct. Mater.* 2005, 15, 1979-1987.

- (11) Swinnen, A.; Haeldermans, I.; vande Ven, M.; D'Haen, J.; Vanhoyland, G.; Aresu, S.; D'Olieslaeger, M.; Manca, J. *Adv. Funct. Mater.* 2006, 16, 760-765.
- (12) Warman, J. M.; de Haas, M. P.; Anthopoulos, T. D.; de Leeuw, D. M. *Adv. Mater.* 2006, 18, 2294-2298.
- (13) Loi, M. A.; Toffanin, S.; Muccini, M.; Forster, M.; Scherf, U.; Scharber, M. *Adv. Funct. Mater.* 2007, 17, 2111–2116.
- (14) Yang, X.; Loos, J. *Macromolecules* 2007, 40, 1353-1362.
- (15) Moule, A. J.; Meerholz, K. *Adv. Mater.* 2008, 20, 240-245.
- (16) Swinnen, A.; Zhao, J.; Van Assche, G.; Vanderzande, D.; D'Olieslaeger, M.; Manca, J.V.; Van Mele, B., in *Proceedings of the Society of Photo-Optical Instrumentation Engineers (SPIE) - Organic Photovoltaics VIII*, eds. Kafafi Z. H.; Lane P. A., Volume: 6656, 65619-65619 (2007).
- (17) Muller, C.; Ferenczi, T. A. M.; Campoy-Quiles, M.; Frost, J. M.; Bradley, D. D. C.; Smith, P.; Stingelin-Stutzmann, N.; Nelson, J. *Adv. Mater.* 2008, 20, 3510-3515.
- (18) Zhao, J.; Swinnen, A.; Van Assche, G.; Manca, J.; Vanderzande, D.; Van Mele, B. J. *Phys. Chem. B* 2009, 113, 1587-1591.
- (19) Bertho, S.; Janssen, G.; Cleij, T. J.; Conings, B.; Moons, W.; Gadisa, A.; D'Haen, J.; Goovaerts, E.; Lutsen, L.; Manca, J.; Vanderzande, D. *Sol. Energy Mater. Sol. Cells* 2008, 92, 753-760.
- (20) Avrami, M. *J. Chem. Phys.* 7 (1939) 1103 ; 8 (1940) 212.
- (21) Supaphol, P.; Spruiell, J.E. *Polymer* 42 (2001) 699–712

BIOGRAPHIC DATA OF PROFESSOR GUY VAN ASSCHE

Prof. Dr. ir. Guy Van Assche behaalde zijn doctoraat aan de Vrije Universiteit Brussel. Na een jaar aan het Kyoto Institute of Technology, startte hij een postdoc rond geavanceerde thermische analyse technieken, waaronder modulated temperature DSC, microcalorimetrie en thermische analyse op een sub-100 nm schaal. Deze worden toegepast in het kader van reactieve polymeersystemen, fasescheiding in waterige polymeeroplossingen en polymeerblends. Momenteel werkt hij aan de ontwikkeling van een nieuwe meettechniek die simultane rheologische en calorimetrische metingen toelaat op enkele milligram materiaal. Hij doceert rond de kinetiek van chemische en fysische processen.



Prof. Dr. ir. Guy Van Assche received his PhD from the Vrije Universiteit Brussel in 1998. After one-year stay at the Kyoto Institute of Technology, he continued as a postdoctoral researcher of the Research Foundation - Flanders, focussing on the development and application of advanced thermal analysis techniques, applied in the context of reactive polymers, polymer solutions, and nano-structured polymer systems, including nanocomposites and, more recently, photovoltaic blends. The main techniques of interest are modulated temperature DSC, rapid-scanning DSC for the analysis of small samples or thin films, AFM-based thermal analysis techniques, and the development of a technique for simultaneous rheological and calorimetric analysis. Since 2001 he is part-time lecturer at the Vrije Universiteit Brussel.

IMPROVED HOLE COLLECTION IN ORGANIC SOLAR CELLS USING DITHIAPYRRANYLIDENE ULTRA-THIN FILMS AS ANODIC INTERLAYERS

Stéphane Berny,^{1,2} Ludovic Tortech,^{1,2} Michelle Véber³ and Denis Fichou^{1,2}

¹CEA-Saclay, Groupe Nanostructures & Semi-Conducteurs Organiques,
IRAMIS/SPCSI, 91191 Gif-sur-Yvette, France

²Institut Parisien de Chimie Moléculaire, UMR CNRS 7201,
Université Paris VI, France

³Université Paris XI, Orsay, France

The Abstract of this lecture is not available!

Stéphane BERNY

Birth 13/10/1983 in Paris
French Nationality

4B Passage du Chemin de Fer
91400 ORSAY
(+33) 6 71 50 60 43
stephane.berny@cea.fr

- RESEARCH EXPERIENCE -----

- Since Dec. 2007 **Ph. D. Student in Materials Science** **CEA, Saclay (91)**
Doctoral Student with Pr. D. Fichou at the Nanostructures and Organic Semiconductors Laboratory on Organic Solar Cells and Organic Spintronics (expected submission: October 2010).
- 2007 (6 months) **Semi-Industrial Research internship in Materials Science** **IS2M, Mulhouse (68)**
SEB Industry, Rumilly (65)
Master Student with Pr. M. F. Vallat at the Adhesion Laboratory of IS2M and with Dr. S. Tuffe at the Materials Research Center of TEFAL.
Thesis title: "*Bulk and Surface Properties of Novel Ceramic Coatings*".
- 2006 (2 months) **Research internship in Chemistry and Materials Physics** **IMN, Nantes (44)**
Master Student with Pr. J. Wéry and J. L. Duval at the Nanostructures and Materials Physics Laboratory of IMN.
Thesis title: "*Towards the Organic Quantic Confining: Photoluminescence properties of PPV-based Nanofibres and Chemical Synthesis of MEH-PPV*".
- 2005 (2 months) **Engineering Internship in Chemistry** **KODAK Industry, Châlon-sur-Saône (71)**
Engineering Student with Dr. M. Perrin at the Chemical Synthesis Research Center of KODAK.
Thesis title: "*Chemical Synthesis of Organic Pigments*".

--ACADEMIC QUALIFICATIONS --

- Since Dec. 2007 **Ph. D.**, Materials Science, CNRS/CEA, Saclay, France.
- 2005 – 2007 **Master Student**, Nano-Objects Physics and Materials Science, University of Haute Alsace, Mulhouse, France - Valedictorian - Upper Second Class Honours.
- 2004 – 2007 **Master's Degree in Engineering**, Chemistry, ENSCMu (Ecole Nationale de Chimie de Mulhouse), Mulhouse, France - www.enscmu.uha.fr.

---SCIENTIFIC PUBLICATIONS ---

5. "Dithiapyranylidenes (DITPY) as Efficient Hole Collection Interfacial Layers in Organic Solar Cells"
S. Berny, L. Torteck, D. Fichou, *Adv. Func. Mat.*, **2010** (submitted).
4. "DITPY- ϕ_4 Tunnel Barriers for the Magnetic Decoupling of Hybrid Organic-Inorganic Ferrite/DITPY- ϕ_4 /Co Heterostructures"
S. Berny, S. Matzen, J.-B. Moussy, L. Torteck, D. Fichou, *Appl. Phys. Lett.*, **2010** (submitted).
3. "2D Self-Assembly Networks of Alcoxy-Dithiapyranylidenes"
S. Berny, S. Quentin, L. Torteck, F. Silly, D. Fichou, **2010** (in preparation).
2. "Influence of a g-Al₂O₃ crystalline barrier on the Growth and Magnetic Behaviour of Ferrite/Al₂O₃/DITPY- ϕ_4 /Co Heterostructures"
S. Berny, S. Matzen, J.-B. Moussy, L. Torteck, D. Fichou, *J. Mater. Chem.*, **2010** (to be submitted in a themed issue in connection with E-MRS 2010).
1. "Dipyrranylidenes derivatives as interfacial anodic layers in electronic devices"
S. Berny, L. Torteck, D. Fichou, *French Patent*, PCT/FR2009/001201, **2009**.

--- MEETINGS IN 2010----

- 03 - 2010 **Meeting of Local Probe Microscopy**, oral communication and poster presentation. Mittelwihr, France
- 05 - 2010 **TPE 10**, oral communication and poster presentations. Rudolstadt, Germany
- 06 - 2010 **E-MRS 2010**, oral communications. Strasbourg, France

OBSERVATION OF CHARGE-TRANSFER COMPLEX ABSORPTION AND EMISSION IN POLYMER SOLAR CELLS

Martin Presselt, Felix Herrmann, Marco Seeland, Maik Bärenklau, Sebastian Engmann, Roland Rösch, Sviatoslav Shokhovets, Harald Hoppe, Gerhard Gobsch

Experimental Physics I, Institute of Physics & Institute of Micro- und Nanotechnologies, Ilmenau University of Technology, Weimarer Str. 32, 98693 Ilmenau, Germany

In bulk heterojunction organic solar cells an essential step of photocurrent generation is the separation of charges at the donor-acceptor interface due to the generation of charge transfer excitons (CTEs). CTE generation occurs upon transferring either an excited electron from the donor lowest unoccupied molecular orbital (LUMO) to the acceptor LUMO or a hole from the acceptor highest occupied molecular orbital (HOMO) to the donor HOMO if the exciton is generated in the donor or the acceptor material, respectively. The presence of CTEs within bulk heterojunctions constituted of P3HT and PCBM or other donor acceptor blends was revealed by the low energetic emission in the photoluminescence (PL) spectra of the blends¹⁻⁵ arising from charge recombination across the donor-acceptor interface. Indeed, CTE dissociation is the dominant process in P3HT:PCBM bulk heterojunctions as proven by the high external quantum efficiencies (EQE > 65%) in those blends^{6,7}, thus causing weak CT emission intensities¹.

Apart from exciton dissociation the direct excitation of the CTE, i.e. a charge transfer transition from the donor HOMO to the acceptor LUMO, is an alternative way of CTE generation. In analogy to CT emission, CT absorption energies are below the individual bandgaps of the pristine donor or acceptor materials⁸⁻¹³.

Further possibilities inducing absorption features below the bandgap are disorder and defect states¹⁴⁻¹⁶. Disorder or dopants are leading to variations of the energy levels of the pristine polymer. Consequently, transition energies lower than the HOMO-LUMO gap of the pristine polymer become possible due to the molecular orbital (MO) energy fluctuations, i.e. a transition from an energetic HOMO maximum to an energetic LUMO minimum.

Particularly, there is a high interest to study absorption and emission from CTEs since the CTE optical energy gap was shown to correlate linearly with the open circuit voltage V_{OC} of the device^{8,9,17} and is consequently a crucial parameter for the device performance. However, in the case of P3HT:PCBM blends subbandgap absorption was assigned to exponential absorption tails and defect related absorption processes.¹⁴⁻¹⁶ Indeed, in more

recent studies focussing on the subbandgap region in external quantum efficiency (EQE) spectra low energetic contributions are attributed to CTE absorption.^{9,10,13,17} In some of these studies the EQE subbandgap region is fitted via a peak profile to determine the CTE optical energy gap.

In our investigations we detected subbandgap absorption in various P3HT:PCBM blends via photothermal deflection spectroscopy (PDS). In case of low PCBM concentrations (1 – 10 % PCBM content) the subbandgap tails possess exponential character in the EQE spectra too. With higher PCBM fractions the EQE-values in the subbandgap region get raised, possessing a maximum for almost balanced blending ratios. Furthermore, increasing the PCBM fraction goes along with a more pronounced curvature of the EQE spectrum in the subbandgap region, as exemplarily shown in figure 1 for fractions of 1, 10 and 60 % PCBM. For PCBM fractions higher than 60 % the curvature gets reduced, thus yielding exponential tails for PCBM fractions higher than 80 %. These trends indicate that disorder and defect related subbandgap absorption revealed by PDS partially contribute to the photocurrent. Consequently, the EQE subbandgap region was fitted by a Gaussian profile accounting for the non-exponential curvature attributed to CTE absorption by Vandewal *et al.*⁹ and an exponential function accounting for disorder induced absorption tails¹⁵ as illustrated in figure 1.

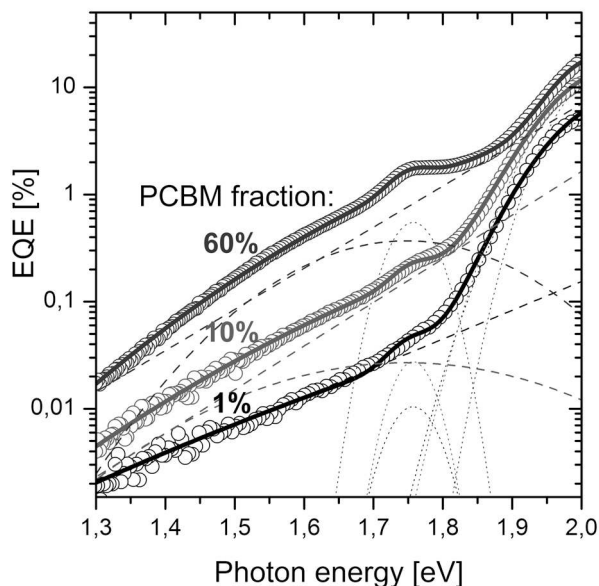


Figure 1: Subbandgap EQE spectra of P3HT:PCBM bulk heterojunction organic solar cells using PCBM weight fractions of 1, 10 and 60 %. The EQE spectra were fitted using Gaussian profiles to describe P3HT and PCBM peaks (dotted lines, centred at 2.03 and 1.76 eV) and the CTE assigned peak as well as an exponential function accounting for disorder and defect induced absorption (dashed straight lines).

Using a Gaussian profile in addition to an exponential function all features of the subbandgap parts (1.3 – 1.7 eV) of the presented EQE spectra could be reliably reproduced. For very low and for very high PCBM concentrations the fits yield negligible amplitudes of the subbandgap Gaussian profiles, thus highlighting the need of using exponential functions to describe the subbandgap EQE spectra reliably.

We gratefully acknowledge financial support from the Deutsche Forschungsgemeinschaft in the frame of SPP 1355 and from the Fonds der Chemischen Industrie.

- (1) Hallermann, M.; Kriegel, I.; Da Como, E.; Berger, J. M.; von Hauff, E.; Feldmann, J. *Advanced Functional Materials* **2009**, *19*, 3662.
- (2) Loi, M. A.; Toffanin, S.; Muccini, M.; Forster, M.; Scherf, U.; Scharber, M. *Advanced Functional Materials* **2007**, *17*, 2111.
- (3) Hallermann, M.; Haneder, S.; Da Como, E. *Applied Physics Letters* **2008**, *93*.
- (4) Veldman, D.; Ipek, O.; Meskers, S. C. J.; Sweelssen, J.; Koetse, M. M.; Veenstra, S. C.; Kroon, J. M.; van Bavel, S. S.; Loos, J.; Janssen, R. A. J. *Journal Of The American Chemical Society* **2008**, *130*, 7721.
- (5) Hasharoni, K.; KeshavarzK, M.; Sastre, A.; Gonzalez, R.; BellaviaLund, C.; Greenwald, Y.; Swager, T.; Wudl, F.; Heeger, A. J. *Journal Of Chemical Physics* **1997**, *107*, 2308.
- (6) Muhsin, B.; Renz, J.; Drue, K. H.; Gobsch, G.; Hoppe, H. *Synthetic Metals* **2009**, *159*, 2358.
- (7) Renz, J. A.; Keller, T.; Schneider, M.; Shokhovets, S.; Jandt, K. D.; Gobsch, G.; Hoppe, H. *Solar Energy Materials And Solar Cells* **2009**, *93*, 508.
- (8) Veldman, D.; Meskers, S. C. J.; Janssen, R. A. J. *Advanced Functional Materials* **2009**, *19*, 1939.
- (9) Vandewal, K.; Gadisa, A.; Oosterbaan, W. D.; Bertho, S.; Banishoeib, F.; Van Severen, I.; Lutsen, L.; Cleij, T. J.; Vanderzande, D.; Manca, J. V. *Advanced Functional Materials* **2008**, *18*, 2064.
- (10) Vandewal, K.; Oosterbaan, W. D.; Bertho, S.; Vrindts, V.; Gadisa, A.; Lutsen, L.; Vanderzande, D.; Manca, J. V. *Applied Physics Letters* **2009**, *95*.
- (11) Panda, P.; Veldman, D.; Sweelssen, J.; Bastiaansen, J.; Langeveld-Voss, B. M. W.; Meskers, S. C. J. *Journal Of Physical Chemistry B* **2007**, *111*, 5076.
- (12) Benson-Smith, J. J.; Goris, L.; Vandewal, K.; Haenen, K.; Manca, J. V.; Vanderzande, D.; Bradley, D. D. C.; Nelson, J. *Advanced Functional Materials* **2007**, *17*, 451.
- (13) Vandewal, K.; Goris, L.; Haeldermans, I.; Nesladek, M.; Haenen, K.; Wagner, P.; Manca, J. V. *Thin Solid Films* **2008**, *516*, 7135.
- (14) Goris, L.; Haenen, K.; Nesladek, M.; Wagner, P.; Vanderzande, D.; De Schepper, L.; D'Haen, J.; Lutsen, L.; Manca, J. V. *Journal Of Materials Science* **2005**, *40*, 1413.
- (15) Goris, L.; Poruba, A.; Hod'akova, L.; Vanecek, M.; Haenen, K.; Nesladek, M.; Wagner, P.; Vanderzande, D.; De Schepper, L.; Manca, J. V. *Applied Physics Letters* **2006**, *88*.
- (16) Goris, L.; Poruba, A.; Purkrt, A.; Vandewal, K.; Swinnen, A.; Haeldermans, I.; Haenen, K.; Manca, J. V.; Vanecek, M. *Journal Of Non-Crystalline Solids* **2006**, *352*, 1656.
- (17) Vandewal, K.; Tvingstedt, K.; Gadisa, A.; Inganas, O.; Manca, J. V. *Nature Materials* **2009**, *8*, 904.

Part VI:

OFET and devices

FROM ULTRA-THIN MODEL SYSTEMS TO FLEXIBLE THIN FILM TRANSISTORS

V. WAGNER*; B. GBUREK; T. BALSTER

Jacobs University Bremen; School of Engineering and Science; Campus Ring 1; 28759 Bremen; Germany

Due to options of wet chemical and low temperature processing together with low cost printing qualitatively new fields of applications for organic/polymeric thin film transistors have become possible. However, improved performance, e.g. by smaller channel lengths, is a major issue. For thiophene-based devices on rigid as well as flexible substrates experimental determination of scaling limits towards smaller dimensions are discussed and compared with theoretical predictions. Standard field-effect transistor (FET) theory predicts a maximum bandwidth of $\mu V_{DS}/L^2$ (linear regime case, μ = mobility, L = channel length, V_{DS} = applied drain-source voltage). However, this is not observed in AC measurements of organic transistor bandwidths [1,2]. Crucial additional limitations for the AC bandwidth not accounted for in the simple formula given above are parasitic capacitances and contact resistance. Most important parasitic capacitances are between the gate electrode and the source or drain electrode of the transistor. To assure a proper covering of the gate electrode with the channel area, the gate electrode has to be structured larger than the channel area typically by the patterning resolution accuracy and the obtainable relative alignment accuracy between different layers. Often for interdigitated source/drain structures the gate electrode will cover the whole interdigitated transistor area and result in parasitic capacitances originating from the full source/drain electrode area with the gate. Detailed analysis yields a correction factor a for the maximum frequency of $a = C_{ch} / (C_{ch} + C_{parasitic}) < 1$, with C_{ch} the channel capacitance with the gate and $C_{parasitic}$ the source+drain electrode capacitance with the gate. Contact properties between the channel and the source and drain electrodes can be described for larger current levels by a channel width W normalized specific contact resistance $\rho_C = (R_{C,S} + R_{C,D}) \cdot W$. Such contact resistance reduces the effective drain voltage in the channel (linear regime) by $\Delta V_{DS} = I_D \cdot \rho_C / W$ and modifies the AC response of the transistor. Thus the maximum bandwidth is further reduced by a second correction factor $c = L / (L + L_C) < 1$, with L the channel length and $L_C = \rho_C / R_S$ the effective contact length. Here, the sheet resistance R_S of the transistor channel is given by $R_S = 1 / (\mu C_i (V_{GS} - V_{th}))$ with C_i the gate-channel capacitance per area and V_{th} the threshold voltage. In summary, the obtainable maximum bandwidth scales actually by including both correction factors with $a \cdot c \cdot \mu V_{DS} / L^2$ and is usually significantly

smaller than expected. It is shown for small molecules and for P3HT polymer, that channel length below a few microns usually does not further improve the bandwidth but show even a degradation of performance with decreasing channel length.

Since the contact resistance is identified as one of the crucial limiting performance factors, proper analysis and determination of this important quantity is required. While the transfer line method is one option to obtain the contact resistance data for a materials system from a sequence of transistors with decreasing channel length, it has specific drawbacks. First, due to the device-to-device performance fluctuation the determined contact resistance has a rather large error bar especially for small contact resistances, second, only the total contact resistance at source and drain together is obtained and no information is obtained if charge injection or charge extraction represents the major bottleneck at the contact. Alternatively, Kelvin probe microscopy can provide a detailed electrical potential mapping of the channel and thus detailed contact properties but is restricted to from the outside directly accessible channels and vacuum environment. In this context we show that contact resistance can be accurately determined via mapping the channel potential by patterning additional sensing electrodes into the active transistor channel. This approach allows for systematic contact property analysis also in application-relevant buried channels (top-gate configuration) for various materials and active layer thicknesses. By this approach various systems are analyzed, e.g. P3HT-field-effect transistors in (encapsulating) top-gate configuration on flexible plastic foil substrates.

- [1] V. Wagner, P. Wöbkenberg, A. Hoppe, J. Seekamp, *Appl. Phys. Lett.* 89 (2006) 243515.1-3
- [2] A. Hoppe, D. Knipp, B. Gburek, A. Benor, M. Marinkovic, V. Wagner, *Org. Elec.* 11 (2010) 626-631

**BIOGRAPHIC DATA OF
PROFESSOR VEIT WAGNER**



1987	Training at IBM research lab Rüschlikon, Zürich, Switzerland
1985-1991	Diploma in Physics, RWTH-Aachen, Germany
1991-1995	Ph.D. in Physics, TU-Berlin and RWTH-Aachen, Germany
1995	awarded „Borchers-Plakette“ of the RWTH-Aachen
1995-1996	Postdoctoral Fellow, Univ. Notre-Dame de la Paix, Namur, Belgium
1996-2001	Habilitation in Physics, University of Würzburg, Germany
since 2002	Professor of Physics, Jacobs University Bremen, Germany
2009	sabbatical stay, Stanford University, California, USA
since 2010	speaker of the Research Center for Functional Materials and Nanomolecular Science at Jacobs University Bremen

THE INFLUENCE OF GAUSSIAN DISORDER ON THE PERFORMANCE OF ORGANIC DEVICES

G. PAASCH^{1*}, S. SCHEINERT²

¹ Leibniz Institute for Solid State and Materials Research Dresden – IFW Dresden, PF 270116, D-01171 Dresden, Germany

² Ilmenau University of Technology, Institute for Solid State Electronics, PF100565, D-98684 Ilmenau, Germany

Introduction: Since the pioneering work of Bäessler [1] much progress has been achieved in understanding hopping transport in disordered organics. Mainly based on the analysis of transport data, it is now usually assumed that these materials are characterized by a distribution of HOMO and LUMO states which is close to a Gaussian one, and which is sometimes approximated by an exponential one in a limited energy range. Actually, this Gaussian density of states (DOS) might be only that part of the total DOS which is close to the gap. For a long time it was essentially the temperature dependency of the mobility which seemed to be of interest. But then Vissenberg and Matters [2] found that hopping in an exponential DOS leads to a strong dependency of the mobility on the carrier concentration. Later Tanase *et al.* [3] realized that the extreme difference between the mobility values measured in diodes and field-effect transistors result just from this concentration dependency. The presence of the Gaussian density of hopping transport states influences the performance of organic electronic devices in different manner. We present here an overview emphasizing recent achievements.

Mobility dependencies on carrier concentration and field: The current characteristics of organic field-effect transistors (OFET) show often a disadvantageous non-linearity at low drain voltages. For bottom contact (BOC) OFETs, Schottky contacts are often stated as origin of the non-linearity. It has been shown by us by a mixed mode simulation that for large ideality factors a Schottky contact only at drain leads to such a non-linearity. But with the same Schottky contacts at drain and source the effect is covered by the high resistance of the contact at source. It is demonstrated with detailed two-dimensional simulations that the combination of the presence of Schottky contacts with a field dependence of the mobility can cause the non-linearity. For the mobility we use the field dependent Pool/Frenkel model, and the models of Limketai *et al.* [4] and

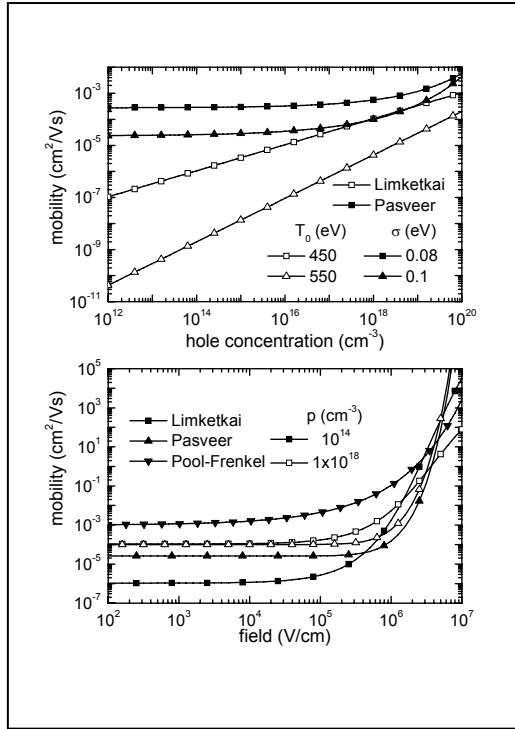


Fig 1. Dependency of the mobility models on the carrier concentration and on the field. T_0 is the decay constant for the exponential DOS in the Limketkai model and σ is the variance of the Gaussian DOS in the Coehoorn/Pasveer model. Fig. taken from [7]

Pasveer/Coehoorn *et al.* [5,6] which depend in addition on the carrier concentration. The dependencies of these models on the carrier concentration and on the field are shown in Fig.1 [7]. There is a clear difference in the concentration dependence. Whereas the Pasveer/Coehoorn model approaches at low concentration a constant value, the Limketkai model shows no saturation. At high concentrations the mobility resulting from the

Pasveer/Coehoorn model increases stronger than the one obtained with the Limketkai model. The field dependency is shown in one case for a low concentration in the concentration dependent models for comparison with the Pool/Frenkel model. The critical field strength at which the increase in the mobility becomes important is largest for the Pasveer/Coehoorn model. Above the critical field the Pasveer/Coehoorn model yields a stronger increase than the other models. For the two concentration dependent models also the field dependence is depicted for a high concentration. Then the increase with the field is stronger and at the same time the critical field is slightly decreased.

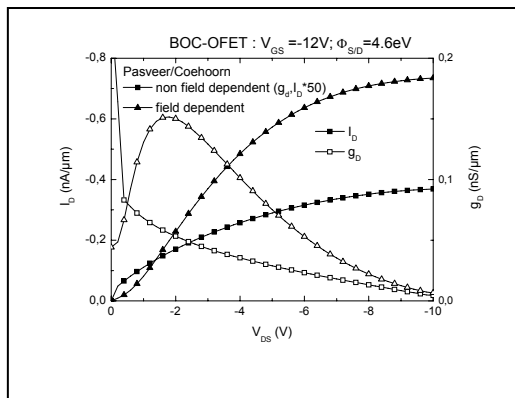


Fig.2. Comparison of the output characteristics and of the drain conductance obtained with the Pasveer/Coehoorn model with and without dependence of the mobility on the field. BOC-OFET at $V_{GS}=-12$ V and Schottky contacts at source and drain (low contact work function $\Phi_{S/D}=4.6$ eV). Fig. taken from [7].

The influence of these dependencies on the device performance has been clarified by simulations. Simulated profiles of concentrations and fields lead to the understanding of the mechanism causing the non-linearity [7]. This mechanism is especially effective for the Pasveer/Coehoorn model which is based on the assumption of a Gaussian DOS for the hopping transport states. In Fig.2 output characteristics and drain conductance are shown

for a BOC OFET calculated with a constant mobility and with the Pasveer/Coehoorn model. It is clearly seen that the non-linearity of the output characteristics (maximum of the drain conductance at finite drain-source voltage) is caused by the special dependencies of the mobility if the source/drain work function is low, i.e. if these contacts are of the Schottky type.

Space charge layers in MIS structures in equilibrium: Space charge layers (SCL) in metal-insulator-semiconductor (MIS) structures are decisive for the operation of field-effect transistors (FET). For many organic semiconductors, transport takes place as hopping in Gaussian or exponentially distributed states. However, existing theoretical descriptions of SCL and advanced device simulation programs suppose a density of states other than a Gaussian or an exponential, employing often the non-degenerate limit for the concentrations. We summarize results of a simulation [8] study for the MIS structure as the basic module of the FET. For broader distributions, the densities deviate strongly from the non-degenerate limit which leads indeed in a MIS structure to a strong deviation of the dependence of the surface electric field (and hence the areal charge) on the surface potential. However, as one can control only the gate voltage directly, the dependency on this quantity determines device operation. For the variations of the layer thickness and gate insulator thickness, and doping in the wide range of interest, this dependency deviates only slightly from the non-degenerate approximation, essentially in the depletion region by a flat-band voltage shift. In the accumulation region, which is determinative for FET operation, the remaining deviation can be removed almost perfectly by considering this flat-band voltage shift.

Band bending and interface dipole at a organics-metal contact: Considered is a thin semiconducting layer on a metal substrate which was extensively investigated by photoelectron spectroscopy to characterize the metal-organics interface occurring at the source/drain contact of FETs and as anode and cathode in organic light emitting diodes. For the thin organic layer on a metal substrate, numerical simulations [8] confirm the applicability of an analytical approximation for band bending and floating potential [9] for the non-degenerate case and for the exponential distribution. Indeed, for small barriers at the interface, a band bending of up to the order of 100meV can occur within the first two nm near the interface. In the interpretation of photoemission data such contribution will appear as part of the measured interface dipole.

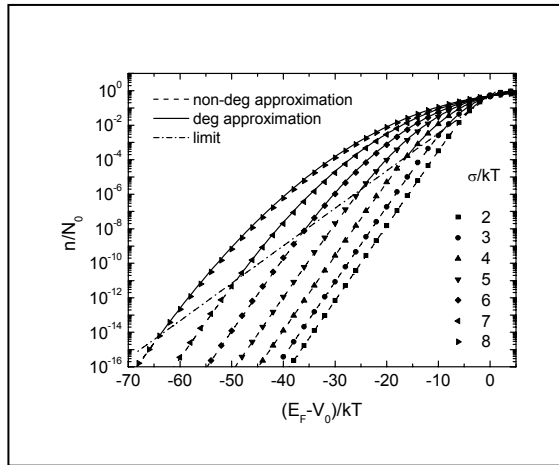


Fig.3. Dependencies of the Gauss-Fermi integral on the Fermi energy relative to the center of the Gaussian DOS for selected values of the variance σ/kT : From numerical integration - only symbols, and the approximations in the non-degenerate and degenerate regions (below and above a limit separating both). The two approximations match continuously and differentiable at the limit. Fig. taken from [10]

Carrier concentration: For the full numerical device simulation one has to solve simultaneously the continuity equations for electrons and holes containing the drift-diffusion equations for the currents, and the Poisson equation, containing all densities of charged species. There occurs a serious problem. The dependency of the carrier density on the local position of the (quasi) Fermi energy needed in the device simulation can be obtained for the Gaussian DOS only by numerical integration. Such procedure has not yet been implemented in any of the advanced device simulation programs. And if implemented, the numerical efficiency of the programs will be significantly reduced. Thus, for a Gaussian density of states (DOS) of the HOMO or LUMO the charge carrier density is needed as the integral over the DOS multiplied with the Fermi-Dirac distribution. We denote this normalized quantity as the Gauss-Fermi integral $G=n/N_0$. It cannot be evaluated analytically and, similarly as in the case of the Fermi-Dirac integral $F_{1/2}$, an analytical approximation is needed for efficient device simulation. We developed such an approximation [10] with different expressions in the non-degenerate and degenerate regions with a continuous and differentiable transition between both regions. The approximation can be implemented in existing device simulation programs and is also applicable to traps with a Gaussian DOS.

Einstein relation: A Gaussian distribution of the hopping transport states modifies the Einstein relation considerably. One has then to use the well-known generalized Einstein relation, which again can be evaluated only numerically. However, with the analytical approximations [10] described before, one obtains also for the Einstein relation in this case a valuable analytical approximation.

References

- 1 H. Bässler, *physica status solidi B*, 175, 15 (1993).
- 2 M.C.J.M. Vissenberg, M. Matters, *Phys. Rev. B* 57, 12964 (1998).
- 3 C. Tanase, E. J. Meijer, P. W. M. Blom, and D. M. de Leeuw, *Phys. Rev.Lett.* **91**, 216601 (2003).
- 4 B. N. Limketkai, P. Jadhav, and M. A. Baldo, *Phys. Rev. B* **75**, 113203 (2007).
- 5 R. Coehoorn, W. F. Pasveer, P. A. Bobbert, and M. A. J. Michels, *Phys. Rev. B* **72**, 155206 (2005).
- 6 W. F. Pasveer, J. Cottaar, C. Tanase, R. Coehoorn, P. A. Bobbert, P. W. M. Blom, D. M. de Leeuw, and M. A. J. Michels, *Phys. Rev. Lett.* **94**, 206601, (2005).
- 7 S. Scheinert, G. Paasch, *J. Appl. Phys.* **105**, 014509 (2009).
- 8 G. Paasch, S. Scheinert, *J. Appl. Phys.* **101**, 024514 (2007).
- 9 G. Paasch, H. Peisert, M. Knupfer, J. Fink, S. Scheinert, *J. Appl. Phys.* **93**, 6084 (2003).
- 10 G.Paasch, S. Scheinert, *J. Appl. Phys.*, in press.

BIOGRAPHIC DATA OF PROFESSOR DR. RER. NAT. HABIL. GERNOT PAASCH

Degrees

- Diplom-Physiker (1967, Technical University Dresden)
- Dr. rer. nat. (1970, Technical University Dresden)
- Dr. sc. nat. (1976; converted into Dr. rer. nat. habil. 1991, Technical University Dresden)



Where I have been

- Technical University Dresden (1967-1977)
- Lomonossov Moscow State University and Institute of Physical Problems Moscow (Postdoc with Prof. M.I. Kaganov, Group of I.M. Lifshiz, 1974-1975)
- Martin- Luther- University Halle- Wittenberg, Dozent (1977-1979)
- Technical University Ilmenau, full Professor for Theoretical Physics (1979-1987)
- Institute for Solid State and Materials Research (since 1988) (formerly Zentralinstitut für Festkörper- und Werkstofforschung), senior scientist, with research Groups Conducting Polymers, Electrochemistry and Conducting Polymers, later with the Group for Theoretical Solid State Physics.
- Technical University Ilmenau, Guest Professor for Nanoelectronics 1996-1998
- Retired since 2007, now with Group Electronic and Optical Properties (part-time employed) at the Leibniz Institute of Solid State and Materials Research

Research

- Conjugated (conducting) polymers: Transport properties, organic devices as organic LED and OFET, systems with polarons and bipolarons as charged states, space charge layers
- Electrochemical impedance spectroscopy and cyclic voltammograms of conducting polymers
- Other low dimensional systems as charge density wave conductors (transport)
- Plasmon dispersion in special low dimensional systems (direct determination of band structure data)
- Microelectronics: Deep submicron scaling of MOSFETs and vertical FETs, non-volatile memories, SOI

PRINTED CMOS-LIKE INVERTERS FOR FAST-SWITCHING ORGANIC LOGIC CIRCUITS

M. CAIRONI^{1*}; E. GILI¹; H. SIRRINGHAUS¹

¹ Cavendish Laboratory, JJ Thomson Avenue, Cambridge CB3 0HE, UK

Direct-write, solution-based, additive printing techniques¹ are an emerging and very versatile approach for low-cost, large-area manufacturing of electronic circuits. Despite this, the poor resolution achievable with standard tools represents a limit for the operative frequencies of printed circuits. This issue was successfully addressed by developing a self-aligned inkjet printing (SAP) technique² based on commercial drop-on-demand systems which allows the fabrication of metal electrodes with sub-micrometer gaps^{3,4}. The SAP technique is based on printing a first conductive electrode line, modifying its surface with a self-assembled monolayer (SAM) to become repulsive to the ink, and then printing a second conductive electrode line along the edge of the first electrode, such that the ink droplets flow off the first conductive electrode and dry in close proximity, but not in electrical contact with the first printed electrode. This demonstration opened the question whether such high resolution printing technique could be capable of defining electrode arrays with gaps on the 100 nm scale without electrical shorts and with a sufficient patterning yield and uniformity. Here we report on an improved configuration for SAP contacts, which enabled the fabrication of low leakage metal electrodes arrays with gaps of 200 – 500 nm with surprisingly high yields of 94-100%⁵. In this new configuration the two electrodes are printed one at 90° with respect to the other and the channel width (30 – 80 μm) is limited and defined by a single droplet. This allows to carefully control the dewetting process, since this is determined by the fluid-dynamics of a single droplet, instead of a series of droplets interacting with each other as in our previous work^{3,6}. This is not only of high practical importance, since it moves the technique within reach of applications, but it also facilitates fundamental scientific understanding of the SAP process. Moreover, given the limited width of the contacts, it is feasible to correlate defects along the channel (e.g. observed with SEM) with the leakage current, providing a powerful tool for failure analysis. In Figure 1 we report the yield and leakage currents of a 6 x 12 array of SAP gold electrodes where all 72 contacts show a leakage current lower than 2 pA at an applied bias of 10 V. Breakdown voltages higher than 2 MVcm⁻¹ were measured. Based on this approach, down-scaled top-gate, bottom-contacts *p*-type and *n*-type field-

effect transistors (FETs) based on high mobility organic semiconductors were developed using the SAP electrodes as source and drain contacts. The successful demonstration of SAP FETs with both polarities is a very important step because it opens up the possibility to realize integrated SAP CMOS-like inverters, basic building blocks for the development of complementary logic. Complementary gates, besides reducing power consumption, offers higher noise margins than unipolar gates, fundamental for the development of robust printed logic circuits. To assess the current uniformity of the printed FETs, critical for the correct operation of circuits where several integrated devices are present, we measured the ON and OFF drain currents of SAP FETs arrays. In Figure 1 ON and OFF currents of an array based on 6,13-bis(triisopropylsilylethynyl) pentacene (TIPS-pentacene) *p*-type FETs are reported. Apart from the only two shorted devices, the ON current and the ON/OFF ratio show good uniformity across the entire array, thus demonstrating a good control over the SAP channels length and width.

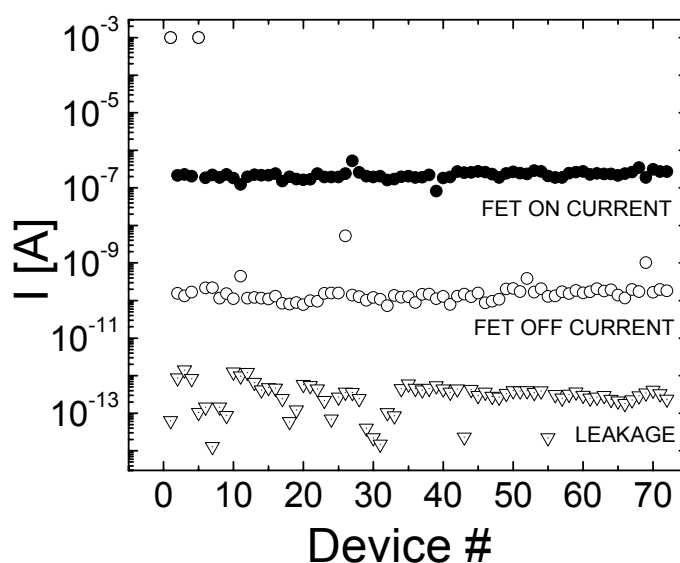


Fig.1: Leakage currents in air at 10 V of single-droplet SAP gold electrodes in a 6 x 12 array (triangles). ON drain currents (gate voltage of -10 V, filled circles) and OFF drain currents (gate voltage of +5 V, empty circles) at an applied drain bias voltage of -1 V for a 6 x 12 array of TIPS-pentacene SAP FET with a channel length of ~ 400 nm, a channel width of ~ 40 μ m and a ~ 130 nm thick CYTOP dielectric. Only 2 devices are shorted and the yield is higher than 97%.

Another important requirement for the integration of printed devices in circuits is that the adopted metallic inks should offer conductivities close to those of bulk metals such as copper or silver in order to reduce parasitic voltage drops along long printed electrodes and

interconnects. Here we replace the commonly thermally evaporated electrode for the top-level metallization (gate-level) with a silver complex ink TEC-IJ-010 (InkTec Co., Ltd.) which can be converted into a highly conducting electrode at low temperatures (130 °C). This sintering temperature is compatible with plastic substrates and avoids degradation of the underlying organic semiconductor and dielectric layers. Thanks to this, fully solution-processed organic FETs were realized, without the use of any mask during the fabrication process.

[1] Sirringhaus, H.; Sele, C. W.; von Werne, T.; Ramsdale, C. In *Organic Electronics, Materials, Manufacturing and Applications*; WILEY-VCH; **2006**, 294-322.

[2] Sele, C. W.; von Werne, T.; Friend, R. H.; Sirringhaus, H. Lithography-Free, Self-Aligned Inkjet Printing with Sub-Hundred-Nanometer Resolution. *Adv. Mater.* **2005**, *17*, 997-1001.

[3] Zhao, N.; Chiesa, M.; Sirringhaus, H.; Li, Y.; Wu, Y.; Ong, B. Self-Aligned Inkjet Printing of Highly Conducting Gold Electrodes with Submicron Resolution. *J. Appl. Phys.* **2007**, *101*, 064513.

[4] Gili, E.; Caironi, M.; Sirringhaus, H. In *Handbook of Nanofabrication*; ELSEVIER, Edited by Gary Wiederrecht; **2009**.

[5] Caironi, M.; Gili, E.; Sakanoue, T.; Xiaoyang, C.; Sirringhaus, H. High Yield, Single Droplet Electrode Arrays for Nanoscale Printed Electronics. *ACS Nano* **2010**, published on-line, DOI: 10.1021/nn9014664.

[6] Noh, Y. Y.; Zhao, N.; Caironi, M.; Sirringhaus, H. Downscaling of Self-Aligned, All-Printed Polymer Thin-Film Transistors. *Nat. Nanotechnol.* **2007**, *2*, 784-789.

BIOGRAPHIC DATA OF DR MARIO CAIRONI

Mario Caironi was born in Bergamo (Italy) in 1978. He studied at “Politecnico di Milano” (Milan, Italy) where, under the supervision of Prof. Marco Sampietro, he obtained his Laurea degree in Electrical Engineering in 2003 and a Ph.D. in Information Technology with honours in 2007, with a thesis on organic photodetectors and memory devices. In March 2007 he



joined the group of Prof. Henning Sirringhaus at the Cavendish Laboratory (Cambridge, UK) as a post-doctoral research associate. He worked in Cambridge for 3 years on high resolution inkjet printing of downscaled organic transistors and logic gates, and on charge injection and transport in high mobility polymers. In April 2010 he has been appointed as a team leader in the Center for Nano Science and Technology of the Italian Institute of Technology (CNST-IIT@Polimi, Milan, Italy). He is author and co-author of more than 20 scientific papers in international journals and books. He is currently interested in solution based high resolution printing techniques for opto-electronic devices fabrication, in the device physics of organic semiconductors based field-effect transistors and their integration in printed circuits, and in solution processed organic photodetectors for imaging and X-rays detection applications.

DESIGN OF ORGANIC SEMICONDUCTORS FOR SELF-ASSEMBLED MONOLAYER FIELD EFFECT TRANSISTORS (SAM-FETs)

**T. MEYER-FRIEDRICHSEN*^a, S. A. PONOMARENKO^b,
O. V. BORSHCHEV^b,**

^a H.C. Starck Clevios GmbH, Research and Development, Chempark Leverkusen, Building B 202, 51368 Leverkusen, Germany.

^b N.S. Enikolopov Institute of Synthetic Polymer Materials, Russian Academy of Sciences, 70 ul. Profsoyuznaya, 117393 Moscow, Russian Federation.

Organic electronics technology is steadily progressing and first products are appearing on the market. One target for this technology is the manufacturing of devices such as transistors for backplane panels and radio frequency identification tags (RFIDs) or printed organic photovoltaic cells in a cheap mass production like roll-to-roll printing. For this purpose the development of suitable materials for organic electronics is still one of the key points to access new application areas with this promising technology.

The most common component in electronic devices are field effect transistors. An organic field effect transistor (OFET) consists of a gate electrode, dielectric layer, semiconductor layer, and the source and drain electrodes. The function of the transistor is mainly influenced by the performance of the semiconductor layer, which depends on the layer morphology and the interface with the dielectric. (Mass-) Production processes have to be in a way that especially these interface structures are obtained in an ideal fashion with very high reproducibility. This issue could be solved if the semiconductor molecules can self assemble on the dielectric surface to perfectly aligned and dense layers.

Recently, bottom-up designed organic circuit devices using self assembled monolayers of semiconductors bound to the oxide dielectric surface of the gate electrode were reported [1]. The potential of this technology was impressively shown by the manufacturing of electronic devices like inverters, ring oscillators and a 15-bit code generator combining more than 300 fully functional SAM-transistors by simple dipping of the structured substrates into the semiconductor solution. We will report on the design and synthesis of such new organic semiconductor materials which are able to chemically link to oxide

surfaces of gate electrodes in order to establish self-assembled monomolecular layers with high ordering of the semiconducting cores.

We have synthesized a range of semiconducting SAM-molecules with diverse anchoring groups and oligothiophene-based semiconducting components as depicted in figure 1. In general, the structure consists of an anchoring group, aliphatic spacer, semiconducting oligothiophene core and an aliphatic end-group. Oligothiophenes were chosen because of their high charge carrier mobility of up to $1.1 \text{ cm}^2/\text{Vs}$ [2] and versatile chemistry. The aliphatic α,ω -substitution of the oligothiophene cores facilitates the anisotropic ordering as is well known for rod-like mesogens in liquid crystals [3,4,5]. The oligothiophenes are also stabilized against oxidation by blocking the α - and ω -position of the cores and this functionalization enhances the solubility of the materials as well.

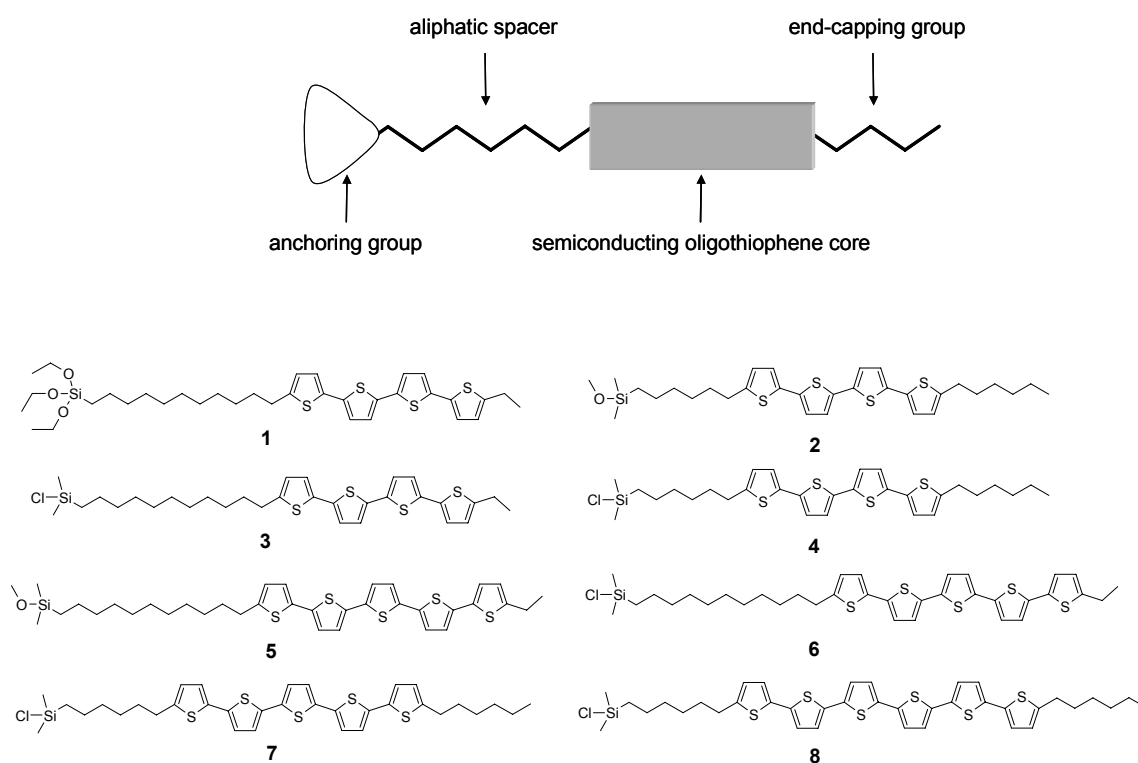


Fig. 1. Top: schematic representation of the general molecular structure for SAMFETs consisting of an anchoring group, aliphatic spacer, oligothiophene semiconducting core and aliphatic end-group; bottom: structural formulas of depicted synthesized SAM-semiconductors.

Devices were assembled and electrically characterized by the group of de Leeuw at the Philips Research Laboratories in Eindhoven [1]. For the device structures, silicon wafers having atomically flat silicon dioxide dielectric surfaces were used. The SAM-

semiconductors chemically bind to the oxide surface. Chlorosilanes or alkoxy silanes are generally used as anchoring groups. The formation of the monolayer proceeds then via a condensation reaction with the hydroxide groups of the hydrolysed silicon dioxide surface. Long range ordered monolayers were obtained using the highly reactive monochlorosilyl group. The synthesis of these compounds were carried out by platinum catalyzed hydrosilylation reaction of the respective alkylene precursor molecule with dimethylchlorosilane as depicted in figure 2 for compound **6**.

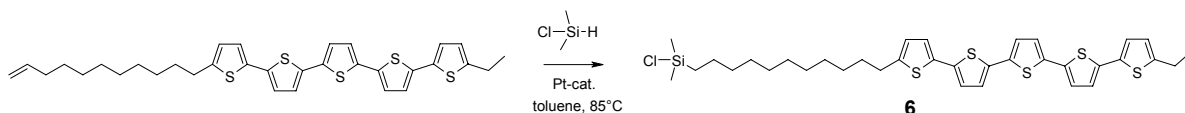


Fig. 2. Synthesis of monochlorosilyl substituted SAM-semiconductor **6** by hydrosilylation reaction of the respective undecenyl substituted oligothiophene precursor.

We will discuss the influence of linker groups, aliphatic spacer and end group length and the role of the side products formed during the hydrosilylation reaction on the formation of the SAM-layers.

Another topic will be the influence of the oligothiophene cores on the electrical properties of the the SAM layers. The semiconducting properties of oligothiophenes depend on the number of thiophene units [2]. The highest mobilities for SAM-layers were observed using the chlorosilyl-functionalized materials **6** and **7** with values of up to 10^{-2} cm^2/Vs . Comparable linear alkyl substituted quinquethiophenes are not solution processable due to their low solubilities. Instead islands of bulk crystalline material are formed if a solution of e.g. α,ω -dihexylquinquethiophene is spin-coated on a silicon wafer substrate. But due to the monolayer self-assembling process, only very low concentrations of **6** or **7** are necessary to obtain full coverage of the surface. With the use of the SAM-semiconductor **6** it was even possible to build complex devices like inverters and ring oscillators with more than 300 fully functional transistors.

The presented results will show that the concept of building OFET devices by molecular self-assembling processes is a powerful technique that can simplify the production of such devices and can be a major step forward to mass-producible, reliable organic electronics. We will show that one key requisite for this technique is the molecular design of the material in order to obtain smooth and dense semiconductor monolayers.

Acknowledgement

Development of the SAM-processing, device design and manufacturing and characterization of the SAMFETs has been done at the Philips Research Laboratories in Eindhoven. We like to acknowledge E. C. P. Smits, S. G. J. Mathijssen, P. A. van Hal, S. Setayesh, T. C. T. Geuns, K. A. H. A. Mutsaers, H. J. Wondergem and Prof. D. M. de Leeuw. For further characterization we like to acknowledge Bert de Boer[†] from University of Groningen, NL, O. Werzer and R. Resel from Institute of Solid State Physics, Graz, Au and E. Cantatore and M. Kemerink from Eindhoven University of Technology, NL.

References

- [1] E. C. P. Smits, S. G. J. Mathijssen, P. A. van Hal, S. Setayesh, T. C. T. Geuns, K. A. H. A. Mutsaers, E. Cantatore, H. J. Wondergem, O. Werzer, R. Resel, M. Kemerink, S. Kirchmeyer, A. M. Muzafarov, S. A. Ponomarenko, B. de Boer, P. W. M. Blom and D. M. de Leeuw, *Nature* **2008**, *455*, 956.
- [2] M. Halik, H. Klauk, U. Zschieschang, G. Schid, S. Ponomarenko, S. Kirchmeyer and W. Weber, *Adv. Mater.* **2003**, *15*, 917.
- [3] A. J. J. M. van Breemen, P. T. Herwig, C. H. T. Chlon, J. Sweelssen, H. F. M. Schoo, S. Setayesh, W. M. Hardeman, C. A. Martin, D. M. de Leeuw, J. J. P. Valetton, C. W. M. Bastiaansen, D. J. Broer, A. R. Popa-Merticaru and S. C. J. Meskers, *J. Am. Chem. Soc.* **2006**, *128*, 2336.
- [4] S. A. Ponomarenko, E. A. Tatarinova, A. M. Muzafarov, S. Kirchmeyer, L. Brassat, A. Mourran, M. Moeller, S. Setayesh and D. M. de Leeuw, *Chem. Mater.* **2006**, *18*, 4101.
- [5] I. McCulloch, M. Heeney, C. Bailey, K. Genevicius, I. MacDonald, M. Shkunov, D. Sparrowe, S. Tierney, R. Wagner, W. Zhang, M. L. Chabinye, R. J. Kline, M. D. McGehee and M. F. Toney, *Nature Mater.* **2006**, *5*, 328.

BIOGRAPHIC DATA OF DR TIMO MEYER-FRIEDRICHSEN

Dr. Timo Meyer-Friedrichsen studied chemistry at the Universities of Oldenburg and Hamburg. He received a PhD in Organometallic Chemistry in 2000 working on the synthesis and characterization of materials for nonlinear optics. He attended a postdoc at the University of Arizona at the group of Prof. Seth R. Marder working on two-photon absorption materials and metal nanoparticles. In 2001 he joined the Central Research Department of Bayer where he worked on organic materials for optical data storage systems. Timo switched to H.C. Starck in 2006 where he is currently responsible for the development of organic semiconductor materials and intrinsic conducting polymers.



APPROACHES IN FLEXIBLE THIN FILM ELECTRONICS

Marcus Halik

Organic Materials & Devices - Institute of Polymer Materials,
University Erlangen – Nürnberg, Martensstr. 07, D-91058 Erlangen, GERMANY;
e-mail: marcus.halik@ww.uni-erlangen.de

Abstract:

Self-organizing molecules are promising components to serve as active layers in high performance, low cost, and flexible electronic devices. The process of self-assembly can be used in or even outperform printing technologies in future device fabrication due to the molecular induced driving force of voluntary film formation – serving surface – and the local selectivity and full control on film thickness. This contribution highlights the use of self-assembled molecular layers in organic transistor development.

Simple n-alkyl molecules (silanes or phosphonic acids) can act as monomolecular dielectric in organic transistors. This concept is suitable for a wide range of semiconductor materials (p- and n-type, nanoparticles, polymers) and enables CMOS like organic electronics with reduced power consumption even on flexible substrates [1,2].

Thereby, the length dependent electrical properties of SAMs based on n-alkyl phosphonic acids are studied in large area thin film devices (transistors and capacitors). In terms of their structural organization the tunnelling currents through the monolayer were interpreted using the Simmons model. Molecular dynamics (MD) simulations provide a deeper insight into the nature of the intermolecular interactions and allow identifying the most realistic molecular assembly of the monolayers. The observed divergence from theory suggests a change in the self-assembled monolayer morphology from an amorphous state for short alkyl chains to a quasi-crystalline state for longer alkyl chains which impacts on the electrical properties. [3,4]

Secondly, a rational molecular design will be introduced, in which we address the advantages of charge transport (p- and n-type) within a monolayer in combination with low voltage operation in organic transistors. For the p-type material, a quaterthiophene unit (4T) serves as suitable π -system with dedicated hole transport properties. The ability to self-assemble and low voltage operation of a resulting SAM is implemented by a non-symmetric substitution pattern with a n-dodecyl-phosphonic acid tail (C₁₂-PA). The molecular design of the n-type semiconductor molecules rely on the electron transport behaviour of fullerene (C₆₀). One n-hexyl-phosphonic acid substitution (C₆-PA) is attached to the C₆₀ core via malonate moiety linkage and enables the SAM formation. Both materials were self-assembled on oxidized Al-gate pattern and operate in self-assembled monolayer field effect transistors (SAMFETs) in the expected performance. By using 4T and C₆₀ moieties, we have obtained hole transport and electron transport respectively in ambient air. The approach provides prospective complementary circuitry based on self-assembled molecules in the future. The air sensitive C₆₀ in particular needs to be protected with a barrier, which we have integrated in the molecular structure. The device

performance critically depends on the effective $\pi\pi$ -interaction in the molecular monolayer and seems to be influenced by the surface roughness of the electrode, rather than by the channel length. Charge transport in functional SAMs could benefit from a more uncritical molecular interaction, provided by spherical π -systems [5].

Finally, a novel concept of an electrically programmable self-assembled molecular gate dielectric layer is provided for OTFTs, that can be reversibly charged and discharged and retains these digital states even when the supply voltage is removed. Due to the small thickness of the dielectric stack (app. 5.7 nm), the memory transistors operate with very small program and erase voltages of ± 2 V. Despite the extremely small dielectric thickness, the retention time is already promising (~ 6 hours with a read voltage of -750 mV applied continuously). The dielectric is a mixed monolayer of aliphatic and C_{60} -functionalized phosphonic acid molecules (app. 2.1 nm thickness) on a patterned and plasma-oxidized aluminum gate electrode on a glass substrate. The monolayer composition is proven by electrically and by AFM experiments. Structure-property relations of various compositions have been studied and strong dependencies of the memory behavior related to the composition of the SAM in capacitor and transistor devices were demonstrated [6].

References:

- [1] M. Halik, H. Klauk, U. Zschieschang, G. Schmid, C. Dehm, M. Schutz, S. Maisch, F. Effenberger, M. Brunnbauer, F. Stellacci, Low-voltage organic transistors with an amorphous molecular gate dielectric, *Nature* 431 (2004) 963–966.
- [2] H. Klauk, U. Zschieschang, J. Pflaum, M. Halik, Ultralow-power organic complementary circuits. *Nature* 445 (2007) 745-748.
- [3] A. Jedaa, M. Burkhardt, U. Zschieschang, H. Klauk, D. Habich, G. Schmid, M. Halik, The Impact of Self-Assembled Monolayer Thickness in Hybrid Gate Dielectrics for Organic Thin-Film Transistors, *Org. Electron.* 10 (2009) 1442-1447.
- [4] M. Novak, C.M. Jäger, H. Kropp, T. Clark, M. Halik, The morphology of integrated self-assembled monolayers and their impact on devices - a computational and experimental approach, *Org. Electron.* (2010) accepted.
- [5] M. Novak, A. Jedaa, A. Ebel, T. Meyer-Friedrichsen, A. Hirsch, M. Halik, Organic Self-Assembled Monolayer Field Effect Transistors – A Rational Design for p- and n-Type Low Voltage Operation (submitted)
- [6] M. Burkhardt, A. Jedaa, M. Novak, A. Ebel, K. Voitchovsky, F. Stellacci, A. Hirsch, M. Halik, Concept of a Molecular Charge Storage Dielectric Layer for Organic Thin Film Memory Transistors, *Advanced Materials* (2010) in Press.

CURRICULUM VITAE

Marcus Halik
Prof. Dr. rer. nat., Dipl.-Chem.

geboren am: 13.01.1971 in Heiligenstadt

Email: Marcus.Halik@ww.uni-erlangen.de

Web: <http://www.umd.uni-erlangen.de>



Education

- 09/1990 – 07/1995 Study of Chemistry at the Technischen Hochschule Leuna-Merseburg and Martin Luther University Halle-Wittenberg
- 09/1995 – 10/1998 Dissertation: “2,2-Difluor-1,3,2-(2H)-dioxaborine als Bausteine zur Darstellung von langwellig absorbierenden Methin-farbstoffen” at the Martin-Luther-University Halle-Wittenberg

Scientific Career

- 03/1999 – 03/2000 Post-Doc with Prof. Dr. S.R. Marder, University of Arizona (USA),
- 04/2000 – 08/2005 Engineer - Infineon Technologies AG
- 09/2005 - W2-Professur für Polymerwerkstoffe (Organic Materials & Devices – OMD) at the Institute of Polymer Materials at the Friedrich-Alexander University Erlangen-Nürnberg

NEW STRATEGIES AND MATERIALS FOR ORGANIC FIELD EFFECT TRANSISTORS

Mihai Irimia-Vladu, *Soft Matter Physics & Linz Institute for Organic Sollar Cells, Johannes Kepler University, Linz, Austria*
Siegfried Bauer, *Soft Matter Physics, Johannes Kepler University, Linz, Austria*
Niyazi Serdar Sariciftci, *Linz Institute for Organic Sollar Cells, Johannes Kepler University, Linz, Austria*

Green technology based on compostable materials is seen as an ultimate goal for solving waste problems. Currently there are large efforts for producing compostable plastic materials that can be used in daily life products, such as plastic bags and disposable dishware. When such daily items are produced with compostable materials, electronics included in such goods should be also based on materials that are easily degradable. Organic electronics has the potential to develop electronic products that are biocompatible, bioresorbable, biodegradable or even capable to metabolize. An ideal solution for the production of such devices involves the fabrication of the electronics either from natural materials, or from materials that have been proved to be at least biocompatible. Organic electronics is envisioned to find a niche in applications involving low-end products, when electronics may be directly integrated in daily-life items to store information, like inventory labels and price tags, use-by-date information *etc.*

Here we report the combination of biodegradable substrates based on caramelized glucose or commercially available plastic foil based on starch, corn and polylactic acid (Ecoflex[®], BASF) with fully natural or socially accepted materials as gate dielectrics and organic semiconductors in low operating voltage organic field effect transistors (OFETs).

For organic dielectric layer, the choice is made from solution processed small molecules (glucose, lactose, fructose, *etc.*) or evaporable small molecules (guanine, adenine, cytosine, caffeine, glucose, *etc.*). The organic semiconductor is chosen either from natural compounds (indigo, beta-carotene) as well as socially accepted molecules of low toxicity (indanthrene yellow G, indanthrene brilliant orange RF, perylene diimide).

In a first example, low operating voltage OFETs are built on commercially available biodegradable plastic foil (Ecoflex[®], BASF), comprising naturally occurring dielectrics: adenine or alternating layers of adenine, guanine, cytosine and widely accepted perylene diimide—a simple red dye used extensively in cosmetic industry.

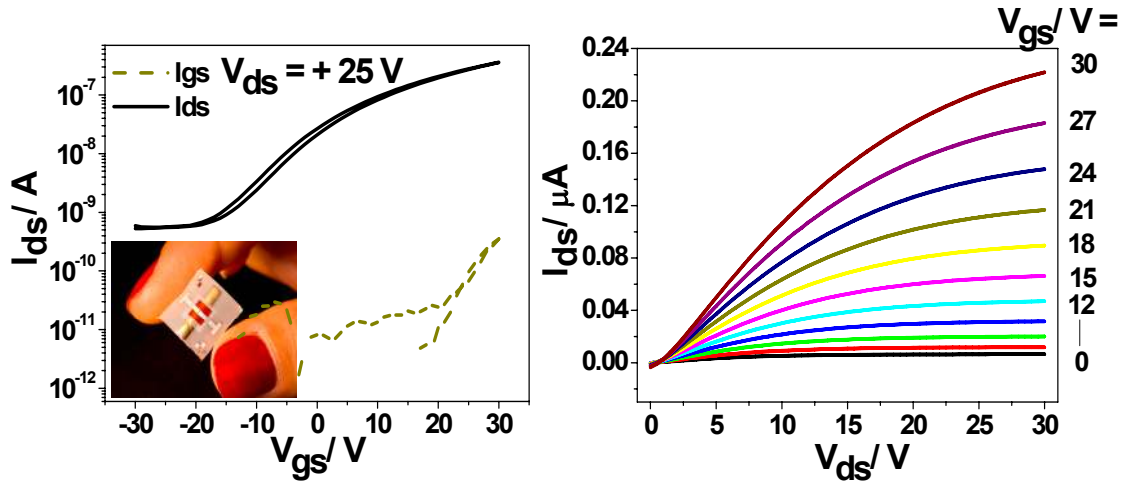


Figure 1: Transfer and output characteristics of OFETs with a 1.75 μm thick adenine gate dielectric and 150 nm perylene diimide semiconductor on plain Ecoflex foil.

In a second example, complete bio-materials based OFETs are introduced based on glucose, lactose, sucrose and caffeine for the gate dielectrics with solution processed beta-carotene as organic semiconductor (Figure 2).

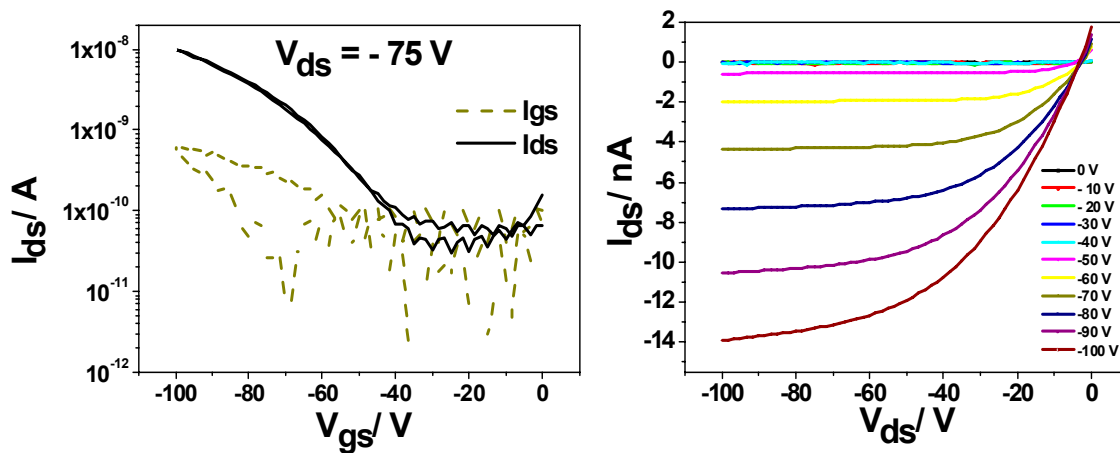


Figure 2: Transfer and output characteristics of field effect transistors on glass substrates with natural p-type (solution processed beta-carotene) as organic semiconductor and glucose with caffeine as gate dielectric.

In a third example, fully degradable devices are produced on caramelized glucose substrate comprising either layers of adenine and guanine for organic dielectrics and indanthrene yellow-a biodegradable vat dye used extensively in textile industry under the name “vat yellow 1” (Figure 3).

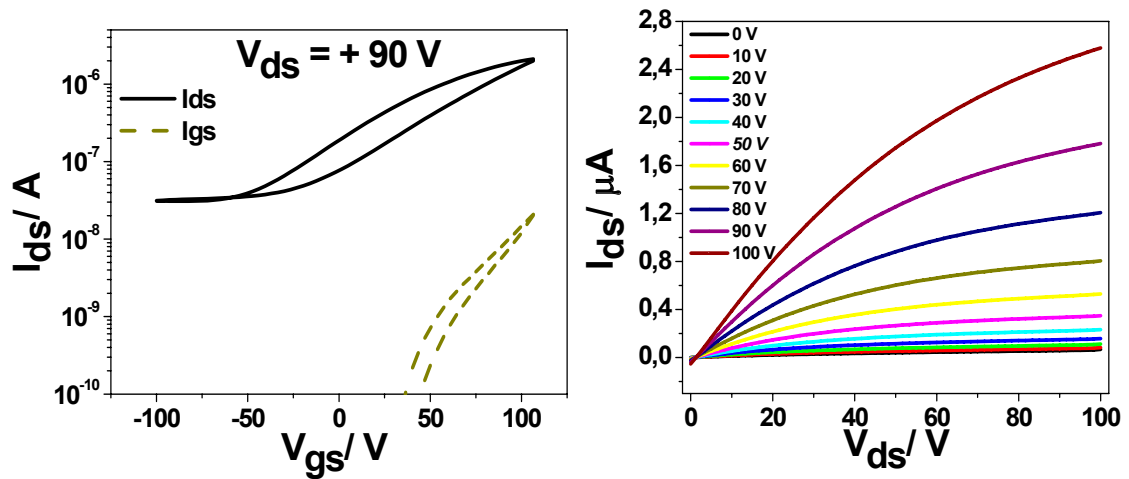


Figure 3: Transfer and output characteristics of bio-compatible (edible) organic field effect transistors on caramelized glucose substrates. A thin smoothing layer of aurin (50 nm) is evaporated on top of the substrate. The gate dielectric is formed by eight alternating layers of adenine and guanine, and indanthrene yellow G is the organic semiconductor.

Tremendous improvement of the OFETs characteristics are feasible simply by employing aurin, a naturally occurring red-orange pigment as a smoothing layer for the Ecoflex plastic foil or by employing the anodization of the aluminium gate electrodes in combination with organic dielectric layers for samples built on glass substrates (Figure 4).

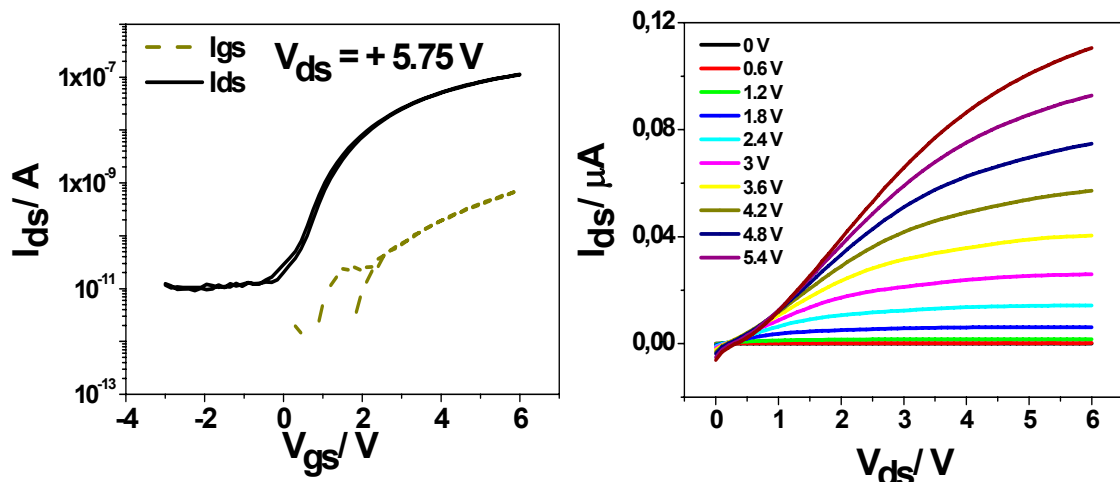


Figure 4: Transfer and output characteristics of an OFET having a combined inorganic (aluminum oxide)-organic (20 nm adenine and 3 nm guanine) for the gate dielectric and 100 nm perylene diimide for the organic semiconductor.

The non toxicity and environmental bio-degradability of these materials copled with their ease of processing on biodegradable substrates, recommend them as a new class of non-toxic compounds for plastic electronic applications. These transistors may be seen at the heart of organic electronic circuits, to be used in low-cost, large volume disposable or throwaway applications, such as food packaging, plastic bags, disposable dishware etc. There is also significant potential to use such electronic items in biomedical implants.

BIOGRAPHIC DATA OF DR. MIHAI IRIMIA-VLADU

Department of Soft Matter Physics & Linz Institute for Organic Solar Cells,
Johannes Kepler University, Linz, A-4040, AUSTRIA
+43(0)732.2468.8767 Mihai.Irimia-Vladu@jku.at



EDUCATION

- 2006 **Ph.D. Materials Engineering** Auburn University,
Alabama (USA)
Dissertation: “*Chemical Sensing Employing pH Sensitive
Emeraldine Base Thin Film For Carbon Dioxide
Detection*”
- 1997 **B.S. Automotive Engineering**, University of Craiova, Romania,
Magna Cum Laudae (ranked 2nd out of 210)

EMPLOYMENT

- 2006 - present **Post Doctoral Research Scientist**, Johannes Kepler University, Linz,
Austria
Soft Matter Physics & Linz Institute for Organic Solar Cells
- 2000 - 2006 **Research and Teaching Assistant**, Auburn University, Alabama, U.S.A.
Materials Engineering Department
- 2005 - 2006 **Teaching Assistant**, Auburn University, Alabama, U.S.A.
School of Pharmacy
- 1997 - 2000 **Mechanical Test & Materials Analysis Engineer**, DAEWOO
Automobiles, Romania, Components Testing & Failure Analysis Division

RESEARCH

Articles in Refereed Journals

1. **M. Irimia-Vladu**, N. Marjanovic, M. Bodea, G. Hernandez-Sosa, A. Montaigne Ramil, R. Schwödiauer, S. Bauer, N.S. Sariciftci and F. Nüesch, “*Small-molecule Vacuum Processed Melamine-C₆₀ Organic Field-Effect Transistors*“, Organic Electronics, Volume: 10, Issue: 3, Pages: 408-415, Published: 2009.
2. **M. Irimia-Vladu**, N. Marjanovic, A. Vlad, G. Hernandez-Sosa, A. Montaigne Ramil, R. Schwödiauer, S. Bauer, N.S. Sariciftci, “*Vacuum Processed, Polyaniline-C₆₀ Organic Field Effect Transistors*“, Advanced Materials, Volume: 20, Issue: 20, Pages: 3887-3892, Published 2008.
3. M. Egginger, **M. Irimia-Vladu**, R. Schwödiauer, A. Tanda, R. Frischauf, S. Bauer and N.S. Sariciftci, “*Mobile Ionic Impurities in Poly(vinyl alcohol) Gate Dielectric: Possible Source of Hysteresis in Organic Field-effect Transistors*“, Advanced Materials, Volume: 20, Pages: 1018-1022, Published: 2008.

4. **M. Irimia-Vladu** and J.W. Fergus, “*Suitability of Emeraldine Base Polyaniline-PVA Composite Film for Carbon Dioxide Sensing*”, Synthetic Metals, Volume: 156, Issue:21-24, Pages: 1401-1407, Published: 2006.
5. **M. Irimia-Vladu** and J.W. Fergus, “*Impedance spectroscopy of Thin Films of Emeraldine Base Polyaniline and its Implications for Chemical Sensing*”, Synthetic Metals, Volume: 156, Issue: 21-24, Pages: 1396-1400, Published: 2006.

Proceedings

1. M. Egginger, **M. Irimia-Vladu**, A. Tanda, S. Bauer, N.S. Sariciftci, “*Ionic Impurities in Poly(vinyl alcohol) Gate Dielectrics and Hysteresis Effects in Organic Field Effect Transistors*“ Mater. Res. Soc. Symp. Proc. Volume: 1091, pages: 1091-AA11-46, Published: 2008.
2. **M. Irimia-Vladu** and J.W. Fergus, “*Emeraldine Base Thin Film Carbon Dioxide Sensor*” in Mater. Res. Soc. Symposium. Proc. “Electroresponsive Polymers and Their Applications” Volume: 889, Pages: 73-78, Published: 2005.

Papers under Review

M. Irimia-Vladu, P.A. Troshin, L. Shmygleva, Y. Kanbur, Melanie Reisinger, G. Schwabegger, M. Bodea, R. Schwödiauer, J.W. Fergus, V. Razumov, H. Sitter, N.S. Sariciftci, S. Bauer, “*Biocompatible and Biodegradable Materials in Organic Field Effect Transistors*”-submitted.

Work in Progress

1. **M. Irimia-Vladu**, Yasin Kanbur, Melanie Reisinger, Günther Schwabegger, Reinhard Schwödiauer, Helmut Sitter, Nyiazi Serdar Sariciftci, Siegfried Bauer, “*Vacuum Processed Polyethylene Gate Dielectrics for Millivolt Operating Organic Field Effect Transistors*”
2. **M. Irimia-Vladu**, Melanie Reisinger, Yasin Kanbur, Günther Schwabegger, Reinhard Schwödiauer, Helmut Sitter, Nyiazi Serdar Sariciftci, Siegfried Bauer, „*Evaporable Polyvinyl Alcohol and Poly Vinylidene Fluoride Gate Dielectrics for Organic Field Effect Transistors*“

Invited talks

1. “*New strategies and materials for organic field effect transistors*”- 4th International Symposium „Technologies for Polymer Electronics” – TPE 10, Rudolstadt, Germany, May 18-20, 2010. Invited by: Prof. Hans-Klaus Roth
2. “*Bio-inspired organic field effect transistors*”- International Society for Optical Engineering (SPIE) Annual Meeting, Conference on Organic Field Effect Transistors IX, San Diego, USA, August 3-5, 2010. Invited by: Prof. Zhenan Bao and Prof. Ian McCulloch

Peer-Reviewed Presented Papers (* indicates the presenter)

1. MRS Spring Meeting, (April 2008 San Francisco, CA, U.S.A.)
M. Irimia-Vladu*, R. Schwödiauer, S. Bauer, N. Marjanovic, A. Montaigne Ramil, A. Vlad, M. Bodea, G. Hernandez-Sosa, N.S. Sariciftci, F. Nüesch, "*Stable, Evaporation Processed Organic Thin Film Transistors on Deformable Plastic Substrates*"
2. EMRS Meeting, (May 2008 Strasbourg, France)
M. Irimia-Vladu*, N. Marjanovic, A. Vlad, A. Montaigne Ramil, R Schwödiauer, S. Bauer, N.S. Sariciftci, "*Evaporation Processed Polyaniline-C₆₀ Organic Field Effect Transistors*"
3. MRS Fall Meeting (November 2005, Boston MA)
M. Irimia-Vladu*, J.W. Fergus, "*Emeraldine Base Thin Film Carbon Dioxide Sensor*"
4. Electrochemical Society -Local Chapter at Georgia Institute of Technology (September 2005), Atlanta, GA, U.S.A.
M. Irimia-Vladu*, J.W. Fergus, "*Emeraldine Base Thin Film Carbon Dioxide Sensor*"
5. 204th Meeting of the Electrochemical Society, (October 2003, Orlando, FL, U.S.A.)
M. Irimia-Vladu*, J.W. Fergus. "*Solid State Carbon Dioxide Sensor Based on a Conducting Polymer Composite*"

INTERFACE ENGINEERING FOR OPTIMISING SOLUTION-PROCESSED HIGH-MOBILITY OTFTS

T. KUGLER^{*}, K. OTHMAN, C. NEWSOME, R. WILSON, J. BURROUGHES

Cambridge Display Technology Limited, Unit 12, Cardinal Business Park, Godmanchester, Cambridgeshire, PE29 2XG, United Kingdom

In order to be applicable to Active Matrix backplanes for Organic Light Emitting Diode (OLED) displays, Organic Thin Film Transistors (OTFTs) need to deliver sufficiently high currents for driving OLED pixels, which translates to a requirement for high mobility OTFTs with low contact resistance. CDT is investigating techniques for understanding and optimising these OTFT properties, in order to achieve device performances suitable for active matrix OLED backplanes.

Specifically, the formation of Self-Assembled Monolayers (SAMs), both on the Source/Drain contacts and on the glass substrate, has been investigated with the aim of optimising the band alignment at the Source – OSC interface, and for controlling the nucleation and resulting morphology of the active OSC layer. Photo-Electron Spectroscopy in Air (PESA) has been used for characterising the band alignment at SAM-modified Source/Drain contacts. Atomic Force Microscopy (AFM) measurements have been performed for understanding the impact of the SAM-treatments on the morphologies of OSC layers based on solution-processed small molecules.

The work presented here has resulted in hole mobilities of up to $0.7\text{cm}^2/\text{Vs}$ in TIPS pentacene devices with 5 micron channel length. Furthermore, using proprietary organic semiconductors from Merck, hole mobilities of up to $1\text{cm}^2/\text{Vs}$ have been obtained at the same channel length.

BIOGRAPHIC DATA OF DR. THOMAS KUGLER



Academic and professional formation:

- 1990 Diploma in chemistry, Tübingen University, Germany
- 1990-1993 PhD work on the surface analysis of organic adsorbates on Si(100)(2x1) surfaces, Tübingen University, Germany
- 1994-1998 EU research assistant with Prof. W.R. Salaneck at Linköping University, Sweden. Photoelectron spectroscopy of conjugated polymer surfaces and interfaces
- 1996-1997 Assistant professor at Linköping University, Sweden
- 1998-2003 Senior Scientist at ACREO AB in Norrköping, Sweden. Applied R&D in polymer electronics.
- 2001-2003 Part-time position as associate professor at the Dept. of Science and Technology (ITN), Campus Norrköping, Linköping University, Sweden
- 2003-2007 Chief Researcher at the Cambridge Research Laboratory of Epson (CRLE).
- Since 2007: Principal Scientist, CTO Office; Cambridge Display Technology Ltd., Godmanchester, Cambridgeshire, UK.

SOLUTION-PROCESSABLE NANOMATERIAL FIELD-EFFECT TRANSISTORS

M. SHKUNOV*, C. OPOKU

Advanced Technology Institute, University of Surrey, Guildford, Surrey GU2 7XH, UK

1 Introduction

Large area printable, flexible and transparent electronics is a new field of research that promises to revolutionise almost every aspect of our everyday life from the ways we access information to the healthcare and solar power generation. Novel fabrication techniques are currently being developed using additive printing and self-assembly processes that do not require high vacuum techniques and energy demanding high-temperature fabrication steps.

Few examples of novel devices include rollable displays and electronic paper, smart packaging, sensor networks, stretchable and wearable electronics.

Field-effect transistors (FETs) are the main building blocks in these electronic applications as they provide pixel switching in displays, form functional logic elements in circuits and comprise three-terminal sensors and memory elements. The performance of these FETs is of paramount importance for efficient operation of devices and high charge carrier mobility is required for a number of applications.

For various device applications FET mobility requirements range from about $1\text{cm}^2/\text{Vs}$ for low information content displays to few tens of cm^2/Vs for higher performance displays, whereas mobility close to $100\text{cm}^2/\text{Vs}$ is needed for logic function circuits.

Printing approaches, although offering outstanding fabrication potential, put some limitations on the semiconducting materials, FET structures and eventually device mobility, especially when compatibility with plastic substrates is required.

2 Materials for solution-processable transistors

2.1 Organic semiconductors

Currently solution processable organic semiconductors are being widely used in large area printed electronics due to their plasticity, very good thin film formation characteristics when deposited from solvent-based formulations, and excellent compatibility with plastic flexible substrates. Yet performance of the best organic-based FETs targeting these applications is only becoming comparable to a-Si with charge carrier mobilities in the order of $1 \text{ cm}^2/\text{Vs}$.¹ Higher mobilities of up to $5 \text{ cm}^2/\text{Vs}$ have been demonstrated on a single-FET scale, though device-to-device parameters' variations are too large for the use in circuits and integration into large area display back-plane electronics.

2.2 Inorganic semiconducting nanowires

Semiconducting nanowire (NW) materials are high-aspect ratio nanoparticles with typical diameters of 10-70 nm and lengths ranging from hundreds of nanometres to tens of micrometres. These materials are offering a potential breakthrough in the area of high performance printable transistors due to their solution processability and high mobility demonstrated per single nanowire. For instance, silicon NW FET with mobility of $1350 \text{ cm}^2/\text{Vs}$ was demonstrated by Lieber's group.²

Inorganic nanowires maintain most of the bulk single crystal properties, including semiconducting behaviour, crystal lattice structure and efficient charge. The synthesis of nanowires is completely separate from the device fabrication process thus allowing two-fold advantage. Controlled growth of nanowires can be tailored to produce high quality single-crystal structures with desired length to width ratio, and secondly these nanomaterials can be formulated into 'inks' for selective low-temperature additive deposition into device structures. If these nanowires can be deposited to 'bridge' the device electrodes then device performance per nanowire is expected to be comparable to that of traditional single crystal semiconductor technology. Clear advantages of nanowire approach are the ease of processing, wide prospects for self-assembly 'bottom-up' fabrication, compatibility with plastic substrates, and also possibility for fast device prototyping based on additive printing technology.

To be able to use full potential of nanowire electronics there are still some challenges to overcome. Due to nanowire high surface-to-volume ratio, interfacial effects

play major role in electronic properties. Ge nanowires, for example, show relatively low hole carrier mobility in FET devices of just $\sim 2\text{cm}^2/\text{Vs}^3$ compared to tabulated value of $1900\text{cm}^2/\text{Vs}^4$ in pure bulk Ge. This dramatic drop in mobility is attributed to high density of surface trap states, caused by amorphous surface oxide layers and adsorbed ambient species, such as polar water molecules.⁵

Metal-oxide semiconducting nanowires⁶ offer a sensible solution to surface oxide problem and the effect of amorphous oxide layer is significantly reduced. In this work ZnO nanowire-based FETs are investigated, where semiconducting layer is deposited using solution-cast methods.

3 Experimental

Bottom-gate top-contact ZnO nanowire FETs have been fabricated on Si/SiO₂ substrates. In this type of devices doped Si provides common-gate electrodes, whereas SiO₂ serves as a good gate dielectric. Nanowires were deposited on the substrate from a dispersion in isopropanol by either drop-casting or spin-coating. Top-electrodes (Cr) were formed on top of nanowires using photolithographic lift-off technique.

All ZnO NW FETs showed n-type enhancement characteristics. Typical transfer characteristics are presented in Figure 1, where source-drain voltage was fixed at 2V, 6V, 10V, and the gate voltage was swiped from -10V to +20V. Turn-on voltage for these devices was small ($\sim 2\text{V}$), and on-off ratio was up to $\sim 10^5$ (at $V_{sd}=10\text{V}$). Subthreshold slope was estimated to be 500mV/dec.

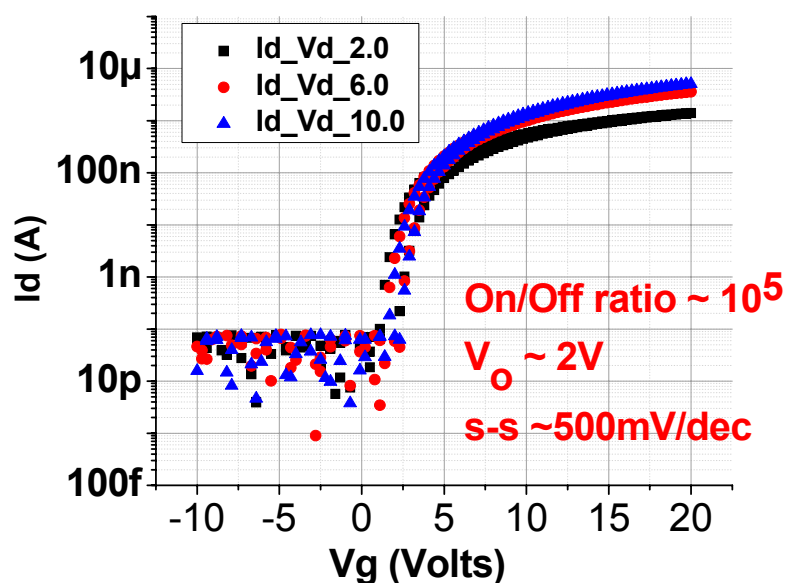


Figure 1 Transfer characteristics of ZnO NW FET

4 Conclusions

Field-effect transistors based on solution-processable ZnO nanowires were fabricated in ambient conditions using low-temperature deposition steps. FETs demonstrated excellent n-type current-voltage characteristics with high current modulation (10^5) and low subthreshold slope.

The results demonstrate high potential of nanowire-based FETs for printed electronics. A number of challenges still remain before this technology can be fully commercialised including large-area solution-based printing of aligned, dense ‘monolayers’ of semiconducting nanowires.

References:

- ¹ M.M. Payne et al., *J. Am. Chem. Soc.* **127** (14), 4986-4987 (2005).
- ² C. Yi, Z. Zhaohui, W. Deli et al., *Nano Letters* **3** (2), 149-152 (2003).
- ³ A. D. Schricker, S. V. Joshi, T. Hanrath et al., *J. Phys. Chem. B* **110** (13), 6816 (2006).
- ⁴ S. M. Sze, *Physics of semiconductor devices*. (Hoboken, Wiley-Interscience, 2007).
- ⁵ T. Hanrath and B. A. Korgel, *JACS* **126** (47), 15466 (2004); T. Hanrath and B. A. Korgel, *J. Phys. Chem. B* **109** (12), 5518-5524 (2005).
- ⁶ W. I. Park, J. S. Kim, G-C Yi et al., *Appl. Phys. Lett.* **85** (21), 5052-5054 (2004).

MOLECULARLY IMPRINTED POLYMER LAYERS FOR THE REGULATION OF L-GLUTAMATE

E. von Hauff*, K. Fuchs, J. Parisi

Institute of Physics, Energy and Semiconductor Research Laboratory,
University of Oldenburg
26111 Oldenburg, Germany

Molecularly imprinted polymers for the uptake and release of the neural transmitter L-glutamate were developed using overoxidised polypyrrole (oPPy) [1,2]. Polypyrrole layers were electrochemically deposited in a three electrode cell on gold working electrodes in aqueous electrolytes containing monosodium L-glutamate. The pyrrole monomer is oxidised with an anodic potential, and polymerises in the solution. Anions, in this case L-glutamate, from the solution are incorporated into the polymer chain to preserve charge neutrality. It was demonstrated using liquid scintillation techniques on radioactively marked glutamate that the resulting films were conductive and doped with glutamate [3]. The PPy layers were then overoxidised after deposition in a controlled manner to expel the glutamate anion and create porous, molecularly selective layers which still adhered to the working electrode surface. In a previous study we optimised the synthesis of the PPy by varying the pH of the deposition solution and the concentration of the electrolyte components to create reproducible polymer layers [3]. In a following study we demonstrated the proof of principle [4] of the voltage regulated enantioselective uptake and release of L-glutamate from the biocompatible oPPy layers. During the uptake and release processes (switching) no changes occur to the L-glutamate molecule. In this study we present further developments of the “glutamate-switch”. Here, the device was characterised to determine the concentration of glutamate which can be regulated by the device, as well as the efficiency and reproducibility of the uptake and release process.

- [1] B. Deore, Z. Chen, T. Nagaoka, ANALYTICAL SCIENCES, 15, 827–828, (1999).
- [2] V. Syritski, J. Reut, A. Menaker, R. E. Gyurcsányi, A. Öpik, ELECTROCHIMICA ACTA, 53, 2729 (2008).
- [3] E. von Hauff, J. Parisi, R. Weiler, Zeitschrift für Naturforschung A, 63a (2008), 359.
- [4] Y. V. Meteleva-Fischer, E. von Hauff, J. Parisi, J. Appl. Polymer Sci., 114, 4051 (2009)
- [5] E. von Hauff, K. Fuchs, J. Parisi, R. Weiler, C. Burkhardt, U. Kraushaar, E. Guenther, submitted.

BIOGRAPHIC DATA OF DR ELIZABETH VON HAUFF

Born on 20.09.1977 in York, Ontario, Canada



Education and Professional Experience

- 1995 – Advanced High School Diploma, Edmonton, Alberta, Canada
- 2000 – BSc Honours in Physics, University of Alberta, Canada
- 2001 – Msc Renewable Energies, University of Oldenburg
- 2005 – PhD (Dr. rer. nat.) in the Faculty of Natural Sciences at the University of Oldenburg “Field effect investigations of charge carrier transport in organic semiconductors”
- 2006-2007 – Post doc at the University of Oldenburg
- Since 2007 – working towards habilitation in the Faculty of Natural Sciences at the University of Oldenburg

Awards

- 2008 – Mentoring Program at the University of Oldenburg

Publication list

J. Benoit, E. von Hauff, A. Saxena. Self-dual bending theory for vesicles. *Nonlinearity* 2004, 17, 57-66.

E. von Hauff, V. Dyakonov, J. Parisi. Study of field effect mobility in PCBM films and P3HT : PCBM blends. *Sol. Energy Mater. Sol. Cells* 2005, 87, 149-156.

I. Riedel, E. von Hauff, J. Parisi, N. Martin, F. Giacalone, V. Dyakonov. Diphenylmethanofullerenes: New and efficient acceptors in bulk-heterojunction solar cells. *Adv. Funct. Mater.* 2005, 15, 1979-1987.

B. Bohnenbuck, E. von Hauff, J. Parisi, C. Deibel, V. Dyakonov. Current-limiting mechanisms in polymer diodes. *J. Appl. Phys.* 2006, 99, no. 024506.

E. von Hauff, J. Parisi, V. Dyakonov. Field effect measurements on charge carrier mobilities in various polymer-fullerene blend compositions. *Thin Solid Films* 2006, 511, 506-511.

E. von Hauff, J. Parisi, V. Dyakonov. Investigations of the effects of tempering and composition dependence on charge carrier field effect mobilities in polymer and fullerene films and blends. *J. Appl. Phys.* 2006, 100, no. 043702.

E. von Hauff, J. Parisi, V. Dyakonov. Investigations of electron injection in a methanofullerene thin film transistor. *J. Appl. Phys.* 2006, no. 073713.

E. von Hauff, C. Deibel, V. Dyakonov. „Device Applications of Organic Materials”. In *Charge Transport in Disordered Solids with Applications in Electronics*, editor S.D. Baranovskii Wiley 2006.

E. von Hauff, J. Parisi, R. Weiler. Binding and Release of Glutamate from Overoxidized Polypyrrole via an Applied Potential for Application as a Molecular Switch. *Z. Naturforsch. a.* 2008, 63, 359-363.

E. von Hauff, N. Spethmann, J. Parisi. A Gated Four Probe Technique for Field Effect Measurements on disordered Organic Semiconductors. *Z. Naturforsch. a.* 2008, 63, 591-595.

Metelva-Fischer Y. V., von Hauff E., Parisi J., Electrochemical synthesis of polypyrrole layers doped with glutamic ions, *J. Appl. Poly. Sci.* 114 2009, 4051.

Da Como E., Hallermann M., Kriegel I., von Hauff E., Feldmann J., Charge transfer excitons in polymer/fullerene blends: the role of polymer chain conformation, *Adv. Funct. Mater.* 19, 3663.

Topp K., Borchert H., Johnen F., Tunc A. V., Knipper M., von Hauff E., Parisi J., Al-Shamery K., Impact of the incorporation of Au nanoparticles into polymer/fullerene solar cells, *J. Phys. Chem. A.*, in press.

Part VII:

OLEDs and related 2

HIGHLY EFFICIENT ORGANIC DEVICES

Karl Leo*

Inst. für Angewandte Photophysik, TU Dresden, 01062 Dresden, Germany

Organic semiconductors with conjugated electron system are currently intensively investigated for optoelectronic applications. This interest is spurred by novel devices such as organic light-emitting diodes (OLED), and organic solar cells. For both devices, high efficiency is a key parameter for many applications. In this talk, I will discuss some of the recent progress on highly efficient OLED and solar cells, in particular results using doped transport layers /1/. The concept of molecular doping allowed to realize green OLED devices with the highest efficiencies reported so far /2/, well exceeding the efficiency of current inorganic GaN LED! The devices were pin-devices where the emitting layer is embedded between a p-doped hole transport layer and an n-doped electron transport layers. It has been shown that these pin-structures can also achieve extremely long lifetimes. White OLED have recently achieved very high efficiencies of 90lm/W /3/, significantly higher than fluorescent tubes, opening the path to a new form of high-efficiency area lighting devices. The doping concepts can be applied in organic solar cells as well. Here, the use of electrically doped transport layers is helpful for an optimized optical design since it yields large freedom in the choice of window layer thickness, this making it easy to put the absorber layers in the electric field maximum in the cavity. Also, doped layers are a key point in efficient charge recombination junctions for tandem solar cells: It has been shown that a pn-junction is an excellent recombination contact causing very small voltage loss. Recently, we have achieved solar cells with certified efficiency exceeding 6% on larger area.

/1/ K. Walzer, B. Maennig, M. Pfeiffer, M. K. Leo, Chem. Rev. **107**, 1233 (2009)

/2/ G. He, M. Pfeiffer, K. Leo, M. Hofmann, J. Birnstock, R. Pudzich, J. Salbeck, Appl. Phys. Lett. **85**, 3911 (2004).

/3/ S. Reineke, F. Lindner, G. Schwartz, N. Seidler, K. Walzer, B. Lüssem, Nature **459**, 234 (2009).

*: I would like thank Jan Blochwitz-Nimoth, Torsten Fritz, Kentaro Harada, Gufeng He, Qiang Huang, Björn Lüssem, Rico Meerheim, Martin Pfeiffer, Sebastian Reineke, Moritz Riede, Rico Schüppel, Gregor Schwartz, Karsten Walzer, Ansgar Werner, Xiang Zhou, and many others for their participation in this work.

RED-LIGHT-EMITTING ELECTROCHEMICAL CELLS BASED ON IRIIDIUM (III) COMPLEXES

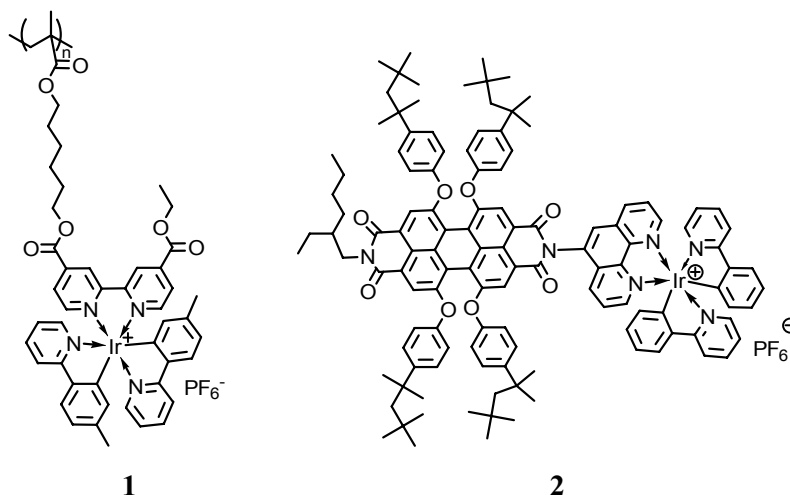
F. FERNÁNDEZ-LÁZARO*¹; J. L. RODRÍGUEZ-REDONDO¹;
F. J. CÉSPEDES-GUIRAO¹; R. D. COSTA²; J. GIERSCHNER²; E. ORTÍ²;
H. J. BOLINK²; Á. SASTRE-SANTOS*¹

¹ División de Química Orgánica; Instituto de Bioingeniería; Universidad Miguel Hernández; Avda. de la Universidad s/n; 03202 Elche; Spain

² Instituto de Ciencia Molecular; Universidad de Valencia; PO Box 22085 Valencia; Spain

Deep-red phosphorescent ionic iridium (III) complexes have been synthesized and incorporated in a polymer (**1**). LEC devices using both the complex and the polymer as the electroluminescent active material have been built up. The polymer version of the complex gives rise to devices with higher stabilities that emit light at longer wavelengths in the red (660 nm) than the devices using the small molecular weight complex (630 nm). The improved stability and the longer emission wavelength are attributed to a more uniform distribution of the active ionic transition-metal complexes imposed by the chemical linkage to the polymer backbone. This is one of the first examples of a polymeric iTMC-based optoelectronic device incorporating iridium (III) complexes that shows bright electroluminescence in a simple sandwiched architecture using air-stable electrodes.

The synthesis and luminescence properties of an iridium (III)-perylene-3,4,9,10-tetracarboxylic diimide dyad (**2**) will be also reported. The new derivatives show efficient fluorescence with high quantum yields (55%). A two-layer light-emitting electrochemical cell device based on the new material emits in the deep-red region with high external quantum efficiency (3.27%).



BIOGRAPHIC DATA OF PROFESSOR FERNANDO FERNÁNDEZ LÁZARO

Fernando Fernández Lázaro studied chemistry at Autónoma University of Madrid. He obtained the PhD degree in 1992 at the same university under the guidance of Prof. Tomás Torres working in the synthesis and study of the electrical properties of hemiporphyrines. He spent a post-doctoral stay in the University of Tübingen (Germany) working with Prof. Michael Hanack in the synthesis of silicon phthalocyanines. He moved to Bordeaux (France) to



work with Dr. Christophe Mingotaud at C.N.R.S. in the preparation of Langmuir-Blodgett films. Then, he went to the University of California Santa Barbara to carry research with Prof. Bruce H. Lipshutz in the synthesis of the family of Coenzyme Qn (n = 1-10).

He joined the recently founded Miguel Hernández University at the end of 1998. Since the beginning of 2001 he is Profesor Titular of organic chemistry at this university.

His current research interest comprises the chemistry of perylenes and phthalocyanines, the study of the energy and electron transfer processes they are involved in, and their application in organic solar cells and light-emitting diodes. He carries also research in photorefractive materials and in the applications of triorganoindium reagents in synthesis.

OPTIMIZING CONTRAST IN DUAL ELECTROCHROMIC DEVICES WITH OPTICALLY TRANSPARENT ION-STORAGE LAYERS

J. PADILLA*¹, M.A. INVERNALE², Y. DING², D.M.D. MAMANGUN²,
G. A. SOTZING²

¹ Department of Applied Physics, ETSII, Technical University of Cartagena (UPCT), C/ Doctor Fleming s/n 30202 Spain

² University of Connecticut, Department of Chemistry and the Polymer Program, 97 N. Eagleville Road, Storrs, Connecticut 06269-3136

Electrochromic devices are electrochemical cells for which at least one of the electrodes changes colour reversibly. Applications for these devices include smart windows or displays, just to cite some of them ¹. For these and any other possible use, there are several parameters that must be optimized to get a viable device. Perhaps the most important one is to get good optical characteristics, which means that, as the primary function of these devices is to show colour changes, these coloured states must be well differentiated. To achieve this goal of optimized contrast, that is, the transmittance difference between two colour states, should be maximized. Another relevant parameter to optimize is the lifetime of the devices; otherwise they will not be useful for a real-world application. Other interesting aspects to study include switching speed or memory effect, although these are critical only for certain applications.

Due to the electrochemical nature of these devices, the reactions occurring at one electrode (oxidation or reduction) must be compensated by their complementary ones (reduction or oxidation, respectively). If this is not carried out by an adequate electrode, it will be found that the device will not work as the redox reaction cannot be completed or that parallel and frequently undesirable reactions occur (electrolyte discharge for instance) to complete it. This often leads to creation of chemicals that will attack and degrade the electrochromic material or the electrode materials, thus effectively destroying the device.

Ion storage layers, able to compensate the electrochromic reaction occurring at the opposite electrode by undergoing their own redox chemistry, have been used since the beginning of the development of electrochromic devices. After a reasonable choice of material (considering its redox and optical properties), the inclusion of an ion storage layer at one electrode guarantees that the lifetime of the electrochromic material at the opposite electrode will mostly depend on its own properties and will not be subjected to deleterious side reactions. In a general sense, the function of these layers is only electrochemical. They

do not take part in the electrochromic response of the device. Ideally, the ion storage layer would be transparent in both states.

A significant advance in the design of electrochromic devices was the dual complementary electrodes approach²: the ion storage layer is also an electrochromic in this system, and if its optical properties are well chosen, complementary and simultaneous colour changes occur at both electrodes. Benefits from this configuration, at first sight, are that we still can guarantee a good lifetime for the device and could improve the optical response, as two electrodes are contributing simultaneously. This configuration has shown clear benefits and is widely used.

From an optical point of view, impressive advances have been made in recent years synthesizing materials with tailored electrochromic and contrast properties, especially for organic materials, and more precisely for conducting polymers. However, the contrast of an electrochromic film is not an intrinsic characteristic of the material, i.e. different film thicknesses of the same material show different contrast, and therefore it is critical to identify the maximum contrast conditions.

According to a modified Beer-Lambert law³, absorbance can be expressed as

$$A = \eta q \quad (1)$$

With q being the redox charge consumed per unit area (charge density) during the color change. η corresponds to coloration efficiency, defined as the charge density consumed per unit of absorbance change.

Transmittance can therefore be defined as

$$T = \exp(-\mu q) \text{ with } \mu = 2.303\eta \quad (2)$$

And finally, contrast, the difference in percent transmittance between two states (denoted as the subscripts c and d for “clear” and “dark”)

$$\Delta T = \%T_c - \%T_d = 100[\exp(-\mu_c q) - \exp(-\mu_d q)] \quad (3)$$

The derivative of this function allows for identifying the maximum contrast of a given material, and the redox charge density needed to achieve it. It constitutes a useful tool to

synthesize the best contrast film for a given material, as redox charge density is an easily identifiable parameter.

As long as the Beer-Lambert law is obeyed, this optical characterization as a function of the redox charge of a film can be extended to several layers by simply adding their absorbances. A dual configuration implies that two films with, in principle, different redox charge densities, are operated together. From an electrochemical point of view, practical combinations are reduced to those with balanced redox charge films, at least for general purposes. However different combinations are allowed (utility of these combinations can be discussed in more detail, although that is not relevant for this study). It seems necessary to identify which of these combinations shows better contrast. If this is carried out for a dual electrochromic configuration, surprising results are obtained⁴. The calculation of the maximum contrast values among the possible combinations of two electrochromic materials reveals that no clear optical benefit is obtained from the dual configuration. Although there are several dual combinations that increase the contrast, compared to the individual values, the maximum contrast achievable for two given materials is obtained when only one film is present. As a consequence, the possible benefits of a dual configuration in terms of lifetime of a device get reduced by the fact that optically this configuration is not so attractive.

Solutions to this include the use of ion storage layers being transparent (in the visible region) so as not to decrease the contrast of the opposite electrode, but still being electrochemically active to compensate the redox reaction. A new conducting polymer, poly(thieno[3,4-*b*]thiophene) or PT34bT, has been used specifically for this purpose. This material has a very low bandgap, 0.85 eV, and has earlier been reported to be highly transmissive and colorless in the oxidized state and a transmissive sky blue in the neutral state⁵. Different films of this material were electropolymerized and the contrast vs. redox charge values identified, obtaining a maximum of ten percent. With such low contrast values, it is expected that the effect of reducing contrast when used as an ion storage layer will also be low.

Several electrochromic devices using PT34bT as ion storage layer were constructed⁶. Opposite electrodes were made with different electrochromic polymers, namely, PProDOT-Me₂ (poly [2,2-dimethyl-3,4-propylenedioxythiophene]), PEDOT (poly[3,4-ethylenedioxythiophene]) and PDiBz-ProDOT (poly[dibenzyl-3,4-propylenedioxythiophene]). Previous to their inclusion into the devices, the contrast vs. redox charge density relationship was also obtained for each material. It was found that, as

expected, the use of PT34bT as an ion storage layer did not reduce the contrast dramatically. In any case, it was always lower than 10%. Table 1 compares the different values of contrast between single materials and with PT34bT as ion storage layer.

Table 1. Photopic contrast values of single electrochromic polymers, PProDOT-Me₂, PEDOT and PDiBz-ProDOT, compared with values obtained using PT34bT as ion storage layer in an electrochromic device.

	Single electrochromic polymer	Device with PT34bT as ion storage layer	
	photopic contrast (%T)		difference (%T)
PDiBz-ProDOT	43	41	2
PProDOT-Me₂	67	59	8
PEDOT	34	27	7

It has been shown that the dual configuration of electrochromic devices could represent a good solution to several issues associated with electrochromic devices, from an electrochemical point of view; however there are some optical limitations in terms of the obtainable contrast. The inclusion of a complementary electrochromic layer could lower the final contrast of the device. A way to avoid this problem consists of the use of materials with good redox properties but which are also transparent in the visible range so as not to contribute to the final optical response of the device. A new low band gap conducting polymer, PT34bT, has been specifically used for this purpose and the viability of its use as an ion storage layer was shown.

References

1. Monk, P.M.S., Mortimer, R.J. & Rosseinsky, D.R. *Electrochromism: Fundamentals and applications*. VCH, Weinheim (1995).
2. Sapp, S.A., Sotzing, G.A., Reddinger, J.L. & Reynolds, J.R. Rapid switching solid state electrochromic devices based on complementary conducting polymer films. *Adv. Mater.* **8**, 808-811 (1996).
3. Padilla, J., Seshadri, V., Sotzing, G.A. & Otero, T.F. Maximum contrast from an electrochromic material. *Electrochem. Commun.* **9**, 1931-1935 (2007).
4. Padilla, J. & Otero, T.F. Contrast limitations of dual electrochromic systems. *Electrochem. Commun.* **10**, 1-6 (2008).
5. Lee, K. & Sotzing, G.A. Poly(thieno[3,4-*b*]thiophene). A new stable low band gap conducting polymer. *Macromolecules* **34**, 5746-5747 (2001).
6. Invernale, M.A. *et al.* Polythieno[3,4-*b*]thiophene as an Optically Transparent Ion-Storage Layer. *Chem. Mater.* **21**, 3332-3336 (2009).

BIOGRAPHIC DATA OF JAVIER PADILLA MARTÍNEZ

Present position

Assistant professor
Polytechnic University of Cartagena, Technical School of Engineering,
Department of Applied Physics
Edif. ETSII. Antiguo Hospital de Marina. Campus Muralla del Mar. C/ Doctor
Fleming, s/n 1ª Planta. 30202 Cartagena. Murcia. Phone number: +34
968325597 Fax: +34 968325337
e-mail: javier.padilla@upct.es



Research lines

Conducting polymers: Electrochemistry and electronics. Applications: Development of electrochromic devices. Organic solar cells.

Academic degrees

June 2001, Degree in Physics, University of Valladolid, Spain
Dec 2006, Phd European doctorate in experimental sciences, Polytechnic University of Cartagena, Spain. Advisor: Prof T.F Otero.

Last relevant publications

- [1] A.Kumar, S.Y.Jang, J.Padilla, T.F.Otero, G.A.Sotzing, *Polymer* 2008, 49, 3686
- [2] J.Padilla, T.F.Otero, *Electrochem. Commun.* 2008, 10, 1.
- [3] J.Padilla, V.Seshadri, J.Filloramo, W.Mino, S.P.Mishra, Radmard B., A.Kumar, G.A.Sotzing, T.F.Otero, *Synth. Met.* 2007, 157, 261.
- [4] J.Padilla, V.Seshadri, G.A.Sotzing, T.F.Otero, *Electrochem. Commun.* 2007, 9, 1931.
- [5] V.Seshadri, J.Padilla, H.Bircan, B.Radmard, R.Draper, M.Wood, T.F.Otero, G.A.Sotzing, *Organic Electronics* 2007, 8, 367.

Collaborations in the last four years

Prof G. A. Sotzing at Institute of Materials Science (UCONN, USA)
Prof K. West at Riso National Laboratory (Denmark)
Prof T.F. Otero at Polytechnic University of Cartagena (Spain)
Prof A. Urbina at Polytechnic University of Cartagena (Spain)
Prof. J. Colchero at Center for Investigation in Optics and Nanophysics (University of Murcia, Spain)
Dr. D. Curiel at University of Murcia (Spain)

Other achievements (Miscellaneous)

Best thesis award (Basic Science) 2008-2009, Polytechnic University of Cartagena
Award for the best oral presentation of young researchers (VIII Escuela Nacional de Materiales Moleculares), Estepona, Málaga, (Spain) May 2007

USER OF LARGE SCIENTIFIC FACILITIES

Rutherford Appleton Laboratory (RAL), UK. Neutron scattering experiment: "Characterization of the structural properties and side-chain dynamics of bulk poly-3-alkylthiophenes" Instrument used: OSIRIS. Exp: 820280. (4-10 July 2008). Exp: RB910412. (17-22 March 2009)

VI Escuela Nacional de Materiales Moleculares (Member of the local organizing committee) (21-29 June 2003)

4th World Congress on Biomimetic, Artificial Muscles and Nano-Bio (Member of the local organizing committee) (6-9 Nov 2007)

19 oral presentations at international conferences

Part VIII:

Materials & Methods 2

PHOTOINDUCED ELECTRON TRANSFER AND TRANSIENT STATES IN ORGANIC COMPOSITES STUDIED BY ESR

H.-K. Roth^{1*}, A. Konkin², V. I. Krinichnyi³ and M.Schroedner¹

¹ TITK Institute Rudolstadt, Department Functional Polymer Systems and Physical Research, Breitscheidstr. 97, D-07407 Rudolstadt, Germany (*e-mail: roth@titk.de)

² Ilmenau University of Technology, Institute for Micro- and Nanotechnologies, Gustav-Kirchoff-Str.7, D-98693 Ilmenau, Germany (e-mail: alexander.konkin@tu-ilmenau.de)

³ Institute of Problems of Chemical Physics, Russian Academy of Sciences, N. N. Semenov Avenue 1, Chernogolovka 142432, Russia (e-mail: kivirus@gmail.com)

Introduction

By this contribution we will show how we can support by electron spin resonance (ESR or EPR) the development of polymer photovoltaic and related fields of organic electronics. Essential processes in organic photovoltaic are the excitation of molecules, the electron transfer, the generation of charge carrier pairs, and the motion of charges. To the study of all mentioned processes ESR can support.

The contributions of ESR are especially high if one has the possibility to use various measuring frequencies, that is, to employ besides the ordinary X-band with 9.5 GHz, for example, the K-band (24 GHz), and/or the Q-band (35 GHz), the W-band (94 GHz), or the D-band (140 GHz). The higher the frequency, the better is the spectral resolution [1-2]. In the solid state the ESR signals are usually influenced by inhomogeneous line broadening caused by unresolved hyper-fine structures and by anisotropic broadening connected with the anisotropy of the g-factor components. K-, Q-, W- and D-band measurements allow to determine the spectral parameters g_i and ΔB_i (line widths) with better accuracy.

As known in polymer electronics thin layers of semiconducting polymers are applied showing often strong anisotropic structures and properties. The ESR offers the opportunity to study the anisotropic behaviour direct on the polarons P^+ generated and moving in polymer chains. If the polymer chains in polymer films exhibit some degree of order and orientation the same is valid also for the polarons. The macroscopic anisotropy of polymer thin film morphology can be confirmed by angular-dependent ESR experiments as made recently, for example, by K-band investigations on films of P3HT/PCBM blends [3].

LESR (light-induced ESR)

According to the topic of the paper especially LESR spectra – that is ESR measured during light illumination - are in the center of interest. The following information can be obtained by analysis of LESR spectra [4]:

1. The main is the detection of cation and anion radicals during and after light excitation including the determination of the estimation of charge carrier concentration.
2. The analysis of the spectroscopic Zeeman splitting factor (g-factor) gives information about the localization of the paramagnetic centre and on the symmetry. The deviation of the average g-factor from the g-factor g_e of the free electron; $\Delta g = g - g_e = \lambda / \Delta E_g$, where λ is the spin-orbit coupling constant and ΔE_g is the polymer band gap, informs about the most probable position (or spin density maximum) of polaron localization on the polymer chain. This is possible because of the significant difference of the λ value for C-atoms of a conjugated polymer ($\lambda = 29 \text{ cm}^{-1}$ for C) from that of other atoms ($\lambda = 78 \text{ cm}^{-1}$ for N and 382 cm^{-1} for S)
3. The LESR signal line-width analysis gives essential information about
 - (a) spin-lattice and spin-spin relaxation times T_1 and T_2 , respectively,
 - (b) exchange and dipole-dipole interactions,
 - (c) anisotropic broadening, connected with the anisotropy of g-factor components,
 - (d) inhomogeneous broadening due to unresolved hyperfine signal structure.
4. The time dependence of the signal amplitude gives information on the kinetics of charge generation and charge recombination processes.

Examples of LESR-spectra of a poly(3-dodecylthiophene){P3DDT} /PCBM {phenyl-C61-butrylic acid methylester} composite registered during laser irradiation at 77 K shows Fig. 1 [2]. The spectra of two overlapping ESR signals are seen where the left hand signals belong to diffusing polarons P^+ and the right hand signals are attributed to the PCBM anion radicals C_{61}^- .

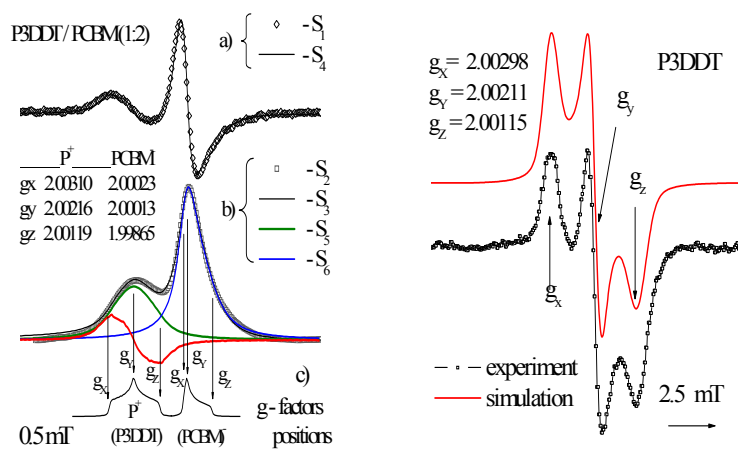


Fig.1 left: X-band LESR spectra of polarons P^+ in P3DDT and of PCBM anion radicals, a) measured (S_1) + simulated (S_4) 1st derivative spectrum, b) absorption spectrum calculated from S_1 , $S_5 =$ extracted P^+ signal, c) schematic representation of anisotropic absorption signals and g-factor components

Fig.1 right: D-band ESR spectra of polarons P^+ in P3DDT

LESR studies have been made also on PPV-PPE/PCBM and PPV-MDMO/PCBM at 77 K [4]. The strong saturation effect of the polaron signal gives the opportunity to investigate the PCBM anion radical de facto separately and in detail. Measured and calculated spectra dominated by the anion radicals are seen in Fig. 2. In the first step the absorption spectrum had been calculated

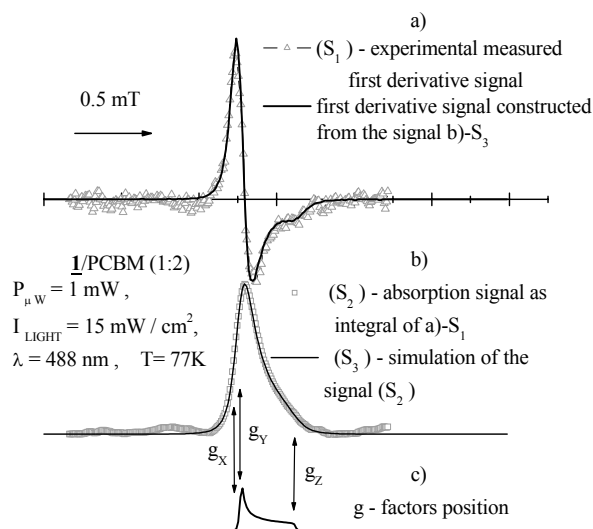


Fig. 2; LESR spectra of a 1:2 composite of PPV-PPE/PCBM registered during laser irradiation

($\lambda = 488 \text{ nm}$, $P = 15 \text{ mW}$) at 77 K (in the X-band)

(a) measured and calculated first derivative spectrum,

(b) constructed absorption spectrum,

(c) schematic representation of the anisotropic absorption signal of the PCBM anion radical (calculated with a small line-width) and positions of the determined g-factor components

PPV-PPE = poly(phenylene vinylene)-poly(phenylene ethynylene)

by integration of the experimentally first derivative ESR signal. In the second step these absorption spectrum were simulated as a glass type spectrum with a Lorentzian line shape. The complete analysis allows to eliminate the anisotropic line width broadening and to estimate the effective spin-spin relaxation time T_2 (and by means of it also the spin-lattice relaxation time T_1). T_1 of the anion radical is significantly influenced by the surrounding structure. (In MDMO-PPV $T_1=7.4 \mu\text{s}$, $T_2=68 \text{ ns}$; in PPV-PPE $T_1=9.4 \mu\text{s}$, $T_2=65 \text{ ns}$.) That in MDMO-PPV T_1 is shorter than in PPV-PPE composites means that the exchange of spin energy with the surrounding occurs in MDMO-PPV faster than in PPV-PPE composites.

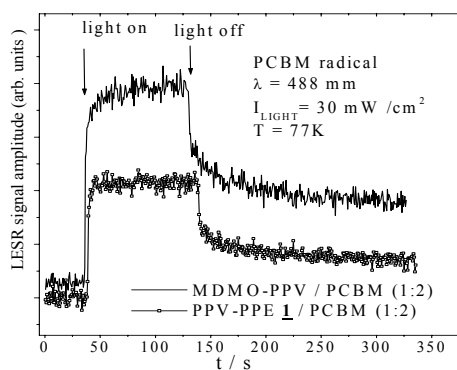


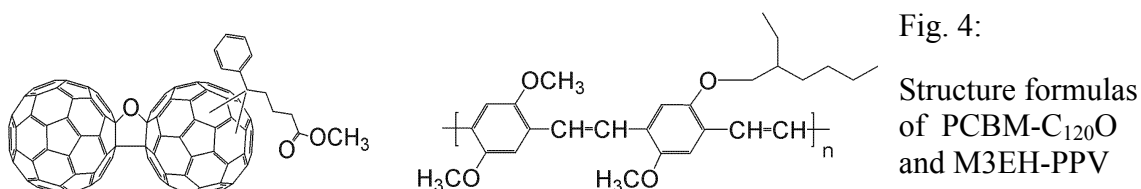
Fig. 3; Rise and decay of the LESR signal of PCBM anion radicals C_{61}^- in two different 1:2 composites measured at 77 K

The upper signal amplitude belongs to MDMO-PPV / PCBM composite and the lower one to a PPV-PPE composite

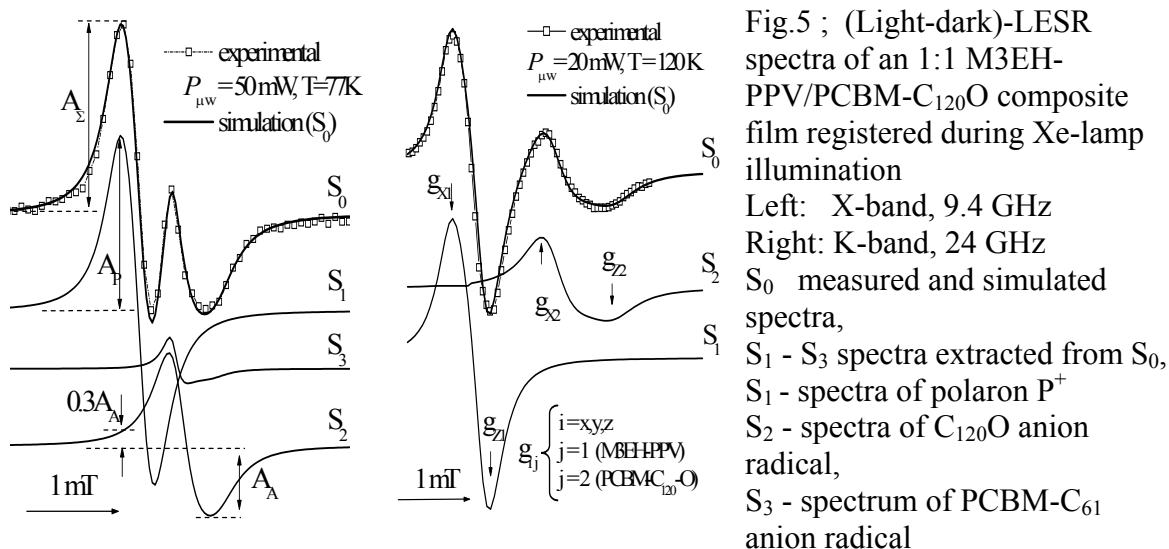
MDMO-PPV = poly[methoxy(dimethyloctyloxy)-phenylene vinylene

In Fig. 3 is to see that also the kinetics of the PCBM anion radical depends strongly on the polymer surrounding. The decay curves can be described successfully by a tunnel model in which the recombination frequency depends only on the distance between the charge carriers. The same model has been used before for the study of organic solar cell composites [6].

The generation of radical pairs normally occurs in the femto- to nano-second time domain. Therefore the time dependence of the ESR signal intensities is mainly caused by their recombination. Different activation energies obtained for P^+ and C_{61}^- are evidences for independence of the motion of the polarons and C_{61} anion radicals [5]. There are also different spin dynamics in this system, namely the polaron diffusion along and between the polymer chains and the dominant rotational diffusion of the PCBM anion radicals.



Similar LESR studies on thin films of M3EH-PPV with the fullerene dimmer PCBM- $C_{120}O$ as electron acceptor have been carried out by X- and K-band ESR at 77 and 120 K [7].



It was found that the isotropic g-factor $g_0 = (g_x + g_y + g_z)$ of the $PCBM-C_{120}O$ anion radical obtained in this blend is with $g_0 = 1.9996$ close to the g-factor of PCBM and of the electrochemical reduced $(C_{120}O)^-$, but it does not coincide with the analogous parameter of the triplet state radical $(C_{120}O)^{2-}$ [8].

ESR give also the opportunity to study the spin and charge dynamics in conjugated polymers like P3DDT [2] and also in P3DDT/PCBM composites with photo-generated radical pairs [5] especially if measuring at various frequencies [9] and as a function of temperature.

TR-ESR (time-resolved ESR)

If we would like to know

- what happens in detail after the absorption of light quanta in the polymer blends,
- from which excited state the photo-induced electron transfer will be introduced,
- the mechanism of the generation of charge carrier pairs and their motion, separation and energy exchange,

in that case the time-resolved ESR is a suitable measuring method. Such TR-ESR studies of the photo-induced electron transfer in poly(3-dodecylthiophene){P3DDT}/maleic anhydride {MA} blend in THF solution have been carried out [10]. The blends have been excited by laser flashes of about 20 ns and the ESR spectra were registered between 100 ns and 10 μ s after the flash.

By TR-ESR investigations a great part of the information on the photo-induced ET (electron transfer) and with it on the formation of radical ion pairs we get from the irregular population of energy levels which are below 1 μ s far away from the population in the thermal equilibrium. The reason for the unusual level population is the so-called Chemically Induced Dynamic Electron Spin Polarization (CIDEP).

One reason for CIDEP is the Triplet Mechanism (TM). Absorption of a photon by a donor molecule M yields an excited singlet state $^1M^*$ which undergoes intersystem crossing to an excited triplet state $^3M^*$ whose Zeeman levels T_{+1} , T_0 and T_{-1} have different energy in the magnetic field of the ESR spectrometer. The ISC is spin selective and creates spin polarization in the triplet state molecule. If the ET and the radical pair formation from a triplet state takes place more quickly than the deactivation by phosphorescence or by the spin-lattice relaxation of the triplet state (3T_1) the unusual spin polarization will be transferred in the doublet states of the radical ions and often we will observe emission spectra which are independent of the magnetic field position of the observed ESR lines. (The radical system acts as a microwave emitter until the occupation of the thermal equilibrium is reached.)

A second reason for CIDEP is the so-called Radical Pair Mechanism (RPM) which effects changes between singlet and triplet states (S-T-mixing) during separation, diffusion and re-encounter of radical pairs. It effects that the spin polarisation in the low-field region is different from that in the high-field region.

Some times CIDEP effects are to observe also in the usual continuous wave ESR spectra if these are registered during steady state illumination with light of a Xenon lamp or a laser as published, for example, in [11, 12]. If the effect of RPM is observed it informs us that radical pairs are formed also if we detect only the spectrum of one radical.

The usual continuous wave ESR register the spectra with modulation technique and the first derivative of the absorption spectra will be observed as seen, for example, in Figs 1, 2, 5... of this paper. For the TR-ESR measurements no field modulation was used but a direct detection have been applied. The transient ESR signals were digitized by a fast digital oscilloscope synchronized with the laser pulses. Photo-excitation was performed by an excimer laser Compex 205 operating at 308 nm and with a pulse repetition rate of 10 Hz. The pulse energy of the Laser was 100 – 200 mJ and the pulse duration was about 20 ns. The time resolution of our detection system is approximately 50 ns.

The effect of TM and the influence of RPM can be seen in Fig. 6 for radicals of maleic anhydride (MA) and in Fig. 7 for radicals in P3DDT/MA [10].

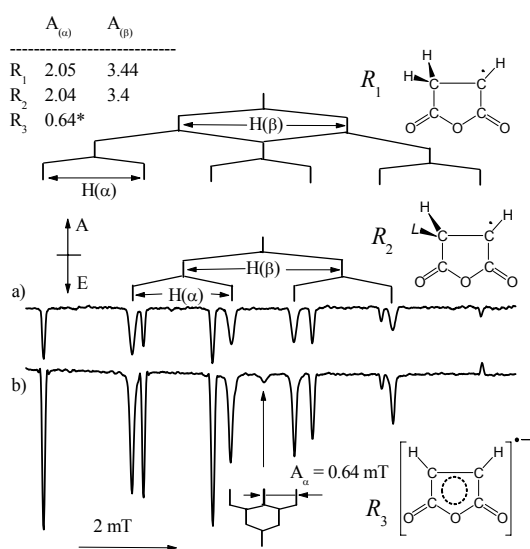


Fig. 6 ; TR-ESR spectra of 3 various radicals of MA radicals and the belonging splitting diagrams
a) in THF solution, b) in butanol
The H-containing solvents are in this contribution labelled as LH. The electrical neutral radicals R_1 and R_2 are formed by attachment of $H\cdot$ and $L\cdot$ via abstraction of H from the LH-molecule ($R_1 = HMA$, $R_2 = LMA$). In butanol $R_3 = MA\cdot^-$ is formed by the attachment of an electron from a solvent molecule.

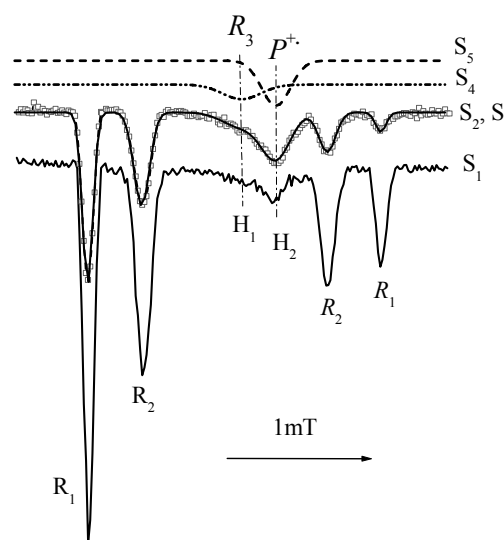


Fig. 7; TR-ESR spectra (S_1 , S_2) of radicals in blends from P3DDT and MA solved in THF.
 S_1 and S_2 are measured 0.35 μs after the laser flash. For the spectrum S_2 about two times more P3DDT has been in the solution than for S_1 . S_3 is the fitted spectrum of S_2 . S_4 and S_5 are extracted spectra from S_3 belonging to the anion radical $R_3 = MA\cdot^-$ and the polaron $P^{+\cdot}$, respectively.

In Fig. 7 the field position H_1 of the central lines of R_3 corresponds to $g = 2.0037$ for the anion radical. The position H_2 corresponds to $g = 2.0022$ which is in agreement with the isotropic g-factor of the polaron $P^{+\cdot}$, estimated from measurements on a film of P3DDT/PCBM [5].

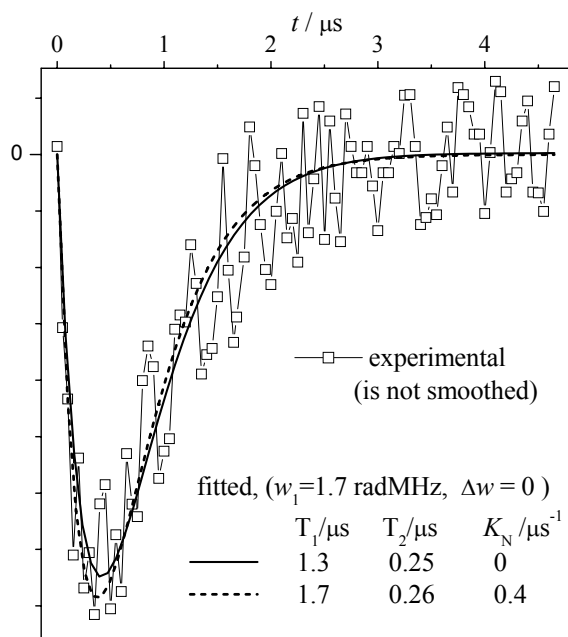


Fig. 8

The measured time dependence of the polaron signal. Although the signal to noise rate is with $S/N \approx 3.5$ low the time dependence is clear and allows in a fitting process the estimation of the relaxation times T_1 and T_2 .

The low spin-spin relaxation time T_2 is caused mainly by the high hole mobility of P^+ in the conjugated polymer P3DDT and is of the same order of magnitude as estimated by a saturation method in a solid PDDT layer [5].

Complete three-line TR-ESR spectra of MA^- have been published by Honma et al, [13] and by He et al. [14], however, not with a conjugated polymer as donor but with a low molecular compound.

Results regarding ET in P3DDT/MA [10].

The simultaneous detection of both ion radicals, the polaron P^+ and the anion radical R_3^- informs us that in solutions of P3DDT/MA blends in THF the most probable version of the formation of R_3 anion radicals will be via the electron attachment from the photo-excited poly(3-dodecylthiophene). The emissive character of the spectra informs that the dominating CIDEP mechanism is the triplet mechanism (TM). That means a precursor of the photo-induced electron transfer is a triplet state generated via intersystem crossing from an excited singlet state.

Additionally the polarization by the radical pair mechanism (RPM) occurs, however, with opposite sign in comparison with the electrically neutral radical pairs R_1 and R_2 where the RPM by S- T_0 mixing effects clear E/A spectra with emissive signals in the low field region and enhanced absorption signals in the high field region of the spectra. In case of the electrically charged radical pairs the polarization is not only influenced by the exchange interaction $J \leq 0$ but especially by dipole-dipole or Coulomb interaction (CI). In such ion radical pair systems a " $J \geq 0$ " behaviour is possible [15], and in the above mentioned system with MA^- radicals the S- T_{-1} mixing seems to be the most plausible polarization mechanism [13].

Also in the case of the radical pair R_3^- and P^+ a " $J \geq 0$ " behaviour is probably influencing the spectra of $R_3 = MA^-$. This behaviour is caused by dipole-dipole or Coulomb interaction

(CI) within the geminately generated ion radical pairs. This is in agreement with the theoretical treatment of Shkrob [15].

The CI is larger in donor/acceptor systems with smaller molecular radius of acceptors than in that with larger acceptor molecules. The CI promotes the back electron transfer, and as a result, limits the efficiency of the charge separation process. The small CI in polymer blends with the acceptor fullerene is probably the reason for the high efficiency of the photo-induced electron transfer in blends of conjugated polymers with fullerene derivatives.

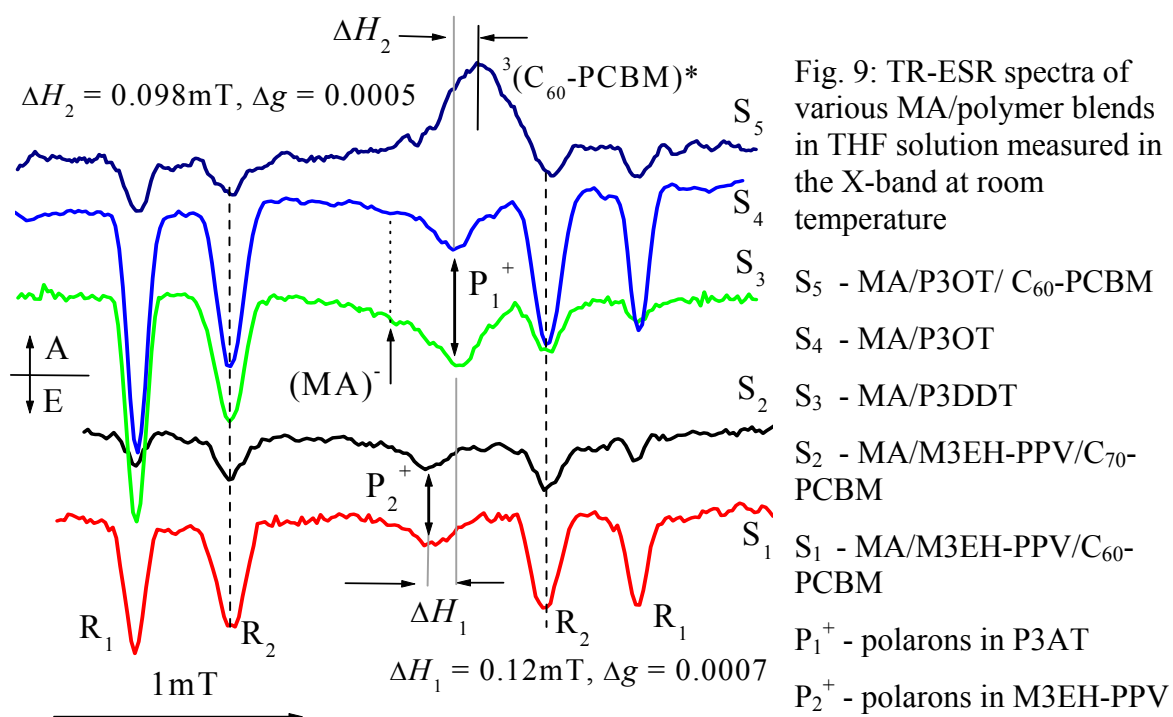


Fig. 9: TR-ESR spectra of various MA/polymer blends in THF solution measured in the X-band at room temperature

- S₅ - MA/P3OT/ C₆₀-PCBM
- S₄ - MA/P3OT
- S₃ - MA/P3DDT
- S₂ - MA/M3EH-PPV/C₇₀-PCBM
- S₁ - MA/M3EH-PPV/C₆₀-PCBM
- P₁⁺ - polarons in P3AT
- P₂⁺ - polarons in M3EH-PPV

Additional experiments with two other conjugated polymers have been carried out with the aim to compare the resonance positions and the spin polarisation (CIDEP) of polarons in different polymers. The spectra are seen in Fig. 9. The spectrum S₃ of Fig. 9 is identical with the spectrum S₂ of Fig. 7.

Concerning the spectra S₁ and S₂ of Fig. 9 it should be pointed out that the TR-ESR spectra have been recorded in the presence of a small concentration ($c \approx 0.001$ M) of C₆₀- and C₇₀-PCBM, respectively, especially because in pure MA/M3EH-PPV solution the signal/noise rate was too low to register polaron spectra of sufficient intensity. The resonance positions of polarons P₂⁺ (in M3EH-PPV) is shifted to the low field direction by 0.12 mT in respect to P₁⁺ (in P3AT). Different g-factors of polarons in P3AT and in M3EH-PPV are the reason for the displacement.

P3OT (Poly-3-octylthiophene) and P3DDT have the same polymer backbone and the polarons have about the same isotropic g_0 -factor of around 2.0021. However, the polarons P_2^+ in M3EH-PPV have a g_0 -factor value $g_0 = 2.0029$. (In Fig. 9 signals of the anion radicals of C_{60} - and C_{70} -PCBM are de-facto not to see because of the small concentration. Its g -factors are about 2.000 and 2.0028, respectively.)

For the spectrum S_5 an about 10-times higher C_{60} -PCBM concentration ($c \approx 0.01$ M) have been applied in the blend with MA-P3OT. The strong absorption signal is caused by excited triplet states of C_{60} -PCBM. It should be pointed out that the $^3(C_{60}\text{-PCBM})^*$ spectrum has been certainly registered by us also in THF solution without MA and polymer, and for example, by Scharber et al. [16]. For the spectrum S_5 the blend with MA has applied mainly because of the opportunity of precise line position determination relative to the spectral lines of R_1 and R_2 of maleic anhydride. The CIDEP signals of $^3(C_{60}\text{-PCBM})^*$ and of the observed polarons have opposite signs. Therefore on the field position labelled with P_2^+ in the spectra S_1 and S_2 are really the resonance signals of P_2^+ and can not be attributed to signals of anion radicals of PCBM.

Concluding remarks

With this contribution it has been shown that ESR spectroscopy allows a deeper insight in the physical processes of the electron transfer and in chemical reactions of radical ions and neutral radicals. By means of ESR spectroscopy relatively fast can be proofed

- whether in a new donor/acceptor material combination photo-induced electron transfer occurs or not
- how various additives influence the electron transfer and the electron back-transfer
- whether in the selected material combination electron back-transfer happens and how fast it is
- how special material treatments like, for example, annealing, solving and re-crystallization influences that process

By means of TR- ESR spectroscopy one can study

- excited triplet state properties of donors:
 - electron transfer rate
 - excited triplet / singlet ground state kinetics,
 - estimation of relative sublevels triplet state populations
- transient precursor states and kinetics of ion radical formation in donor-acceptor organic composites under the light excitation

Without doubt, ESR spectroscopy contributes not only to the fundamental research but it is also of practical worth for developers of solar cell materials and for related subjects of development.

References

- [1] a) Roth, H.-K., Krinichnyi, V. I.; *Synth. Met.* 137 (2003) 1431-1432
b) Krinichnyi, V. I., Roth, H.-K.; *Appl. Magn. Reson.* 26 (2004) 395-415
- [2] Konkin, A., Roth, H.-K., Krinichnyi, V. I., Schroedner, M., Aganov, A., Nazmutdinova, G., Sensfuss, S.; *Proceedings TPE 04* (2004) 167-170
- [3] Konkin, A., Roth, H.-K., Scharff, P., Aganov, A., Ambacher, O., Sensfuss, S.; *Solid State Communications* 149 (2009) 893-897
- [4] Konkin, A. L., Sensfuss, S., Roth, H.-K., Nazmutdinova, G., Schroedner, M., Al-Ibrahim, M., Egbe, D. A. M.; *Synth. Met.* 148 (2005) 199-204
- [5] Krinichnyi, V. I., Roth, H.-K., Sensfuss, S.; Schroedner, M., Al-Ibrahim, M.; *Physica E* 36 (2007) 98-101
- [6] Schultz, N. A., Scharber, M. C., Brabec, C. J., Sariciftci, N. S.; *Phys. Rev. B.* 64 (2001) 245210
- [7] Konkin, A., Ritter, U., Scharff, P., Roth, H.-K., Aganov, A., Sariciftci, N. S., Egbe, D. A. M.; *Synth. Met.* 160 (2010) 485-489
- [8] Balch, A. L., Costa, D. A., Fawcett, W. R., Winkler, K.; *J. Phys. Chem.* 100 (1996) 4823-4827
- [9] Mizoguchi, K., Kuroda, S. in: Nalwa, H. S. (Ed), *Handbook of Organic Conductive Molecules and Polymers*, Vol. 3, John Wiley & Sons, New York 1997, pp. 251-317
- [10] Konkin, A., Sensfuss, S., Roth, H.-K., Scharff, P., Ambacher, O., Aganov, A., Schroedner, M.; *J. Molecular Liquids* 141 (2008) 54-61
- [11] Roth, H.-K., Keller, F., Schneider, H.; *Hochfrequenzspektroskopie in der Polymerenforschung*, Akademie-Verlag, Berlin 1984
- [12] Roth, H.-K., Wünsche, P.; *Acta Polymerica* 32 (1981) 491-511
- [13] Honma, H., Murai, H., Kuwata, K.; *Chem. Phys. Letters* 195 (1992) 239-242
- [14] He, G., Li, X., Chen, C., Xu, G.; *J. Photochemistry and Photobiology* 108 (1997) 155-158
- [15] Shkrob, I. A.; *Chem. Phys. Letters* 264 (1997) 417-423
- [16] Scharber, M. C., Brabec, C. J., Dyakonov, V., Sariciftci, N. S.; *Synth. Met.* 101 (1999) 356

BIOGRAPHIC DATA OF PROFESSOR DR HANS-KLAUS ROTH

Hans-Klaus Roth received his master degree in Experimental Physics and his PhD in Molecular and Polymer Physics under the mentorship of Prof. W. Holzmüller at the University of Leipzig in 1962 and 1969, respectively.

Until 1974 scientific assistant or co-worker in the Department of Physics at the University of Leipzig, research on the field of polymer physics and rf-spectroscopy.

From 1974 a two years post-doctoral stay in the Institute for Polymer Physics at the University of St. Petersburg with Prof. V. N. Zwetkow.



1976 Habilitation at the University of Leipzig with a thesis on Molecular dynamic processes in radicals and during polymerisation. From 1976 to 1983 he worked as Docent (senior lecturer) in the Department of Physics at the University of Leipzig with research on the field of applied molecular physics.

In 1983 he was appointed as full Professor with Chair in Experimental Physics at the Leipzig University of Technology. Research interest includes methodical aspects of ESR spectroscopy and the study of novel materials, especially magnetic and conducting polymers, including laser processing of conducting polymers.

1993 three months guest professor at the Tokyo Metropolitan University in the Department of Physics, ESR investigations on conducting polymers with Prof. K. Mizoguchi.

From 1994 to 2003 head of the new established Department of Physical Materials Research at the TITK institute in Rudolstadt/Germany. Besides he gives lectures at the Ilmenau University of Technology. His main research activities are organic functional polymers and its application in polymer electronics and photovoltaics. Since 2003 retired and senior consultant at TITK as part-time employment and as hobby.

MOLECULAR DYNAMICS OF POLY-ALKYL-THIOPHENES: EXPERIMENTAL STUDY BY NEUTRON SCATTERING, RHEOLOGY AND CALORIMETRY

A. URBINA*¹, V. GARCÍA-SAKAI², M. TYAGI³, N. ESPINOSA¹, C. DÍAZ-PANIAGUA⁴, R. GARCÍA VALVERDE¹, J. PADILLA¹, J. ABAD⁵, AND F. BATALLÁN⁴

¹ Universidad Politécnica de Cartagena, Plaza del Hospital 1, 30202 Cartagena, Murcia, Spain.

² ISIS Spallation Neutron Source. Rutherford-Appleton Laboratory, Chilton, Didcot OX110QX, United Kingdom.

³ Center for Neutron Research, National Institute of Standards and Technology, Gaithersburg, Maryland 20899, USA.

⁴ Instituto de Ciencia de Materiales de Madrid, ICMM-CSIC, Spain.

⁵ Universidad de Murcia, Departamento de Física, Campus de Espinardo, 30100 Murcia, Spain.

Poly-alkyl-thiophenes are conjugated polymers which have been widely used as active layers in organic electronic devices such as field-effect transistors, organic light emitting diodes and organic solar cells [1]. In particular, blends of P3HT and functionalized fullerenes in tandem devices have been the most successful realization of the bulk-heterojunction concept in which two interpenetrated networks of materials perform as electron donors or acceptors [2]. The morphology of the blends is strongly correlated with the performance of the devices, but a deep understanding of the molecular dynamics of these polymers at different temperatures is still lacking. We present a detailed study carried on solutions and bulk samples of P3OT and P3HT, the experimental techniques that we have used include quasielastic neutron scattering measurements in pulsed (OSIRIS spectrometer at ISIS-RAL, UK) and continuous neutron sources (IN10 at ILL, France, and HFBS at NIST, USA, both high resolution back-scattering spectrometers) [3, 4, 5], as well as calorimetric and rheological studies of the same samples. Our findings include the description of a low temperature glass transition, the characterization of the side chain and backbone dynamics, and the experimental determination of the crystallinity of the samples. Blends of poly-3-hexyl-thiophene (P3HT) and 6,6-phenyl-C₆₁ butyric acid methyl ester (PCBM) are the most promising candidates for active layers of plastic solar cells with high efficiency in power conversion. The morphology of the blends is strongly dependent on the solvent used in the preparation of the layers, as well as thermal annealing cycles in the post-preparation stage. The PCBM tends to aggregate and therefore destroy the path needed for *n*-type carrier transport. A huge effort is devoted in order to understand the dynamical processes which drive such aggregation. Different solvents and deposition

* antonio.urbina@upct.es

methods (spin coating, spray pyrolysis, ink-jet printing) are being tested.

We have performed measurements of quasielastic neutron scattering in different poly-alkyl-thiophenes both in solution and bulk samples, and small angle neutron scattering of functionalized carbon nanotubes in solution [4, 5, 6]. The experiments presented in the following paragraphs will focus into the detailed study of blends of P3HT and PCBM by quasielastic neutron scattering performed in the instruments mentioned above.

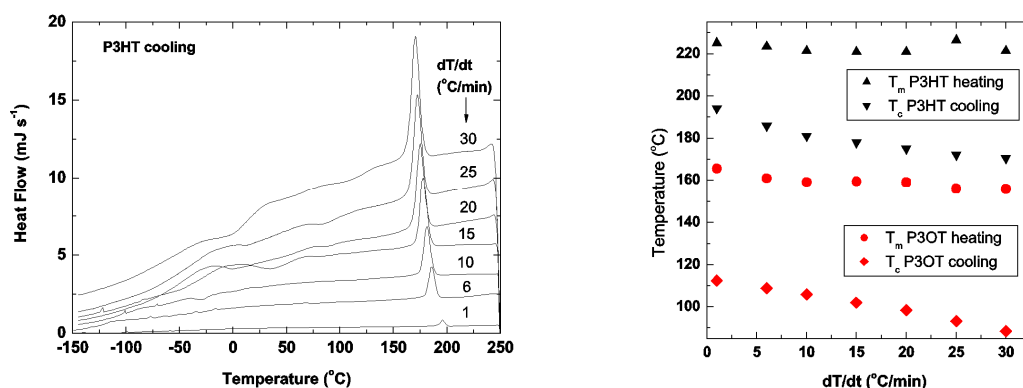


Figure 1. Differential Scanning Calorimetry of a bulk sample of P3HT, cooling scans at different cooling rates are plotted (left). From crystallization peaks as well as from melting peaks in cooling and heating scans for P3HT and P3OT, the critical temperatures can be obtained and are plotted as a function of the temperature scanning rate (right).

Our previous calorimetric measurements on the pure P3HT and P3OT bulk samples allowed us to determine the temperature ranges of interest, defining the melting and crystallization temperatures as well as the onset of some dynamics indicating a possible glass transition at low temperature (Figure 1). Differential scanning calorimetry was performed at different temperature scan rates and the obtained melting and crystallization temperatures extrapolated to infinitely slow scans are $T_m=496\text{K}$, $T_c=465\text{K}$ for P3HT and $T_m=438\text{K}$, $T_c=385\text{K}$ for P3OT. The enthalpies of fusion of the 100% crystalline materials can be found in the literature, and are $\Delta H_0(\text{P3HT}) = 99\text{Jg}^{-1}$ and $\Delta H_0(\text{P3OT}) = 74\text{Jg}^{-1}$ [7]; then we can obtain a percentage of crystallinity, $X(\%)$, using the approximation given by $X = \Delta H/\Delta H_0$. For our measured values for the enthalpy of fusion, we obtain the crystallinity ratio after each one of the heating scans which is for P3OT and P3HT around 7% and 15% respectively and do not depend on the scan rate of the cooling/heating cycles.

Neutron scattering experiments measure the double-differential scattering cross-section $\delta^2\sigma/(\delta E\delta\Omega)$, which is the probability that a neutron is scattered into a solid angle ($\delta\Omega$) having exchanged energy (δE) and momentum ($\mathbf{Q} = \mathbf{k}_i - \mathbf{k}_f$) with the sample. In our

samples, which are hydrogenated polymers, the scattering is dominated by the incoherent contribution, and for molecular motions within a fixed volume, the incoherent scattering law describing rotational motions of side groups is given by [8]:

$$S_{inc}^{rot}(Q, \omega) = A_0(Q)\delta(\omega) + S_{inc}^{qel}(Q, \omega)$$

Where $A_0(Q)$ is the elastic incoherent scattering function (EISF), related with the geometry of the molecular motion, and $S_{inc}^{qel}(Q, \omega)$ is the quasi-elastic scattering process. Further elaboration, taking into account the case of methyl group rotation, which is present at the end of all side-chains in P3HT and P3OT gives [9]:

$$S_{inc}^{rot}(Q, \omega) = \exp\left(\frac{-Q^2 \langle r^2 \rangle}{3}\right) \left(A_0(Q)\delta(\omega) + \frac{1}{\pi} [1 - A_0(Q)]L(\omega) \right)$$

Where $\delta(\omega)$ is the Dirac delta, $L(\omega) = \Gamma/(\Gamma^2 + \omega^2)$ is a Lorentzian function, and the exponential factor is the Debye-Waller Factor (DWF) in the harmonic approximation which allows us to obtain the temperature-dependent mean square displacement $\langle r^2 \rangle$ by fitting the EISF experimental data. At $T \approx 100\text{K}$ a deviation of the harmonic behaviour is observed, similar for P3HT and P3OT, and at higher temperatures, a branching in the $\langle r^2 \rangle$ temperature dependence for both polymers is obtained. It is an insight on the onset of two different dynamics at intermediate temperatures.

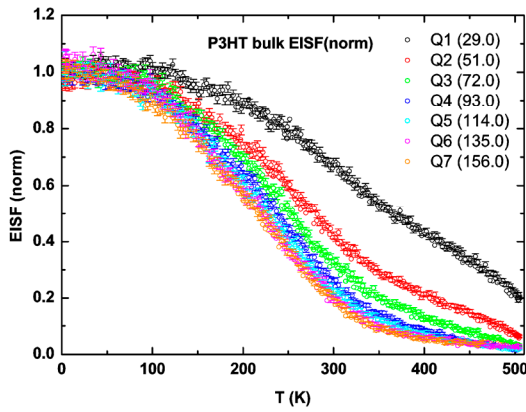


Figure 2. Temperature dependence of the Elastic Incoherent Scattering Function (EISF) for bulk P3HT. The different momentum transfers that were measured are displayed in the plot (ILL-IN10 instrument, fixed elastic window scans).

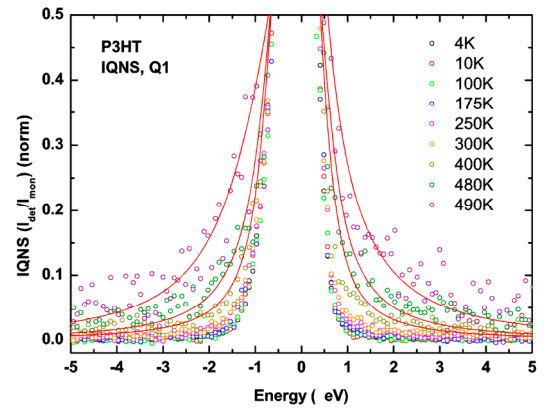


Figure 3. Incoherent Quasielastic Neutron Scattering for a single momentum transfer at different temperatures. A fit to the data using a dynamical model with two Lorentzian peaks is superimposed for the three highest temperatures (ILL-IN10 instrument).

In Figure 2, some examples of the EISF for P3HT, the special case where the energy exchange is zero and we measure the Q and T dependence of the elastic signal (a particular case of scattering function, $S(Q, 0)$) is shown. In this case, $L(\omega)$ can be approximated by

$\arctan(\Gamma_{\text{res}}/\Gamma)$, where Γ_{res} is the width of the spectrometer resolution function (at fwhm) and Γ is the width of the Lorentzian quasi-elastic peak, which broadens according to the Arrhenius law [10]:

$$\Gamma = \Gamma_0 \exp\left(\frac{-E_a}{RT}\right)$$

where $R = 8.31\text{JK}^{-1}\text{mol}^{-1}$ is the gas constant, and E_a is the activation energy, related to the height of the potential barrier that the rotational motion has to surpass (Γ_0 is the line width at $T=\infty$). By fitting our experimental data we obtain a narrow distribution of activation energies centred around $E_a \approx 12.5\text{kJmol}^{-1}$, with $\sigma \approx 3.2\text{kJmol}^{-1}$.

Secondly, some examples of quasielastic incoherent neutron scattering spectra (IQNS), showing the Q and temperature dependence of the quasielastic peaks are plotted as a function of the energy transfer (Figure 3). From the fit with a set of Lorentzian functions (plus a Dirac delta), the experimental parameters which describe the observed dynamics are calculated, the most frequent data treatment is the study of the FWHM as a function of Q or T , provided that a good fit is obtained and the movements can be identified. Other usual treatment is to perform a Fourier transform to obtain an experimental $S(Q, t)$, called “intermediate scattering function” which gives a set of time coefficients obtained from fitting the slopes of the plots [10].

In Figure 3, a more detailed data treatment is shown: Lorentzian fits are performed on each spectra (in this case two Lorentzian peaks plus a Dirac delta), shown here for the three highest temperatures. In the case that the different movements can be separated, which is not always the case, we can consider that: $S(Q, \omega) = S_{\text{tr}} \otimes S_{\text{rot}} \otimes S_{\text{vib}}$, and each of the Lorentzians gives information of the distances and the time-scale involved in each movement, provided that the experimental window allows us to “see” that particular movement. Since we have carried out for this sample two sets of experiments (at ISIS-OSIRIS and ILL-IN10), we have covered a large energy range, or equivalently, a large time window and we can claim that we are “seeing” at least two well defined movements, that we can consider related to side-chain dynamics, the first one to the rotation of the methyl groups found at the end of all the side-chains, and the second one (slower) related to a rotation of the whole side chain, exploring a bigger space where movement is allowed because we have a high degree of disorder in the bulk polymers. The difficulty in obtaining a single relaxation time is related to the different environment that affect the side-chain

dynamics in different ways and therefore explaining the existence in such an heterogeneous environment of a distribution of jump frequencies.

We will also present the potential of other neutron scattering techniques such as small angle neutron scattering (SANS) and neutron reflectivity in the study of the structure and dynamics of polymeric multilayered organic electronic devices.

- [1] C.J. Brabec, et al., *Advanced Functional Materials*, **11**, 15 (2001)
- [2] Y. Kim, et al., *Nature Materials*, **5**, 197 (2006)
- [3] V. García-Sakai, et al., *Current Opinion in Colloid & Interface Science*, **14**, 381 (2009)
- [4] A. Urbina, et al., *Physical Review B*, **78**, 045420 (2008)
- [5] A. Urbina, et al., *Journal of Physics: Condensed Matter*, **20** 104208 (2008)
- [6] B. Perez-García, et al., *Nanotechnology*, **19**, 065709, (2008)
- [7] S. Malik, et al., *Journal of Polymer Science Part B-Polymer Physics*, **40**, 2073, (2002).
- [8] J. S. Higgins and H. C. Benoît, "Polymers and Neutron Scattering"; Oxford University Press: Oxford (1994).
- [9] M. T. F. Telling, et al., *Journal of Physical Chemistry B*, **112**, 10873 (2008)
- [10] V. Arrighi, et al. *Macromolecules*, **28**, 4622 (1995).

BIOGRAPHIC DATA OF DR ANTONIO URBINA

Dr. Antonio Urbina (born 1967 in Madrid, Spain) graduated in Physics (1991) at Universidad Complutense de Madrid and finished his PhD thesis in Physics (1996) at Instituto de Ciencia de Materiales de Madrid ICMM-CSIC. He has been postdoctoral research fellow at the Department of Engineering of the University of Cambridge, UK, visiting associated professor at the Department of Chemistry of the University of Wisconsin (Madison, USA) and visiting research fellow at the Centre for Environmental Policy, Imperial College London, UK.



He is now lecturer of Electronic Engineering at Universidad Politécnica de Cartagena, Spain, where he leads the Group of Molecular Electronics (2 physicists, 1 chemist and 2 electronic engineers). Antonio Urbina has worked in experimental studies of electronic transport processes. He begun his work studying quantum conductance in III-V quantum well heterostructures measuring the Quantum Hall Effect and Shubnikov-de Haas oscillations in environments of high magnetic fields and low temperatures. More recently, he has studied the transport properties of carbon nanostructures (carbon nanotubes and fullerene derivatives) and extended the characterization of materials to Surface Force Microscopy, developing measurement techniques which allows us to relate the nanostructure of the materials with their macroscopic electronic properties. Now he is devoted to the study of new devices based in bulk heterojunctions of conjugated polymers, fullerene derivatives and nanoparticles/nanorods percolative networks. These blends have been studied with the aim of developing efficient organic photovoltaic devices. Also thin films, solutions and suspensions of such materials have been studied by neutron scattering techniques, where quasielastic and small angle scattering measurements give useful information aimed to understand the self-assembly and nanostructuration processes produced during the fabrication procedures of organic devices from solution. He has published 28 articles in scientific journals, with more than 180 citations, two books and three book chapters. He has great interest in the application of cheap and reliable photovoltaic technologies to sustainable rural electrification projects in developing countries.

PAPER BASED SUBSTRATES FOR POLYMER ELECTRONICS

W. SCHMIDT

Felix Schoeller jr Foto- und Spezialpapiere GmbH & Co. KG; R&D; Burg Gretesch; 49086 Osnabrück; Germany

Paper-based substrates show several advantages above glass plates and plastic foils for printing and coating processes used in the manufacturing of polymer electronics, especially for large scale industrial processes. Paper-based media exhibit unique mechanical properties regarding flexibility, elasticity, stiffness and dimension stability due to its fibrous structure and non-plastic behavior. Furthermore paper is made mainly from pulp, an inexpensive and renewable raw material.

The surface of uncoated plain paper is porous and highly liquid absorbing, which is advantageous for many material depositing methods like gravure or offset printing, as the functional material is efficiently transferred from the printing plate to the substrate by capillary forces. But due to the large pore size of paper, generally in the order of several μm to several $10 \mu\text{m}$, the functional ink containing active ingredients which are much smaller like nanoparticles, macromolecules or even small molecules penetrate into the pore system. This may greatly impart the functionality, as the active material is dispersed and not building up film like structures.

In this presentation is shown how the properties of paper-based substrates can be customized to different types of functional inks and printing or coating processes by using coating and laminating technologies already well established on an industrial scale. For example, surface smoothness - or template structuring of the surface- down to nanometer scale is achieved by extrusion coating with thermoplastic polymers like polyethylene onto the base paper. Layers resulting from this process also serve as very efficient liquid barriers and are inert to many printing chemicals and solvents. The surface energy and adhesion of printing inks may be additionally controlled by coating a customized primer formulation onto the thermoplastic layer.

By polymer extrusion coating the absorptivity and porous nature of paper is completely lost. For some inks and most printing processes, a controlled porosity in the nm-scale was shown to be advantageous over a completely closed surface. Such surfaces can be obtained

by coating paper, resin coated paper or a plastic film with nanoparticle dispersions containing low amounts of binder. Nanopigments, mostly synthetic silica or alumina, are available with different structures, primary and secondary particle size. By choosing a specific pigment or pigment mixture, the pore size of the surface can be tuned in a range from some nm to more than 100 nm.

When selecting the right relation of pore size of the substrate surface and particulate size of the functional material in the printing ink or coating solution, an “ultrafiltration” or “nanofiltration” process can be achieved *in situ* during subsequent printing or coating, leading to instant separation of the functional material and the carrier liquid, and a clearly defined layer deposition of the functional material on the top of the substrate.

Furthermore, the filtration process can be used to separate different ingredients in the printing ink or coating solution based on their particulate size. Examples are shown using silver inkjet inks containing nanosilver with particle size of about 60 nm printed on a coated paper with a surface pore diameter of about 30 nm. Metallic conductivity of the printed structures was observed directly after printing without any sintering steps. The interpretation of these experiments is that the filtration process leads to an efficient removal of ink additives like dispersants and stabilizers from the printed silver material. The additives needed for ink stability, but due to their electrically insulating nature they prevent inter-particle conductivity as long as they are present in printed and dried functional layers. Conventionally they are removed in the “sintering” or “curing” step, which seems to be more an evaporation or combustion process for the ink additives than a melting or fusing of the silver particles themselves.

By using mesoporous or nanoporous coatings, the poorly up-scalable step of sintering or curing can be avoided. Using such substrates adapted to the specific ink therefore allows e.g. printing of conducting lines after printing thermally instable materials or structures, or printing with inks which usually need curing onto thermally instable substrates.

Furthermore, using the described filtration process may lead to new options for ink or coating solution formulation. It is highly recommended that inks and substrate surfaces are jointly developed in the future to fully exploit the potential of this tool.

DEPOSITION OF PEDOT:PSS DISPERSIONS WITH INDUSTRIAL INKJET PRINTHEADS

W. VOIT^{1*}, I. REINHOLD¹, W. ZAPKA¹, D. GAISER²

¹ XaarJet AB, Advanced Application Technology Group, Elektronikhöjden 10, 17526 Järfälla, Sweden

² H.C. Starck Clevios GmbH, Chempark B 202, 51368 Leverkusen, Germany

PEDOT:PSS is an intrinsically electrical conductive polymer that finds increasing interest for polymer electronics. This material is especially attractive as it combines a relatively high conductivity with high transparency, while it can be brought into a stable fluidic dispersion and thus be applied with various coating techniques. Potential applications for PEDOT:PSS range from the use as transparent conductive coatings for various applications, as hole injection layers for OLEDs and organic photovoltaics, to the use as electrode material for organic transistors¹ and organic memories.²

In this paper the development of an inkjet printing process of highly conductive CLEVIOS™ P Jet grades from H.C. Starck Clevios with Xaar 1001 inkjet printheads is presented. These printheads utilize an ink through-flow principle and enable single-pass printing with high resolution and reliability, giving the potential for a roll-to-roll based industrial scale digital printing process. A special focus is put onto the development of optimized driving waveforms to achieve high-quality drop formation and reduced satellite formation, while still maintaining high printing reliability. Furthermore, achievable printing results on some substrates are presented, and suitable printing strategies are discussed.

H.C. Starck Clevios has developed a range of inkjettable PEDOT:PSS formulations, that are available under the trade name CLEVIOS™ P Jet.³ CLEVIOS™ P consists of a aqueous dispersion of the polymer complex poly(3,4-ethylenedioxythiophene) polystyrene sulfonate (PEDOT:PSS). The dispersions are formulated of submicrometer sized gel particles which upon drying form a continuous film which is conductive and transparent.

In this stage, two high-conductivity grades of CLEVIOS P Jet dispersions were utilized for the development of a jetting process with the Xaar 1001 printhead. The evaluated formulations were CLEVIOS™ P Jet HC V2, which allows for layers conductivities in the range of 300-500 S/cm, and CLEVIOS™ P Jet N V2 with a partly neutralized pH-value (increased to 5-7 from the original pH-value of about 2) and resulting layer conductivities higher than 200 S/cm. The pH neutralization of CLEVIOS™ P Jet N V2 is expected to be

beneficial for the lifetime of the inkjet printhead. Both fluid formulations exhibit a shear-thinning behaviour, with a viscosity of around 20 mPa.s at low shear rates, which decreases to well below 10 mPa.s at the high shear rates that are present at the printhead nozzles.

The Xaar 1001 is the latest generation of printheads from Xaar, with 1000 nozzles arranged in two rows, allowing single pass printing with 360 dpi and typically 8 greylevels.⁴ The printhead produces subdrops of 6 pL volume at high frequency, and different greylevels are produced by ejecting trains of subdrops by appropriate electrical pulses, which form a single droplet when leaving the nozzle. The total drop volumes are thus multiples of the subdrop volume with a maximum of $n \times 6$ pL for a n drops-per-dot (dps) waveform.

Furthermore, this printhead allows high jetting reliability by utilizing the Through-Flow TechnologyTM (TFT). A specific external ink system provides a constant circulation of ink through the ink channels, and simultaneously controls the negative meniscus pressure at the nozzle. While air intake through the nozzle into the ink channels may occur under certain circumstances, these air bubbles cannot accumulate in the ink channel and can be easily removed by the ink flow from the recirculating ink system, enabling self-recovery without the need for additional purging steps. By controlling the temperature of the ink in the through-flow system, it also provides an easy way to control the printhead temperature and to adjust this temperature to higher or lower values. Furthermore, there are indications that the latency times, i.e. the time that the printhead can be idle and startup of the jetting process without further interception is still possible, is increased with the ink through-flow of the Xaar 1001.

For typical applications of inkjet printed PEDOT:PSS patterns, high-quality jetting performance and reliability is needed, as missing ink drops could cause electrical breaks, and undesired drops or satellites could produce electrical shorts. Thus, a well controlled drop formation with high placement accuracy, and virtually no satellite drops or misfiring behaviour is required. This was achieved by optimizing the electrical driving waveform and jetting conditions for the Xaar 1001 printhead. It was also found that best jetting performance could be accomplished by cooling the ink and printhead down to 20 °C, as this counteracts the reduced viscosity of the shear-thinning PEDOT:PSS ink at jetting conditions, and well as it minimizes the ink evaporation.

With optimized driving waveforms for all greylevels of the printhead, a stable and reliable jetting process at full duty cycle and without the occurrence of satellite drops was realized at a drop speed of around 5 m/s at jetting frequencies up to 4-5 kHz. For low duty cycle printing,

e.g. when only partial layer coverage is needed, this jetting frequency could even be increased to the maximum drop ejection frequency of the printhead of about 6 kHz.

Figure 1 (a) and (b) show examples for stroboscopic images of the drop formation in flight with CLEVIOS™ P Jet N V2, producing 1 dpd drops and 7 dpd drops at 4 kHz, respectively. In these images the nozzle guard of the printhead is visible at the top, and distances of 0.5 mm and 1 mm from the nozzle guard are marked in the images. The drops are ejected at full duty cycle and in the 3 cycle mode that is typical for Xaar-type printheads, i.e. only every 3rd channel is jetting a drop at a time. The drop volume was measured with about 7 pL per subdrop, and latency times of at least 30 min were achievable at an ink temperature of 20 °C. Ink circulation and through-flow was carried out with a custom-built small-volume ink system. However, due to the shear-thinning behaviour of the fluid, only a lower flow rate through the printhead of about 65 mL/min could be applied.

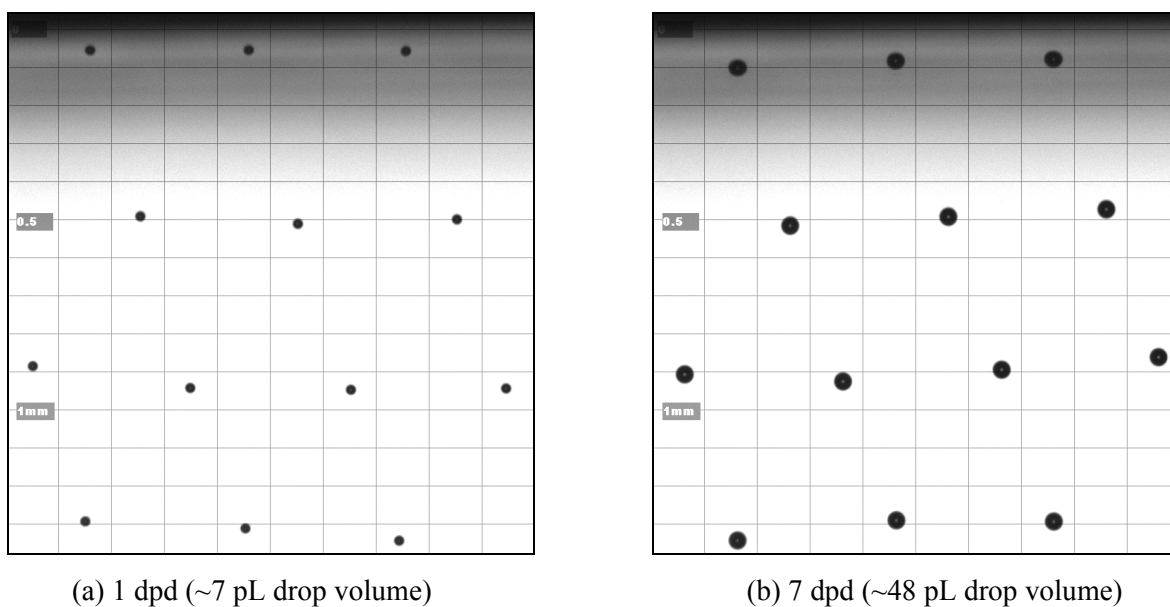


Figure 1: Drop formation with CLEVIOS™ P Jet N V2 at 4 kHz, 20 °C; 5 m/s drop velocity in both cases

Simple test structures with lines and dots were printed onto both PET substrates and photo paper, in order to assess achievable structure dimensions and line width when printing at different processing conditions and with different greylevels of the printhead.

A first part of the test prints was carried out on photo paper, to enable easier visualization of the printed pattern with the nearly transparent PEDOT:PSS layers. Figure 2 (a) and (b) shows two examples of lines printed with CLEVIOS™ P Jet N V2 onto Epson glossy photo paper, where the brighter features in the images are the printed PEDOT:PSS lines, produced by

jetting with every 2nd channel across the printhead to result in a 141 μm pitch of the lines. The lines in Figure 2 (a) were printed with 7 dpd drops at 360 dpi printing resolution and a print speed of 0.3 m/s, yielding a line width of about 76 μm . However, there is still certain raggedness visible for the lines produced under these conditions and on this substrate type, indicating that the dot spacing should be further reduced. For smaller drop volumes the resolution in printing direction was thus increased to be able to achieve continuous lines. The best printing resolution for obtaining highly regular lines with 1 dpd drops (corresponding to about 7 pL drop volume) was found to be 847 dpi, as can be seen on the roughly 38 μm wide lines visible in Figure 2 (b). The diameters of single dots on photo paper were slightly larger than the corresponding line width, with 84 μm for 7 dpd dots and 42 μm for 1 dpd dots. No satellite drops could be seen on all print samples.

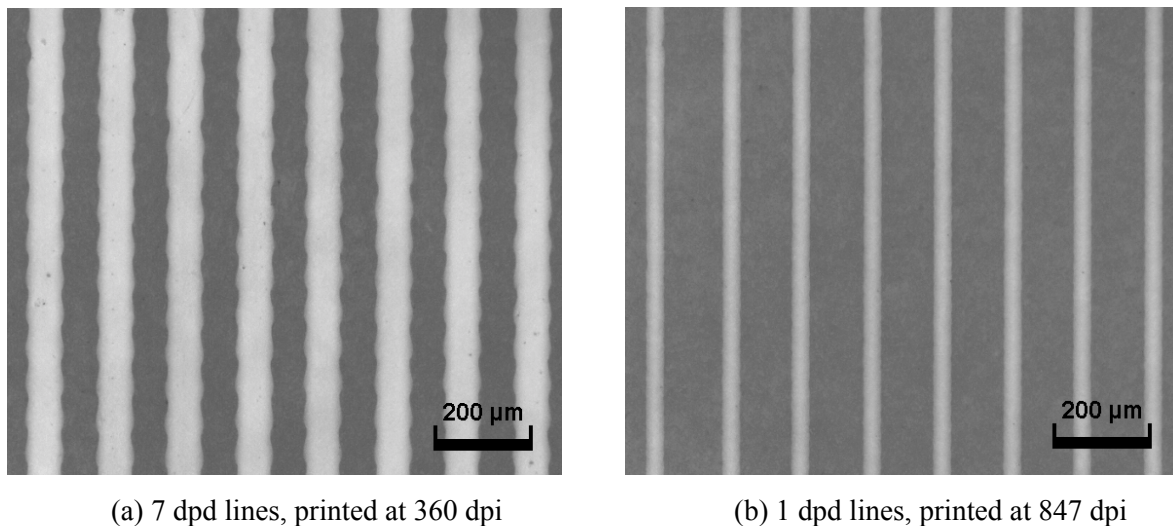


Figure 2: Lines produced with different dpd-levels (i.e. different drop volumes) on photo paper; width of the 7 dpd lines is approx. 76 μm , and width of the 1 dpd lines is approx. 38 μm

Further printing tests were performed on Melinex® 505, a pretreated PET substrate from DuPont Teijin Films. For these tests the substrate was kept at different temperatures during printing, to influence the drying times after drop impact and enable additional control of the structure dimensions. Evaluated substrate temperatures were room temperature (RT, around 25 °C), 40 °C and 60 °C. Similar to photo paper, it was observed as well on the Melinex® 505 substrates that continuous lines with 7 dpd could be achieved at 360 dpi, whereas a resolution of 847 dpi (dot spacing of 30 μm) was required to obtain regular and continuous lines with the smallest 1 dpd drops. For resolutions lower than 847 dpi for 1 dpd drops, occasional breakage of the lines did occur. This relation of the best suitable printing resolution for a given drop

volume was found to be relatively independent of the substrate temperature, but the pre-heating had a major influence on the achievable line width, with a reduction from 170 μm down to 105 μm for 7-dpd lines, and from 70 μm down to 45 μm for 1-dpd lines, when going from room temperature to a substrate temperature of 60 $^{\circ}\text{C}$. The line width obtained with the Xaar 1001 printhead on Melinex[®] 505 substrates for 1 dpd and 7 dpd at the different processing conditions, along with the diameters of single dots, are summarized in Table 1.

Substrate temperature	1 dpd drops (~7 pL volume)		7 dpd drops (~48 pL volume)	
	1dpd line width at 847 dpi	diameter 1 dpd dots	7dpd line width at 360 dpi	diameter 7 dpd dots
RT (~ 25 $^{\circ}\text{C}$)	70 μm	58 μm	170 μm	135 μm
40 $^{\circ}\text{C}$	60 μm	50 μm	150 μm	120 μm
60 $^{\circ}\text{C}$	45 μm	47 μm	105 μm	105 μm

Table 1: Line width and dot diameter for 1 dpd and 7 dpd, for printing CLEVIOS[™] P Jet N V2 onto Melinex[®] 505 PET substrates pre-heated to different temperatures; the values given are approximate average values.

The applicability of inkjet printed PEDOT:PSS pattern for polymer electronics depends on the achievement of a highly reliable printing process, where even the first drops of a printing swathe should be ejected in a well-defined way. However, as the evaluated CLEVIOS[™] P Jet formulations are designed to dry in a reasonable time on the substrate, they have a tendency to start to dry or cross-link at the nozzle plates of the printhead, resulting in difficulties to immediately start off the jetting process when the printhead is idle for longer periods. To overcome these start-up problems, different strategies could be applied, like regular maintenance with capping and purging steps, or the printing of ‘dummy’ drops at an idle position or outside the targeted printing area.

Although the constant ink through-flow of the Xaar 1001 printhead already seems to allow prolonged latency times, it still takes a certain amount of drops to regain standard jetting performance after longer idling times. To improve this further, an additional technique was evaluated when printing the CLEVIOS[™] P Jet inks with the Xaar 1001 printhead, namely the application of a ‘tickle pulse’, i.e. a short, non-jetting pulse that just causes an ink meniscus movement without actually ejecting ink drops. For a test with 10 minutes idling time without such a tickle pulse it could take up to several hundred of drops until all channels of the heads were jetting again. With this tickle pulse activated during the idling phase, drops from all

nozzles were appearing immediately in the first printed line, first with some directionality errors but regaining good placement quality after a few drops.

Conclusion and Outlook

We have demonstrated that a well-controlled jetting process can be achieved when printing PEDOT:PSS formulations with the Xaar1001 inkjet printhead. Smallest lines of approx. 40 μm are feasible when printing with 7 pL drops, but it is also obvious that the printing and processing conditions have to be adjusted for each substrate type and application type. The reliability of the jetting process for continuous printing runs, as well as the long-term performance of printheads with CLEVIOS™ P Jet inks still need to be further evaluated.

References

-
- ¹ H. Sirringhaus, T. Kawase, R. H. Friend, T. Shimoda, M. Inbasekaran, W. Wu, E. P. Woo, 'High-Resolution Inkjet Printing of All-Polymer Transistor Circuits', *Science*, Vol. 290. no. 5499, pg. 2123 – 2126 (2000)
 - ² W. Voit, W. Zapka, P. Dyreklev, O.J. Hagel, A. Hägerström and P. Sandström, 'Inkjet Printing of Non-Volatile Rewritable Memory Arrays', *Proc. Digital Fabrication 2006*, pg. 34-37 (2006)
 - ³ www.clevios.com, 2010
 - ⁴ www.xaar.com, 2010

BIOGRAPHIC DATA OF WOLFGANG VOIT

Wolfgang Voit is member of the Advanced Application Technology group at Xaar. He received his diploma from the University of Applied Sciences in Regensburg, Germany. In 1997 he joined MIT Inkjet, Järfälla, Sweden, and Xaar in 1999. In the past 12 years he gained thorough experience in both inkjet printhead technology as well as developing new inkjet applications, specifically in the area of printing functional and non-conventional fluids for coatings and devices.

METALLOCOMPLEXES OF FULLERENES FOR POLYMER SOLAR CELLS WITH ENHANCED PHOTOVOLTAGE

A.A. GROMCHENKO¹; S.A. ZAPUNIDI¹; V.V. BRUEVICH¹;
 N.A. KHLOPKIN¹; V.A. DYAKOV¹; I.A. GVOZDKOVA²;
 M.V. TSIKALOVA³; YU.N. NOVIKOV³; D.YU. PARASCHUK^{1*}

- ¹ Faculty of Physics & International Laser Center; Lomonosov Moscow State University; 119991 Moscow; Russia
² State University of Management; Rayzanskii pr. 99; 109542 Moscow, Russia
³ Nesmeyanov Institute of Organoelement Compounds; Russian Academy of Sciences; ul. Vavilova 28; 119991 Moscow; Russia

The most efficient organic solar cells are based on blends of conjugated polymers and fullerenes. One of the promising strategies to enhance the performance of polymer-fullerene solar cells is enhancing the open-circuit voltage (V_{oc}) by increasing the energy gap between the polymer HOMO and fullerene LUMO (Fig. 1). Indeed, the LUMO-HOMO difference in the most studied P3HT:PCBM solar cells is abundantly large, i.e., it is essentially higher than that needed for efficient exciton dissociation (exciton binding energy) as illustrated in Fig. 1. As a result, the V_{oc} in P3HT:PCBM solar cells is limited to ~ 0.6 V. The fullerene LUMO energy can be decreased by attaching an organic addend to the fullerene cage that typically results up to ~ 0.15 eV lower LUMO as compared to the parent C_{60} [1, 2]. Meanwhile, an

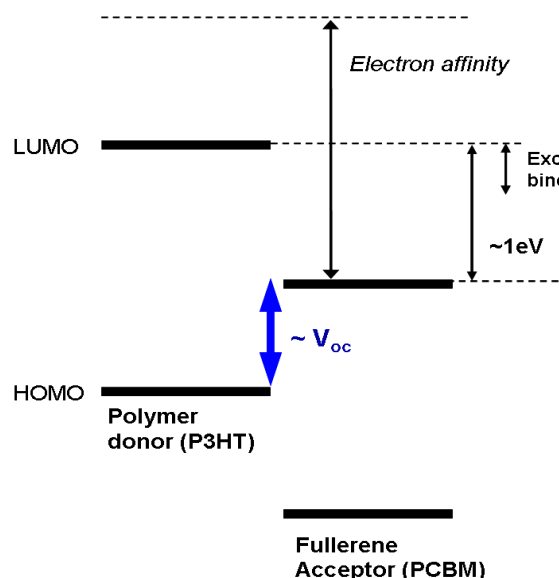


Fig. 1. Relative energies of frontier molecular orbitals of P3HT and PCBM.

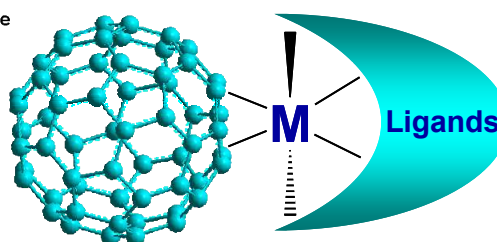


Fig. 2. Schematic of exohedral fullerene metallocomplex, M is a metal atom.

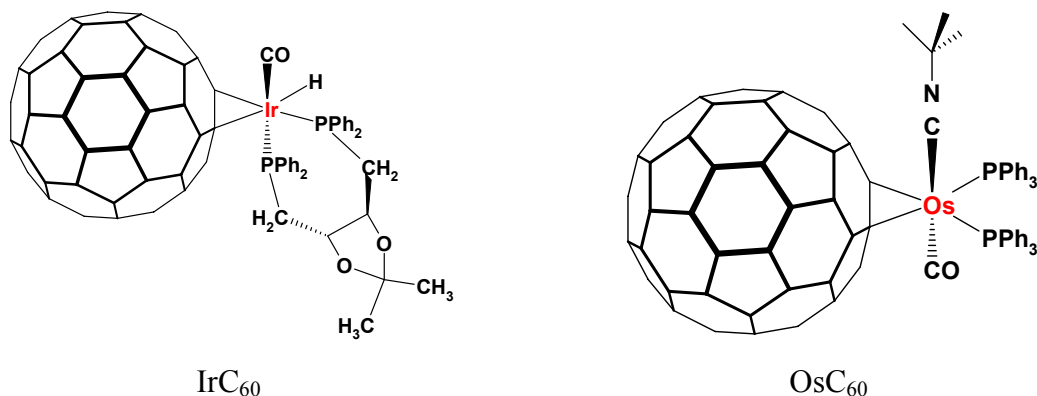


Fig. 3. Structural formulas of $(\eta^2\text{-C}_{60})\text{IrH}(\text{CO})[(+)\text{DIOP}]$ (left) and $(\eta^2\text{-C}_{60})\text{Os}(\text{CO})(t\text{BuNC})(\text{PPh}_3)_2$ (right).

essentially lower LUMO energy can have fullerene compounds with a metal atom attached to the fullerene cage. The metal moiety donates the electron density to the fullerene cage that results in a lower LUMO energy. Recent studies have demonstrated that endohedral fullerenes lead to V_{oc} up to 0.89 V in P3HT: $\text{Lu}_3\text{N}@C_{80}$ bulk-heterojunction solar cells [3]. However, endohedral fullerenes are difficult to synthesize, and because of this exohedral metal-fullerene compounds could be much more technologically attractive. Our recent studies suggest that exohedral fullerene metallocomplexes (FM) could be a promising type of acceptors for polymer solar cells [4, 5]. Fig. 2 presents a structural formula of FMs. According to the electrochemistry data [6], FMs have the LUMO energy at least 0.4 eV lower than that of C_{60} , and their ligands can be used to control the solubility. In addition, FMs have considerably stronger optical absorption than PCBM [4, 5] that could provide higher photocurrent. In this work, we study IrC_{60} and OsC_{60} [7] FMs (Fig. 3) as acceptors for polymer solar cells.

We have recently shown that in MEH-PPV: IrC_{60} blends the polymer photoluminescence is efficiently quenched, and long-lived charges are generated, under polymer photoexcitation [4, 5]. Similar results have been obtained in this work for polymer: OsC_{60} blends. These data indicate efficient photoinduced charge transfer from the polymer to FMs.

The active layer of devices was sandwiched between an ITO/glass substrate covered by PEDOT:PSS and Ca:Al electrode. The active layer (FM, P3HT:FM or P3HT:PCBM blend) was deposited by spin-coating from ortho-dichlorobenzene solution. To measure the electron mobility in FM films, space-charge-limited current (SCLC) technique was used.

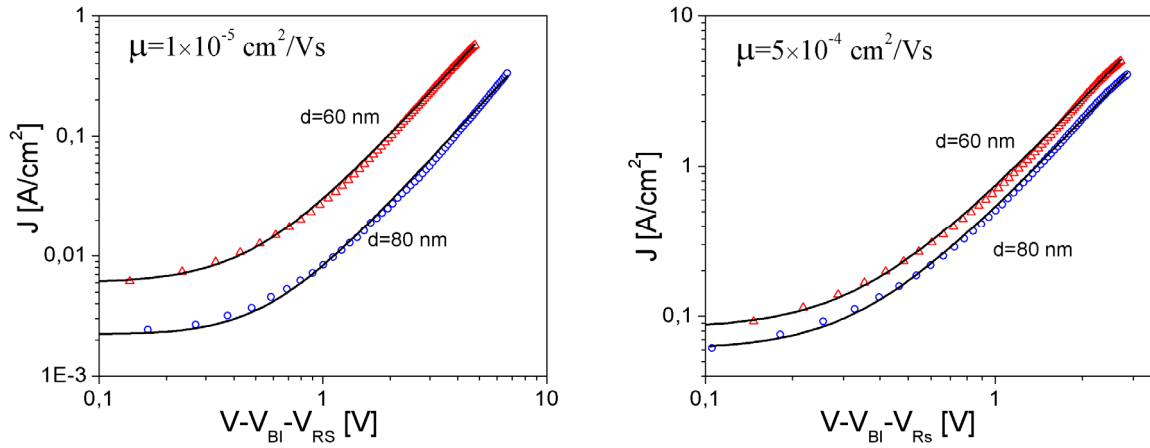


Fig. 4. Experimental (symbols) and calculated (solid lines) J - V characteristics of ITO/PEDOT:PSS/OsC₆₀/Ca:Al (left, V_{BI} =2.4 eV, R_s =60 Ω and ϵ =3.9) and ITO/PEDOT:PSS/IrC₆₀/Ca:Al (right, V_{BI} =2.3 eV, R_s =30 Ω and ϵ =3.9) devices with FM thickness d =60 and 80 nm.

Fig. 4 show the J - V characteristics for OsC₆₀ and IrC₆₀ devices with the applied voltage corrected for the built-in voltage V_{BI} and series resistance R_s . The J - V curves were fitted by the Child law assuming a field-independent mobility. The SCLC electron mobility μ for IrC₆₀ was found to be 5×10^{-4} cm²/Vs, and for OsC₆₀ 1×10^{-5} cm²/Vs. The electron mobility of IrC₆₀ is expected to be quite sufficient for efficient polymer:FM solar cells.

IrC₆₀ and OsC₆₀ were used as an acceptor in polymer:fullerene solar cells with P3HT as a donor. As a reference, P3HT:PCBM solar cells with a 1:1 weight ratio were fabricated. Fig. 5 compares the J - V characteristics of the P3HT:IrC₆₀ and P3HT:PCBM solar cells.

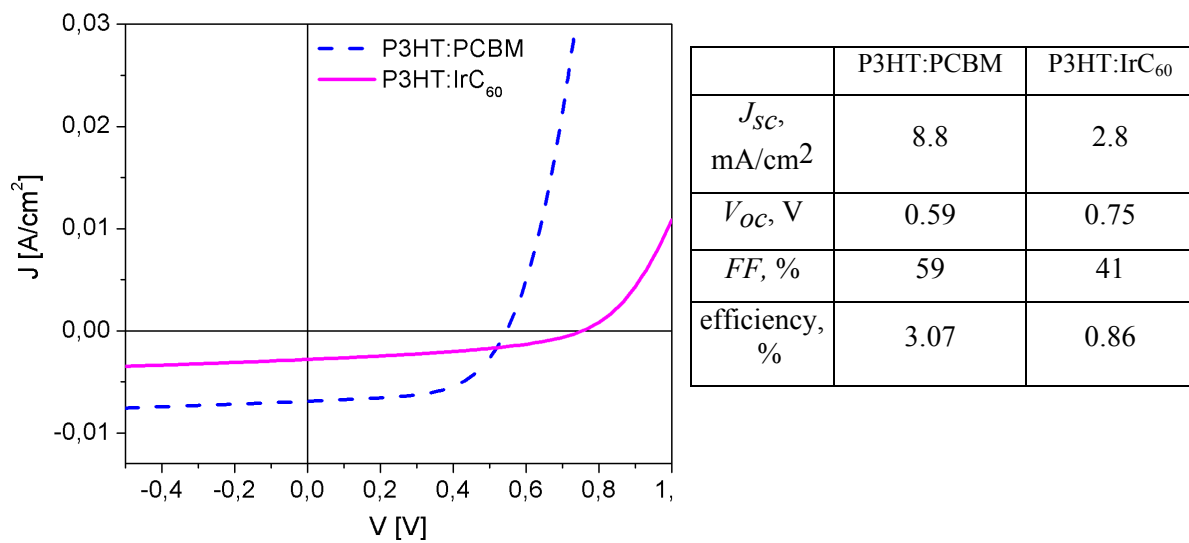


Fig. 5. J - V curves (left) and photoelectric data (right) for 1:1 P3HT:PCBM and P3HT:IrC₆₀ cells measured under AM 1.5 illumination conditions (1000 W/m^2).

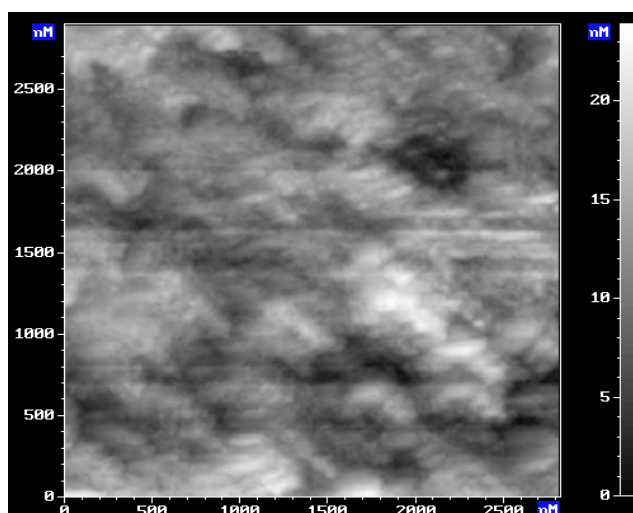


Fig. 6. Atomic force microscopy (AFM) image (3x3 μm) of 1:1 P3HT:IrC₆₀ blend.

Although the V_{oc} of the P3HT:IrC₆₀ cell was 0.75 V that is by 0.16 V higher than that of the P3HT:PCBM cell, the short-circuit current of P3HT:IrC₆₀ solar cell is about three times lower than that of the reference cell. As a result, the efficiency of the P3HT:IrC₆₀ solar cell is below 1%. Note that according to the IrC₆₀ LUMO energy [6] the V_{oc} in P3HT:IrC₆₀ solar cells is expected to be up to 0.9 V. Possibly, the low performance of P3HT:FM devices is associated with non-optimized morphology of the active layer. Fig. 6 shows a typical AFM image of P3HT:IrC₆₀ blend film: reasonable scale of donor-acceptor phase separation is observed. Optimization strategies for polymer-FM cells (varying FM:polymer ratio, deposition conditions, annealing conditions etc.) are discussed.

This work is partially supported by the program "Scientific and scientific-pedagogical personnel of innovative Russia" (contract #02.740.11.5155).

- [1] F. B. Kooistra *et al.*, *Org. Lett.* **9**, 551 (2007).
- [2] Y. J. He *et al.*, *J. Am. Chem. Soc.* **132**, 1377 (2010).
- [3] R. B. Ross *et al.*, *Nat. Mater.* **8**, 208 (2009).
- [4] S. A. Zapunidi *et al.*, *J. Pure and Appl. Chem.* **80**, 2151 (2008).
- [5] S. A. Zapunidi *et al.*, Proceedings of the 3rd International Symposium Technologies for Polymer Electronics - TPE 08, Rudolstadt, Germany, 2008, p. 164.
- [6] S. M. Peregodova *et al.*, *Russ. J. Electrochem.* **44**, 249 (2008).
- [7] A. V. Usatov *et al.*, *Eur. J. Inorg. Chem.*, 2041 (2003).

BIOGRAPHIC DATA OF DR DMITRY YU. PARASCHUK

Dmitry Yu. Paraschuk graduated Faculty of Physics, M.V. Lomonosov Moscow State University (MSU), Russia, and finished his PhD thesis in 1991 and DrSci thesis in 2005 at MSU. At present he is a team leader on photophysics of organic nanomaterials at Faculty of Physics & International Laser Center, MSU. His main research interests are spectroscopy of semiconducting polymers and related materials (Raman, ultrafast, photothermal, electroabsorption etc.), organic photovoltaics, and picosecond photoacoustics.



Part IX:

Solar cells / OPV 2

Functionnalized single wall carbon nanotubes significantly improve the performances of polymer solar cells

H. Derbal^{a,c}, C. Bergeret^b, J. Cousseau^b, J.-M. Nunzi^{d,e} *

^a PPF Cellules Solaires Photovoltaïques Plastiques, Université d'Angers, 2 Bd. Lavoisier, 49045 Angers, France

^b Institut des Sciences et Technologies Moléculaires d'Angers, UMR CNRS 6200, Université d'Angers, 2 Bd. Lavoisier, 49045 Angers, France

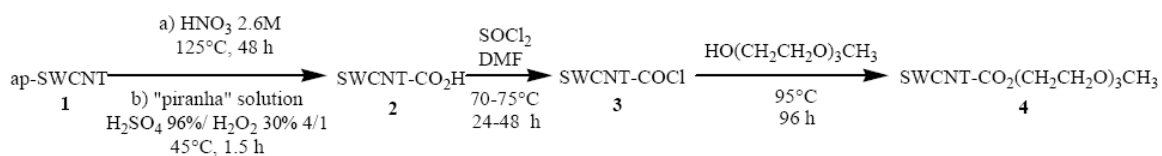
^c IM2NP Laboratory, Equipe OPTO-PV, casier 231, Paul Cézanne University, L'escadrille Normandie Niemen, Aix Marseille III, France.

^d Department of Physics and Department of Chemistry, Queen's university, Kingston, Ontario K7L 3N6, Canada

^e XLIM CNRS UMR 6172, Université de Limoges, 123 Av Albert Thomas, 87060 Limoges, France

Several attempts to incorporate carbon nanotubes in the active layer of bulk heterojunction solar cells (BJH) have been reported. E. Kymakis et al. very early reported a solar cell in which single walled carbon nanotubes (SWCNTs) replaced the fullerene in the polymer BHJ.¹ Interestingly, such cells could result in a large open-circuit voltage of 0.75V,² whereas the open circuit voltage of fullerene BHJ cells is currently in the range of 0.6 V.³ CNTs should be present as few wt% quantities in the polymer:fullerene BHJ to yield acceptable efficiencies and promising applications.⁴⁻⁶ B. Pradhan *et al.* have introduced functionalized multi walled carbon nanotubes (MWNTs) into the BHJ,⁴ while Berson *et al.* have reproduced state-of-the-art results by incorporating pristine SWCNTs or MWCNTs in the BHJ without annealing procedure.⁵ More recently Stylianakis *et al.* also obtained state-of-the-art results with large fill factor by insertion of functionalized SWCNTs in the BJH.⁶ In this paper, we report on the achievement of an exceptionally large open circuit voltage V_{oc} above 0.8 V, together with large fill factor and short circuit current, through the incorporation of HiPco ester-functionalized SWCNT in a poly(3-hexylthiophene) (P3HT) : 1-(3-methoxycarbonyl) propyl-1-phenyl[6,6]C₆₁ (PCBM) bulk heterojunction.

The pristine HiPco SWCNTs **1** were transformed into corresponding ester derivatives **4**, in order to obtain carbon nanotubes easily dispersible in organic media. This overall transformation is achieved after three main steps, as depicted in Scheme 1: *i*) purification-oxidation in order to eliminate metallic catalysts and amorphous carbon, and to create carboxylic acid groups,⁷⁻⁹ *ii*) formation of corresponding acid chloride group,^{7,9,10} *iii*) esterification through reaction with the alcohol CH₃-(OCH₂-CH₂)₃-OH.



Scheme 1. Synthesis of SWCNT ester derivatives **4**

Characterization of the functionalized SWCNT **2** and **4** was achieved through use of thermogravimetric analyses (TGA) and infra-red spectra. On that basis, the average degree of functionalization in SWCNT derivatives **4** was estimated as one ester group for each *ca.* 45 carbon atoms.

In order to precisely evaluate the influence of SWCNT **4** on the photovoltaic characteristics of cells composed of SWCNT **4**:P3HT:PCBM blends, the blends were prepared as follows. A SWCNT **4**/P3HT mixture was first prepared, starting from the previous SWCNT **4** dispersion in chlorobenzene : a v volume (mL) of this dispersion was added to P3HT (10 mg) dissolved in a chlorobenzene volume $v' = (1-v)$ mL, so that the obtained mixture contains 0.1-0.4 wt% SWCNT **4** related to P3HT in a final 1 mL volume. Then PCBM (8mg) is added to the solution. The final blend is thus characterized by three constants: the amounts of P3HT (10mg) and PCBM (8mg), and the chlorobenzene volume (1 mL). As a consequence, the thickness of the active layer of the corresponding BHJ cells is expected to be invariable whatever the SWCNT **4**:P3HT:PCBM blend studied.

Current/voltage characteristics of the various devices: ITO/PEDOT: PSS/ SWCNT **4**:P3HT: PCBM: /LiF-Al, before and after annealing, are presented in Figure 1.

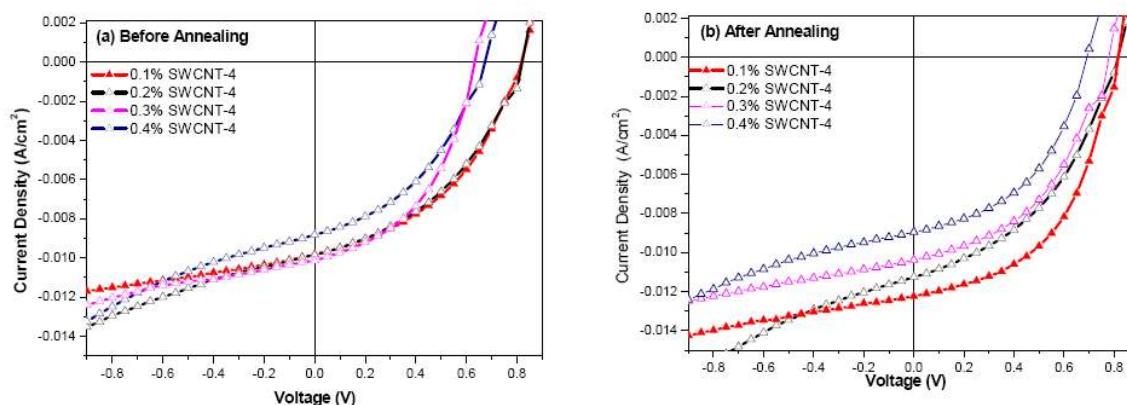


Figure 1: J-V characteristics under illumination with 107 mW/cm² of the organic solar cells based on the composites SWCNT **4**:P3HT: PCBM, before (a) and after annealing (b) at 100°C for 10 min.

<i>P3HT:PCBM</i> (1:0.8) :x% SWCNT	<i>Before annealing</i>				<i>After annealing</i>			
	V_{oc} (V)	J_{sc} (A/cm ²)	FF	$\eta\%$	V_{oc} (V)	J_{sc} (mA/cm ²)	FF	$\eta\%$
0 %	0.53	6.8	0.50	1.9	0.58	12.1	0.54	4.0
0.1 %	0.84	9.8	0.42	3.2	0.83	12.2	0.49	4.7
0.2 %	0.82	9.8	0.41	3.1	0.81	11.3	0.42	3.6
0.3 %	0.64	10	0.46	2.8	0.77	10.4	0.45	3.4
0.4 %	0.67	8.8	0.41	2.3	0.69	8.9 0	.47	2.7

Table 1. Photovoltaic parameters under 107 mW/cm² illumination, before and after annealing at 100°C during 10 minutes.

Photovoltaic parameters extracted from the J-V characteristics in Figure 1 are given in Table 1. Figure 1 confirms that the presence of SWCNT **4** in the active layer improves the PV characteristics of the solar cells before annealing.⁵ The best improvement is obtained with cells incorporating 0.1 and 0.2 wt% SWCNT **4**. State-of-the-art efficiencies are obtained after annealing of the BHJ.³ Most importantly, a record open circuit voltage of 0.83 V is obtained with 0.1% SWCNT **4**, whereas the open circuit voltage of pristine annealed solar cells is 0.58 V. Interestingly, a large open circuit voltage is a common feature to all the SWCNT-doped cells studied in this work.

The influence of SWCNT **4** on the active layer was studied by UV-Visible spectroscopy before and after annealing. The evolution of the shoulders at 550 and 610 nm in the absorbance correlates with the increase of the π - π -stacking of the conjugated polymer in the BHJ.³ The behaviour is also strongly correlated with X-ray diffraction (XRD) data.

In conclusion, we have obtained a significant improvement in the photovoltaic properties of P3HT/PCBM based PV cells through the incorporation of SWCNT-ester derivative **4** into the active layer. We may expect that the improvement is mostly due to the fact that the covalent functionalization of pristine SWCNTs strongly diminishes, if not suppresses, the metallic character of the initial carbon nanotube network, as previously observed.^{11,12} Furthermore the maximum open circuit voltage that is accessible to a solar cell is related to the energy difference between the conduction level of the acceptor material and the valence level of the donor material (the flat band regime)¹³, minus a voltage drop that is related to the build-up of a space charge field either at the electrode interfaces or inside the BHJ.¹⁴ The 0.3 V drop that was currently admitted can be overcome by the use of lower bandgap photovoltaic polymers in which, at constant open-circuit voltage, the short circuit current

can be increased significantly.¹⁵ The idea was successfully applied by several authors in order to break successively the world record efficiency accessible to BHJ- cells.¹⁶⁻¹⁸ The technique demonstrated herein may open new margins for an extra *ca.* 30% efficiency enhancement using state-of-the-art low band-gap BHJ solar cells through the increase of the open-circuit voltage.

Acknowledgements:

We acknowledge the Région des Pays de la Loire (UNIVALOIRE) and the Conseil Général de Maine-et-Loire for supporting Drs. Hassina Derbal and Céline Bergeret, respectively.

Research at Queen's University was supported by the Natural Sciences and Engineering Research Council, the Canada Research Chair program on Chiral Photonics and the Canada Foundation for Innovation.

REFERENCES:

- 1 – E. Kymakis, G.A.J. Amaratunga, *Appl. Phys. Lett.* **2002**, 80, 112.
- 2 – E. Kymakis, I. Alexandrou, G.A.J. Amaratunga, *J. Appl. Phys.* **2003**, 93, 1764.
- 3 – G. Dennler, M.C. Scharber, C.J. Brabec, *Adv. Mater.* **2009**, 21, 1323.
- 4 – B. Pradhan, S.K. Batabyal, A.J. Pal, *Appl. Phys. Lett.* **2006**, 88, 093106.
- 5 – S. Berson, R. de Bettignies, S. Bailly, S. Guillerez, B. Jusselme, *Adv. Funct. Mater.* **2007**, 17, 3363.
- 6 – M.M. Stylianakis, J.A. Mikroyannidis, E. Kymakis, *Sol. En. Mater. Sol. Cells* **2010**, 94, 267.
- 7 – J. Liu, A.G. Rinzler, H. Dai, J.H. Hafner, R.K. Bradley, P.J. Boul, A. Lu, T. Iverson, K. Shelimov, C.B. Huffman, F. Rodriguez-Macias, Y.-S. Shon, T.R. Lee, D.T. Colbert, R.E. Smalley, *Science* **1998**, 280, 1253.
- 8 – A.G. Rinzler, J. Liu, H. Dai, P. Nikolaiev, C.B. Huffman, F.J. Rodriguez-Macias, P.J. Boul, A.H. Lu, D. Heymann, D.T. Colbert, R.S. Lee, J.E. Fischer, A.M. Rao, P.C. Eklund, R.E. Smalley, *Appl. Phys. A* **1998**, 67, 29.
- 9 – J. Chen, M.A. Hamon, H. Hu, Y. Chen, A.M. Rao, P.C. Eklund, R.C. Haddon, *Science* **1998**, 282, 95.
- 10 – D. Bonifazi, C. Nacci, R. Marega, S. Campidelli, G. Ceballos, S. Modesti, M. Meneghetti, M. Prato, *Nano Lett.* **2006**, 6, 1408.
- 11 – C. Bergeret, J. Cousseau, V. Fernandez, J.-Y. Mevellec, S. Lefrant, *J. Phys. Chem. C* **2008**, 112, 16411.
- 12 – M. Kanungo, H. Lu, G.G. Malliaras, G.B. Blanchet, *Science* **2009**, 323, 234.
- 13 – A. Moliton, J.M. Nunzi, *Polymer Int.* **2006**, 55, 583.
- 14 – P.W.M. Blom, V.D. Mihailetschi, L.J.A. Koster, D.E. Markov, *Adv. Mater.* **2007**, 19, 1551.
- 15 – M.C. Scharber, D. Mühlbacher, M. Koppe, P. Denk, C. Waldauf, A.J. Heeger, C.J. Brabec, *Adv. Mater.* **2006**, 18, 789.
- 16 – S.H. Park, A. Roy, S. Beaupre, S. Cho, N. Coates, J.S. Moon, D. Moses, M. Leclerc, K. Lee, A.J. Heeger, *Nature Photonics* **2009**, 3, 297.
- 17 – H.-Y. Chen, J. Hou, S. Zhang, Y. Liang, G. Yang, Yang Yang, L. Yu, Y. Wu, G. Li, *Nature Photonics* **2009**, 3, 649.
- 18 – Y. Liang, Z. Xu, J. Xia, S.-T. Tsai, Y. Wu, G. Li, C. Ray, L. Yu, *Adv. Mater.* **2010**, 22, 1

CURRICULUM VITAE

NUNZI, Jean-Michel, Professor, Tenured



DEGREES:

Ph.D., Physics, Pierre et Marie Curie, Paris, 1984
MSc., Ecole Supérieur de Physique et Chimie, Paris 1982
B.Sc., Pierre et Marie Curie, Paris, 1980

EMPLOYMENT HISTORY:

2009 Professor, University of Limoges, XLIM
2006 - Professor, Chemistry Department, Physics Department,
 Queen's
2000 - 2006 Professor, Physics, Université d'Angers, POMA
1984 - 2000 Full researcher, Electronics, Atomic energy Commission,
 France

HONOURS:

- Tier 1 Canada research Chair in Chiral Photonics, 2006
- Habilitation à Diriger les Recherches, Orsay, France, 1999

PROFESSIONAL ACTIVITIES:

2010 Co-chair of 'Nanophotonics' SPIE Conference, Brussels, April
2008 Co-chair of 'Linear and Nonlinear Optics of Organic Materials'
 SPIE annual meeting, San Diego, CA, August 2008 Co-chair of
 'Nanophotonics' SPIE Conference, Strasbourg, France, April
2007 Chairman of the "The 7th International Symposium on
 Advanced Organic Photonics (ISAOP7)", Angers - France,
 June 14 - 15, 2007 <http://ead.univ-angers.fr/~isaop7/>
2007 Chairman of 'Linear and Nonlinear Optics of Organic Materials'
 SPIE annual meeting, San Diego, CA, August
2006 Co-chair of 'Nanophotonics' SPIE conference, Photonics
 Europe, Strasbourg, France, April
2006 Programme committee of ISOPL4 conference, Dingle, Ireland
 June
2006 Co-chair of 'Linear and Nonlinear Optics of Organic Materials'
 SPIE annual meeting, San Diego, CA
2000 - 2010 Program committee of 'Organic Photonics Materials and
 Devices' SPIE Conference, Photonic West, San Jose, CA,
 January

GRADUATE SUPERVISION:

Completed: 12 Ph.D. since past 7 years

NAME OF STUDENTS currently supervised:

Feng Liu	PhD Queen's Chem	2007
Sunny Rao	Master Queen's Phys	2007
Andrew Fraser	Master Queen's Chem	2007
Thomas Kraft	Master Queen's Chem	2008
Nicole Day	Master Queen's Chem	2009
Ahmad Elhajj	Master Limoges	2010

EXTERNAL RESEARCH FUNDING:

<u>Year</u>	<u>Source</u>	<u>Type*</u>	<u>Amount per year</u>	<u>Purpose**</u>
2006 - 2013	CRCHAIRS - CRC		\$200000/year	research
2010 - 2015	NSERC - DG		\$60000/year	research
2006 - 2007	CFI - Infrastructure		\$221600	equipment
2006 - 2007	MRI - Infrastructure		\$221600	equipment
2008 - 2009	NSERC RTI		\$143329	equipment
2008-2009	Hutchinson SA		\$10000	research

SELECTED RECENT PUBLICATIONS:

- 'Up-conversion injection in Rubrene/Perylene-diimide-heterostructure electroluminescent diodes', A.K. Pandey, J.-M. Nunzi, *Appl. Phys. Lett.* 90, 263508 (2007)
- 'Spontaneous photoinduced patterning of azo-dye polymer films: the facts', C. Hubert, C. Fiorini-Debuisschert, L. Rocha, P. Raimond, J.-M. Nunzi, *JOSA B* 24, 1839-1846 (2007)
- 'Optical modeling of the efficiency limits of (Pentacene: N, N'-ditridecylperylene-3, 4, 9, 10-tetracarboxylic diimide)-blend solar cells', F. Monestier, A.K. Pandey, J.-J. Simon, P. Torchio, L. Escoubas, J.-M. Nunzi, *J. Appl. Phys.* 102, 034512 (2007)
- 'Rubrene fullerene heterostructures with half-gap electroluminescence threshold and large photovoltage' A.K. Pandey, J.M. Nunzi, *Adv. Mater* 19, 3613-3617 (2007)
- 'Size effect on organic optoelectronics devices: example of photovoltaic cell efficiency', A.K. Pandey, J.-M. Nunzi, B. Ratier, A. Moliton, *Physics Letters A* 372, 1333-1336 (2008)
- 'Cognitive ability process at the molecular level', R. Barille, S. Ahmadi Kandjani, J.M. Nunzi, E. Ortyl, S. Kucharski, *Int. J. Nanotech.* 5, 885-895 (2008)
- 'Tunable circularly polarized lasing emission in reflection distributed feedback dye lasers', F. Chen, D. Gindre, J.-M. Nunzi, *Optics Express* 16, 16746-16753 (2008)
- 'Effect of metal cathode reflectance on the exciton- dissociation efficiency in heterojunction organic solar cells', A.K. Pandey, P.E. Shaw, I.D.W. Samuel, J.M. Nunzi, *Appl. Phys. Lett.* 94, 103303 (2009)
- 'Near infrared emission in rubrene:fullerene heterojunction devices', A.M.C. Ng, A.B. Djuricic, W.K. Chan, J.M. Nunzi, *Chem. Phys. Lett.* 474, 141-145 (2009)
- 'Surface Relief Grating formation on nano-objects', R. Barillé, P. Tajalli, S. Zielinska, E. Ortyl, S. Kucharski, J.M. Nunzi, *Appl. Phys. Lett.* 95, 053102 (2009)
- 'Spontaneous formation of optically induced surface relief gratings' H. Leblond, R. Barille, S. Ahamadi-Kandjani, J.M. Nunzi, E. Ortyl, S. Kucharski, *J. Phys B.* 42, 205401 (2009)
- 'An isomerization-induced dynamic heterogeneity in a supercooled glass-former', V. Teboul, M. Saiddine, J.M. Nunzi, *Phys. Rev. Lett.* 103, 265701 (2009)
- 'Metal Plasmon Enhanced Europium Complex Luminescence', F. Liu, G. Aldea, J.M. Nunzi, *J. Lumin.* 130, 56-59 (2010)
- "Photoinduced deformation of azopolymer nanometric spheres" R. Barillé, P. Tajalli, S. Kucharski, E. Ortyl J.-M. Nunzi, Accepted, *Appl. Phys. Lett.* (L10-01434R)

IMPROVEMENTS OF THIENOPYRAZINE POLYPHENYLENE VINYLENE BASED POLYMER SOLAR CELLS BY THIOL ADDITIVES

S. Sensfuss^{1*}; L. Blankenburg¹, H. Schache¹, S. Shokhovets², G. Gobsch²,
A. Konkin³, S. Sell⁴, E. Klemm⁴, A. Dellith⁵, G. Andrae⁵

¹ TITK Rudolstadt, Dept. Functional Polymer Systems and Physical Research,
Breitscheidstr. 97, D-07407 Rudolstadt, Germany, *e-mail: sensfuss@titk.de

² Ilmenau Technical University, Institute for Physics, Weimarer Str.32, D-98684 Ilmenau,
Germany

³ Ilmenau Technical University, Center for Micro- and Nanotechnologies, Gustav-
Kirchhoff-Str.7, D-98693 Ilmenau, Germany

⁴ Jenpolymer Materials Ltd. & Co. KG, Wildenbruchstr. 15, D-07745 Jena, Germany

⁵ Institute of Photonic Technology, Dept. Photonic Silicon, Albert-Einstein-Str.9, D-07745
Jena, Germany

Abstract

The thienopyrazine-based low-bandgap poly(phenylene-vinylene) (PPV) PM-19 was successfully applied in flexible and rigid polymer:fullerene solar cells. [6.6]-Phenyl-C₆₁₍₇₁₎-butanoic acid methyl ester ([60]-PCBM, [70]-PCBM) were used as acceptors. The comparison of the device parameters of PM-19:[60]-PCBM vs. PM-19:[70]-PCBM (1:2 w/w) yield an increased short circuit current applying [70]-PCBM but finally nearly the same power conversion efficiencies (2.32% vs. 2.38% on ITO PET, 2.86 % vs. 2.84 % on ITO glass substrates). For PM-19:[70]-PCBM (1:2 w/w) devices with 1,8-octanedithiol as an additive we found a strong influence on the film morphology, the external/ internal quantum efficiency, the charge carrier separation and consequently on the solar cell efficiency in dependence on the amount of the thiol given to the polymer:fullerene solution. The best results were obtained with an polymer: thiol weight ratio (w/w) in the range of 1:0.1 to 1:0.25 with an enhanced power conversion efficiency to about 3.23% on ITO PET vs. 2.32 % without thiol. Light-induced electron spin resonance (LESR) spectroscopy exhibits that the charge transfer to PCBM as acceptor occurs quite normally and that the ESR line double integral intensity decreases if the thiol content is increased from 1:0.1 to 1:2.4 polymer:thiol w/w.

Introduction

The technology and cost benefit for reel to reel processed solar cells based on soluble conjugated polymers is undoubted. The development of new low-bandgap polymers (LBP) whose absorption match the solar spectrum better than the well-known poly(3-hexylthiophene) (P3HT) is a key issue. Up to now only a few low-bandgap polymers yield

high power conversion efficiencies in the range of 5.1-6.1% (on glass substrates) [1-4], but the majority of this kind of polymers typically show cell efficiencies <1.1% (seldom >2%) [5] mostly linked to problems with the charge transport. In some cases clearly improved cell efficiencies of P3HT:[60]-PCBM [6-7] and LBP:[70]-PCBM [1-2] devices were obtained with the help of processing additives. Here we report the optical, electrical and photovoltaic properties of a low-bandgap thieno[3,4-*b*]pyrazine phenylene-vinylene copolymer (PM-19). The influence of a dithiol additive on the film morphology, the external (EQE)/ internal (IQE) quantum as well as solar cell efficiency applying [70]-PCBM as acceptor is reported.

Materials

The well-defined strictly alternating thieno[3,4-*b*]pyrazine phenylenevinylene copolymer PM-19 was synthesized by a Horner polycondensation route [8-9]. Figure 1 shows the chemical structure of the photoactive donor material (PM-19). [60]-PCBM and [70]-PCBM were used as acceptors (Solenne 99.5 and 99% purity, respectively).

Based on the cyclic voltammetric data measured in solid state the HOMO/ LUMO level positions of PM-19 amount to -5.10 eV and around -3.11 eV, respectively (for PM-19 no reduction peak could be obtained but for very similar polymer structures). The HOMO position is energetically increased and the LUMO decreased related to the well known MDMO-PPV homopolymer (poly[2-methoxy-5-(3',7'-dimethyloctyloxy)-1,4-phenylenevinylene], HOMO: -5.31 eV, LUMO: -2.83 eV). The UV-VIS absorption spectrum of a PM-19 film (from chlorobenzene) shows 3 peaks at 356, 468 and 660 nm and the absorption edge is shifted to lower photon energies indicating a lower optical bandgap (1.6 eV) than MDMO-PPV (2.2 eV).

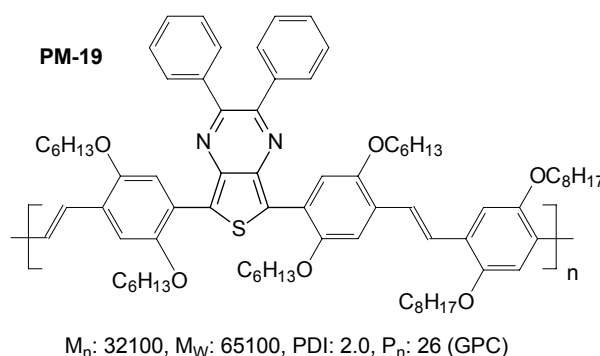


Figure 1: Chemical structure of the low-bandgap PPV (PM-19)

Solar cell devices without an additive

PM-19:[60]-PCBM (1:2 w/w) and PM-19:[70]-PCBM (1:2 w/w) solar cell devices were prepared on indium tin oxide (ITO) covered polyester (PET) films (Cadillac Plastic, 100 nm

ITO, surface resistance: 60 Ω /square) or on ITO glass substrates (Merck Displays, 125 nm ITO, 13 Ω /square). The usual device configuration was applied by spin-coating a thin layer (~80 nm) of PEDOT:PSS (poly(3,4-ethylenedioxythiophene)-poly(styrenesulfonate) (Baytron PH or Baytron AI 4083, H. C. Starck/ Germany) followed by a drying step (5-10 min at 80-120°C). Subsequently, the photoactive polymer:fullerene composite layer (~70-100 nm, solvent: chlorobenzene) was deposited again by spin-coating without a subsequent annealing (film preparation outside a glovebox). The aluminum cathode was thermally deposited (~ 50 nm) through a shadow mask, the I/V curves were recorded on ambient conditions.

Table 1: Photovoltaic parameters of PM-19:[60]-PCBM and PM-19:[70]-PCBM devices with and without 1.8-octanedithiol (Aldrich, purity >97%) as an additive (P_{IN} : 100 mW/cm², AM1.5 white light, Steuernagel solar simulator, A: 25 mm²)

PM-19:PCBM 1:2 w/w (PM-19:thiol w/w)	I_{SC} [mA/cm ²]	V_{OC} [mV]	FF	$\eta_{AM1.5}$ [%]
[60]-PCBM (1:0)*	6.20	584	0.64	2.32
[60]-PCBM (1:0)**	7.71	553	0.67	2.86
[70]-PCBM (1:0)*	7.40	606	0.53	2.38
[70]-PCBM (1:0.1)*	8.74	606	0.61	3.23
[70]-PCBM (1:1)*	4.95	597	0.57	1.68
[70]-PCBM (1:2.4)*	4.17	603	0.51	1.28
[70]-PCBM (1:0)**	8.24	564	0.61	2.84
[70]-PCBM (1:0.25)**	8.59	616	0.60	3.17
[70]-PCBM (1:2.4)**	5.20	581	0.54	1.63

* on ITO-PET (Cadillac Plastic, 60 Ω /□),

** on ITO glass (Merck Displays, 13 Ω /□), thiol: 1.8-octanedithiol

The comparison of the device parameters of PM-19:[60]-PCBM vs. PM-19:[70]-PCBM (without any additive, Table 1) show mainly an increased short circuit current (I_{SC}) applying [70]-PCBM, whereas a less decreased V_{OC} (open circuit voltage) or FF (fill factor) finally yield nearly the same power conversion efficiencies. This is the case on ITO PET (2.32% vs. 2.38%) as well as on ITO glass (2.86 % vs. 2.84 %). It agrees with the external quantum efficiencies (EQE), which give nearly the same overall EQE for both composites, but the spectrum with [70]-PCBM shows less features. The EQE peak value comes up to ~42 % for the blend with [60]-PCBM (Figure 2, IQE peak value ~54%) and is among the best for low-bandgap polymers [5]. The higher I_{SC} results from the clearly lower optical bandgap of [70]-PCBM (~1.75 eV) related to [60]-PCBM (~2.4 eV), which contributes to the light absorption [10]. The appearance of the film colour changes from olive-green to red brown going from PM-19:[60]-PCBM to PM-19:[70]-PCBM (1:2 w/w).

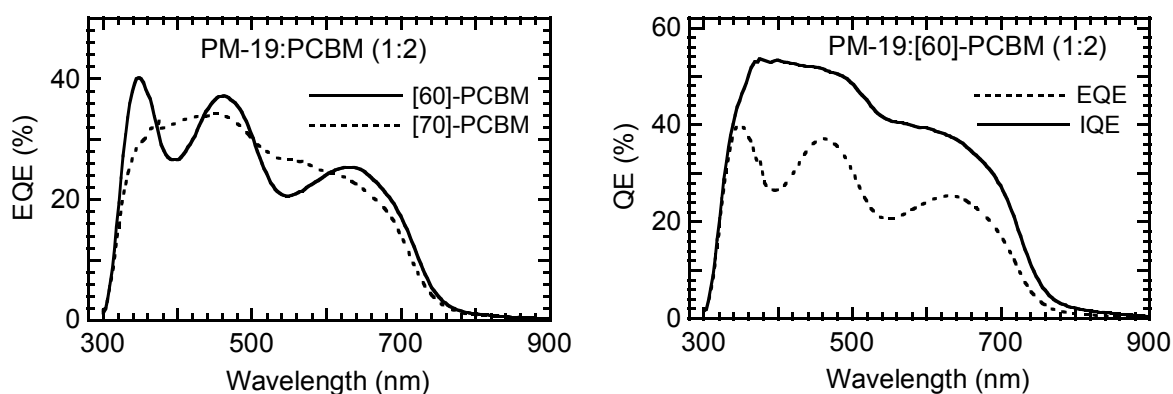


Figure 2: Comparison of the external quantum efficiencies for devices with [60]-PCBM and [70]-PCBM (left) as well as EQE vs. IQE for the device with [60]-PCBM (right, in both figures without an additive)

Solar cell devices with a thiol additive

Peet et al. [1] and Lee et al. [2] reported about a clearly enhanced power conversion efficiency of low-bandgap polymer:[70]-PCBM solar cell devices in the presence of dithiols with different alkyl spacer length [1] and different 1,8-functionalized alkanes [2]. Both attributed the role of the additive as a processing agent, which mainly acts via its higher boiling point than the host solvent applied for the film preparation as well as by a selective solubility of [70]-PCBM.

For PM-19:[70]-PCBM (1:2 w/w) devices with 1,8-octanedithiol as the additive we found a strong influence on the film morphology, the external and internal quantum efficiency, the charge carrier separation and finally on the solar cell efficiency in dependence on the amount of the thiol given to the polymer:fullerene solution. The PM-19:fullerene phase separation is lower and the surface roughness smoother related to the reference (Figure 3) applying less thiol (PM-19:thiol 1:0.1 w/w, Figure 3b) and is strongly increased using much thiol (PM-19:thiol 1:2.4 w/w, Figure 3d) (AFM surface roughness: without thiol 3.82 nm, PM-19:thiol 1:0.1 - 1.08 nm, PM-19:thiol 1:1 - 1.22 nm, PM-19:thiol 1:2.4 - 13.88 nm/ root mean square deviation, internal value of the Anfattec AFM apparatus). The AFM and the field emission scanning electron microscopic (SEM) images show for the highest thiol content broad hill-like features with a diameter of ~500 nm attributed to large fullerene clusters (Figure 3d, 4b). A special circular phase distribution was observed only for PM-19:thiol (1:1 w/w, Figure 3c).

The short circuit current is clearly increased after addition of less thiol (PM-19:thiol 1:0.1 w/w) and the power conversion efficiency enhanced to about 3.23% on ITO PET (vs. 2.32 % of the reference cell without thiol, Table 1/ Figure 5). A thiol content higher than 1:0.25 polymer:thiol drastically decrease the device performance due to a too large phase separation.

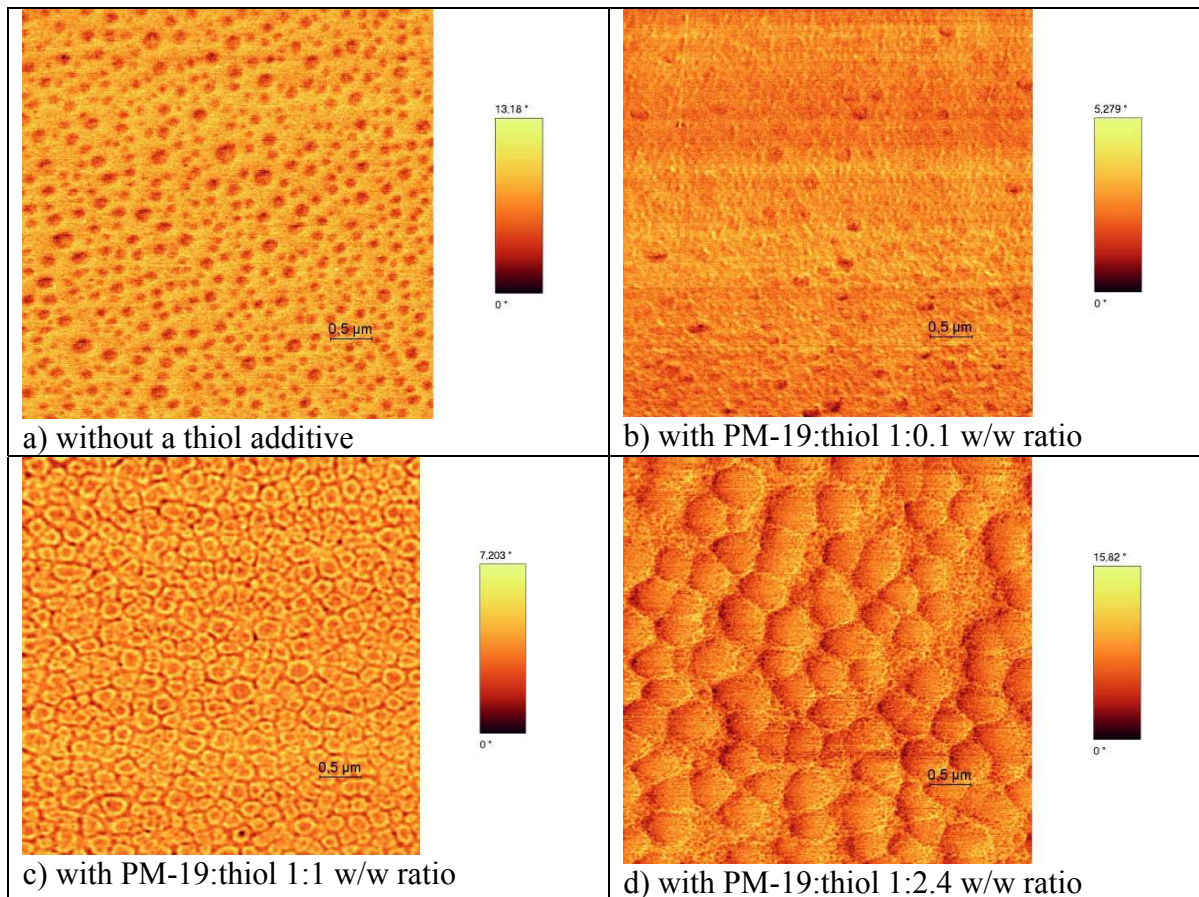


Figure 3: Influence of the amount of 1,8-octanedithiol on the AFM film morphology of PM-19:[70]-PCBM (1:2 w/w) layers (phase images, 5 x 5 μm, on ITO PET)

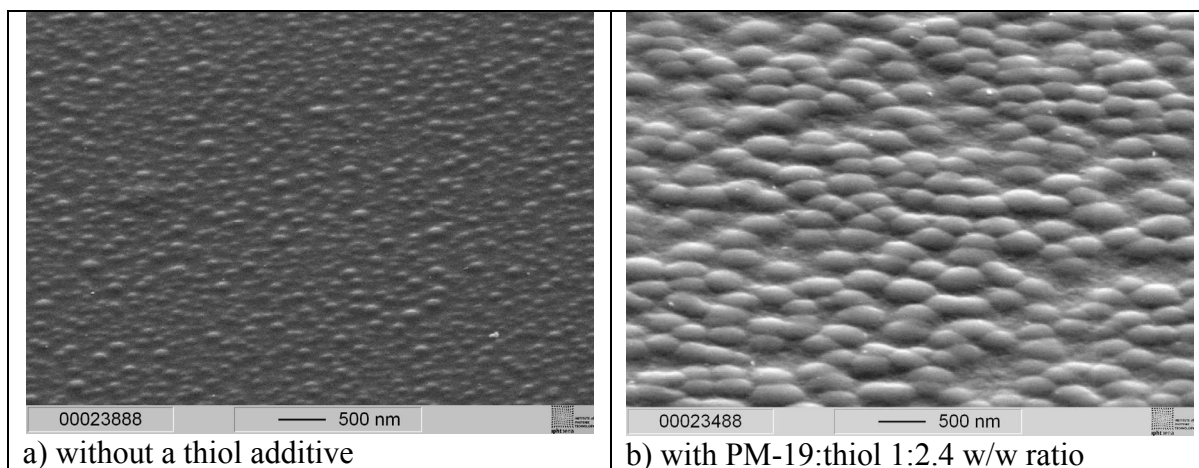


Figure 4: Scanning electron microscopic images of a PM-19:[70]-PCBM (1:2 w/w) films on ITO PET (SEM: JEOL JSM 6300-F FESM recorded @ 5 kV)

The higher device performance is also proved comparing the external and internal quantum efficiencies before and after less thiol addition (Figure 6). The EQE rises up from 34 to 58% and the IQE from 40 to 64% at ~460 nm. Although these values are among the best ones reported for low-bandgap polymer based solar cells [5] the clear difference between EQE and IQE demonstrates the considerable reserves concerning an optimal thickness of the

photoactive layer. Here the interplay between the spectral dependence of the optical constants and interference effects plays an important role.

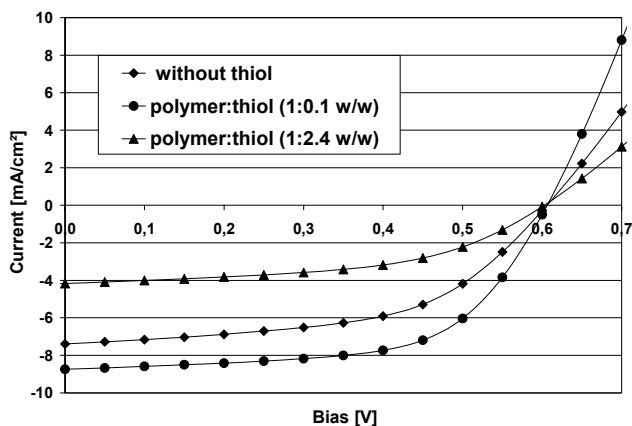


Figure 5: I-V characteristics of PM-19:[70]-PCBM (1:2 w/w) devices on ITO PET (Cadillac Plastic, $60 \Omega/\square$) with different 1.8-octanedithiol content (P_{IN} : 100 mW/cm^2 , AM1.5 white light, Steuernagel solar simulator, A: 25 mm^2)

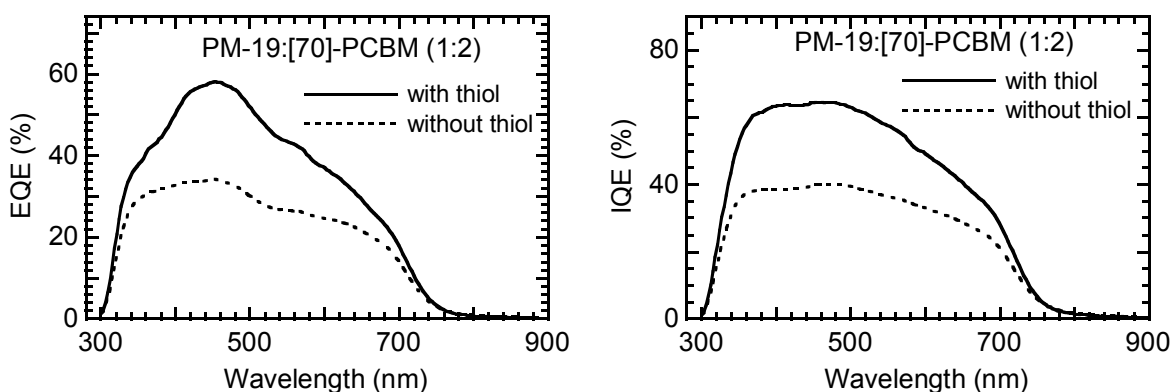


Figure 6: Comparison of the external (left) and internal (right) quantum efficiencies for PM-19:[70]-PCBM devices without and with 1.8-octanedithiol (polymer:thiol 1:0.25 w/w)

Additionally, an influence of the amount of added thiol on the charge separation process could be detected by light-induced electron spin resonance (LESR) technique. Figure 7 shows the recorded LESR spectra of frozen solutions of pure PM-19 (S_1) and of PM-19:[70]-PCBM (1:2 w/w, S_2) (in chlorobenzene, T: 77 K, CW Xe-lamp illumination, Bruker X-band spectrometer ELEXYS E500 operating at 9.4 GHz). The frozen solution spectra are better resolved (smaller spectral linewidth) and more intensive (PM-19) than the spectra of film samples. Therefore they were used to clarify the spectroscopic data of the complicated superposed donor (PM-19) and acceptor ([70]-PCBM) spectra. The experimental LESR spectrum of PM-19 exhibits an inhomogeneous line shape (S_1 , Figure 7) and corresponds to the positive polaron ($P^{\bullet+}$) on the polymer chain. S_4 in Figure 7 is the simulated PM-19 polaron spectrum obtained with $S_4 = n \cdot S_1$ (here $n = 4.2$ determined by the simulation). Subsequently, the [70]-PCBM $^{\bullet-}$ radical

anion (S_3) may be extracted as the difference spectrum of $S_3=S_2-S_4$. The determined g-factor components of the PM-19 polaron (P^+) as well as the [70]-PCBM radical anion (R^-) are listed on top of Figure 7. To the best of our knowledge the g-factor components of [70]-PCBM $^{\bullet-}$ are still not reported to date. LESR using thin solid dropcasting films ($0.6\pm 0.1 \mu\text{m}$) of PM-19:[70]-PCBM show that the ESR line double integral intensity (DI_{NM}) decreases continuously if the thiol content is increased starting from a polymer:thiol ratio of 1:0.1 to 1:0.25 to 1:2.4 w/w. This fully agrees with the photovoltaic parameters (Table 1, Figure 5). The normalised double integral intensities (DI_{NM}) in dependence on the thiol content (X) are inserted (F7) in Figure 7. However, the maximum point of DI_{NM} , which should be correlated with the best solar cell, was not determined definitely.

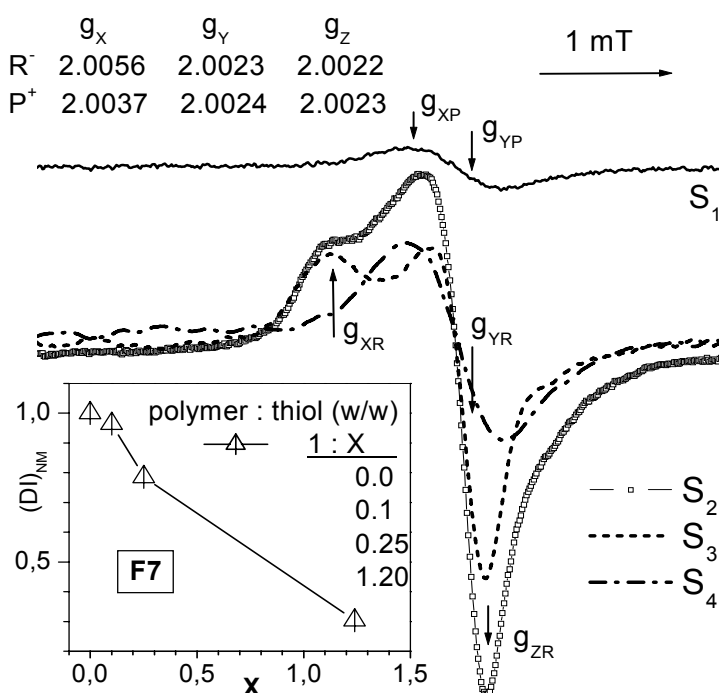


Figure 7: Recorded LESR spectra of frozen solutions of pure PM-19 (S_1), PM-19:[70]-PCBM (1:2, S_2) (in chlorobenzene, T: 77 K, CW Xe-lamp illumination, X-band, 9.4 GHz) and the simulated spectra for the PM-19 $^+$ polaron (S_4) and the extracted [70]-PCBM $^{\bullet-}$ radical anion ($S_3 = S_2-S_4$). The insert F7 shows the dependence of the normalised double integral intensities (DI_{NM}) on the thiol content X measured at PM-19:[70]-PCBM films.

Conclusion

The thienopyrazine-based low-bandgap PPV PM-19 was successfully applied in flexible and rigid polymer:fullerene solar cells. The LESR exhibits that the charge transfer to PCBM as acceptor occurs quite normally differently to many other low-bandgap polymers in the literature [5]. The comparison of the device parameters of PM-19:[60]-PCBM vs. PM-19:[70]-PCBM (without any additive) show an increased short circuit current applying

[70]-PCBM, whereas a less decreased V_{OC} or FF finally yield nearly the same power conversion efficiencies.

For PM-19:[70]-PCBM (1:2 w/w) devices with 1,8-octanedithiol as an additive we found a strong influence on the film morphology, the external and internal quantum efficiency, the charge carrier separation (detected by LESR) and finally on the solar cell efficiency in dependence on the amount of the thiol given to the polymer:fullerene solution. The best results were obtained with a polymer:thiol ratio in the range of 1:0.1 to 1:0.25 w/w.

The understanding of the thiol as a processing agent [1, 2] is possible, because its strong influence on the film morphology is undoubted and also clearly shown by our investigations. But based on our LESR results and the notice, that small amounts of the thiol give the highest solar cell efficiency enhancement, it seems to be another approach, that the thiol additionally improves the charge carrier separation and transport by an easier overcoming of deep traps and finally modifying the product of charge carrier mobility and lifetime. Peet et al. [6] discussed it in a similar way and Pivrikas et al. [7] proved a strong decay of the charge carrier mobility with the time for cells without n-octanedithiol but a nearly time-independent mobility after addition of this thiol to P3HT:[60]-PCBM composites.

Acknowledgement

Financial support from the Federal Ministry of Education and Research (BMBF project No. 03SF0333C) is gratefully acknowledged.

References

- [1] J. Peet et al. Efficiency enhancement in low-bandgap polymer solar cells by processing with alkane dithiols. *Nature Materials* **6**, 497-500 (2007).
- [2] J. K. Lee et al. Processing Additives for Improved Efficiency from Bulk Heterojunction Solar Cells. *J. Am. Chem. Soc.* **130**, 3619-3623 (2008).
- [3] Y. Liang et al. Development of New Semiconducting Polymers for High Performance Solar Cells. *J. Am. Chem. Soc.* **131**, 56-57 (2009).
- [4] S. H. Park et al. Bulk heterojunction solar cells with internal quantum efficiency approaching 100%. *Nature Photonics* **3**, 297-303 (2009).
- [5] E. Bundgaard, F. C. Krebs. Low band gap polymers for organic photovoltaics. *Solar Energy Materials & Solar Cells* **91**, 954-985 (2007).
- [6] J. Peet et al. Method for increasing the photoconductive response in conjugated polymer/fullerene composites. *App. Phys. Lett.* **89**, 252105 (2006).
- [7] A. Pivrikas et al. Substituting the postproduction treatment for bulk-heterojunction solar cells using chemical additives. *Organic Electronics* **9**, 775-782 (2008).
- [8] A. Drury, S. Maier, M. R  ther, W. J. Blau, J. Mater. Chem. **13**, 485-490 (2003)
- [9] M. Shahid, R. S. Ashraf, E. Klemm, S. Sensfuss, *Macromolecules*, **39**, 7844-7853 (2006)
- [10] M. Wienk et al. Efficient Methano[70]fullerene/MDMO-PPV Bulk Heterojunction Photovoltaic Cells. *Angew. Chem. Int. Ed.* **42**, 3371 – 3375 (2003).

USE OF NANOFIBERS IN BULK HETEROJUNCTION SOLAR CELLS: THE EFFECT OF ORDER AND MORPHOLOGY ON THE PERFORMANCE OF P3HT:PCBM BLENDS.

D. J. M. Vanderzande^{1,2*}, W. D. Oosterbaan¹, V. Vrindts², S. Bertho¹, J. C. Bolsée¹,
A. Gadisa¹, K. Vandewal¹, J. Manca^{1,2}, L. Lutsen², T. J. Cleij¹, J. D'Haen¹, J. Zhao³
G. Van Assche³, B. Van Mele³

¹ University of Hasselt, Institute for Materials Research (IMO), Agoralaan Bld D, B-3590 Diepenbeek, Belgium

² IMEC/ IMOMEC, Wetenschapspark 1, B-3590 Diepenbeek, Belgium

³ Vrije Universiteit Brussel (VUB), Pleinlaan 2, B-1050 Brussel, Belgium.

The observation of electron transfer between a conjugated polymer and a C₆₀ molecule,^[1] and the development of the bulk-heterojunction concept in polymer:fullerene devices,^[2, 3] have led together with several developments in materials and device design to polymer solar cells nearing 6% efficiency.^[4] A well-documented example of a polymer:fullerene bulk heterojunction solar cell (BHJ solar cell) is the poly(3-hexylthiophene) (P3HT): [6,6]-phenyl -C₆₁-butyric acid methyl ester (PCBM) solar cell, a materials combination for which several research groups reported efficiencies near 5%.^[5-7] P3HT has favourable electronic and optical properties and a good processability. Furthermore, it has a strong tendency to crystallize. Well-developed crystals of P3HT have a fibrillar shape, can be several micrometers long and have a cross section of approximately 20 × 4 nm.^[8-10] More importantly, these fibers have been identified as the main hole conducting channels in optimally annealed, state-of-the-art BHJ solar cells^[11] and field-effect transistors (FETs).^[12]

The goal of the presented work is to establish the effect of the alkyl side chain length of P3ATs on device properties.^[13] Nanofibers offer an attractive way to study the influence of alkyl chain length on material and device properties on a more equal footing, since nanofiber formation by crystallization in solution is expected to give more evolved and relaxed systems than those that can be obtained by thermal annealing.

The regioregular P3ATs were synthesized by us from 2,5-dibromo-3-alkylthiophenes using the Rieke method (Figure 1). This yielded polymers P3Pr(opyl)T to P3N(onyl)T in 50—80% yield with high regioregularities ($RR \geq 94.5\%$).^[14] Molecular weights were measured with GPC *versus* a polystyrene standards. The \bar{M}_n values obtained for P34T to P39T are in a fairly narrow range; between 17 and 28 kg mol⁻¹.

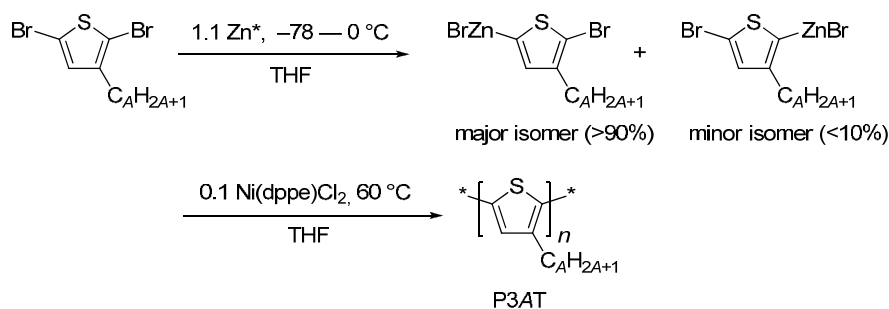


Figure 1: Synthesis of poly(3-alkylthiophene)s (P3AT).

Fibers were prepared by the slow cooling to room temperature of a heated solution of P3AT in a suitable solvent.^[8,10] To allow for spin-coating layers of sufficient thickness (>20 nm), we aimed at fiber formation in the concentration range of ~0.3 to 1 wt %.

The UV-Vis spectra of thin films of the isolated fibers of P3PrT to P3NT clearly show (Figure 2) that the increase in alkyl chain length in going from P3PrT to P3PT induces a strong increase in the vibrational structure. Also the band maximum red-shifts with increasing alkyl side-chain length. Simultaneously, the relative intensity of the first vibronic transition around 610 nm slightly increases at the cost of the third vibronic transition around 520 nm.

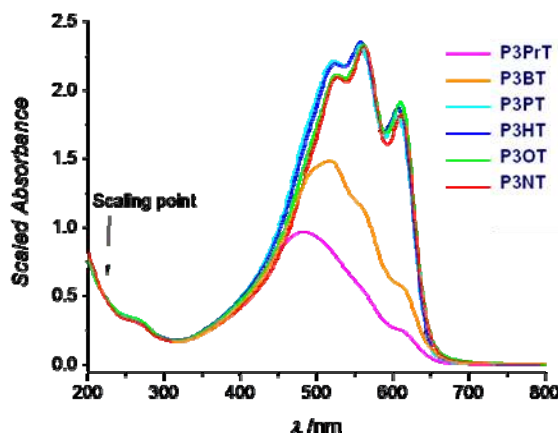


Figure 2: UV-Vis spectra (normalized for an absorbance of 0.2 at 250 nm) of drop-casted films of the isolated fibers of P3PrT to P3NT on quartz.

The motivation to use nanofibers to produce BHJ solar cells was based on the phase diagram that was determined for P3HT:PCBM blends.^[15] For that purpose, different compositions of P3HT and PCBM were produced by dissolving the components in chlorobenzene. Subsequently the solutions were deposited by drop-casting on large glass plates in a glove box under a nitrogen atmosphere to form films. After drying the remaining solid films were scratched off the glass substrates in the powder form and

collected for the DSC and MTDSC measurements. The collection of all data delivers the phase diagram depicted in figure 3. The most important result towards practical applications relates to the evolution of the glass transition temperature (T_g) in function of blend composition. No indication of phase separation in the molten state of the blends is found, as a single glass transition is observed for all compositions. This T_g of the blend starts at the T_g of pure P3HT (= 12 °C) increases as the PCBM content increases till the T_g of pure PCBM (= 131 °C). The phase diagram also shows that the morphology of the blends with an f_w^{PCBM} of 45-50 wt%, giving the highest performance in a solar cell, is intrinsically unstable at the desired maximum operating temperature of 80 °C, as the T_g is less than 40 °C. Possibly the use of nanofibers to produce solar cells can create a kind of thermostable state not relying on a phase separation process.

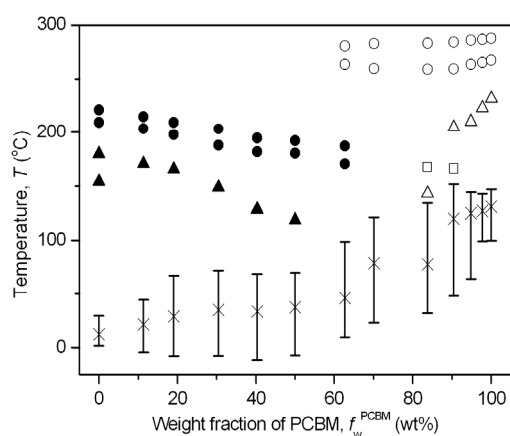


Figure 3: Phase diagram of P3HT:PCBM blends: melt crystallization temperature (▲) and melting temperature (●) of P3HT; melt crystallization temperature (Δ), cold crystallization temperature (□), and melting temperature (○) of PCBM; and T_g (×) with its range (vertical bar) of the blends.

Crystallinity in P3AT:PCBM solar cells has previously been shown to be important for solar cell performance. For P3HT nanofibers, we can show that the fiber content can be easily controlled by varying the solution temperature. In this way, the overall MW of the P3HT in the blend is kept constant^[16,17]. Also fiber isolation is not needed and the use of solvent mixtures is avoided. We found an optimal efficiency at a 42 % fiber content of the casting solution and show that it can be linked to the morphology of the active layer^[18].

The fiber content was determined using UV/Vis measurements of the dispersion. The results obtained show that the fiber content of the solution is very sensitive to temperature. When raising the temperature from 37 to 50 °C, the fiber content of the solution decreases from 60 % to 14 %. The solar cell efficiency displays an optimal efficiency of ~ 3.2 %

found for a solution temperature of 45 °C. At this temperature, the fiber content was as stated 42 %.

From Transmission Electron Microscopy (TEM) images and Selected Area Electron Diffraction (SAED) measurements of the active layers^[18] it was established that the initial increase in efficiency with temperature of the casting solution is caused by an increased solubility of PCBM in the casting solution. At lower temperatures PCBM forms large (> 50 µm) needles in the casting solution, resulting in poorly mixed active layers and low efficiencies. At temperatures equal or above 45 °C, the PCBM dissolves well and, after reaching its maximum, the solar cell efficiency decreases again with decreasing fiber content. The variation, so observed, in characteristics of the nanofiber solar cell can be understood as a consequence of variation in the nanomorphology of the active layer.

Also the extent to which P3AT side chain length as such, influences photovoltaic characteristics of P3AT:PCBMBHJ solar cells^[19] was investigated. For that purpose blends of P3BT:PCBM (1:0.8), P3PT:PCBM (1:1), and P3HT:PCBM (1:1) were used to produce BHJ solar cells. The active layers were prepared by spin-coating from solutions in *o*-dichlorobenzene at 90 °C, followed by an annealing step of 5 minutes at 140°C.

Table 3: Photovoltaic parameters of the best performing P3BT:PCBM (1:0.8), P3PT:PCBM (1:1), and P3HT:PCBM (1:1) BHJ solar cells (thickness 260 ± 10 nm).

Blend	J_{sc} (mA/cm ²)	V_{oc} (V)	FF	$Efficiency$ (%)
P3BT:PCBM	11.2	0.54	0.53	3.2
P3PT:PCBM	12.5	0.55	0.62	4.3
P3HT:PCBM	12.0	0.57	0.68	4.6

These processing conditions should also allow to achieve similar conditions of morphology development for all blends, as *o*-dichlorobenzene is a good solvent for all derivatives. Table 3 depicts all the photovoltaic characteristics for the three types of solar cells produced. The photo-current was recorded under white light (A.M. 1.5) of intensity 100 mW/cm². It is quite surprising that all polymers yield highly efficient BHJ solar cells. In all cases high photo-currents are observed (> 10 mA/cm²) irrespective of the length of the side chain. To probe the effect of balanced charge-transport, the bipolar transport in the polymer:PCBM blends in OFET devices was investigated for the non-annealed as well as thermally annealed films. Mobility values were extracted from the slope of the OFET

transfer characteristics in the linear regime. According to these data, the hole mobility of the P3BT:PCBM blend is about an order of magnitude larger than its electron mobility under all treatment conditions. Similar results were obtained for the hole and electron mobilities of the P3PT:PCBM blend. These differences are reduced upon annealing at 140° C. In the P3HT:PCBM film, however, holes and electrons exhibit well balanced mobility for both thermally annealed and non-annealed samples. The varying bipolar transport with side chain length can be attributed to local morphology variations ^[19]. These results indicate that unbalanced bipolar charge-transport in P3BT and P3PT devices does not crucially limit the photo-current output of the different devices. It, however, affects fill factor significantly. In conclusion, using *o*-dichlorobenzene as a solvent for producing P3B(utyl)T, P3P(enty)T and P3HT based BHJ solar cells power conversion efficiencies of 3.2, 4.3, and 4.6 % were obtained, respectively. This implies that P3PT is proved to be a potentially competitive material compared to P3HT.

- [1] Sariciftci N.S., Smilowitz, L., Heeger, A.J. & Wudl, F. "Photoinduced electron transfer from a conducting polymer to buckminsterfullerene", *Science*, 258 1474-1476 (1992)
- [2] Halls J.J.M., C.A., W., Greenham, N.C., Marseglia, E.A., Friend, R.H., Moratti, S.C. & Holmes, A.B. "Efficient photodiodes from interpenetrating networks", *Nature*, 376 498-500 (1995)
- [3] Yu G., Gao, J., Hummelen, J.C., Wudl, F. & Heeger, A.J. "Polymer photovoltaic cells: enhanced efficiencies via a network of internal donor-acceptor heterojunctions", *Science*, 270 1789-1791 (1995)
- [4] Kim J.Y., Lee, K., Coates, N.E., Moses, D., Nguyen, T.Q., Dante, M. & Heeger, A.J. "Efficient tandem polymer solar cells fabricated by all-solution processing", *Science*, 317 (5835), 222-225 (2007)
- [5] Li G., Shrotriya, V., Huang, J.S., Yao, Y., Moriarty, T., Emery, K. & Yang, Y. "High-efficiency solution processable polymer photovoltaic cells by self-organization of polymer blends", *Nature Mat*, 4 (11), 864-868 (2005)
- [6] Ma W., Yang, C., Gong, X., Lee, K. & Heeger, A.J. "Thermally stable, efficient polymer solar cells with nanoscale control of the interpenetrating network morphology", *Adv Funct Mater*, 15 1617-1622 (2005)

- [7] Reyes-Reyes M., Kim, K. & Carroll, D.L. "High-efficiency photovoltaic devices on annealed poly(3-hexylthiophene) and 1-(3-methoxycarbonyl)-propyl-1-phenyl-(6,6)C₆₁ blends", *Appl Phys Lett*, **87** (083506), (2005)
- [8] Ihn K.J., Moulton J. and Smith P., *Journal of Polymer Science Part B-Polymer Physics*, **31**, 735-742 (1993).
- [9] Chang J.-F., Clark J., Zhao N., Sirringhaus H., Breiby D. W., Andreasen J. W., Nielsen M. M., Giles M., Heeney M. and McCulloch I., *Physical Review B*, **74**, 115318 (2006).
- [10] Berson S., De Bettignies R., Bailly S. and Guillerez S., *Adv. Funct. Mater.*, **17**, 1377-1384 (2007).
- [11] Yang X., Loos J., Veenstra S. C., Verhees W. J. H. , Wienk M. M., Kroon J. M., Michels M. J. A. and Janssen R. A. J., *Nano Lett.*, **5**, 579-583 (2005).
- [12] Surin M., Leclère P., Lazzaroni R., Yuen J. D., Wang G., Moses D., Heeger A. J., Cho S. and Lee K., *J. Appl. Phys.*, **100**, 033712 (2006).
- [13] J. M. Vanderzande, W. D. Oosterbaan, V. Vrindts, S. Bertho, J. C. Bolsée, A. Gadisa, K. Vandewal, J. Manca, L. Lutsen, T. J. Cleij, J. D'Haen, J. Zhao, G. Van Assche, B. Van Mele, *Organic Photovoltaics X*, edited by Zakya H. Kafafi, Paul A. Lane, Proc. of SPIE, Vol. 7416, 741605 (2009)
- [14] Oosterbaan, W. D. Vrindts V., Berson S., Guillerez S., Douhéret O., Ruttens B., D'Haen J., Adriaensens P., Manca J., Lutsen L., Vanderzande D., *J. Mater. Chem.*, **19**, 5424 (2009).
- [15] Zhao J., Swinnen A., Van Assche G., Manca J., Vanderzande D., and Van Mele B., *J. Phys. Chem. B*, **113** (6), 1587-1591 (2009)
- [16] Ma W., Kim J. Y., Lee K., Heeger A. J., *Macromol. Rapid Commun.* **28**, 1776 (2007).
- [17] Schilinsky P., Asawapirom U., Scherf U., Biele M., Brabec C. J., *Chem. Mater.* **17**, 2175 (2005).
- [18] Bertho S., Oosterbaan W. D., Vrindts V., D'Haen J., Cleij T. J., Lutsen L., Manca J., Vanderzande D., *Org. Electron.* , **10** (7), -1248-1251 (2009).
- [19] Gadisa A., Oosterbaan W. D., Vandewal K., Bolsée J. C., Bertho S., J. D'Haen J., Lutsen L., Vanderzande D., Manca J. V., *Adv. Func. Mat.*, **19** (20), 3300-3306 (2009).

BIOGRAPHIC DATA OF PROFESSOR DIRK VANDERZANDE

Name: Dirk Vanderzande

Address: University of Hasselt, Institute of Material Research (IMO), Agoralaan, Building D, B-3590 Diepenbeek, Belgium

Tel.: +32 1126.83.21, Fax: +32 1126.83.01,

E-mail: dirk.vanderzande@uhasselt.be

Born: 12-6-1957, Genk, Belgium.

Master in Chemistry at KULeuven in 1979;

PhD at KULeuven in 1986 in Organic synthesis and studies of mechanisms of thermal induced rearrangement reactions of ortho-quinodimethane systems.



Permanent position as senior post-doc researcher since January 1987 at the University of Hasselt (Belgium) joining the research group “Organic and Polymeric Chemistry”. Expert domains: Organic Synthesis, Polymer Synthesis, Advanced Organic and Polymeric Materials for Optical and Electronic applications.

1988: Start up of his research in the field of conjugated polymers. Two topics were started. The first topic relates to low band gap conjugated polymers, their synthesis, structural characterization and the underlying polymerization mechanisms. The second topic relates to the polymerization behavior of p-quinodimethane systems towards the synthesis of precursors for conjugated polymers.

1992: Appointed as assistant professor at U Hasselt.

1992: A new route was developed and optimized at the level of synthetic routes towards the monomer, the polymerization conditions and conditions of conversion of the precursor polymer.

1995: appointed as associated professor at U Hasselt.

1997 Concerning latter topic important breakthroughs were achieved and the so developed methodologies extended towards other systems. Start of material development specific towards polymer LEDs in collaboration with Philips and Covion.

1999: Appointed as “hoogleraar” at U Hasselt.

2000: Extending the efforts of material development towards applications of conjugated polymers in thin film FET transistors and organic solar cells. Start of studies related to defect structures in conjugated polymers.

2001: Start of association of the group as a division IMOMECE in IMEC vzw.

2003: Appointed as full professor (gewoon hoogleraar) at U Hasselt.

2003: New route was discovered towards Poly(Thienylene Vinylene) via the so called dithiocarbamate route which is under further investigation;

Full partner in many EC research projects in collaboration with industry over the last 10 years.

More than 190 refereed papers in international journals.

Eight original patents in the field of synthetic routes towards conjugated polymers.

EXPLORING DEVICE CONCEPTS FOR EFFICIENT, STABLE AND COST EFFECTIVE PRINTED POLYMER PV

S.C. VEENSTRA^{*,1}, W.J.H. VERHEES¹, L.H. SLOOFF¹, J.M. KROON¹,
Y. GALAGAN², N. GROSSIORD², R.A. ANDRIESSEN²

¹ ECN Solar Energy, P.O. Box 1, 1755 ZG Petten, The Netherlands

² Holst Center/TNO, High Tech Campus 48, 5656 AE Eindhoven, The Netherlands

One of the anticipated attractive features of flexible polymer solar cells is the high production speed. One can use conventional roll-to-roll deposition technologies to deposit an ink containing a polymer:fullerene mixture, onto a suitable substrate. Investigated roll-to-roll deposition technologies include printing technologies, for example ink jet, gravure and flexo-graphic, and coating technologies such as curtain and slot die coating. These deposition techniques enable production speeds in the order of square meters per second.

In a conventional polymer solar cell the photoactive layer, consisting of the polymer:fullerene blend, is sandwiched between two asymmetric electrodes. The hole collecting electrode is formed by an ITO layer, coated with PEDOT:PSS, whereas the electron collecting electrode is a low workfunction metal such as Ca, Ba or LiF/Al. It is a challenge to fabricate this complete layer stack with roll-to-roll deposition technologies at a high speed against low cost with satisfactory power conversion efficiencies and lifetimes that are sufficient for the first commercial applications

In order to meet the demands with respect to performance, stability and/or applicability, several novel device structures have been developed which have anticipated benefits, compared to conventional polymer solar cells. The application of metal-oxide layers in polymer solar cells enables the fabrication of these unconventional devices. Transparent solar cells have added value because of to the unique optical properties and appearance, while inverted solar cells may show increased lifetimes and enable polymer solar cells on metal foil. In all these novel polymer photovoltaic devices, the metal-oxide layer plays a crucial role.

We report on the proof-of-principle of a series of unconventional device concepts, enabled by the inclusion of thin solution processable metaloxide layers in polymer solar cells. Finally, we discuss efforts to replace the relative expensive and brittle ITO by a printable transparent composite anode based on a highly conductive transparent polymer (PEDOT:PSS) supported by a metal grid structure.

BIOGRAPHIC DATA OF DR SJOERD VEENSTRA

Sjoerd Veenstra (1972): studied Polymer Chemistry at the University of Groningen (The Netherlands) where he graduated in 1997 after a study on organic based bulk-heterojunctions. He stayed at the same university where he received his PhD-degree under the supervision of Prof. G. Hadziioannou and Prof. Dr. G. A. Sawatzky, on a thesis entitled: ‘The Electronic Structure of Molecular Systems’, in 2002. After his PhD, he accepted a position as researcher on polymer based solar cells at the Energy Research Centre of the Netherlands (ECN). Since 2009, ECN and the Holst Centre in Eindhoven (The Netherlands) have a joint program on Organic Photovoltaics. Sjoerd Veenstra went for an internship to the University of California at Santa Barbara in the group of Prof. A. J. Heeger (1997) and as visiting scientist to the group of Prof. G. G. Malliaras at Cornell University (2005). Since 2008 he gives a course on ‘Solar Cells’ together with Prof. J.C. Hummelen at the University of Goningen.



SOLUBILITY AND MOLECULAR STRUCTURE EFFECTS OF DONOR AND ACCEPTOR MATERIALS IN BULK HETEROJUNCTION ORGANIC SOLAR CELLS

Pavel A. Troshin,^A Diana K. Susarova,^A Ekaterina A. Khalina,^A Andrey E. Goryachev,^A Daniel Egbe,^B Sergei A. Ponomarev,^C N. Serdar Sariciftci^B and Vladimir F. Razumov^A

[A] Institute for Problems of Chemical Physics of Russian Academy of Sciences, Semenov Prospect 1, Chernogolovka, Moscow region, 142432, Russia. E-mail: troshin@cat.icp.ac.ru

[B] Linz Institute for Organic Solar Cells (LIOS), Johannes Kepler University Linz, Altenbergerstrasse 69, A-4040 Linz, Austria

[C] Enikolopov Institute of Synthetic Polymer Materials, Russian Academy of Sciences, 70 ul. Profsoyuznaya, 117393 Moscow, Russia

We report the investigation of photovoltaic performance of ca. 200 composite systems composed of 20 different fullerene derivatives blended with 10 different conjugated polymers. We showed previously that efficiency of organic solar cells based on poly(3-hexylthiophene) (P3HT) is strongly influenced by the solubility of the fullerene derivative used as electron acceptor counterpart. However, it was unclear if the solubility/structure/device performance relationships revealed for P3HT-based cells will be valid for systems comprising other donor polymers. To answer this question we investigated 10 different polymers combined with various fullerene derivatives in photoactive layers of organic solar cells. This comprehensive study showed that photovoltaic performance of every polymer/fullerene system indeed is governed by relative solubility of the materials and their molecular structures. However, exact fashion in which solar cell performance depends on the solubility of the fullerene-based component might be different for different types of polymers. Molecular structure, in particular, side chain effects are supposed to be responsible for the observed behavior.

CORRELATION BETWEEN THE ENERGY LEVEL ALIGNMENT AND DEVICE PERFORMANCE IN ORGANIC FIELD EFFECT TRANSISTORS

P. STADLER^{1*}; A. M. TRACK²; M. ULLAH³; H. SITTER³; G. J. MATT³; H. NEUGEBAUER¹; T. B. SINGH⁴; N. S. SARICIFTCI¹; G. KOLLER²; M. G. RAMSEY²;

¹ Johannes Kepler University Linz, Institute for Organic Solar Cells (LIOS) and Institute for Physical Chemistry; Altenbergerstraße 69, 4040 Linz, Austria

²University of Graz, Institute of Physics, Universitätsplatz 3, 8010 Graz, Austria

³Johannes Kepler University Linz, Institute for Semiconductor and Solid State Physics, Altenbergerstraße 69, 4040 Linz, Austria

⁴CSIRO Molecular and Health Technologies, Ian Wark Laboratory, Bayview Ave, Clayton VIC 3168, Australia

Interface engineering in organic field effect transistors (OFETs) has become the key issue implementation of high-performance devices. The crucial part is to design the interface between the dielectric and the organic semiconductor. State of the art OFETs usually apply bilayer dielectrics consisting of an oxide which is modified with an organic interlayer on top. Thin polymeric insulators and resins as well as self assembled monolayers (SAMs) grown on silicon dioxide and Al₂O₃ serve as surface modifiers [1]. Recent studies show that the overall device performance improves when interlayers are applied [2].

The role of such modifiers is often interpreted as passivating the oxide surface removing hydroxyl groups which are considered to act as traps. Factors ranging from changes in film morphology through to issues of electronic level alignment could all be playing a role. While device activity has concentrated on modifying the inorganic dielectric surface with SAMs or polymer dielectrics, little work has considered the possibility of charge rearrangements at the interface of such modifiers with the organic semiconductor. Recently theoretical modelling has suggested that improvements in transfer characteristics and ridged shifts of the threshold voltage can result from the introduction of permanent space charge or dipole layers at the organic semiconductor / dielectric interface [3]. In particular the introduction of a BCB divinyltetramethyldisiloxane-bis(benzocyclobutene) interlayer between the inorganic dielectric (Al₂O₃, SiO₂) and the organic semiconductor has been reported to yield low operating voltages and high mobilities [4]. Apart from suggestions of it acting as a passivation layer little is known of

its function. We focus on the energy level alignment at the interface, which is characterized in a combined device and photoemission study. We present a method probing the electronic levels directly at the interface by means of photoemission spectroscopy and we find a direct correlation between the energy level alignment and the transistor performance [5].

Transistors using C_{60} as semiconductor and a bilayer of BCB – Al_2O_3 have been reported to excel in low threshold voltage and high mobility ($<3 \text{ cm}^2\text{V}^{-1}\text{s}^{-1}$). This system is chosen to explore the role in the improved performance due to the BCB interlayer. We present a complementary study of two device structures, with and without BCB. We compare the performance of the field effect transistors and show that the improvement of the OFET with BCB can be directly related to the differences in energy level alignment as measured by ultra-violet and X-ray photoemission spectroscopy: When BCB-interlayer is applied the secondary electron cut-off – the work function – and the valence bands as well as C 1s core levels of the C_{60} shift concomitantly to lower binding energies. Compared to the oxide-only structure the organic interlayer exhibits a huge dipole. The investigations indicate that this dipole is *the* prime determinant for enhancement of the transistor performance. Moreover, from studies of each interface the improvement in device performance arising from the BCB interlayer is shown to be generated by an inbuilt potential at the interlayer/organic semiconductor interface. The magnitude and mechanism of the inbuilt-potential suggests detailed studies into tailoring organic-organic interfaces on the gate dielectric could be very promising for optimizing device performance.

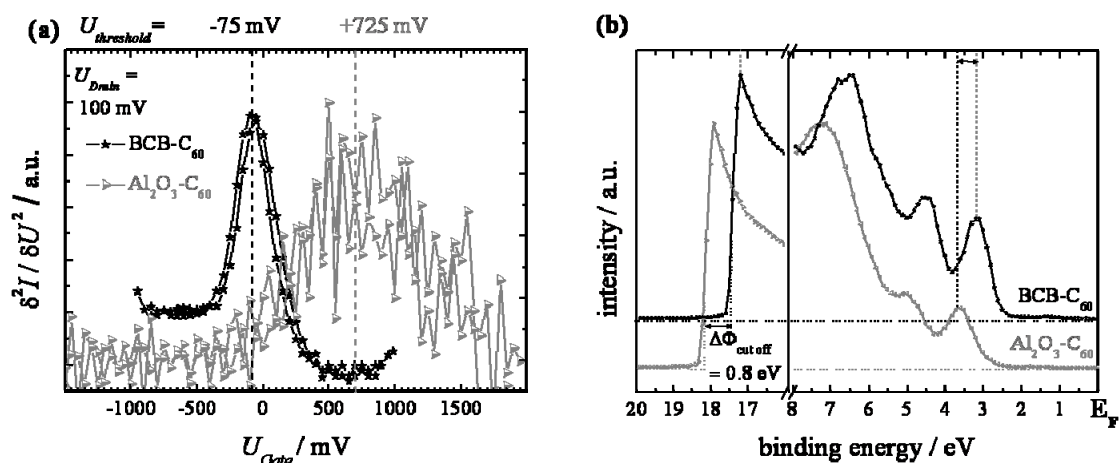


Figure 1. (a) Shift of threshold voltage $\Delta U_{threshold}$ in the second derivative of the transfer characteristics in OFETs with (dark) and without (light) BCB layer. (b) The UPS of C_{60} on

Al₂O₃ (light) and on BCB (dark) referenced to the E_F . The shift in the valence bands and in the secondary electron cut-off $\Delta\Phi$ is indicated.

- [1] H. Klauk, U. Zschieschang, M. Halik, J. Appl. Phys. 102 (2007) 074514
- [2] L.-L. Chua, J. Zaumseil, J.-F. Chang, E. C.-W. Ou, P. K.-H. Ho, H. Sirringhaus, R. H. Friend, Nature 434 (2005) 195
- [3] W. Osikowicz, M. P. de Jong, W. R. Salaneck, Adv. Mater. 19 (2007) 4213–4217
- [4] X.-H. Zhang, B. Domercq, B. Kippelen, Appl. Phys. Lett. 91 (2007) 092114
- [5] P. Stadler, A. M. Track, M. Ullah, H. Sitter, G. J. Matt, G. Koller, T. B. Singh, H. Neugebauer, N. S. Sariciftci, M. G. Ramsey, Org. Electr. 11 (2010), 207-211

BIOGRAPHIC DATA OF Philipp STADLER

*Linz Institute for organic solarcells (LIOS)
Institute for Physical Chemistry
Johannes Kepler University Linz
Altenbergerstrasse 69, A-4040 Linz
AUSTRIA
Tel: +43-732-2468 8753
Fax: +43-732-2468 8770
E-mail: philipp.stadler@jku.at
<http://www.lios.at>*



1st March 2007 – today

Philipp Stadler is a PhD candidate under the supervision of Prof. Sariciftci at the Johannes Kepler University (JKU) of Linz. He received his master degree in January 2007 at JKU in the Institute for Physical Chemistry. His research topic is organic photovoltaic cells and the characterization of organic semiconductors in general, especially in transistor and related devices. His recent publications include the combination of devices and spectroscopy such as photoemission and FTIR studies on organic semiconductors. Part of his work includes lecturing namely the exercises in physical chemistry and supervision of diploma students. He is currently in the final stage of PhD and completing his thesis.

2000 - 2007:

Study of chemistry at the JKU Linz, Austria with sponson for Master of Science in chemistry. Topic of the master thesis: " Hysteresis in Bio-organic field effect transistors"

1991 - 1999 :

Study and graduation at the Bundesgymnasium Freistadt, Austria

Membership in Professional Societies:

Member of the Materials Research Society
Member of the Austrian Chemical Society (GOECH)
Member of the Austrian Physical Society (OEPG)

List of Scientific Publications:

Philipp Stadler has 79 citactions, Hirsch Index= h-index =3 (2010)

Refereed Full Papers:

- [5] “Dependence of Meyer-Neldel energy on energetic disorder in organic field effect transistors”, M. Ullah, I. I. Fishchuk, P. Stadler, A. Pivrikas, C. Simbrunner, V. N. Poroshin, N. S. Sariciftci, H. Sitter, *Organic Electronics and Photonics* (2010), in press
- [4] “The role of the dielectric interface in organic transistors: A combined device and photo-emission study”, P. Stadler, A. M. Track, M. Ullah, H. Sitter, G. J. Matt, G. Koller, T. B. Singh, H. Neugebauer, N. S. Sariciftci, M. G. Ramsey, *Organic Electronics* **11** (2010), 201-211
- [3] “Substituting the postproduction treatment for bulk-heterojunction solar cells using chemical additives”, A. Pivrikas, P. Stadler, H. Neugebauer, N.S. Sariciftci, *Organic Electronics* **9** (2008), 775-782
- [2] “Organic field-effect transistors and memory elements using deoxyribonucleic acid (DNA) gate dielectric”, P. Stadler, K. Oppelt, B. Singh, J. Grote, R. Schwödiauer, S. Bauer, H. Piglmayer-Brezina, D. Bäuerle, N.S. Sariciftci, *Organic Electronics* **8** (2007), 648-654
- [1] ”Fabrication and characterization of solution-processed methanofullerene-based organic field-effect transistors”, B. Singh, N. Marjanovic, P. Stadler, M. Auinger, G. Matt, S. Guenes, N.S. Sariciftci, R. Schwödiauer, S. Bauer, *Journal of Applied Physics* **Vol 97** (2005), 083714

Papers as Contributions in Conference Proceedings:

- [3] “Negative Differential Resistance in C₆₀ Diodes”, P. Stadler, A. Fuchsbauer, G. Hesser, T. Fromherz, G. Matt, H. Neugebauer, N.S. Sariciftci, Interface Controlled Organic Thin Films, *Springer Proceedings in Physics*, Vol **129** (2009), 189
- [2] “Rubrene thin film characteristics on mica substrates”, S.M. Abd Al-Baqi, G. Hernandez-Sosa, H. Sitter, B. Singh, P. Stadler, N.S. Sariciftci, *Springer Proceedings in Physics*, Vol **129** (2009), 43
- [1] “Current filamentation and negative differential resistance in C₆₀ diodes”, P. Stadler, G. Hesser, T. Fromherz, G. Matt, H. Neugebauer, N.S. Sariciftci, *physica status solidi (b)* **245**, No. 10 (2008), 2300-2302

Contributions to international conferences (chronological Order):

July 2006 :

Oral presentation at the International Conference on Synthetic Metals ICSM 2006, Dublin, Ireland

March 2007:

Poster presentation at the German physical society meeting (DPG-Tagung) in Regensburg, Germany

May 2007:

Poster presentation at the Optical Probes, OP2007, Turku, Finland

September 2007:

Oral presentation at the Nationales Forschungsnetzwerk (NFN) project meeting in Admont, Austria

May 2008

Oral presentation at the European Material Research Society (EMRS) Spring Meeting in Straßbourg, France

July 2008

Oral presentation at the International Conference on Synthetic Metals, ICSM 2008, Recife, Brasil

September 2008

Oral presentation at the Nationales Forschungsnetzwerk (NFN) project meeting in Eisenerz, Austria

February 2009

Poster presentation at the GOECH Meeting “Sub-group physical chemistry” in Innsbruck, Austria

February 2009

Oral presentation at the Nationales Forschungsnetzwerk (NFN) project meeting in Leoben, Austria

March 2009

Poster presentation at the International Winterschool on the Electronic Properties of Novel Materials IWEPM 2009 in Kirchberg i. Tirol, Austria.

April 2009

Poster presentation at the Material Research Society (EMRS) Spring Meeting in San Francisco, USA

May 2009

Poster presentation at the European Material Research Society (EMRS) Spring Meeting in Straßbourg, France

July 2009

Invitation to workshop the International Akademie in Traunkirchen, Austria

September 2009

Oral presentation at the Nationales Forschungsnetzwerk (NFN) project meeting in Admont, Austria

April 2010:

Poster presentation at the Material Research Society (MRS) Spring Meeting in San Francisco, USA

April 2010:

Invitation to Department of electrical engineering, University of South Florida, Tampa, USA

TOWARDS ROLL-TO-ROLL PROCESSING OF FLEXIBLE POLYMER SOLAR MODULES

Harald Hoppe¹, Maik Baerenklau¹, Aart Schoonderbeek², Roland Roesch¹, Burhan Muhsin¹, Uwe Stute², Dieter Teckhaus³, and Gerhard Gobsch¹

1 Institute of Physics, Ilmenau University of Technology, Ilmenau, Thuringia, Germany.

2 Laser Zentrum Hannover e.V., Hannover, Lower-Saxony, Germany.

3 SK Kassetten GmbH & Co. KG, Neuenrade, Nordrhein-Westfalen, Germany.

Abstract

Efficient polymer solar modules require a thoughtful design of the device layout based on the constraints arising from the choice of electrode materials – especially when considering the high sheet resistance in transparent conducting oxide.[1] Therefore the series resistance of monolithically interconnected solar cells has to be optimized according to sheet and contact resistances. Here geometrical factors play an important role.[2] Our approach for polymer solar cell processing is based on the slot dye coating technique, allowing a fast, precise and economic use of feed materials. Since the coating is a full area deposition, an additional structuring process is required. To minimize inactive area losses, we apply laser ablation for very fine structuring of the solar cell interconnects.[1, 3, 4] We present first results of solar modules processed by this technology.

References:

- [1] B. Muhsin, J. Renz, K. H. Drue, G. Gobsch and H. Hoppe, Efficient polymer solar cell modules, **Synth. Met.** **159**, p. 2358 (2009).
- [2] B. Muhsin, J. Renz, K. H. Drue, G. Gobsch and H. Hoppe, Influence of polymer solar cell geometry on series resistance and device efficiency, **Physica Status Solidi a-Applications and Materials Science** **206**, p. 2771 (2009).
- [3] G. Dennler, C. Lungenschmied, H. Neugebauer, N. S. Sariciftci and A. Labouret, Flexible, conjugated polymer-fullerene-based bulk-heterojunction solar cells: Basics, encapsulation, and integration, **J. Mater. Res.** **20**, p. 3224 (2005).
- [4] R. Rösch, B. Muhsin, M. Bärenklau, A. Schoonderbeek, G. Gobsch, L. Richter, R. Kling, D. Teckhaus and H. Hoppe¹, TOWARDS ROLL-TO-ROLL PROCESSING OF FLEXIBLE POLYMER SOLAR CELL MODULES, presented at: 24th PV SEC, Hamburg, (2009).

List of Authors

A

Abad, J.	123, 176
Allegramente, G.	199
Andae, G.	150
Andriesen, R.A.	166
Assche, van G.	56, 158
Auner, C.	181

B

Babenko, S.D.	253
Backlund, T.	51
Balster, T.	68
Bärenklau, M.	65, 175
Barge, S.	16
Barret, M.	262
Batallán, and F.	123
Battaglini, N.	29
Bauer, S.	89
Baumann, R.	22
Bergeret, C.	143
Berggren, M.	13
Bernardi, A.	199
Berny, S.	62, 187, 254
Berson, S.	262
Bertho, S.	56, 158
Blankenburg, L.	150, 186
Bober, P.	188
Bodö, P.	246
Bolin, M.	13
Bolink, H.J.	105
Bolsée, J.C.	158
Borchert, H.	191
Borshchev, O.	81
Bott, A.	206
Brabec, Ch.	55
Braga, D.	29
Brande, van d. N.	56
Brookes, P.	51
Bruevich, V.V.	138
Burroughes, J.	95

C

Caironi, M.	77
Canisius, J.	51
Carbonera, C.	199
Carrasco-Orozco, M.	51
Céspedes-Guirao, F. J.	105
Cleij, T.J.	158
Colchero, J.	176
Colsmann, A.	206
Como, da E.	20, 225
Costa, R.D.	105
Cousseau, J.	143

D

Das, A.	42
Dellith, A.	150
Demir, F.	56
Derbal, H.	143
Deshmukh, K.D.	243
Diaz-Paniagua, C.	123
Dieudonné, M.	262
Ding, Y.	107
Dittrich, C.	226
Do, T.H.	206
Dyakov, V.A.	138

E

Egbe, D.	168
Egginger, M.	258
Engmann, S.	65
Espinosa, N.	123, 176, 209

F

Feldmann, J.	20, 231
Feldmeier, E.	32
Fernández-Lázaro, F.	105
Fichou, D.	1, 62, 187, 254
Finger, F.	22
Fuchs, K.	101

G

Gadisa, A.	158
Gaiser, D.	131
Galagan, Y.	166
Garcia-Cascales, M.S.	209
Garcia-Sakai, V.	123
Garcia-Valverde, R.	123, 209
Gburek, B.	68
Georgakopoulos, S.	221
Gerken, M.	264, 267
Getachew, A.	240
Geyer, U.	267
Ghani, F.	263
Giannotta, G.	199
Gierschner, J.	105
Gili, E.	77
Gobsch, G.	65, 150, 175
Gold, H.	181
Goryachev, A.E.	168
Grell, M.	42
Grogger, W.	181
Gromchenko, A.A.	138
Grossiord, N.	166

Guetlein, J.	267	Kristen, J.	263
Guillerez, S.	262	Kroon, J.M.	166
Gvozdikova, I.A.	138	Kruszynska, M.	191
		Kugler, T.	95
H		Kuna, L.	246
Haase, A.	181	Kwiatkowska, M.	257
Haber, T.	181		
Haen, J.D.	158	L	
Halik, M.	86	Larsson, K.	13
Hallermann, M.	20, 231	Lemmer, U.	206, 267
Hasselgruber, M.	22	Leo, K.	104
Hauff, von E.	101, 191, 261	Lloyd, G.	51
Hauss, J.	267	Lokteva, I.	191
Heinemann, M.D.	191	Lutsen, L.	158
Herrmann, F.	65		
Hoppe, H.	65, 175	M	
Horowitz, G.	29	Madec, M.B.	42
Hübler, A.C.	243	Madjarov, A.	239
Huska, K.	267	Magnien, J.	246
		Malliaras, G.	27
I		Mamangun, D.	107
Invernale, M.	107	Manca, J.	158
Irimia-Vladu, M.	89	Matzen, S.	254
		May, C.	22
J		Maydell, K.	191
Jabbour, G.	54	Mele, van B.	56, 158
Jager, E.	13	Melzer, C.	32
Jakopic, G.	181, 246	Meyer-Friedrichsen, T.	81
		Miskiewicz, P.	51
K		Morrison, J.J.	42
Kaiser, I.	267	Moskvin, Yu.L.	253
Katz, H.E.	243	Mourao, J.	262
Kell, D.B.	42	Moussy, J.-B.	254
Kempa, H.	243	Muhsin, B.	175
Kergoat, L.	29	Müller, D.	51
Kettle, J.	42		
Khalina, E.A.	168, 234	N	
Khlopkin, N.A.	138	Nakayama, K.	37
Kim, H.	29	Nazmutdinova, G.	235
Kirchmeyer, S.	48	Neher, D.	16
Klemm, E.	150	Neugebauer, H.	169
Kohlbusch, T.	226	Newsome, C.	95
Koller, G.	169	Novikov, Yu.N.	138
Kolny-Olesia, J.	191	Nunzi, J.-M.	143
Konkin, A.	112		
Konkin, A.	150	O	
Konyushenko, E.N.	228	Oosterbaan, W.D.	158
Kostyanovskiy, V.A.	234	Opoku, C.	97
Kraker, E.	246	Orti, E.	105
Krenn, J.R.	246	Othman, K.	95
Krinichnyi, V.I.	112		

P		Seggern, von H.	32
Paasch, G.	71	Sell, S.	150
Padilla, J.	107, 123	Sensfuss, S.	150, 186
Palfinger, U.	181	Sezen, M.	181
Paraschuk, D.Yu.	138	Shkunov, M.	97, 221
Parisi, J.	101, 191,261	Shokhovets, S.	65, 150
Pellegrino, A.	199	Simon, D.	13
Peregudov, A.S.	240	Singh, T.B.	169
Persson, K.	13	Sinwel, D.	252
Petukhou, Yu.	257	Sirringhaus, H.	77
Pierron, P.	262	Sitter, H.	169
Po, R.	199	Slooff, L.H.	166
Ponomarenko, S.A.	81, 168	Solntsev, A.	257
Pradana, A.	264	Song, A.	42
Presselt, M.	65	Sonntag, P.	262
Pütz, A.	206	Sotzing, G.A.	107
R		Sparrowe, D.	221
Raabe, D.	235	Stadler, P.	169
Rädler, M.	264	Stadlober, B.	181, 246
Radychev, N.	191	Steinhäuser, F.	239
Ramsey, M.	169	Stejskal, J.	188, 228, 272, 275
Razumov, V.F.	168, 240,253	Stürmer, M.	239
Reinhold, I.	131, 239	Stute, U.	175
Reuter, K.	243	Subocz, J.	257
Richardson, T.H.	42	Susarova, D.K.	168, 240, 253
Richter-Dahlfors, A.	13	Sutter, T.	239
Riedel, B.	267	Svennersten, K.	13
Riedel, I.	191	T	
Riegler, H.	263	Teckhaus, D.	175
Rodriguez-Redondo, J.L.	105	Threm, D.	264
Roesch, R.	65, 175	Tierney, S.	51
Roslaniec, Z.	257	Todt, U.	22
Roth, H.-K.	112	Tortech, L.	62, 187, 254
S		Track, A.M.	169
Sapurina, I.	272, 275	Trchová, M.	188, 228, 272, 275
Sariciftci, S.	46, 89, 168, 169, 258	Troshin, P.A.	168, 240, 253
Sastre-Santos, A.	105	Tsikalova, M.V.	138
Savoini, A.	199	Tunc, A.V.	255
Sawatdee, A.	246	Turner, M.	42
Schache, H.	150, 186,235	Tyagi, M.	123
Scheinert, S.	71	Tybrandt, K.	13
Scheipl, G.	246	U	
Schidleja, M.	32	Uglov, V.	257
Schmidt, W.	129	Ullah, M.	169
Schoonderbeek, A.	175	Urbina, A.	123, 176, 209
Schroedner, M.	112, 186,235		
Schubert, U.	6		
Schultheis, K.	186		
Seeland, M.	65		

V

Valozhyn, A.	257
Vanderzande, D.	56, 158
Vandewal, K.	158
Véber, M.	62
Veenstra, S.	166
Verhees, W.J.H.	166
Vogeler, H.	206
Voit, W.	131, 239
Vrindts, V.	158

W

Wagner, V.	68
Wedge, D.C.	42
Wilson, R.	95
Witt, F.	191

Y

Yeates, S.G.	42
--------------	----

Z

Zapka, W.	131, 239
Zapunidi, S.A.	138
Zenker, M.	257
Zhao, J.	56, 158
Zhdanok, S.	257
Zirkl, M.	246
Zutz, F.	191